Behavior of laterally loaded pile group model in sand

Shawqi Juma Al Mandeel

Civil Engineering

May 2000

Abstract

The behavior of laterally loaded pile groups can be studied easily in the laboratory on small scale model, saving a lot of expenses, efforts and time. This research presents investigations on small scale closely spaced pile groups embedded in sandy soil in order to understand the behavior of such model when subjected to lateral load. The experimental program consisted of studying the behavior of twelve models by varying the following parameters: number of piles, loading conditions (static or cyclic) and sand saturation conditions (dry or submerged). The static and cyclic loading were achieved by means of specially designed loading actuator. The cyclic loading represents the wave action exerted on offshore structures. Experimental blending moment and deflection along the pile length were compared with semi-empirical ones. The behavior of the small scale model was compared to full scale model which shows reasonable results. Experimental results have shown that the behavior of pile groups was greatly influenced by the study parameters. Finally, the samll scale model in laboratory can be used to study the behavior of laterally loaded closely spaced pile groups.

INFORMATION TO USERS

This manuscript has been reproduced from the microfilm master. UMI films the text directly from the original or copy submitted. Thus, some thesis and dissertation copies are in typewriter face, while others may be from any type of computer printer.

The quality of this reproduction is dependent upon the quality of the copy submitted. Broken or indistinct print, colored or poor quality illustrations and photographs, print bleedthrough, substandard margins, and improper alignment can adversely affect reproduction.

In the unlikely event that the author did not send UMI a complete manuscript and there are missing pages, these will be noted. Also, if unauthorized copyright material had to be removed, a note will indicate the deletion.

Oversize materials (e.g., maps, drawings, charts) are reproduced by sectioning the original, beginning at the upper left-hand corner and continuing from left to right in equal sections with small overlaps.

Photographs included in the original manuscript have been reproduced xerographically in this copy. Higher quality 6" x 9" black and white photographic prints are available for any photographs or illustrations appearing in this copy for an additional charge. Contact UMI directly to order.

ProQuest Information and Learning
300 North Zeeb Road, Ann Arbor, MI 48106-1346 USA
800-521-0600

BEHAVIOR OF LATERALLY LOADED PILE GROUP MODEL IN SAND

BY

Shawqi Juma Al Mandeel

A Thesis Presented to the

DEANSHIP OF GRADUATE STUDIES

KING FAHD UNIVERSITY OF PETROLEUM & MINERALS

DHAHRAN, SAUDI ARABIA

In Partial Fulfillment of the
Requirements for the Degree of

MASTER OF SCIENCE

In

CIVIL ENGINEERING

MAY 2000

UMI Number: 1406095

Bell & Howell Information and Learning Company
300 North Zeeb Road
P.O. Box 1346
Ann Arbor, MI 48106-1346

KING FAHD UNIVERSITY OF PETROLUEM & MINERALS

DHAHRAN 31261, SAUDI ARABIA

DEANSHIP OF GRADUATE STUDIES

This thesis, written by

SHAWQI JUMA AL MANDEEL

under the direction of his thesis advisor and approved by his thesis committee, has been presented to and accepted by Dean of Graduate Studies, in partial fulfillment of the requirements for the degree of

MASTER OF SCIENCE IN CIVIL ENGINEERING.

THESIS COMITTEE:

Prof. Sahel N. Abduljauwad, Chairman

Prof. Ghazi J. AlSulaimani, Co-Chairman

Dr. Saad A. Aiban, Member

Dr. Naser A. Al Shayea, Member

Department Chairman

Dean of Graduate Studies

عمادة الدراسات العليا
DEANSHIP OF GRADUATE STUDIES

Date : ١٤٢٢/٤/١٢

This thesis is dedicated to my parents, my wife and my family.

ACKNOWLEDGEMENT

Acknowledgement is due to King Fahd University of Petroleum and Minerals for support of this research.

I wish to express my appreciation to Professor Dr. Sahel N. AbdulJauwad who served as my thesis committee major advisor for his support and patience. I also wish express my appreciation to Professor Dr. Ghazi J. AlSulaimani who served as my thesis committee co-advisor for his continuous support during this research. I also wish to thank other members of my Thesis committee Dr. Saad A. Aiban and Dr. Naser A. AlShayea for their great assistance and valuable suggestions.

I wish to acknowledge the great assistance given by all laboratory staff during the experimental part of my research. I also express my thanks to Mr. Hassan Zakria for helping me in maintaining laboratory equipment and for the great effort.

I owe my family an expression of gratitude for their patience, understanding and continuous encouragement.

Lastly, I am thankful to all KFUPM faculty, colleagues and friends who help me during my study.

TABLE OF CONTENTS

LIST OF TABLES

LIST OF FIGURES

LIST OF PLATES

THESIS ABSTRACT

SHAWQI JUMA AL MANDEEL

BEHAVIOR OF LATERALLY LOADED PILE GROUP MODEL IN SAND

CIVIL ENGINEERING

MAY 2000

The behavior of laterally loaded pile groups can be studied easily in the laboratory on small scale model, saving a lot of expenses, efforts and time. This research presents investigations on small scale closely spaced pile groups embedded in sandy soil in order to understand the behavior of such model when subjected to lateral load. The experimental program consisted of studying the behavior of twelve models by varying the following parameters: number of piles, loading conditions (static or cyclic) and sand saturation conditions (dry or submerged). The static and cyclic loading were achieved by means of specially designed loading actuator. The cyclic loading represents the wave action exerted on offshore structures. Experimental bending moment and deflection along the pile length were compared with semi–empirical ones. The behavior of the small scale model was compared to full scale model which shows reasonable results. Experimental results have shown that the behavior of pile groups was greatly influenced by the study parameters. Finally, the small scale model in laboratory can be used to study the behavior of laterally loaded closely spaced pile groups.

مـلـخـص الرسـالـة

الاســـــــــــم : شوقي جمعه المنديل

عنوان الرسالـــة : مسلك نموذج مجموعة الخوازيق المحملة جانبياً في الرمل

التخصـــــــص : هندسة مدنية

تاريخ التخـــرج : مايو ٢٠٠٠

إن دراسة مسلك مجموعة الخوازيق المحملة جانبياً ليس بالأمر الصعب ويسهل تحقيقه في المختبر باستخدام نموذج بمقيـــاس مصغر، مما يوفـــر الكثير من النفقـــات والجهد والوقت. يتميز هذا البحث بتهيئة عمليات الاستقصاء والبحث على أساس مقياس مصغر بالنسبة لمجموعات الخوازيق المتقاربة في تربة رملية ليتسنى دراسة وإدراك مسلك مثل هذا النموذج عند تعرضه لحمل جانبي. حيث أن البرنامج المختبري يتضمن دراسة مسلك إثنى عشر نموذج بالاعتماد على المتغيرات التالية: عدد الخوازيق في المجموعة، وضعية التحميل (ساكن أو متردد) ووضعية التشبع في الرمل (جاف أو مغمور). إن التحميل الساكن أو المتردد قد تم تحقيقه باستخدام آلة حمل محفزة صممت خصيصاً لذلك. اذ أن التحميل المتردد يمثل تأثير الأمواج على المنشآت البحرية. إن كمية العزم والانحناء التجريبي على طول الخازوق قد تمت مقارنتها بمثيلاتها المقدرة من الحلول الشبه تجريبية. إن مسلك النموذج القياسي المصغر قد قورن بنموذج قياسي كامل مما أظهر نتائج معقولة. كما أن النتائج التجريبية قد أظهرت بان مسلك نموذج مجموعة الخوازيق تتأثر بفعالية كبيرة بالمتغيرات المدروسة. وأخيراً فإنه يمكن استخدام النموذج القياسي المصغر في المختبر لدراسة مسلك مجموعة الخوازيق المتقاربة والمحملة جانبياً.

CHAPTER ONE

INTRODUCTION

1.1 General

Piles are defined as structural members imbedded into soil; they are needed to transfer loads from the superstructure to a lower strata of the soil. They are usually constructed from steel, concrete or timber. Laterally loaded piles are usually subjected to axial and lateral loading or a combination of lateral loads, axial loads and moments. Understanding the behavior of laterally loaded piles is one of the major problems concerned with the soil structure interaction. The laterally loaded piles have a number of uses as foundations of structures such as: High-rise buildings subjected to wind and earthquake loadings and offshore structures (e.g. platforms).

Figure 1.1 shows piles subjected to various types of loading. For example, Figure1.1a shows a pile subjected to a lateral load only, which is a rare case in real life implementation, such as an anchor pile. Figure 1.1b is a case of a pile subjected to lateral loading and a moment transferred from the superstructure above, such as in the case of an advertising signboard or claddings. Figure 1.1c is a pile subjected to a lateral load only and fixed against rotation at the top, such as, a pile supporting a reinforced concrete retaining wall. Figure 1.1d

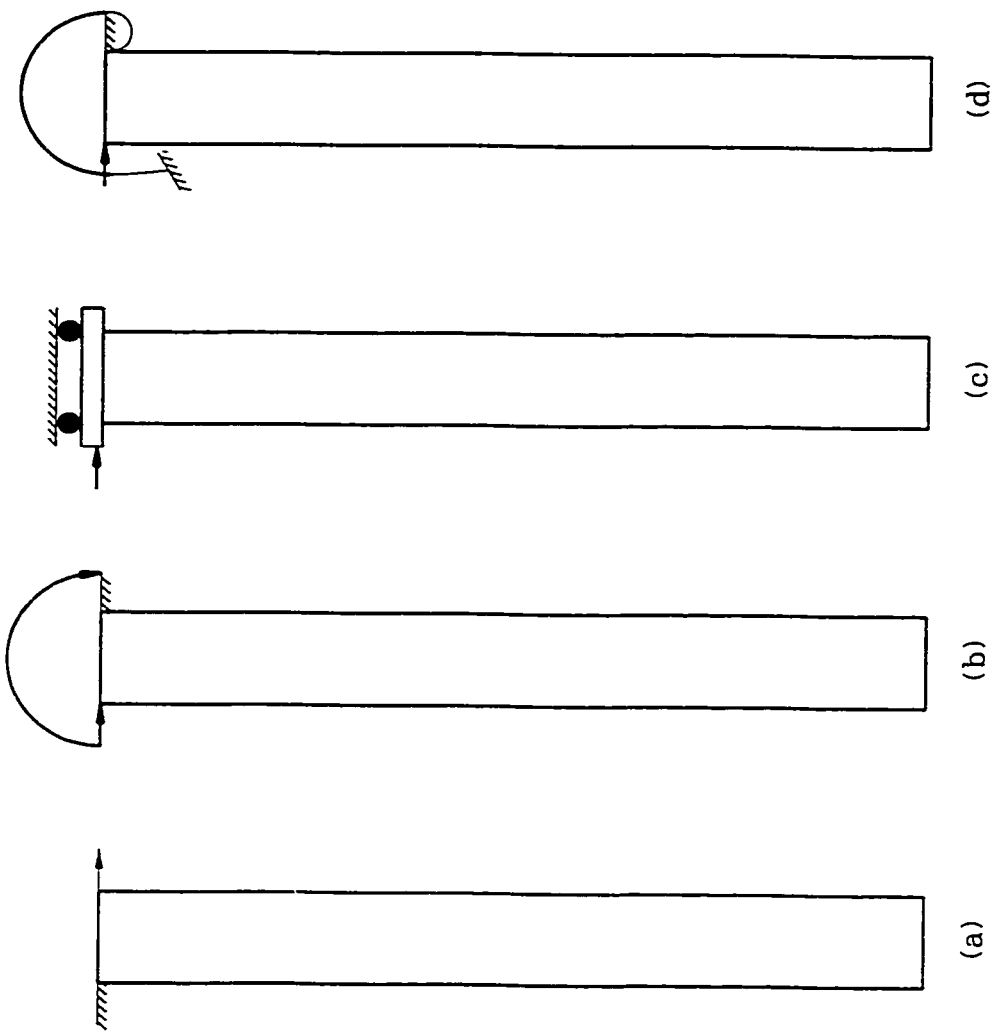

Figure 1.1: Lateral Loading Type (Reese 1977).

representing a pile supporting an offshore drilling platform, where the pile extends upwards and becomes a part of the flexible structure subjected to lateral load. In designing and constructing the piles, two factors are important: strength and serviceability of the pile. These two factors can be satisfied by knowing shear force, the bending moment and the deflections along the length of the pile. The stresses along the pile are essential in determining the load carrying capacity of pile material.

The current analysis methodologies are mostly applicable to a single pile. However piles are usually used as a group such as in offshore foundations or in bridge construction as shown in Figure 1.2. Similar analysis are conducted on group of piles with some modifications to account for group behaviour and actions.

1.2 Importance of the Research

Studying the behaviour of laterally loaded pile group requires the knowledge of the following design parameters: bending moment, shear force deflection, and soil response along the pile length. Thus, the most ideal procedure is to test a full scale pile group model under actual lateral loading conditions. Moreover, these parameters can be drawn from theoretical solutions using numerical procedures with reasonable assumptions or approximations. The latter procedure need to be correlated to the former one (full scale testing). However, conducting a full scale testing is rather expensive and requires a lot of time and great efforts, especially for pile groups.

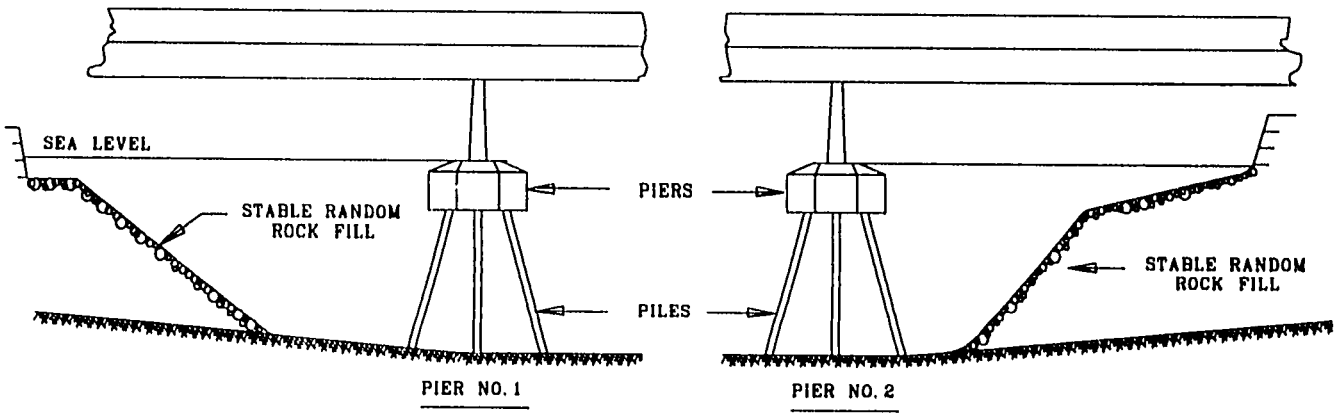

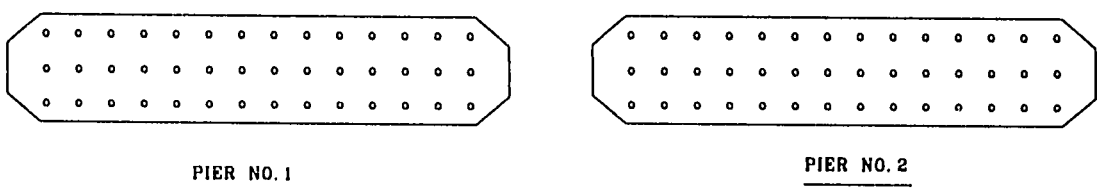

Figure 1.2: Example of Pile Group

Even though full scale testing is the most suitable and beneficial type of testing to study the behaviour of laterally-loaded pile groups, small scale testing produce similar behaviour to full scale model to some extent. Therefore, small scale testing model in the laboratory is still applicable and reliable within certain limits, by applying a similar field conditions as close as possible to those in the full scale testing model.

In this research, tests were conducted on a small-scale piles group model in the laboratory which will reflect the behaviour of full scale pile group model. The initial part of this research is the modification of the experimental set up for pile group, including the development of a fully reversible cyclic loading actuator and a pile cap.

1.3 Research Objective

The main objective of this research is to develop a testing setup of a small scale model for pile groups and study their behavior when subjected to static and cyclic loadings, then compare their behavior with full-scale testing. The specific objectives are as follows:

1. To develop a lateral loading system to simulate the actual loading condition (i.e. static and cyclic loadings) for small scale pile groups.
2. To study the behavior of a single pile.
3. To study the behavior of model pile groups (four and nine pile groups).
4. To compare the behavior of piles in the groups with that of single pile.
5. To study the soil resistance under different testing parameters.

The test parameters which are considered include (as shown in Figure 1.3):

1. Soil condition
    a) Dry
    b) Fully Submerged
2. Lateral loading condition
    a) Static
    b) Cyclic
3. Number of piles in the group
    a) Single pile
    b) Four piles with two piles per row (2 X 2)
    c) Nine piles with three piles per row (3 X 3)

1.4: Organization of the Thesis

This research discusses the behavior of small-scale model pile groups. Chapter one stated in general the behavior of laterally loaded piles and their use in nature. Also, it lists the research importance, objectives and the scope of work. Chapter two investigates the previous works and researches carried out in this field and other related works. In Chapter three the material used and their characteristics were indicated. Moreover, the experimental setup was presented in details for each equipment and the operational procedure was thoroughly discussed. Chapters four and five discuss the research results and findings in

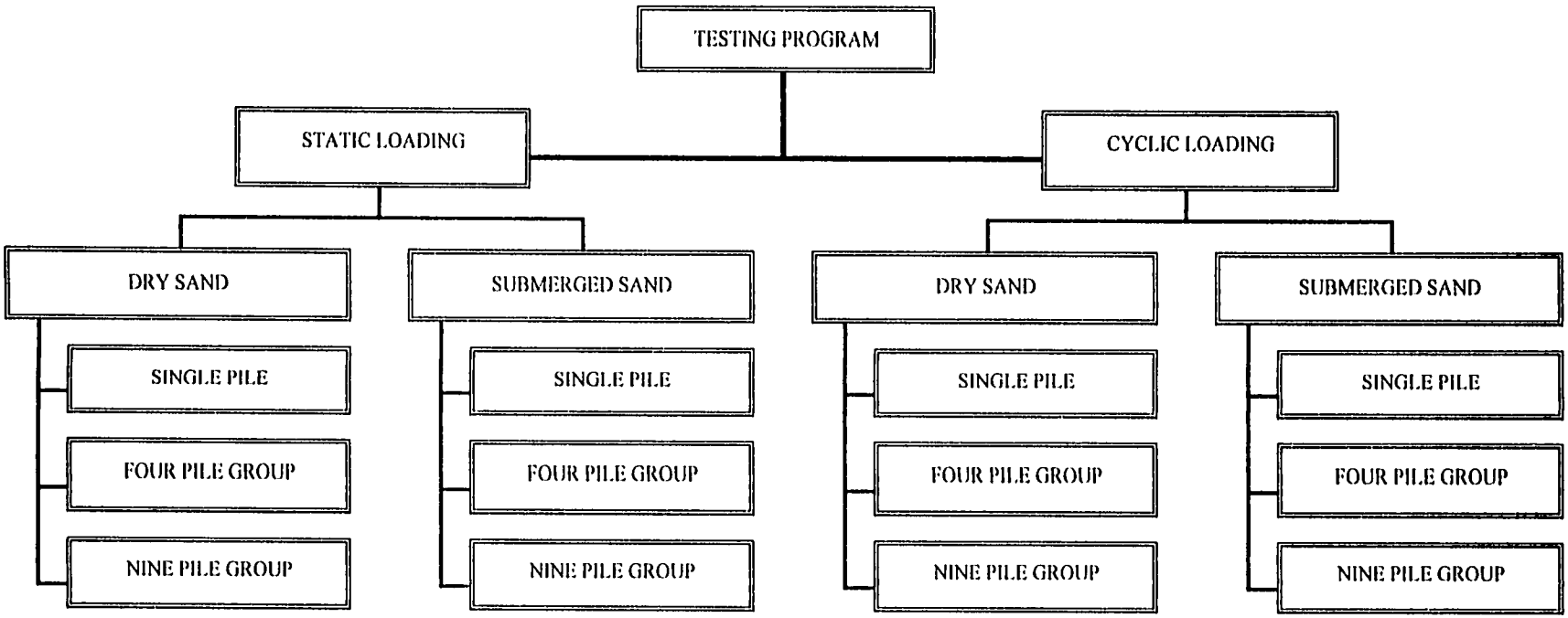

Figure 1.3: Experimental Program

details. In chapter four, the behavior of laterally loaded piles subjected to static lateral load was discussed. First, the analysis methodology used was discussed in details. Then, the discussion included the behavior of single piles, four pile groups and nine pile groups that were embedded in different sand conditions i.e. dry and submerged. Similarly, in chapter five, the behavior of laterally loaded piles subjected to cyclic lateral load was discussed on the same pile groups arrangement discussed in chapter four. Finally, chapter six presents the conclusions drawn out of this research and presented the recommendations for further works on the same topic.

CHAPTER TWO

LITERATURE REVIEW

2.1 Introduction

The fast development of oil investigations and production facilities involves a lot of offshore platforms constructions which are supported by pile foundations. These piles are subjected to lateral loads due to wind and wave action. Therefore, the need to study this pile behavior, in general, leads to the necessity to carry out researches on such type of piles, i.e. laterally loaded piles. Moreover, piles usually exist in form of pile groups. Such researches involved modeling of full scale and small-scale piles testing in the field as well as in the laboratory. This chapter deals with the review of previous work conducted in this area.

2.2 Behavior of Laterally Loaded Piles

2.2.1 General

Laterally loaded piles are considered boundary value problems that require the satisfaction of equilibrium and compatibility conditions. The main problem consists of the prediction of soil properties and pile response. Numbers of proposals have been made in the past to solve and clarify this problem. One proposal is the point of fixity in which the pile is fixed against rotation at some distance below ground line, the distance from the ground surface to the point of fixity is a measure of the strength of the soil (Reese et al, 1984). This method violates the equilibrium and compatibility conditions.

In the design of such pile systems the main engineering concerns is the knowledge of deflection of the pile and bending moment along the pile. The bending moment is required in sizing the pile, while deflection would be important with regard to serviceability of the supported structure (Reese et al, 1984). The complete form of the solution is shown in Figure 2.1, in terms of the deflection y, slope S, bending Moment M, and soil reaction p, as functions of depth. This set of curves is only for one loading level. Therefore, solutions should be worked out for loadings below and above the design loads. This is because of the non-linearity of soil response and properties. These sets of curves can be used to solve the problems associated with serviceability and stability of the pile.

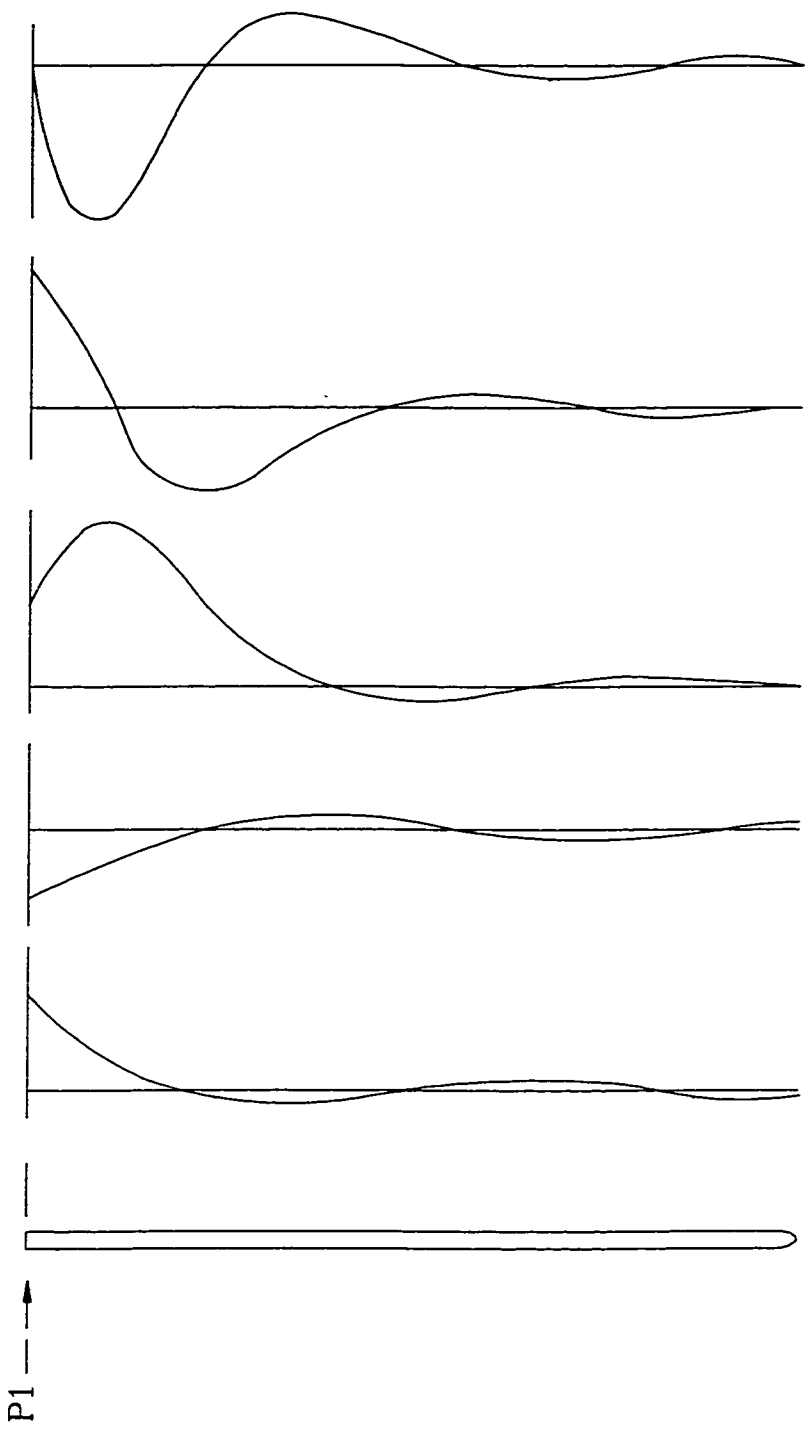

Figure 2.1: The Complete Form of the Solution, (Reese et al 1984).

For the solution of these curves the following well-known fourth order differential equation, which has been suggested by many authors, can be used (Reese 1977):

$$EI\frac{d^4y}{dx^4}+P_x\frac{d^2y}{dx^2}+E_sy=0 \qquad 2.1$$

Where

P_x = Axial load
y = Deflection
x = Length along the pile
E_s = Soil Modulus
EI = Flextural Rigidity of the Pile

The solution of this differential equation can be achieved by satisfying the equilibrium and compatibility conditions. These boundary conditions can be satisfied by using appropriate representation of soil response by selecting a reasonable value of soil modulus. (Reese 1977 and Reese et al 1984).

2.2.2 Method of Presenting the Soil Response and Behavior

The soil response can be described by p-y curve which shows the soil response (p) as a function of deflection (y) at any depth (x) below ground surface. Figure 2.2 presents the idea of the p-y curve. (Shameem 1988 and Reese 1977).

The inter-relation of (p) and (y) is non-linear and depends on many factor, including soil type, depth, pile stiffness, method of installation, type of loading and history of loading

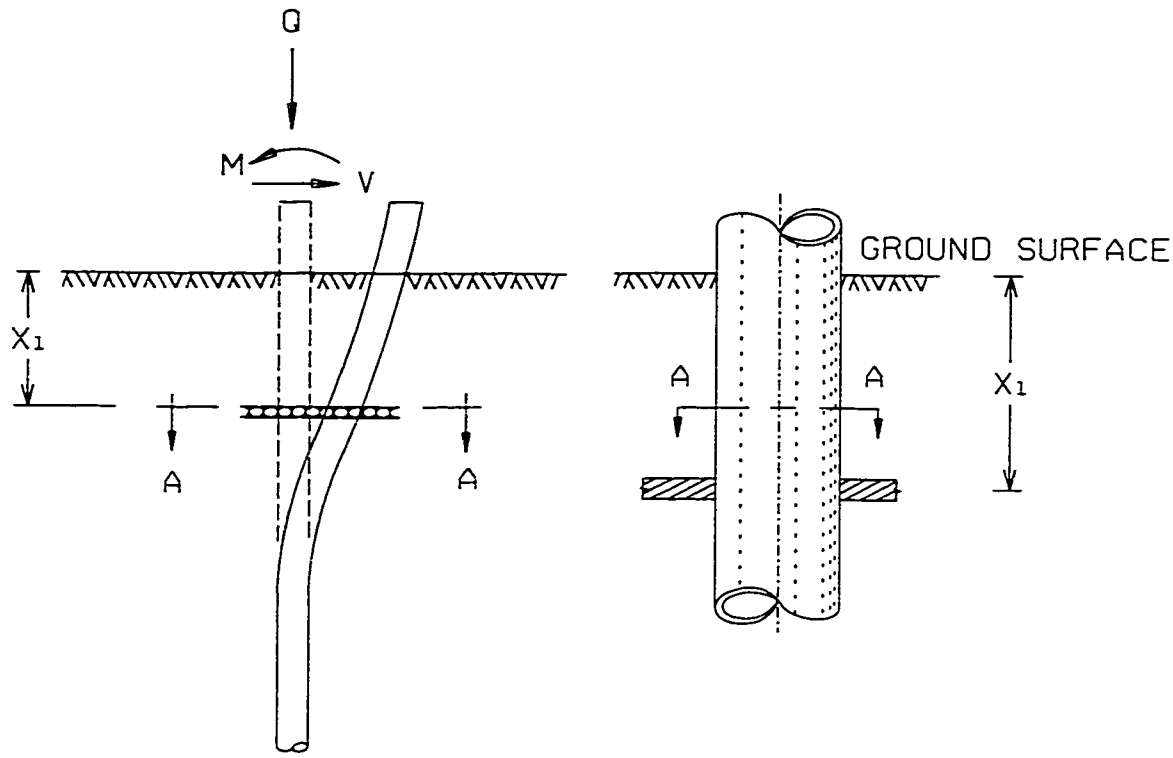

(a) Pile Under General Loading System

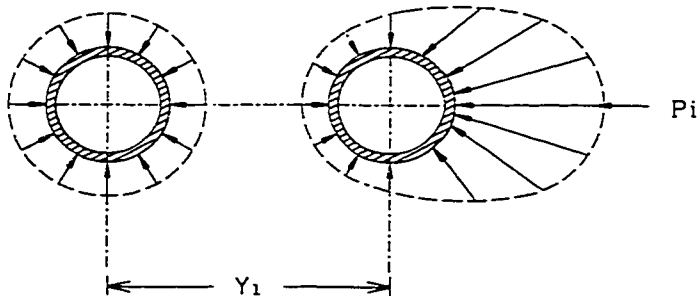

(b) View A-A Earth Pressure Distribution Prior To Lateral Loading

(c) View A-A Earth Pressure Distribution After Lateral Loading

Figure 2.2 : Soil - Pile Interaction; Distribution of p and y, (Shamem,1988).

(Cox 1984 and Reese 1977). However, the modulus of the soil ($E_s = -p/y$) often varies with depth in a linear manner (Reese 1977) .

Figure 2.2 shows a section of pile at a depth x and the soil stress distribution around it. Figure 2.2b represents the earth-pressure distribution after installation and before loading the pile laterally. Figure 2.2c shows the distribution of pressure after loading the pile laterally (assuming the pile was straight during driving and before loading). The deflection y (as shown in Figure 2.2c) generates an unbalanced pressure distribution which yields in unbalanced force p per unit length of the pile.(Reese et al, 1977 and 1984).

A set of p-y curves must be predicted for the solution of the laterally loaded pile at different depths as shown in Figure 2.3 (Reese et al, 1984). If these p-y curves exist, the solution for the differential equation can be found. From the solution of the above differential equation pile deflection, bending moment, shear and soil reaction can be found for any loading level. According to Winkler assumption, the soil reaction at a point is dependent essentially on the pile deflection at that point and not on pile deflection above and below that point. Thus for the purposes of analysis the soil can be removed and replaced by a set of discrete mechanism with load-deflection characteristics of the type shown in Figure 2.3 (Reese et al 1977 and Shameem 1988).

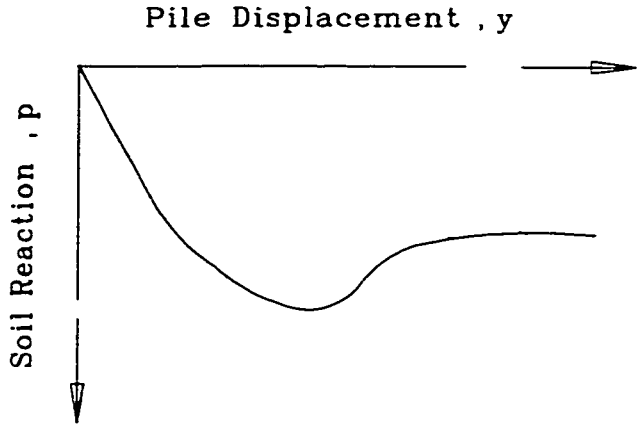

a) Single p - y Curve

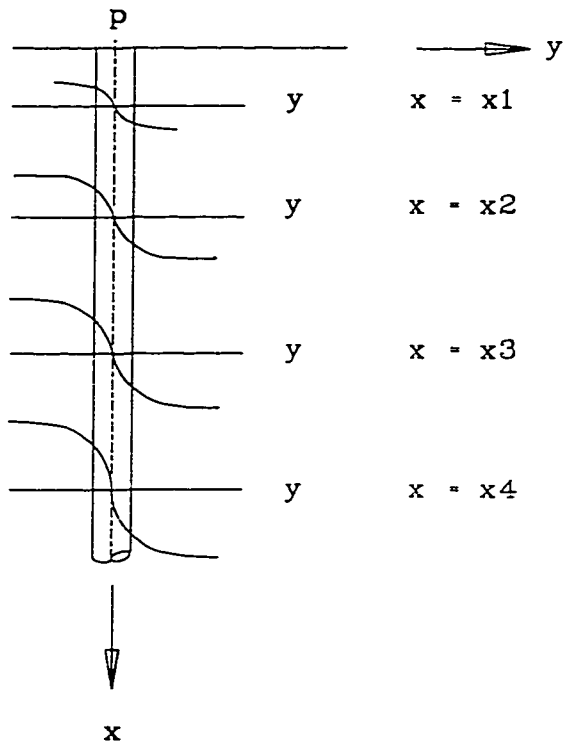

b) Set Of p - y Curves

Figure 2.3: Family of p-y Curves, (Reese et al 1977).

From number of field tests for obtaining the p-y curves, values of p and y points along the pile can be described as:

$$y = \iint \frac{M(x)}{EI} dx^2 \qquad 2.2$$

$$p = \frac{d^2M(x)}{dx^2} \qquad 2.3$$

Theses two equation requires appropriate boundary conditions.

The boundary conditions are as follows:

1. At the top of the pile: depending on the loading at the field.
2. At the bottom there will be zero rotation and deflection: moment is assumed to be zero.
3. The shear is assumed to be zero at the bottom.
4. Horizontal force on the base of pile is considered as horizontal force just above the base, (Reese et al, 1984).

For the calculation of the p-y curves an iterative mathematical procedure is used. This procedure is presented in the following paragraph for the case of static and cyclic laterally-loaded piles embedded in sand. Cox et al (1984) and Reese et al (1984) represent procedure for other piles embedded in various types of soils and for various loading conditions.

2.3 Method of Calculating Empirical p-y Curves for Piles Embedded in Sand

Many procedures were developed to obtain p-y curves which were determined after carrying out a lot of experiments. The experimental data were obtained from tests conducted on model piles in the laboratory and in the field for different loading types and levels.

Cox and McCann (1984) as well as Desai and Reese (1984) are strongly recommending the use of the method developed by Reese et al (1974) for calculating empirical p-y curves. This method is considered to be the most reliable and well established procedure available. The method is capable of establishing the p-y curves for static as well as cyclic loading conditions.

The p-y curves for sand under static and cyclic loadings are four segment curves consisting of three straight lines and one parabolic shape, as shown in figure 2.4. As shown in the figure, a family of p-y curves is needed for analyzing laterally loaded piles. The procedure given below is for development of one of these curves at depth (x).

The step by step procedure is as follows:

1. Determine the angle of friction of the sand, ϕ.

2. Assign the following values:

$$\alpha = \phi/2 \, , \beta = 45 + \phi/2, K_0 = 0.4;$$
$$K_a = \tan^2(45 - \phi/2); \qquad 2.4$$
$$K_p = \tan^2(45 - \phi/2);$$

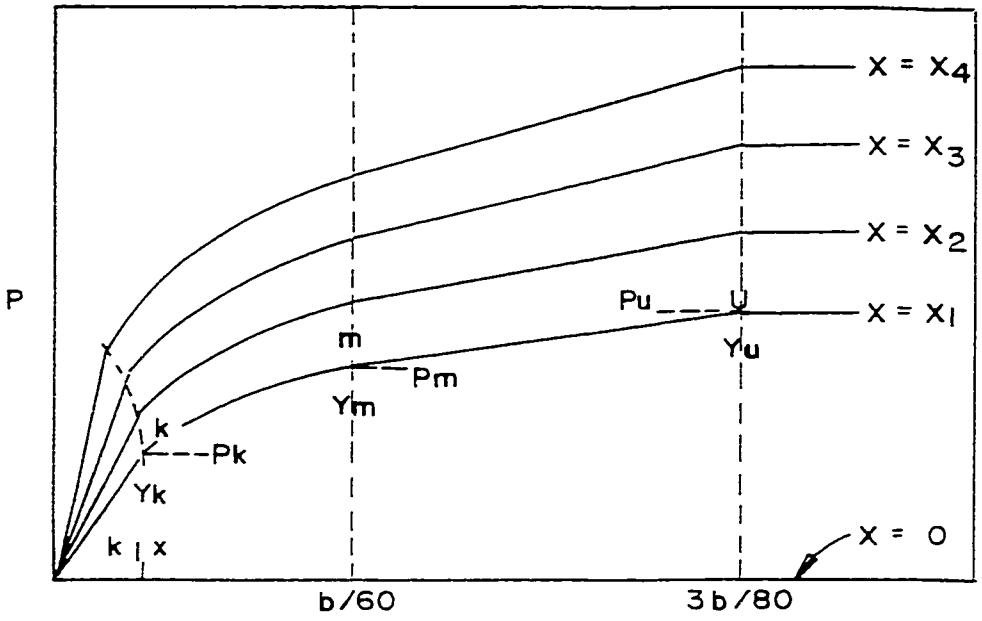

Figure 2.4: Family of p-y Curves for Static and Cyclic Loading in Sand, (Reese 1974).

Where,

K_0 = Earth pressure coefficient at rest,

K_a = Active earth pressure coefficient, and

K_p = Passive earth pressure coefficient.

3. Use the following equation for computing soil resistance:

a. Ultimate resistance near ground surface:

$$p_u = A\,\gamma\,x\,(b\,F_1 + x\,F_2) \qquad 2.5$$

b. Ultimate resistance well below ground surface :

$$p_u = A\,\gamma\,x\;b\,F_3 \qquad 2.6$$

Where, A is a nondimensional coefficient given in figure 2.5a for either the static or cyclic case, and b is the outside diameter of the pile. Also,

$$F_1 = K_p - K_a \qquad 2.7$$

$$F_2 = \tan(45 + \phi/2)\,(F_4 + F_5) \qquad 2.8$$

$$F_3 = K_p^2\,(K_0 \tan\phi + K_p) - K_a \qquad 2.9$$

$$F_4 = (K_p - K_0)\tan\phi/2 \qquad 2.10$$

$$F_5 = K_0\,\tan\phi\,\sin(45 + \phi/2)\,\left(1 + \frac{1}{\cos\phi/2}\right) \qquad 2.11$$

Values of F_1, F_2 and F_3 for different values of ϕ are given in Table 2.1.

4. Find depth x_r where equations 2.5 and 2.6 have equal value. Therefore,

$$x_r = b\left(\frac{F_3 - F_1}{F_2}\right) \qquad 2.12$$

The value of x_r can be determined from the nondiminsional values of x_r/b tabulated in Table 2.1 for values of ϕ.

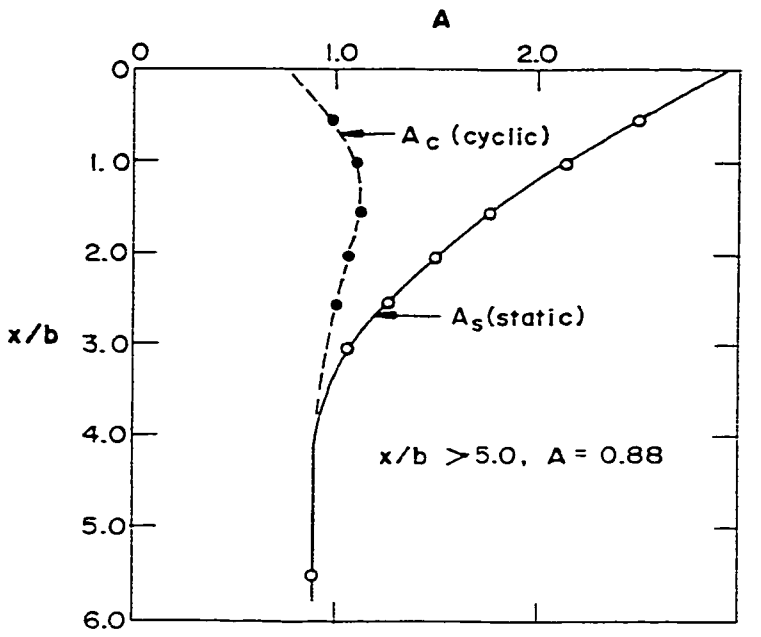

(a) Non-Dimensional Coefficient 'A'

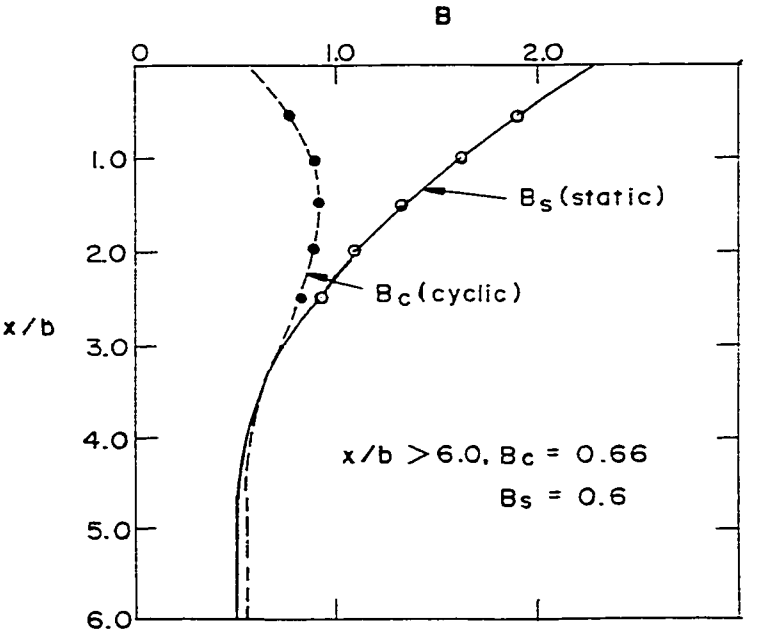

(b) Non-Dimensional Coefficient 'B'

Figure 2.5: Non-Dimensional Coefficient 'A' & 'B', (Reese 1974).

Table 2.1: Coefficient for Ultimate Soil Resistance for Sand, Reese 1974.

ϕ	F_1	F_2	F_3	x_r/b
15	1.1096	0.4454	4.6195	7.881
16	1.1932	0.4982	5.2494	8.142
17	1.2788	0.5553	5.9522	8.417
18	1.3666	0.617	6.7374	8.704
19	1.4567	0.6838	7.6159	9.007
20	1.5493	0.7562	8.6001	9.325
21	1.6447	0.8344	9.7042	9.659
22	1.7430	0.9191	10.9446	10.011
23	1.8445	1.0109	12.3399	10.382
24	1.9495	1.1103	13.9116	10.774
25	2.0581	1.2181	15.6846	11.187
26	2.1706	1.3350	17.6874	11.624
27	2.2874	1.4618	19.9533	12.085
28	2.4088	1.5995	22.5206	12.574
29	2.5351	1.7491	25.4339	13.092
30	2.6667	1.9117	28.7451	13.641
31	2.8039	2.0887	32.5149	14.225
32	2.9473	2.2813	36.8140	14.845
33	3.0973	2.4913	41.7255	15.505
34	3.2544	2.7204	47.347	16.208
35	3.4192	2.9704	53.7935	16.958
36	3.5922	3.2438	61.2007	17.760
37	3.7742	3.5428	69.7295	18.617
38	3.9659	3.8703	79.5711	19.535
39	4.1680	4.2295	90.9533	20.519
40	4.3815	4.6240	104.1481	21.576
41	4.6073	5.0576	119.4823	22.713
42	4.8465	5.5351	137.3486	23.939
43	5.1002	6.0616	158.2214	25.261
44	5.3699	6.6431	182.6759	26.690
45	5.6569	7.2863	211.4116	28.239

Table 2.2: Recommended Values of k_1 for Static and Cyclic Loading, Reese 1974.

RELATIVE DENSITY	k_1 (LB/IN^3) FOR SUBMERGED SAND	k_1 (LB/IN^3) FOR SAND ABOVE WATER TABLE
LOOSE	20	25
MEDIUM	60	90
DENSE	125	225

5. Establish point u such that:

p_u = Equation 2.5 at depths $\leq x_r$

p_u = Equation 2.6 at depths $\geq x_r$

$$y_u = 3b/80. \qquad 2.13$$

6. Establish point m such that:

$$p_m = B\, p_u / A \qquad 2.14$$

$$y_m = b / 60 \qquad 2.15$$

Use the appropriate value of B from figure 2.5b for the particular nondimensional depth and for either the static or cyclic case. Use the appropriate equation of p_u .

7. Establish point k as follows:

$$p_k = k_1 \times y_k \qquad 2.16$$

$$y_k = \left(\frac{p_m}{k_1 \times y_m^{1/n}} \right)^{n/(n-1)} \qquad 2.17$$

where

$$n = \frac{p_m (y_u - y_m)}{y_m (p_u - p_m)} \qquad 2.18$$

Select appropriate value of k_1 from Table 2.2.

8. Compute appropriate number of points on the parabola between k and m from the following formula:

$$p = \left(\frac{p_m}{y_m^{1/n}} \right) y^{1/n} \qquad 2.19$$

9. This completes the development of p-y curve for the desired depth. Since family of these curves is required, any number of curves can be obtained by repeating steps 5 to 8 above for each depth needed.

2.4 Laterally Loaded Single Pile

The prediction of lateral pile response is one of the important considerations in the analysis of offshore pile foundations. This is because soils, in general, have non-homogeneous behavior in nature. Moreover, the behavior of the laterally loaded piles is also non linear which makes the analysis of such a problem even more difficult.

Georgiadis et al (1992) conducted an investigation on the behavior of piles in sand subjected to lateral load. Model piles of three different diameters and flexural stiffness were tested in a centrifuge apparatus to determine prototype pile behavior. The piles were treated as elastic beams on non-linear springs to produce theoretical and numerical analysis of bending moments, deflection and soil response (p-y curves). In the present-day practice, laterally loaded piles are usually analyzed by using the well-known p-y method, that is depending on the beam theory to represent the pile and non-linear springs to represent the soil. During the past years, several researchers have proposed criteria for determining p-y curves. Some of them have used codes of practice such as the American Petroleum Institute (1984). In order to compare the performance of existing p-y relationship for sand, a series prototype-size piles subjected to lateral loads were modeled in a medium-sized centrifugal testing machine. The results of these tests were compared with numerical predictions proposed by Reese et al (1974), Scot (1980), Murchison and O'Neill (1984), and Veritas (1980).

In these tests the experimental setup is shown in Figure 2.6, the angular velocity in all tests was 207 rpm, corresponding to a centrifugal acceleration of 50g at a third of the soil depth.

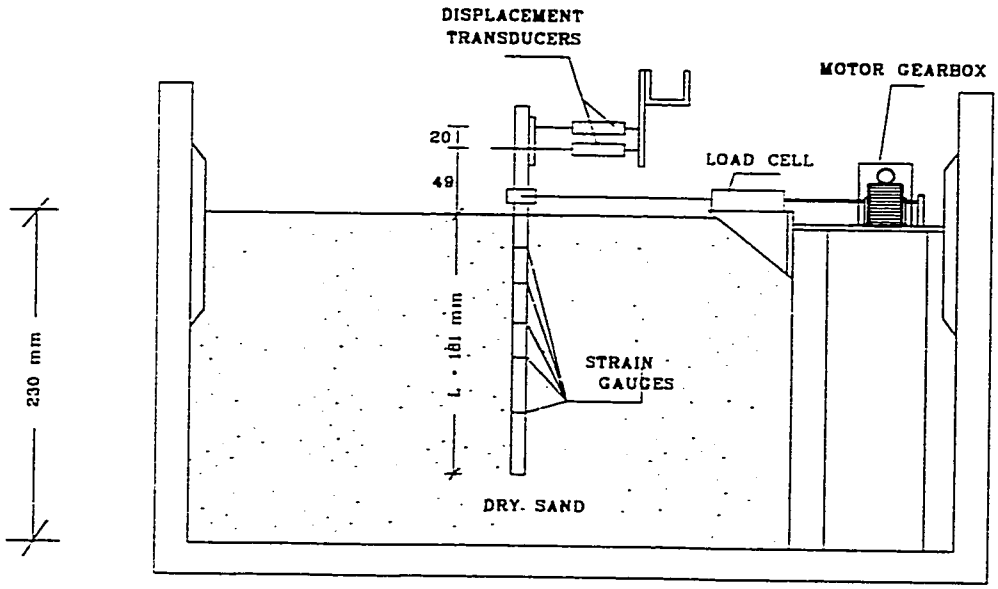

Figure 2.6: Experimental Setup, (Georgiadis et al 1992).

This acceleration resulted in the use of centrifugal scaling factor N=50. The lateral loads were applied to the piles via an aluminum pile cap by gear box motor unit. Typical bending moment diagrams, shear force diagrams, soil reaction diagrams, and deflection of piles are presented in figure 2.7 to figure 2.10, respectively. Points defining p-y curves at several depth are shown in figure 2.11 for two tests, which almost reflect the same results. From their results, it was noted that the p-y curves were sensitive to the value of the soil friction angle ϕ. An increase in ϕ by 2^{o} resulted in an increase of the ultimate soil reaction by 15%. It was concluded that, since the actual pile characteristics (dimensions and flexure stiffness) are used, the validity of the analysis is not affected by the fact that the piles used in the present study were not long piles, where deflections and soil reaction are zero at the pile tip. Moreover, it was clarified that the p-y curves of others (Figure 2.12) underestimated the measured maximum moment as shown in figure 2.13. This is due to the higher initial stiffness recommended in these methods.

A study on laterally loaded single pile model was conducted at King Fahd University of Petroleum & Minerals by Shameem (1988). The tests were carried on small scale model piles embedded in sand in the laboratory to study the effects of various variables on the behavior of the piles. The experimental program consisted of carrying investigations on eleven model piles by varying the following parameters: embedded length to pile diameter ratio, pile diameter to wall thickness ratio, condition of the sand (Dry or Submerged) and loading conditions (static or cyclic). Shameem (1988) concluded the following: First, the small-scale model can be used to explain the behavior of piles subjected to lateral load.

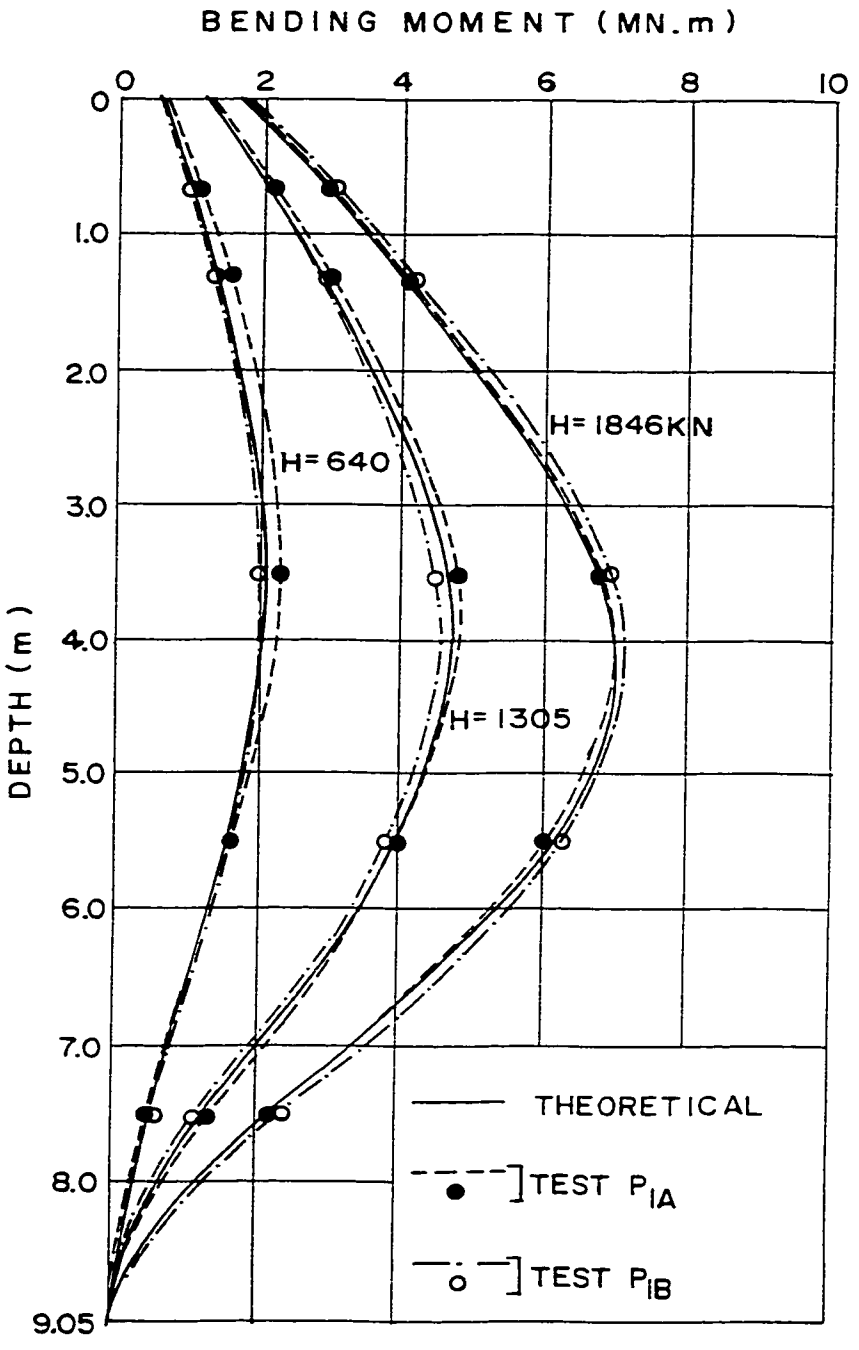

Figure 2.7: Bending Moment Distribution Along the Pile, (Georgiadis et al 1992).

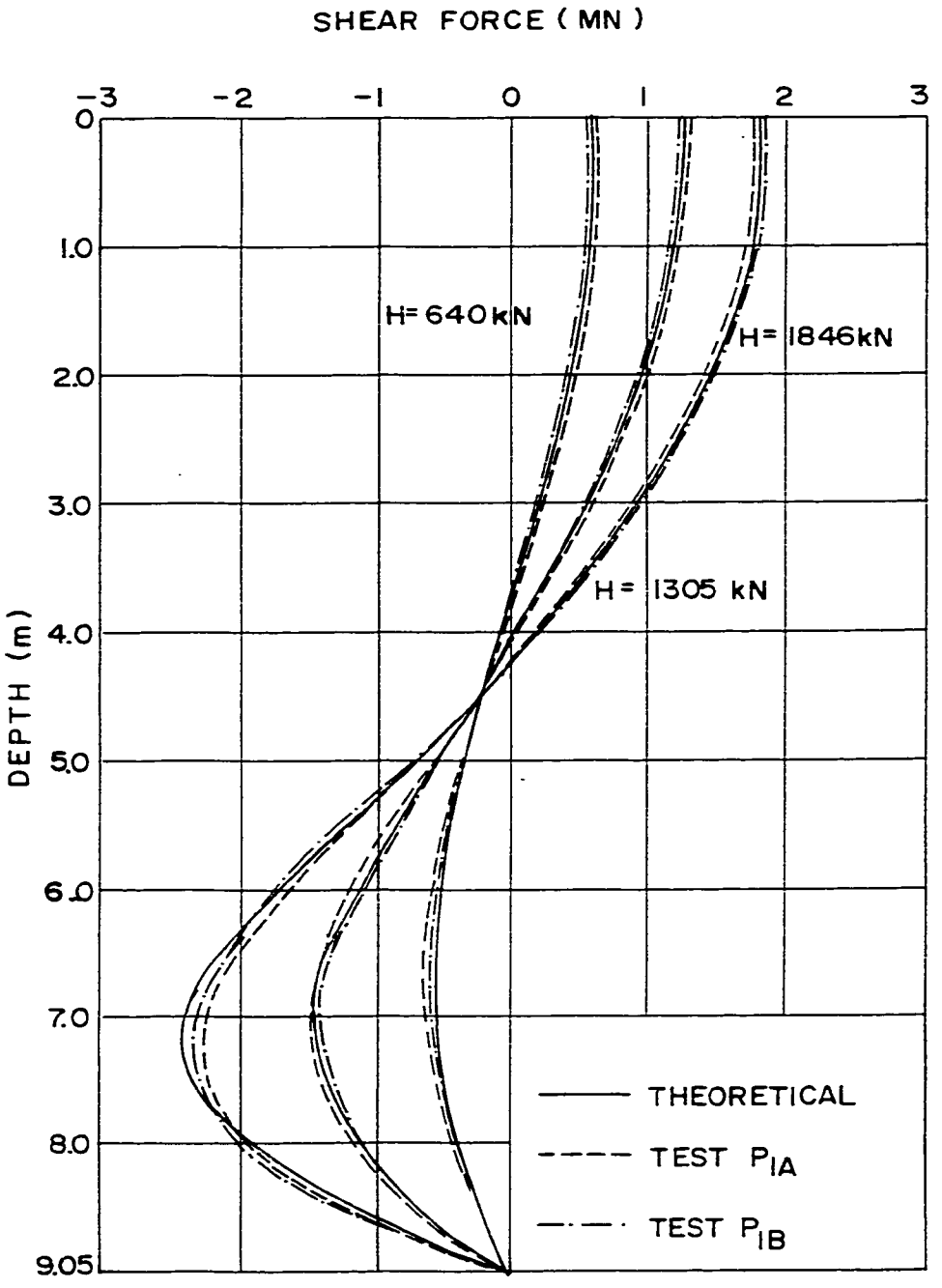

Figure 2.8: Shear Force Distribution Along the Pile, (Georgiadis et al 1992).

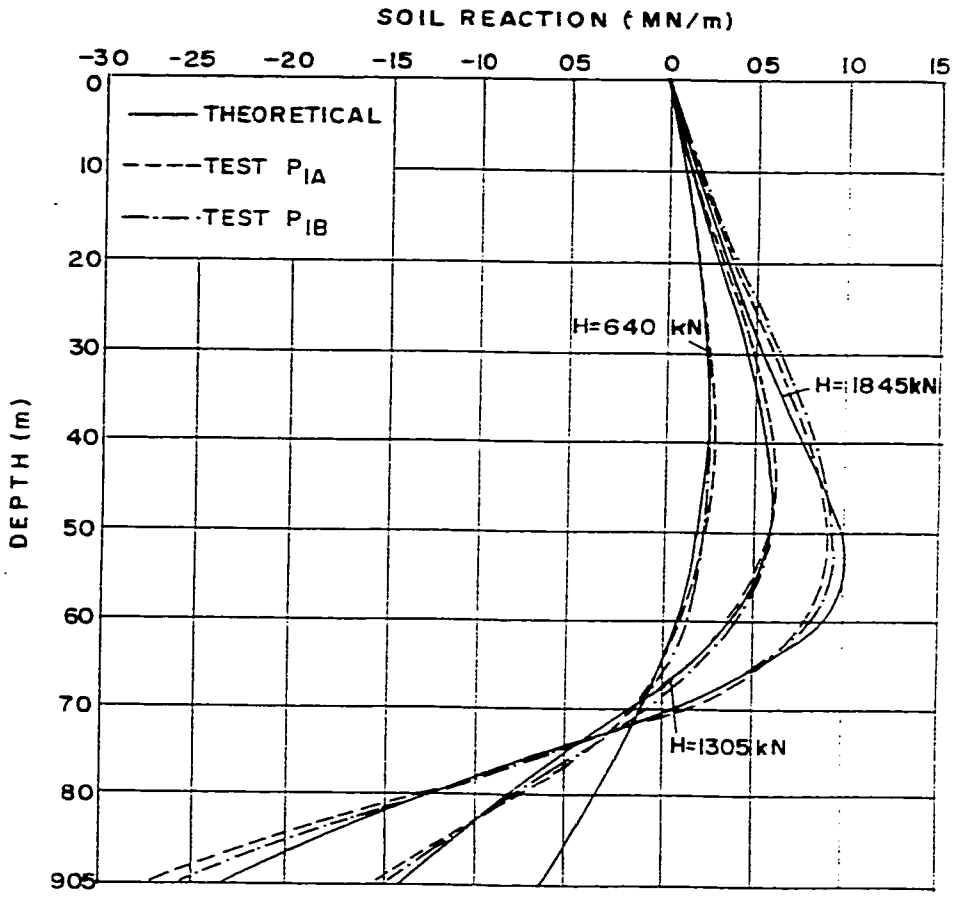

Figure 2.9: Soil Reaction Along the Pile, (Georgiadis et al 1992).

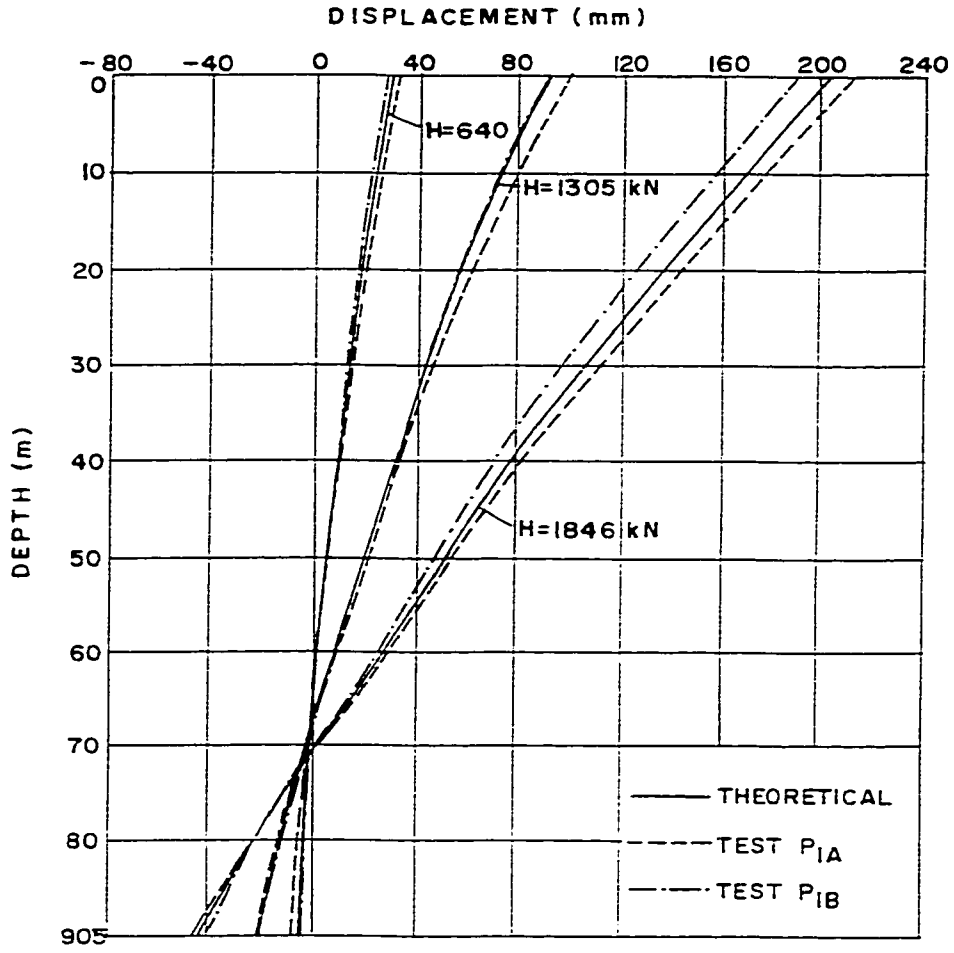

Figure 2.10: Deflection of the Pile, (Georgiadis et al 1992).

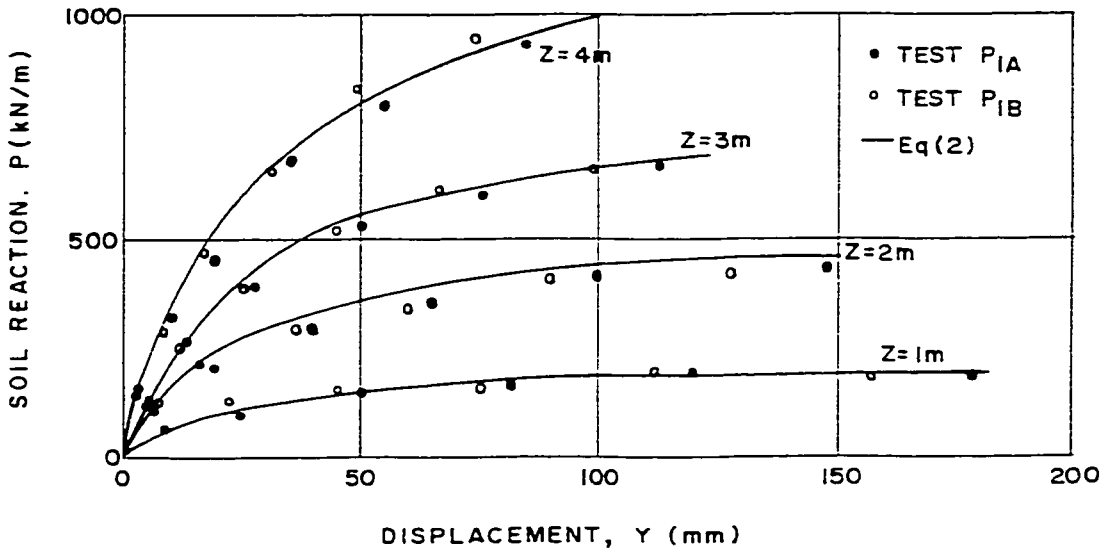

Figure 2.11: The p-y Curves for the Pile, (Georgiadis et al 1992).

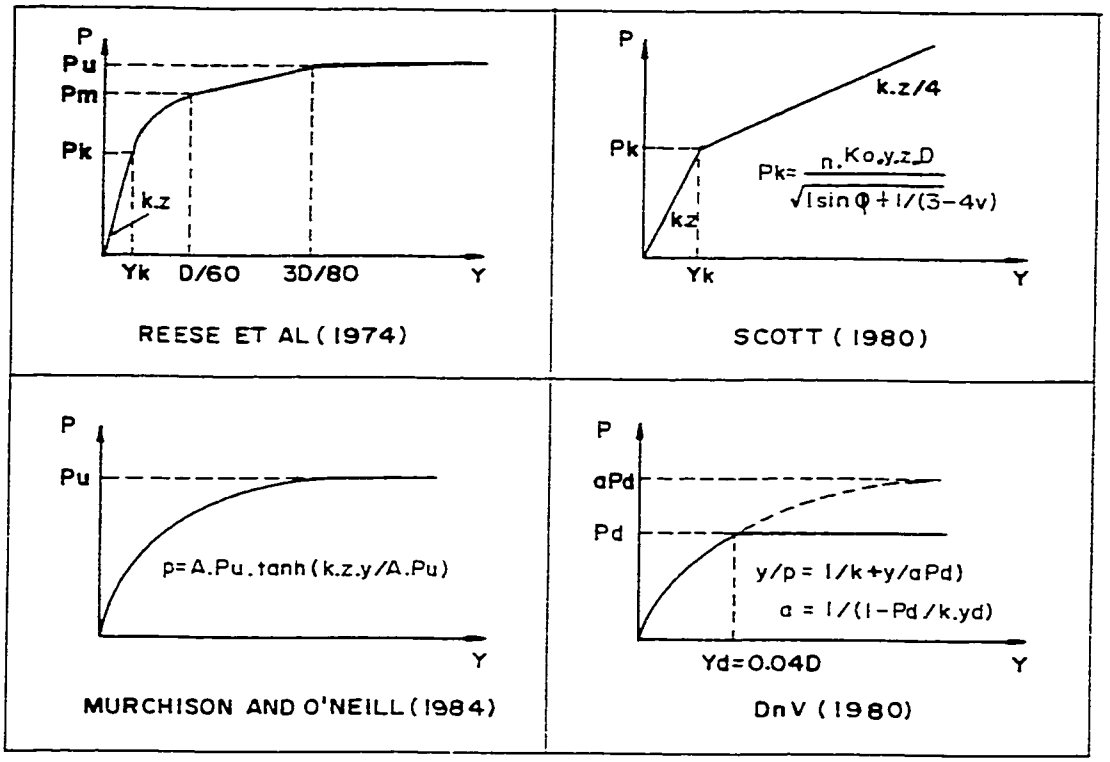

Figure 2.12: Schematic Presentation of Other Load Transfer Relationships for Sand, (Georgiadis et al 1992).

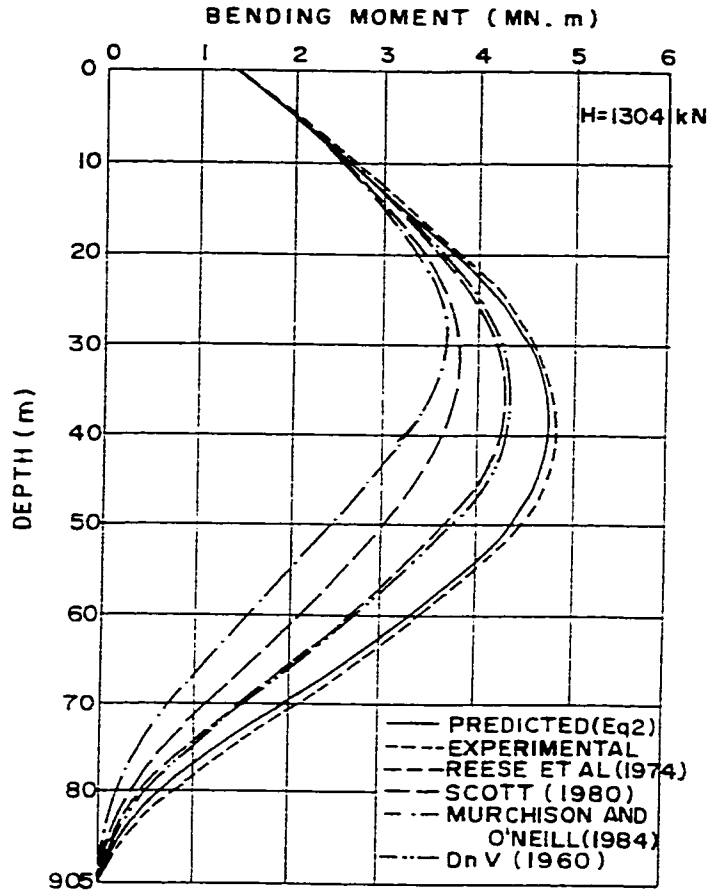

Figure 2.13: Comparison of Predicted and Measured Bending Moment Distributions for the Pile, (Georgiadis et al 1992).

Second, for a given load level, bending moment and deflection along the length of the pile increase with the increase in length/diameter ratio due to larger pile surface contact which increases the soil resistance, while insignificant variations due to changes in diameter/thickness ratio as presented in figures 2.14 and 2.15, respectively. Third, higher bending moments and deflections were found for submerged sand condition when compared with dry sand condition, due to reduction in soil resistance by reducing the effective soil density as shown in figure 2.16. Fourth, experimental p-y curves were less stiff than semi-empirical curves, Figure 2.17. Fifth, the bending moments obtained for peak load decreases slightly upon cycling, while it increase upon cycling for the minimum sustained load and tends to stabilize at large number of cycles, as shown in figure 2.18. Finally, deflection and the bending moment along the pile increase with increasing the number of cycles and stabilize at large number of cycles.

2.5 Laterally Loaded Pile Groups

The previous section discussed the behavior of isolated single piles whereas piles usually exist in groups. The following paragraphs present experiments conducted on closely spaced full size pile group model when subjected to cyclic lateral load.

A full scale testing on model piles was conducted at the University of Texas to study the behavior of a closely spaced pile group when subjected to cyclic lateral loading. These piles were embedded in submerged dense sand. This study was carried out by Brown et al, (1988). The test included large-scale load test of a group of nine (3 x 3) steel piles and an

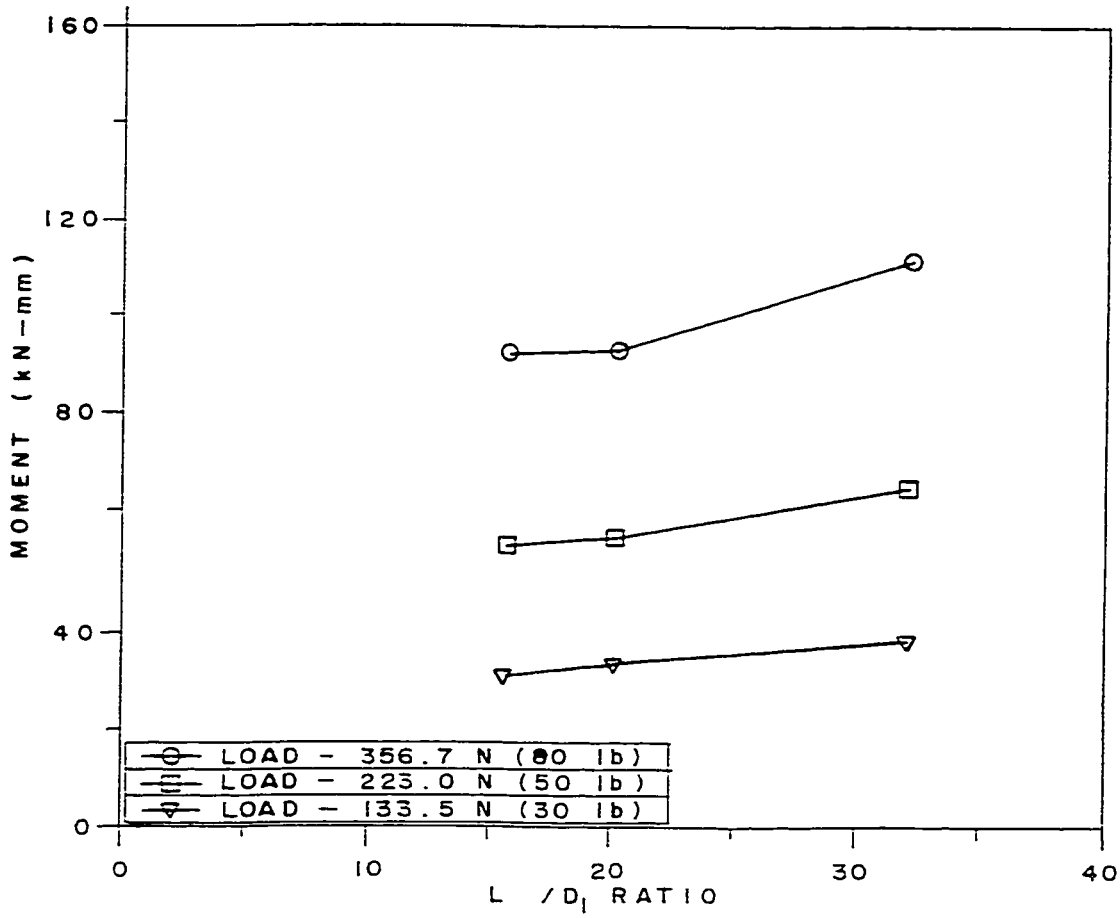

Figure 2.14: Maximum Moment Variation with Length/Diameter Ratio, (Shamem 1988).

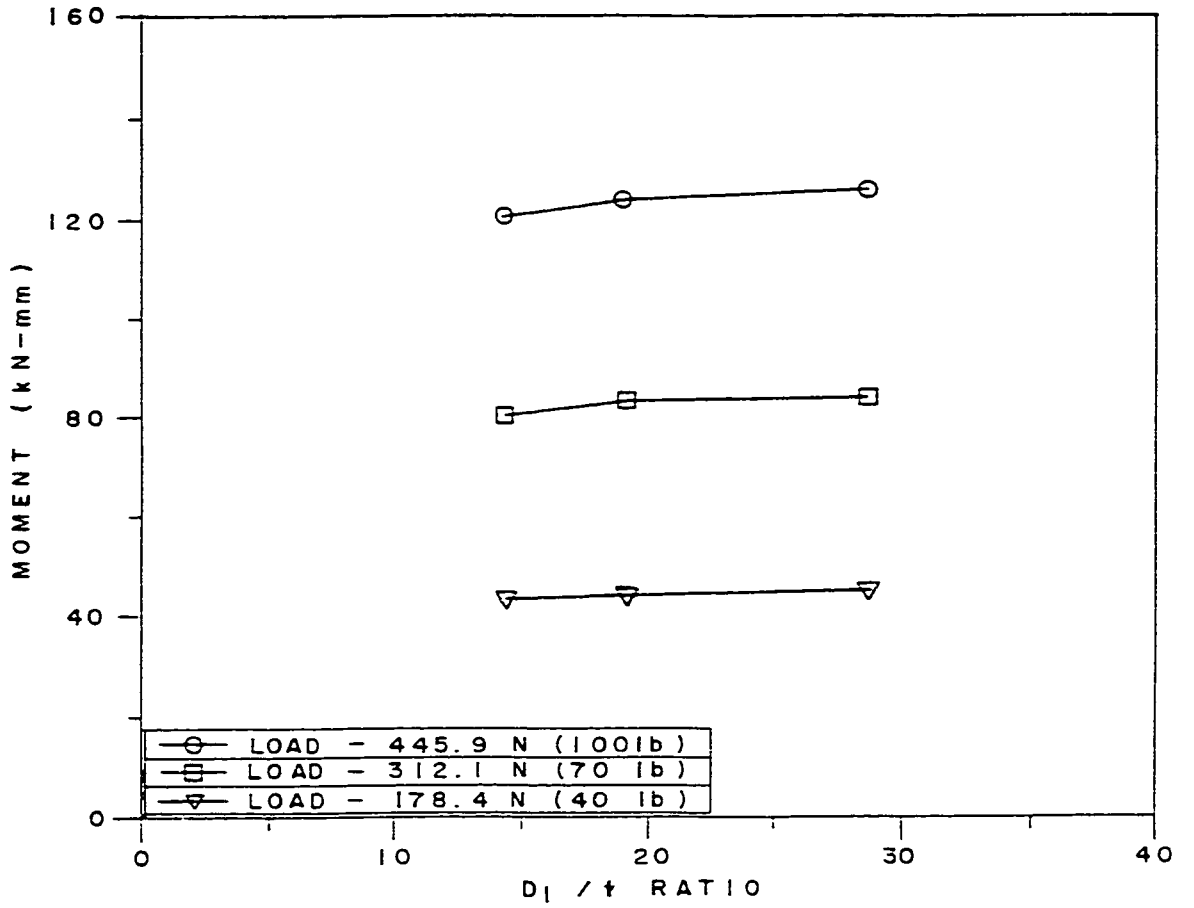

Figure 2.15: Maximum Moment Variation at Different Load Levels with Diameter/Thickness Ratio, (Shamem 1988).

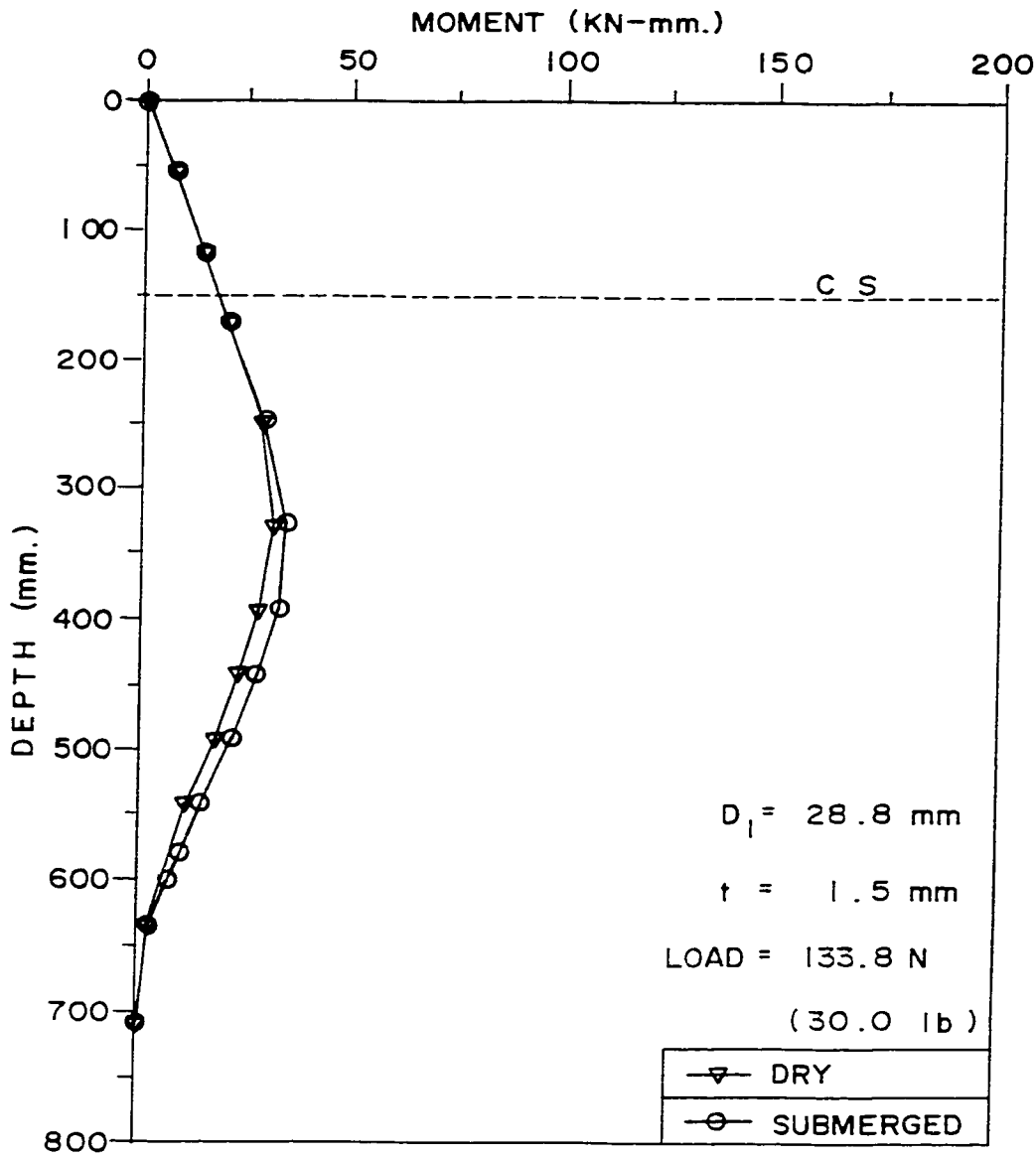

Figure 2.16: Comparison of Bending Moment for Dry and Submerged Sand Conditions, (Shamem 1988).

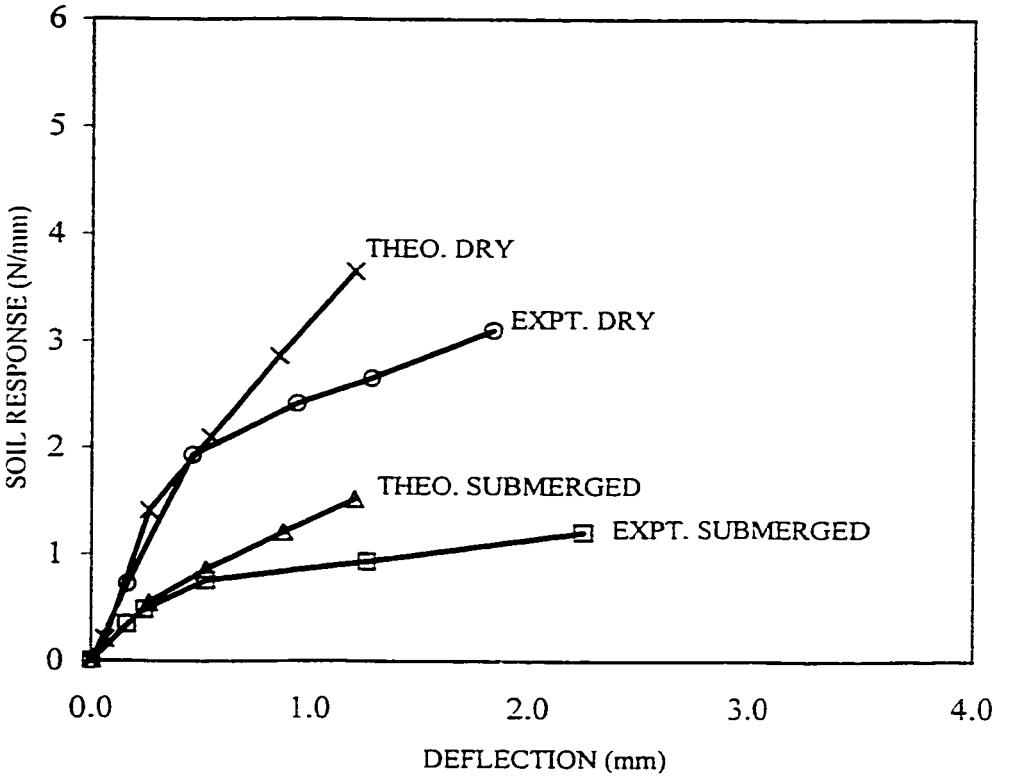

Figure 2.17: Comparison of p-y Curves for Sand at Depth 291mm, (Shamem 1988).

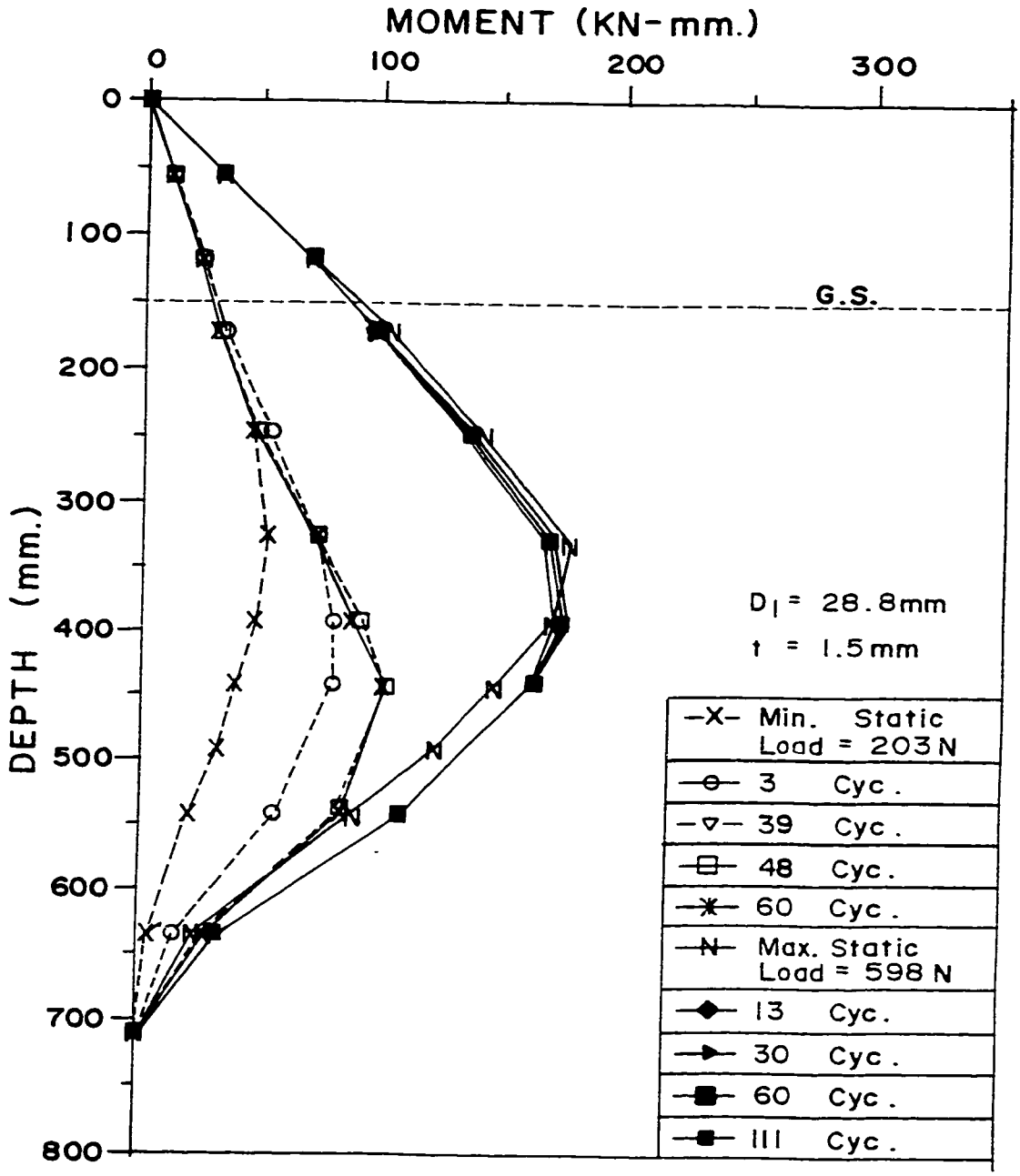

Figure 2.18: Moment Variation Along the Pile Length at Minimum Sustained and Peak Load, (Shamem 1988).

isolated single pile. The soil used was medium to dense saturated sand where the piles were considered fixed at the bottom by very stiff clay layer. Cyclic loading was applied using a computer-driven actuator to produce a sinusoidal curve of pile trend deflection versus time. The deflection was monitored for both directions until 100 - 200 cycle was reached at each load level. The frequency of loading was 0.067 Hz which is 15 seconds period. Figure 2.19 represents the pile head load versus the maximum bending moments for cycle 1 for single pile and pile group. The measured bending moment and the normalized moments are shown in figure 2.20. Finally, out of all the results found in this study, the authors concluded the following:

1. The deflection of pile is greater for the pile group than that for single pile for the same average load per pile.
2. The reduced efficiency of the group under lateral load was due to the effect of "Shadowing". The soil resistance for the piles in the trailing row is greatly reduced due to the influence of the leading row piles on the soil. Slight reduction in soil resistance for the piles in leading row in comparison with the single pile was observed.
3. Bending moment:
    a) Similar behavior for single pile and piles in the leading row.
    b) The maximum moments for the piles in trailing rows occurred at greater depth and were greater in magnitude when normalized by pile head load.
    c) The maximum bending moment occurred in the leading row piles due to greater proportion of load distribution.

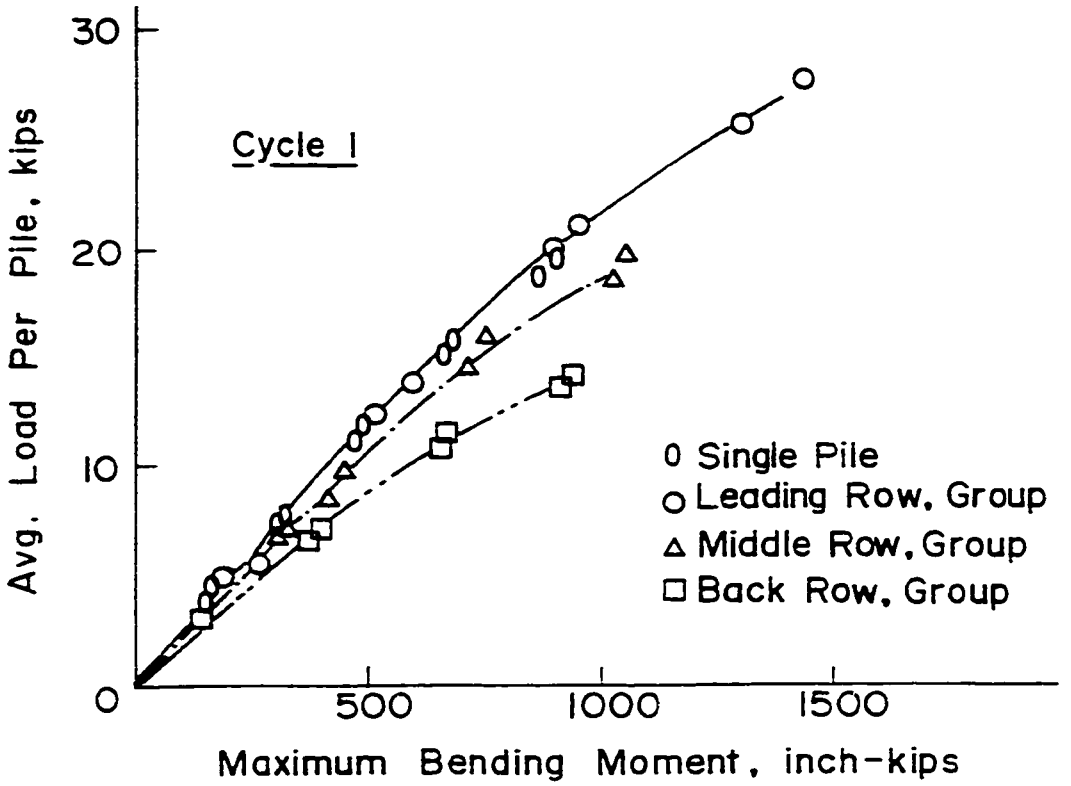

Figure 2.19: Plots of Pile Head Load vs. Maximum Bending Moment for Single Pile and for Pile Group by Row Position, (Brown et al 1988).

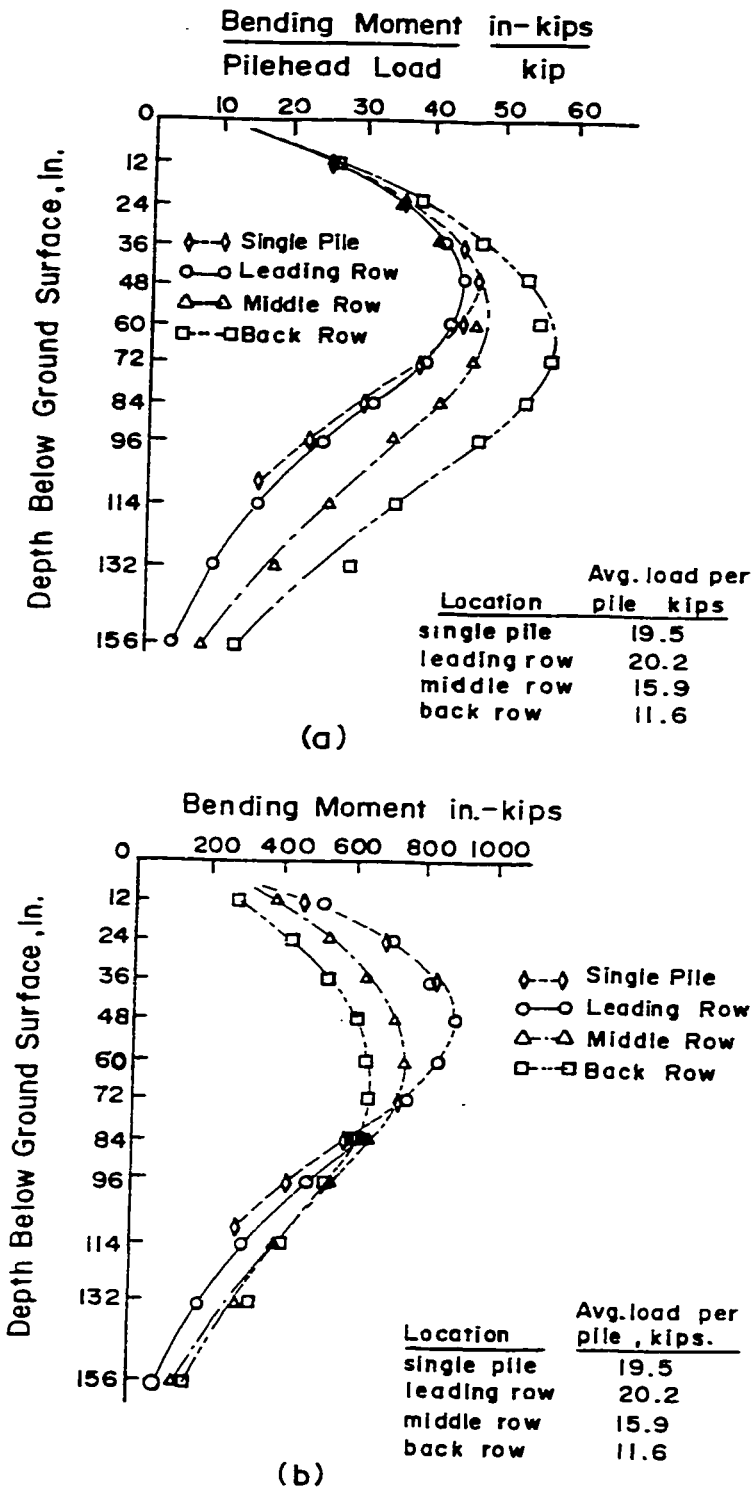

Figure 2.20: Plots of Bending Moment vs. Depth for Single Pile and for Pile Group by Row Position, (Brown et al 1988).

4. Some softening of the response of the piles in the group was observed at large loads; almost no effect occurred at small loads.
5. There is a small loss of soil resistance in the directional cyclic loading due to the significant densification for the soil. Therefore, load history is a very important factor in laterally loaded piles in sand.
6. The design of pile groups for lateral loading is greatly depended on the shadowing effect on the trailing rows. The loss of soil response in the leading row piles is less significant.

Another study conducted by Brown (1989) with slightly different arrangement. In this study the soil condition was fully submerged stiff clay. In addition, he proved that the cyclic loading effects on laterally loaded piles may be accentuated by the group effect.

Brown (1989) summarized the results into two main effects, namely group effects and cyclic loading effect. First, the overall grouping factor has the following influences on the pile group:

1. The deflection of the group was significantly greater than that of the single pile under a load equal to the average load per pile.
2. The bending moments in the piles in the group were greater than those of the single pile.
3. The maximum moments were shifted deeper in the pile group, specially for the piles in trailer rows.
4. The largest proportion of the distributed group load was for the piles in the leading rows.

5. The variations of load and moments within the group were more significant with increasing the load level.
6. The reduced load to the piles in the trailing rows was associated with reduction in the maximum soil resistance which was due to shadowing as resulted from experimental p-y curves.

Second, the influence of cyclic loading on pile response are presented below:

1. The load distribution is governed by the row position only.
2. Figures 2.21 presents the variations in bending moment distribution, which is normalized by pile head load, for piles in the first row with reference to depth and number of cycles. The figures show a relative increase in the bending moment with increase in number of cycles. Moreover, moments increased by significantly greater amount in the pile group than the single pile. Also, the effect of cyclic loading appears to be more significant on the trailing row piles than in the front row.
3. The soil resistance is presented in figures 2.22a, b & c. The figures clearly show that the soil resistance for the front row piles were significantly greater than the one in the trailing rows. Similar trends for each row for the significant decline in soil resistance at the upper part of pile, and this decline continued for 200 cycles. In addition, the reduction in the soil resistance is more significant in the leading row piles.
4. The cyclic loading effect is more significant when the soil resistance exceeds half the maximum value. Moreover, the soil resistance values continue to decline with increasing number of cycles.

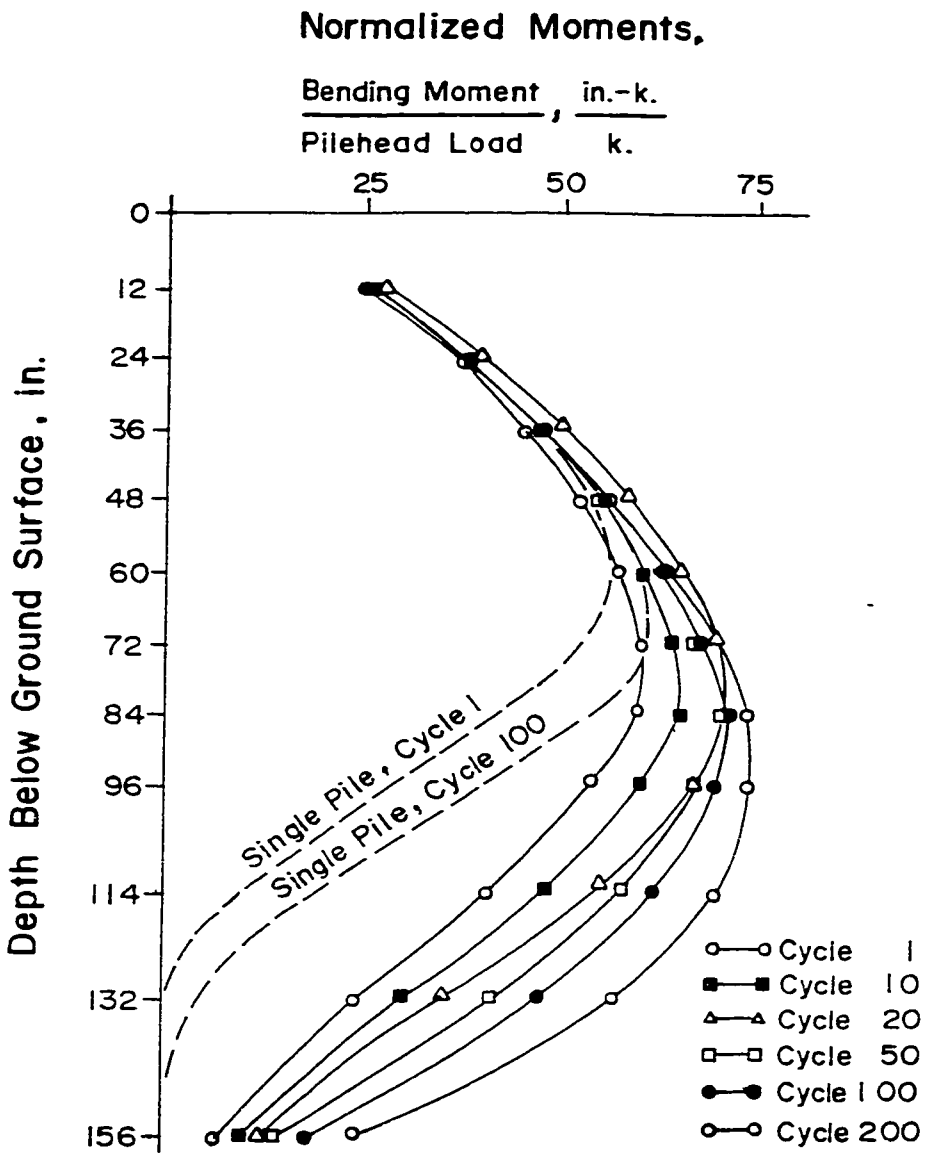

Figure 2.21a: Normalized Bending Moment Distribution Along the Pile for Front Row Pile, (Brown et al 1989).

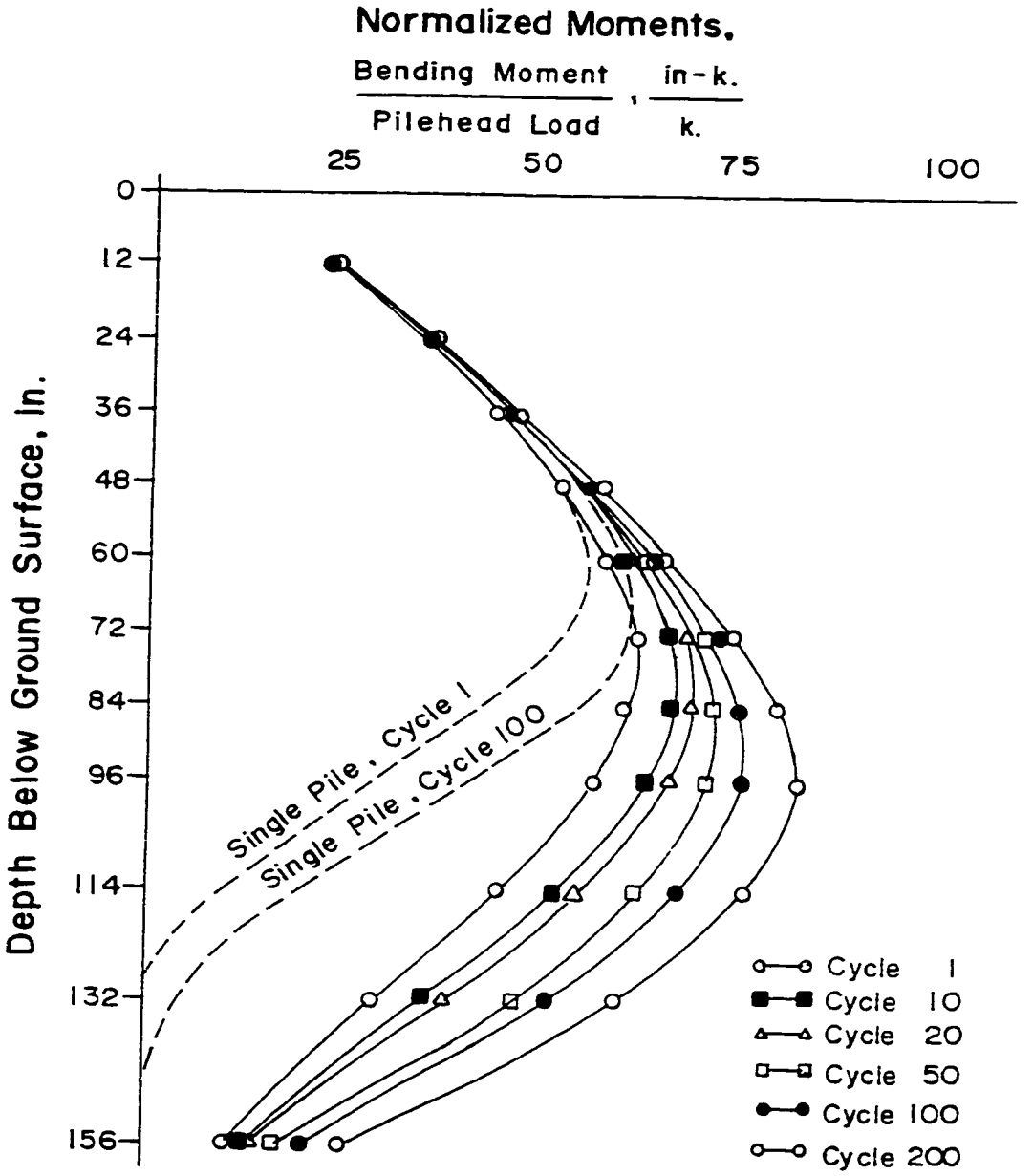

Figure 2.21b: Normalized Bending Moment Distribution Along the Pile for Middle Row Pile, (Brown et al 1989).

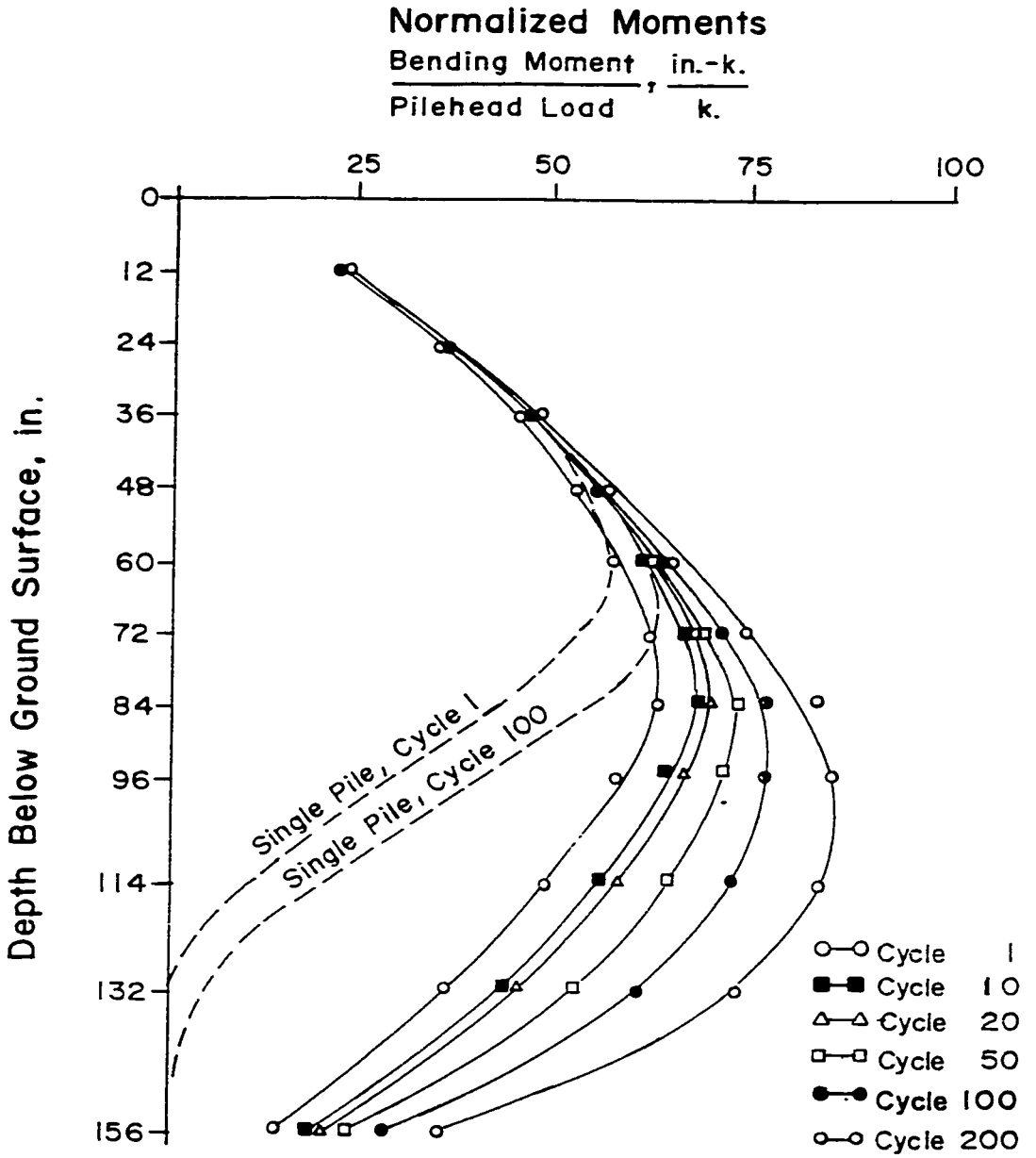

Figure 2.21c: Normalized Bending Moment Distribution Along the Pile for Back Row Pile, (Brown et al 1989).

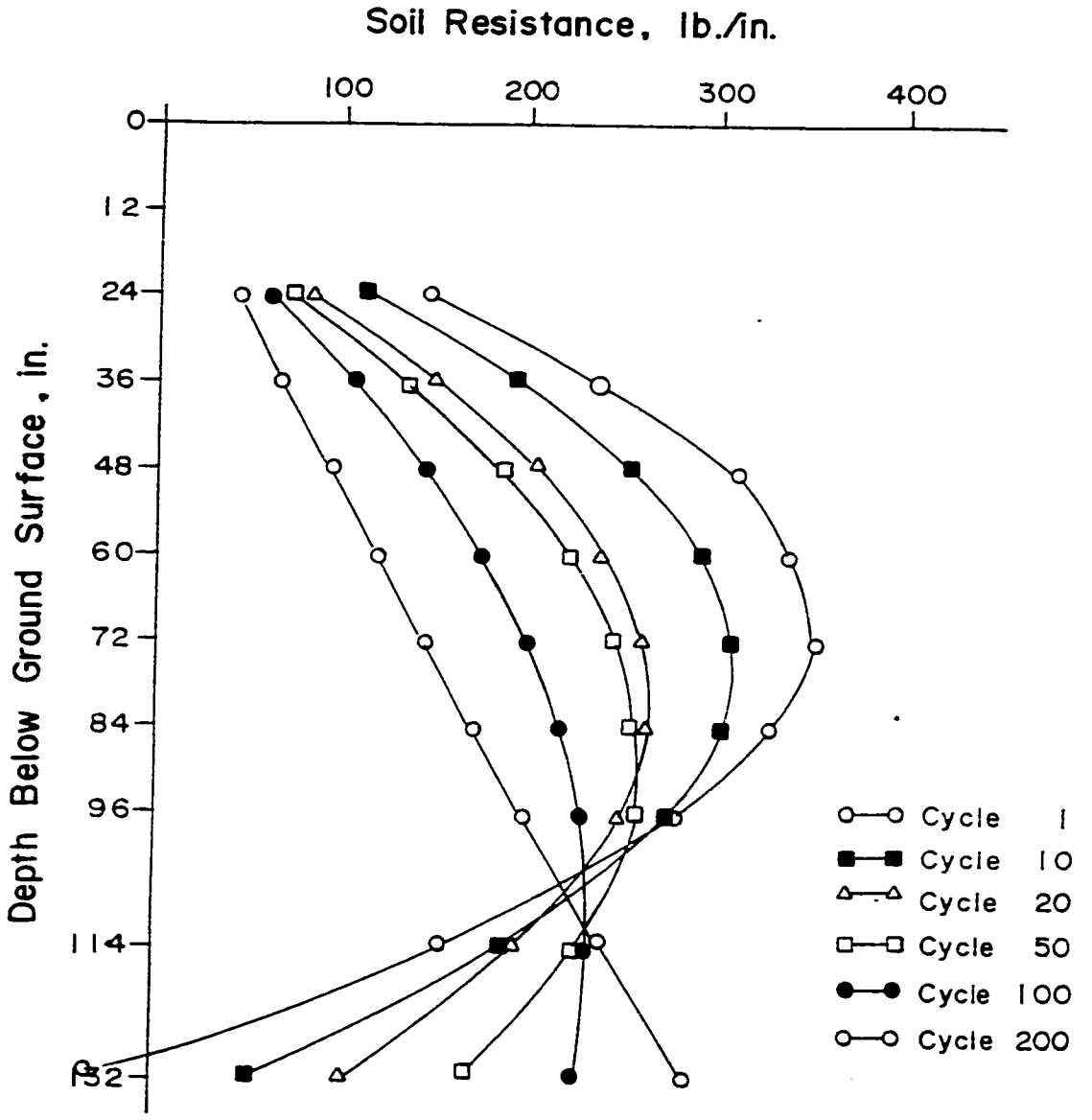

Figure 2.22a: Soil Resistance Along the Pile for Front Row Pile, (Brown et al 1989).

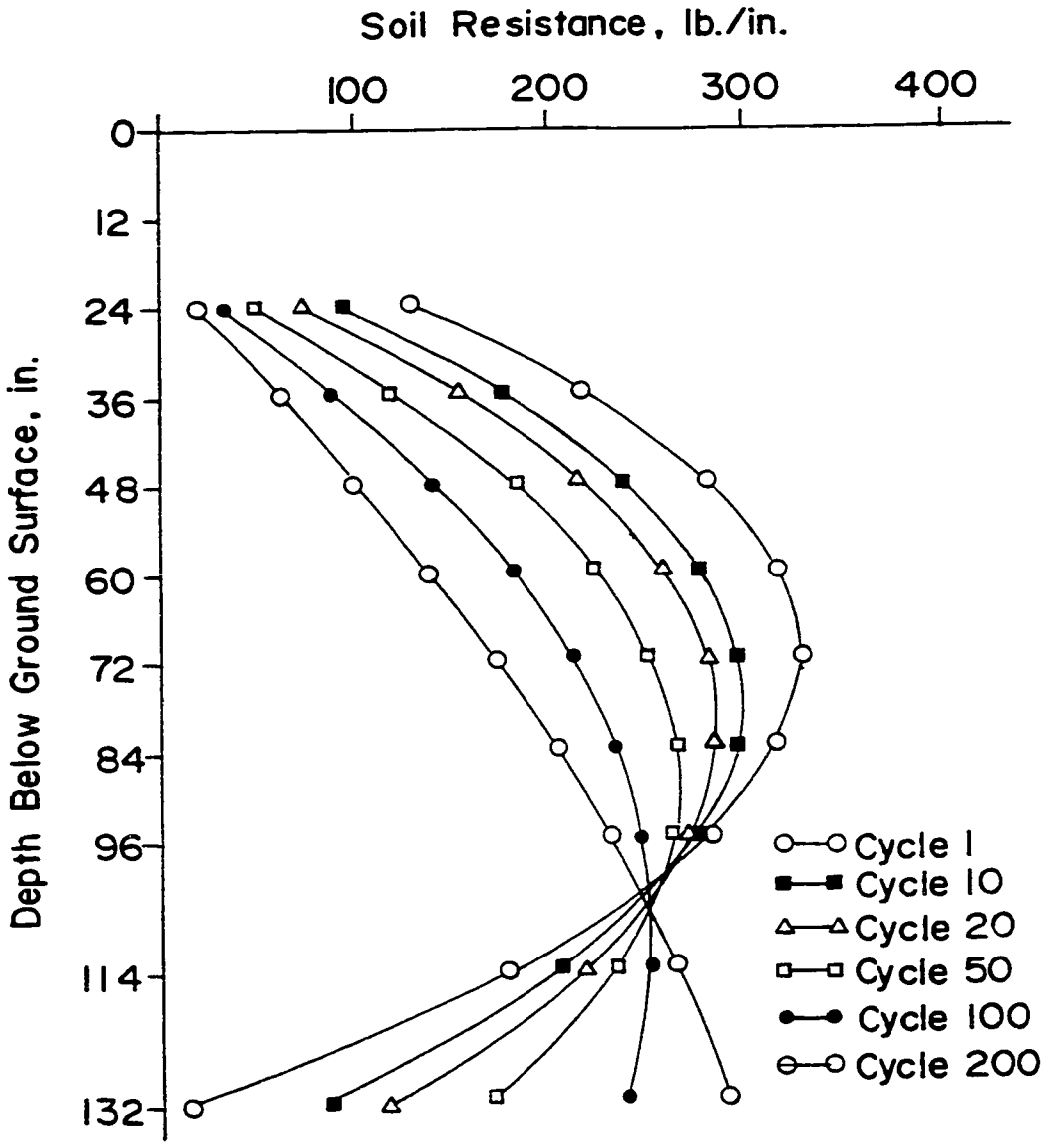

Figure 2.22b: Soil Resistance Along the Pile for Middle Row Pile, (Brown et al 1989).

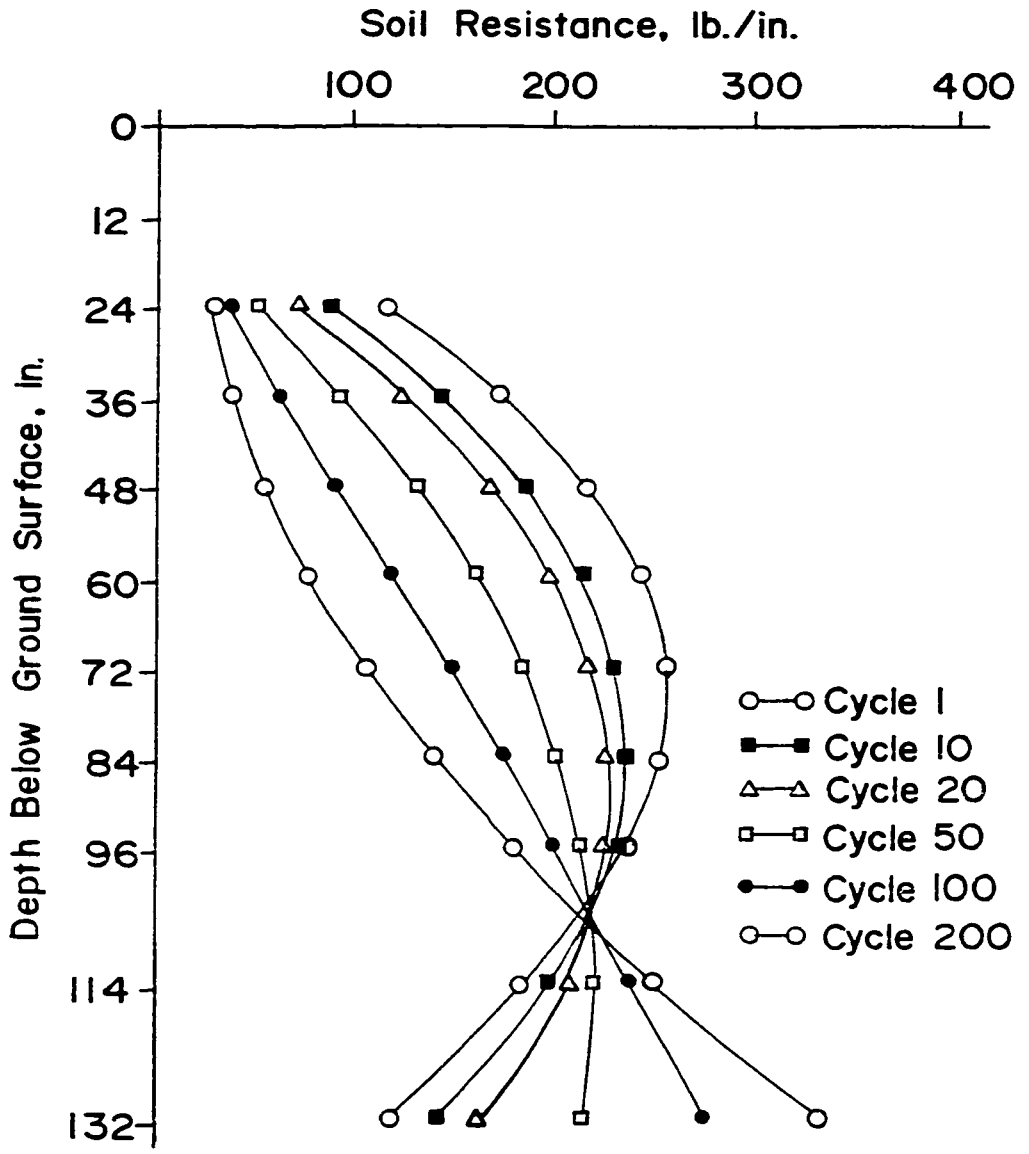

Figure 2.22c: Soil Resistance Along the Pile for Back Row Pile, (Brown et al 1989).

In short, Brown (1989) concluded that the increased load in the group relative to single pile, and the reduced load distribution to the piles in trailing rows have contributed to the shadowing effects as found by Reese et al (1988) above. Furthermore, since the group effects increased the deflections for a given loading, the effect of cyclic loading on the pile response was more significant.

CHAPTER THREE

EXPERIMENTAL PROGRAM AND MATERIAL CHARACTARISTICS

3.1 Introduction

To study the behavior of laterally loaded pile groups, model piles instrumented with strain gages along the pile are placed into a test tank, which is later filled with sand. These piles are fixed at the bottom by means of a bottom cap and hinged at the top by a top cap to produce uniform pile group movement. These caps can be used for single pile, a group of four pile and a group of nine pile. The top cap is hinged to a loading actuator which can apply static and cyclic loading. This actuator is fabricated in order to apply fully reversible cyclic loading. Deflections at the top of piles are measured by means of Linear Variation Displacement Transducers (LVDT's). During loading, a high speed logging system controlled by a personal computer is used to record readings from the strain gages, deflections, and loading level. In the case of submerged tests, an adjacent water tank connected to the test tank through plastic pipes is used in order to slowly flood the sand. This chapter discusses in details the materials, equipment, experimental procedure, and program set-up used in this study.

3.2 Small Scale Model Development

The model developed in this study is identical to the one used by Brown et al (1988) mentioned earlier in chapter two but at smaller size setup. Brown et al (1988) model consist of large scale testing setup. This setup consist of steel pipes with length embedded in sand slightly more than ten times the external pipe diameter. The sand depth was extended to such depth in order that the response of the piles to lateral loading is dominated by the sand only and not disturbed by the stiff clay layer at the bottom of the pile.

The small scale model developed for this study was based on the same concept of producing pile behavior dominated by the sand layer only. Therefore, 40mm diameter aluminum pipes were used to represent the pile in order to obtain a similar behavior because the aluminum pile is more flexible if compared to the steel pipes at such small scale model. The length of the pile embedded in the sand layer was maintained to be slightly more that ten times the outside diameter of the pile i.e. 440mm. Several trials on this model were carried out at the initial stages of the research until this model was finally developed and adopted. These trails were implemented on different pile diameter, pile length, loading actuator, loading pattern, pile caps and pile bottom cap location. The following paragraphs discussed in details the properties of materials used, the model mechanism and the experimental setup.

3.3 Materials

In this research, the materials used were as follows:

i) Fine dune sand for soil, and

ii) Aluminum pipes for piles.

3.3.1 Sand

The sand used was brought from the sand dune at the King Fahd University of Petroleum and Minerals (KFUPM) Beach. To determine the properties of the sand the following tests were carried out:

a) Sieve Analysis to determine the grain size distribution according to ASTM D421-58 & D422-63 as shown in figure 3.1.

b) Relative Dry Density of the sand was determined from maximum and minimum dry densities according to ASTM D2049-69.

c) Direct Shear Test to determine the shear strength parameters namely: angle of internal friction (ϕ) and cohesion (C) as shown in figure 3.2.

A summary of Sand properties is shown in table 3.1.

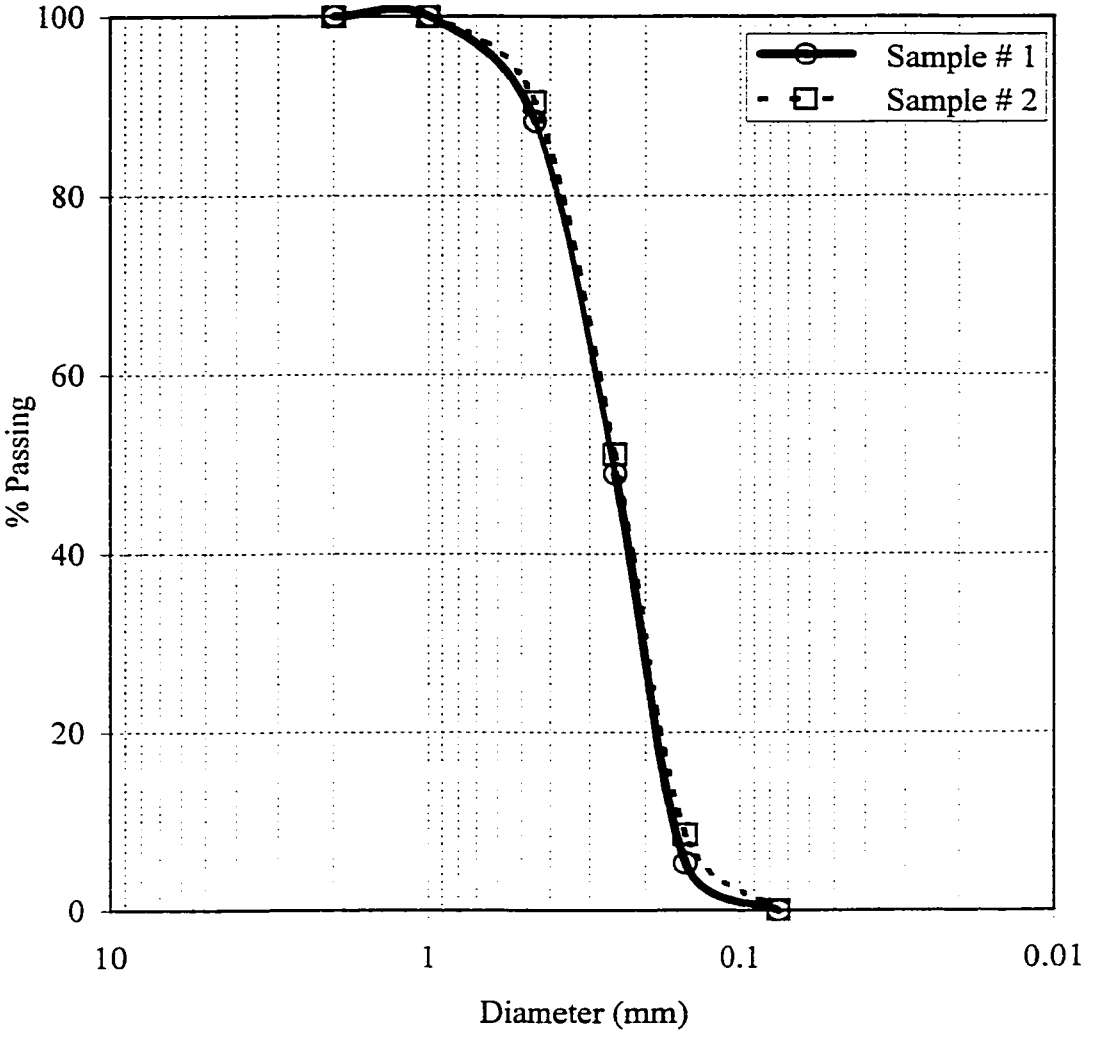

Figure 3.1: Sand Grain Size Distribution

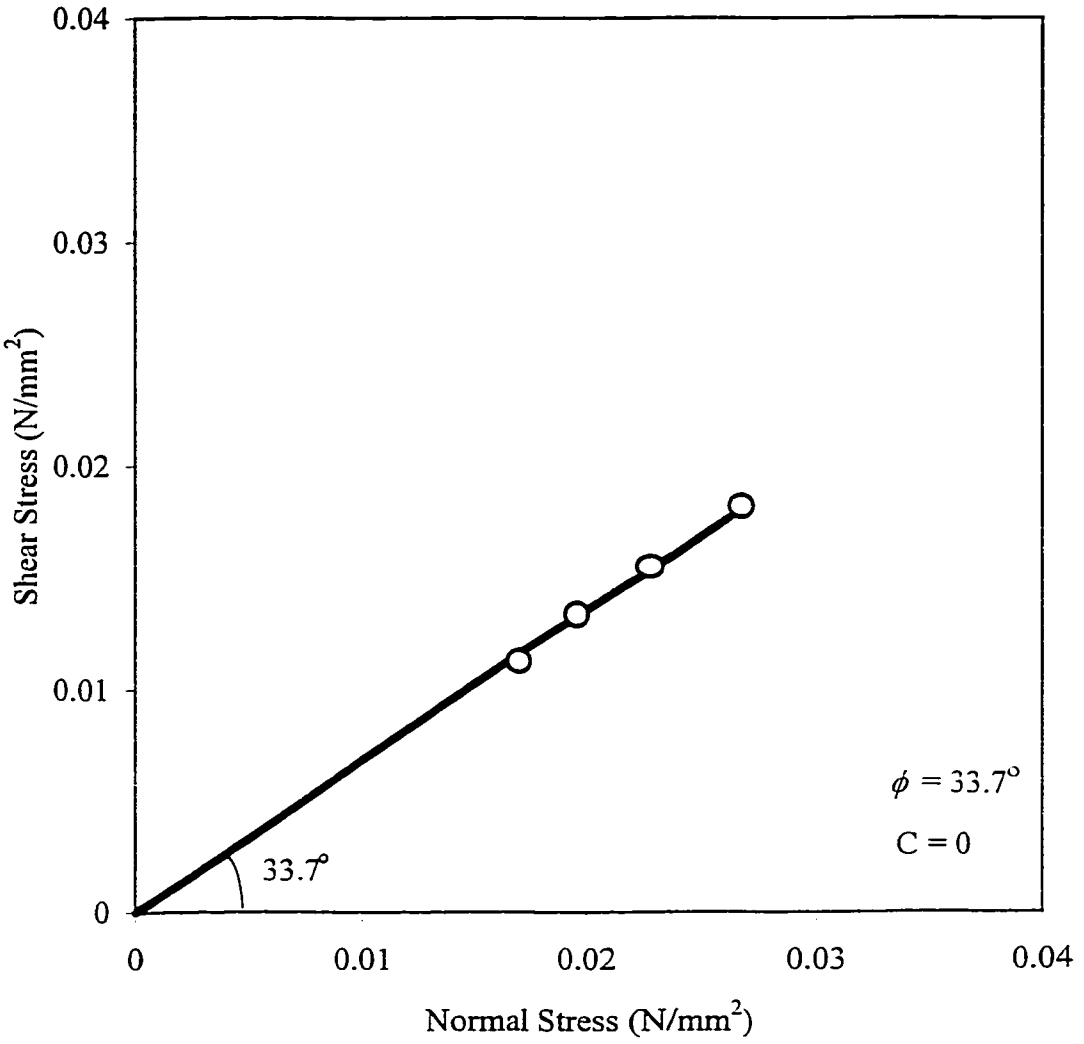

Figure 3.2: Angle of Internal Friction Based on the Direct Shear Test

Table 3.1 SUMMARY OF TEST RESULTS FOR SAND

Maximum Dry Density (KN/m^3)	17.71
Minimum Dry Density (KN/m^3)	14.73
Used Measured Density (KN/m^3) (At the Beginning of the Experiment)	16.71
Used Relative Density (%)	73.4
D_{10} (mm)	0.15
Uniformity Coefficient $C_u = D_{60} / D_{10}$	1.73
Coefficient of Curvature $C_c = D_{30}^2 / (D_{10} * D_{60})$	1.03
Angle of Internal Friction (ϕ)	33.7°
Cohesion (C) (KN/mm^2)	0.0

3.3.2 Aluminum Pipes

Aluminum pipes were used to represent the small scale testing piles for both single and pile groups. These pipes have an outer diameter of 40mm, an inner diameter of 36mm and were prepared and cut to the required length (i.e. 750mm) at the Civil Engineering Lab. Tensile tests were conducted on a sample of these pipes according to ASTM-A370 to determine the Modulus of Elasticity (E), which is required for the analysis of the pile behavior. Special metal plugs were used to prevent the pipe from crushing under the force of testing machine jaws during tensile testing. These plugs were inserted inside the specimen from both sides leaving a middle gap between them to measure the pipe elongation (gage length) according to ASTM requirements as shown in figure 3.3. A strain gage was fixed at the outer surface of the specimen to measure the elongation. The gage length used in the test was 40mm. The load and the elongation were recorded by data logger until the specimen fractured. Figure 3.4 shows the stress-strain curve obtained from these tests and a summary of mechanical properties.

3.4 Experimental Set-up

3.4.1 Introduction

The required testing set-up for this research consisted of the following:

a) Test Tank

b) Flooding Tank

c) Sand Laying Machine

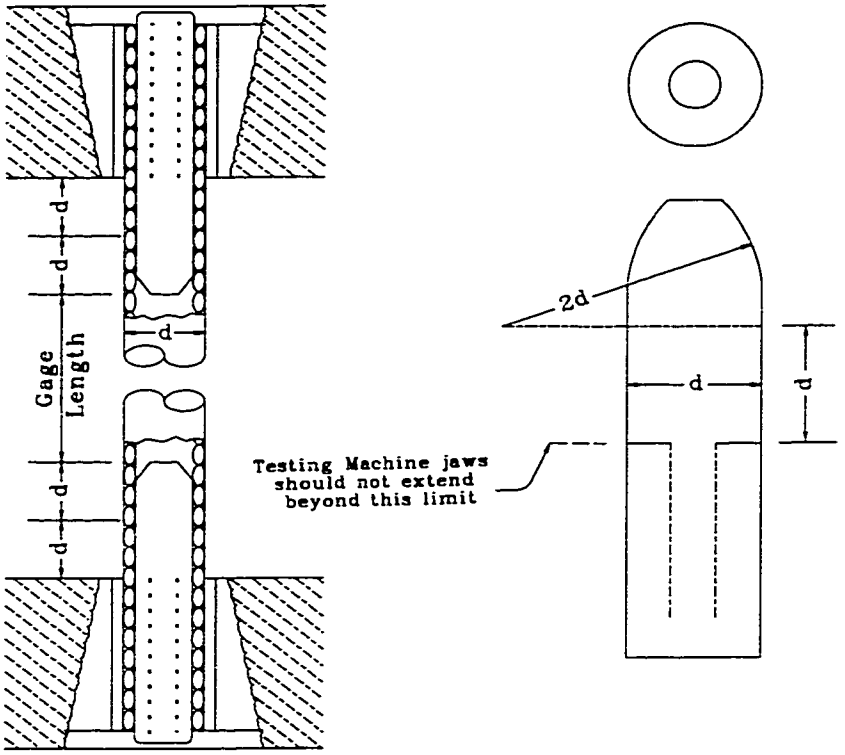

Figure 3.3: Standard Metal Plugs For Tension Test, (Shamem 1988)

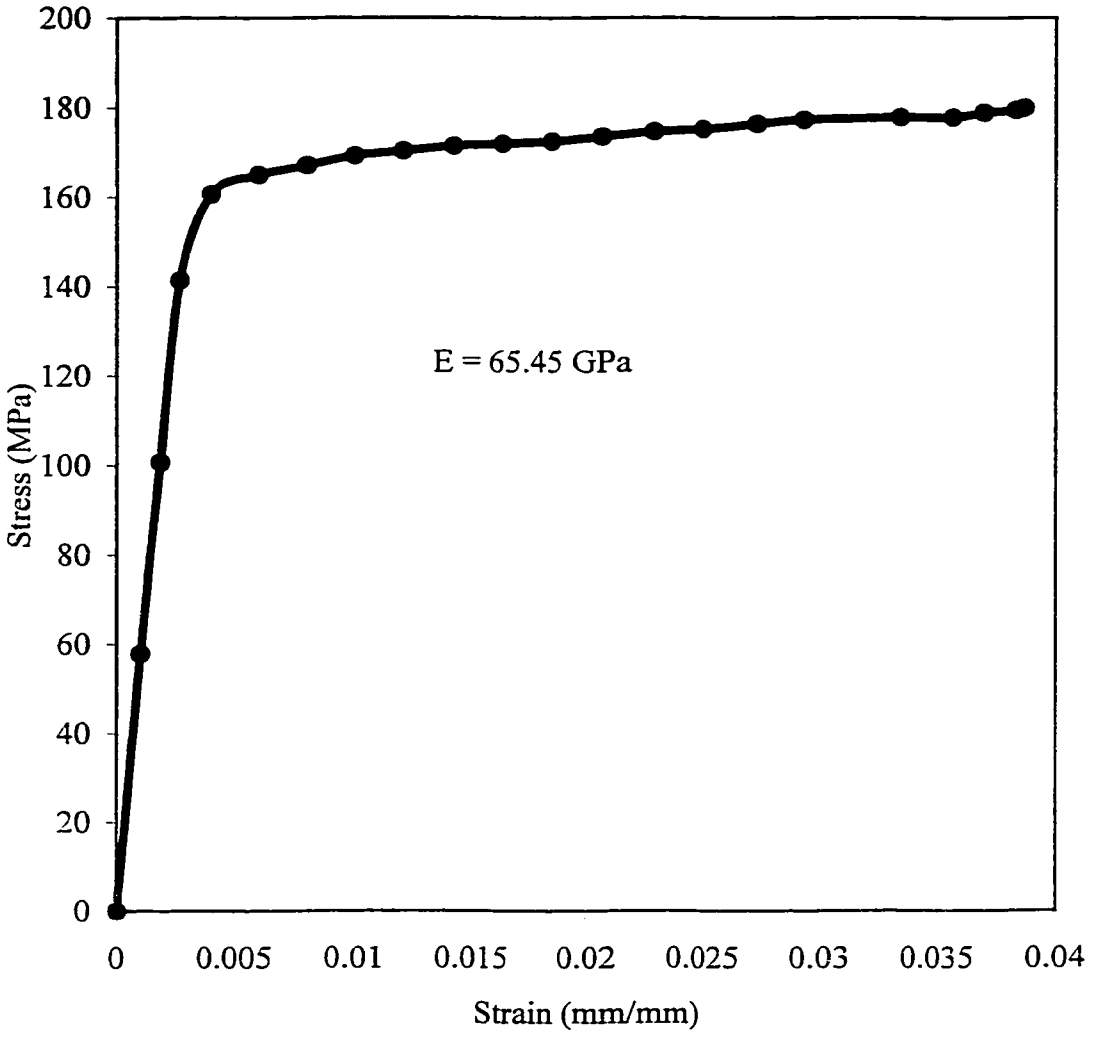

Figure 3.4: Stress-Strain Curve for Aluminum Pipes

d) Model Piles (Aluminum 40mm outside diameter and 36mm inner diameter)

e) LVDT's (Linear Variation Displacement Transducer) and LVDT holder

f) Top Cap for piles group to produce hinges support at top of the piles

g) Bottom Cap to produce fixed end condition at bottom of piles

h) Loading Device for both Static and Cyclic Loading

3.4.2 Test Tank

The test tank is made from plexiglass sheets. The tank dimensions are 1200mm length, 800mm width and 600mm height. It is stiffened with steel frame to prevent it from bulging out when filled with sand. The test tank is prevented from movement when subjected to load by steel bracing fixed to the ground. The test tank setup is shown in figure 3.5 and plate 3.1.

3.4.3 Flooding Tank

Another tank is used to flood the sand through plastic pipes connected to and going through the test tank. The dimensions of this tank are 800mm in length, 200m in width and 1200mm depth as shown in figure 3.5. The water is supplied to the sand at slow rate by increasing the water level slowly in the flooding tank. Therefore, the water level is raised slowly to prevent quick sand condition, in the submerged test case.

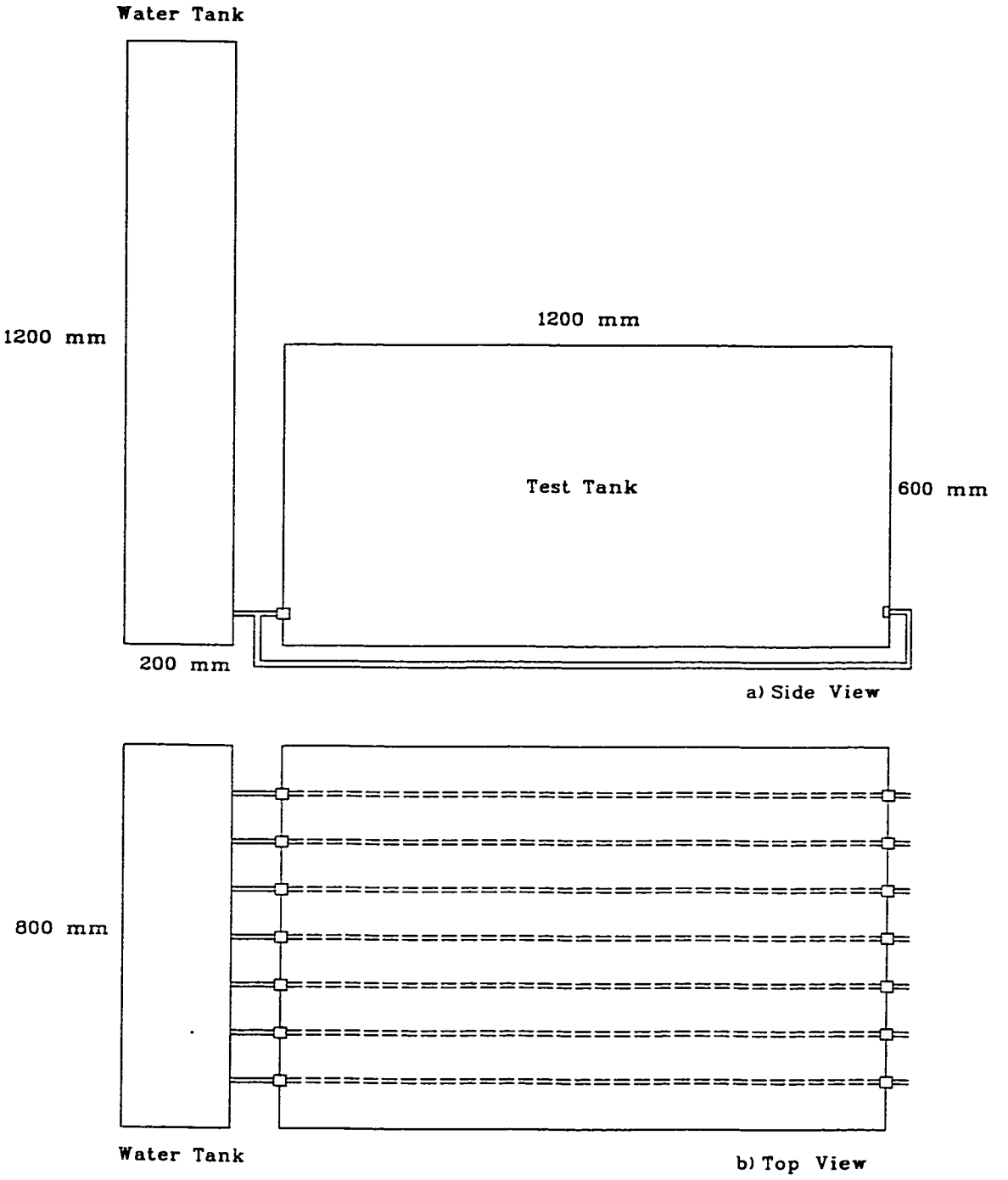

Figure 3.5: Test and Saturation Tanks

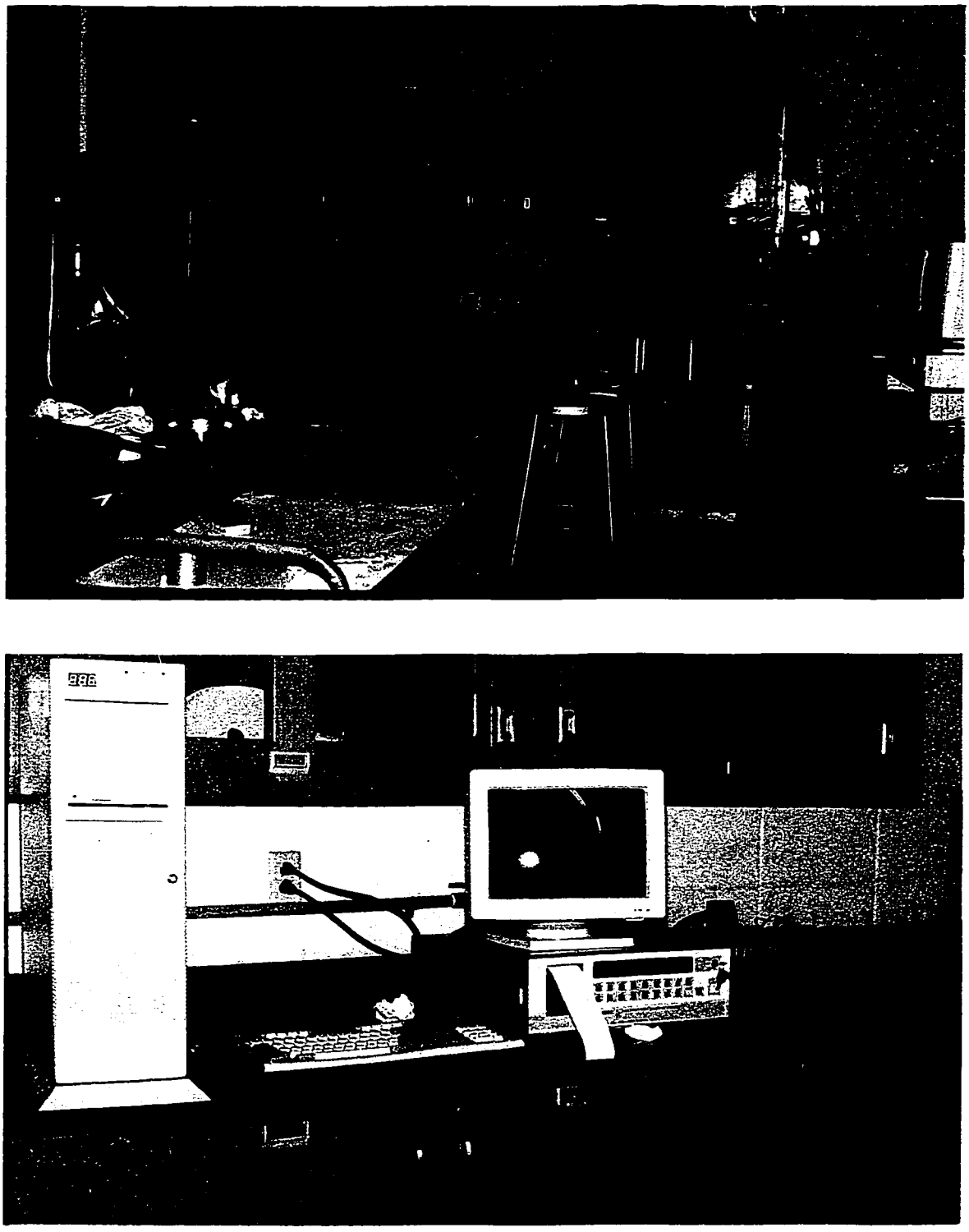

Plate 3.1: Experimental Setup

3.4.4 Submerged Sand Test

The research program involves testing the piles models in dry and fully submerged condition of sand. In case of submerged condition the tank was filled with water from the adjacent water tank through the plastic pipes. The water level was raised in small increments in order to avoid quick sand condition. The procedure is to add little water to the adjacent tank and keep it until the water stabilizes in both tanks before adding any water. Enough time between successive increments must be given until equilibrium in both tanks is achieved.

3.4.5 Sand Laying Machine

An automatic traversing sand laying machine similar to the machine used by the Danish Geotechnical Institute (Steenfelt, 1973) was constructed at the Central Research Workshop at the KFUPM (Shameem 1988). It consists of two parts as shown in figure 3.6. The upper part consists of two vertical screw spindles from which the receptacle is suspended. The rotation of the screw spindles is produced by an electric motor combined with a gear. The spindle's function is to raise the receptacle automatically as the sand surface raises. The receptacle traverses forwards and backwards on two rails placed along the sides of the test tank. It is driven by an electric motor and a gear box. The direction of the traversing is shifted automatically when receptacle reaches the end of the test tank.

The horizontal traversing speed of the receptacle is about 40 mm/sec, and it is raised at a vertical speed of 0.175 mm/sec. The type of opening used at the receptacle's bottom was a

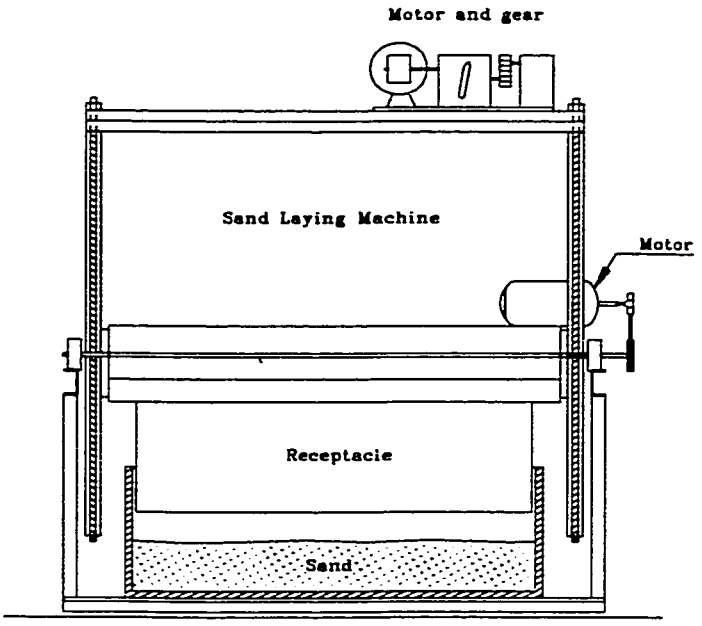

a) Front View

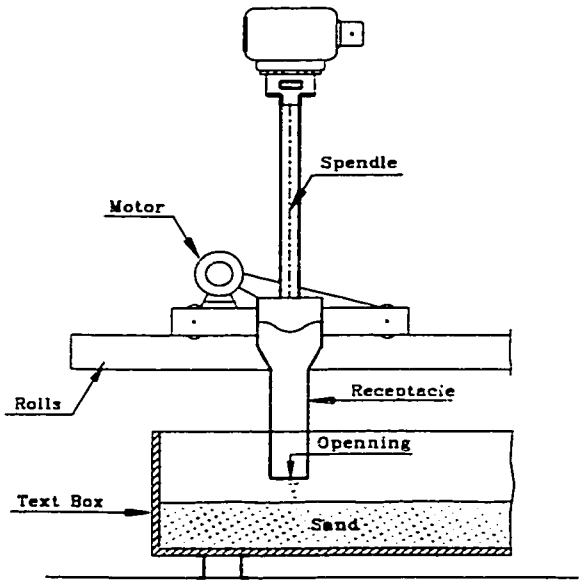

b) Side View

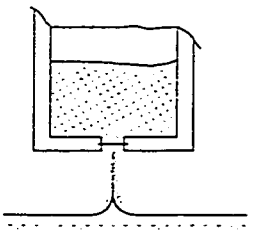

c) Openning Of Receptacle

Figure 3.6: Sand Laying Machine, (Shamem 1988).

continuous horizontal slot 3mm wide at the two ends, and 2mm in the middle. This configuration was adopted in order to minimize the sand heap produced along the middle part of the test tank.

3.4.6 Sand Deposition

This procedure follows directly the load calibration step, discussed later in section (3.3.12). The sand deposition was conducted by using the sand laying machine. To get a uniform density at all points within the test tank, the height of fall was fixed at 80 cm. Shameem (1988) conducted a trial run for sand deposition on the same height of fall to get the density at different locations in the tank. He measured the densities by using metal cans placed at certain locations as shown in figure 3.7. Densities were also measured around the pile in order to know the effect of the presence of the pile. He also measured the overall density by knowing the volume of the tank and the weight of sand deposited. Table 3.2 represents the dry density at different locations by metal cans as well as the overall dry density. For each experiment, sand deposition is carried out at the same fall height (80 cm) to get a uniform and homogeneous density all over the tank.

3.4.7 Model Pile

The model piles used are aluminum pipes with an outer diameter of 40mm and thickness of 2mm which have been cut to the required length of 750mm. A hole is drilled at the top of the pile to connect the pile with the top cap through a screw to simulate a hinge support at the top of the pile. The screw size is exactly the same size as the hole to avoid any impact

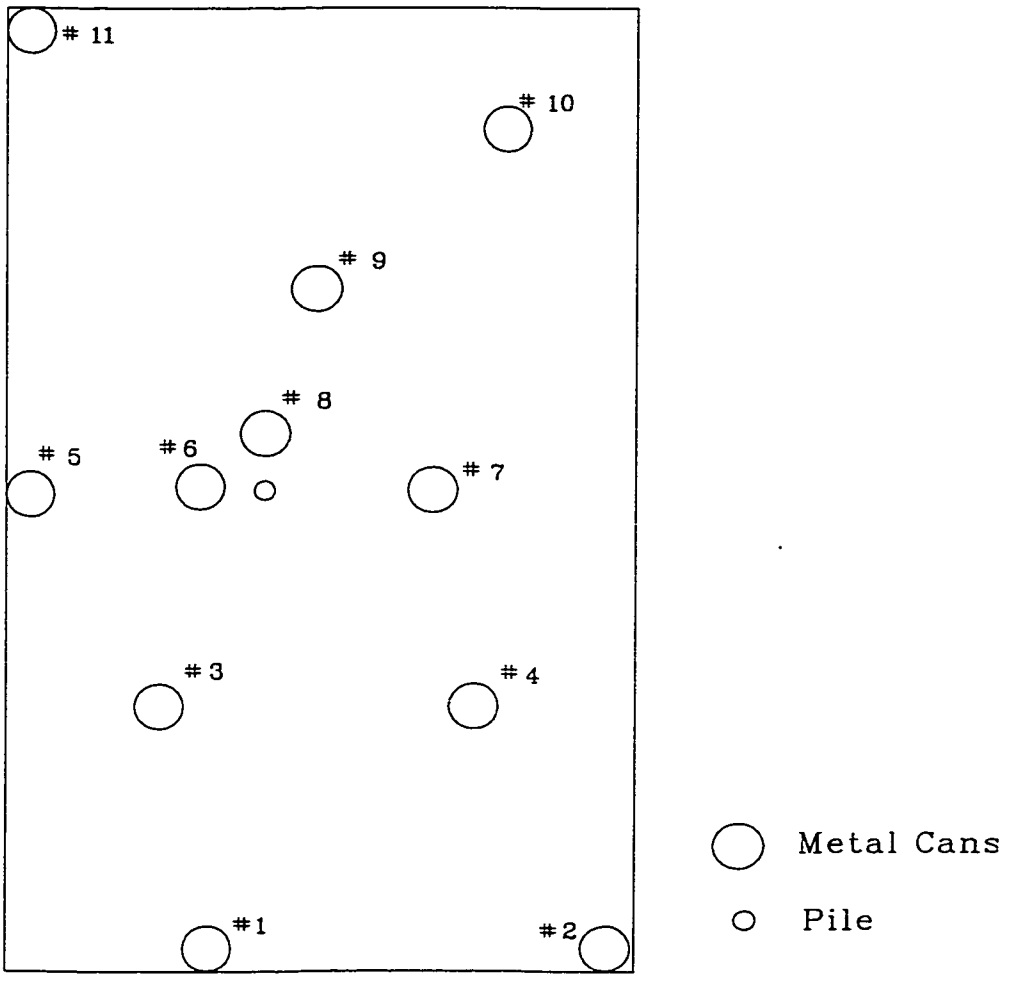

Figure 3.7: Soil Density Measurement by Metal Cans.

Table 3.2: Soil Density Measured By Metal Cans

a) Cans Location Individual Density

CAN POSITION	DENSITY (KN/m^3)
1	16.61
2	16.60 (min.)
3	16.68
4	16.78
5	16.78
6	16.63
7	16.72
8	16.89 (max.)
9	16.76
10	16.60 (min.)
11	16.72

b) Overall All Density

WEIGHT (KN)	DIMENSION (m^3)	DENSITY (KN/m^3)
9.30	1.20 * 0.80 * 0.58	16.70

effect on the pile during loading. Eleven strain gages were placed at equal spacing on one side of the pile surface in the loading direction. These strain gages are protected against sand friction and water by special epoxy coating ARALDITE AW2100. The epoxy is lift to dry for one day to gain its full performance.

In case of pile groups, one pile in each row was instrumented with strain gages due to similarity within the same row. This similarity helps tremendously in reducing the number of data channels and therefore reducing the reading time for these channels. Hence, the time gaps between readings the first and the last channel is negligible.

3.4.8 Top Cap

In case of group of piles, a specially designed pile cap was constructed at KFUPM Civil Engineering Workshop. The cap was needed to distribute the load to all piles that were equally spaced and to provide the hinging support at the top of the piles. This is to simulate the continuity between piles top and the steel jacket in offshore platforms. The top pile cap is shown in Figure 3.8. This pile cap was used for nine and four pile groups. For nine piles group (3 X 3), the center to center spacing of the piles is twice the pile diameter, while for four pile group (2 X 2), the center to center spacing is four times the pile diameter. It should be noted that the single pile is hinged at its top without the need of a top cap.

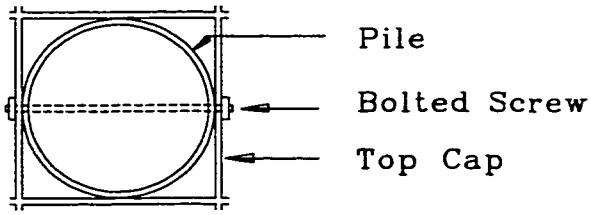

a) Top View of Sample Pile Connection

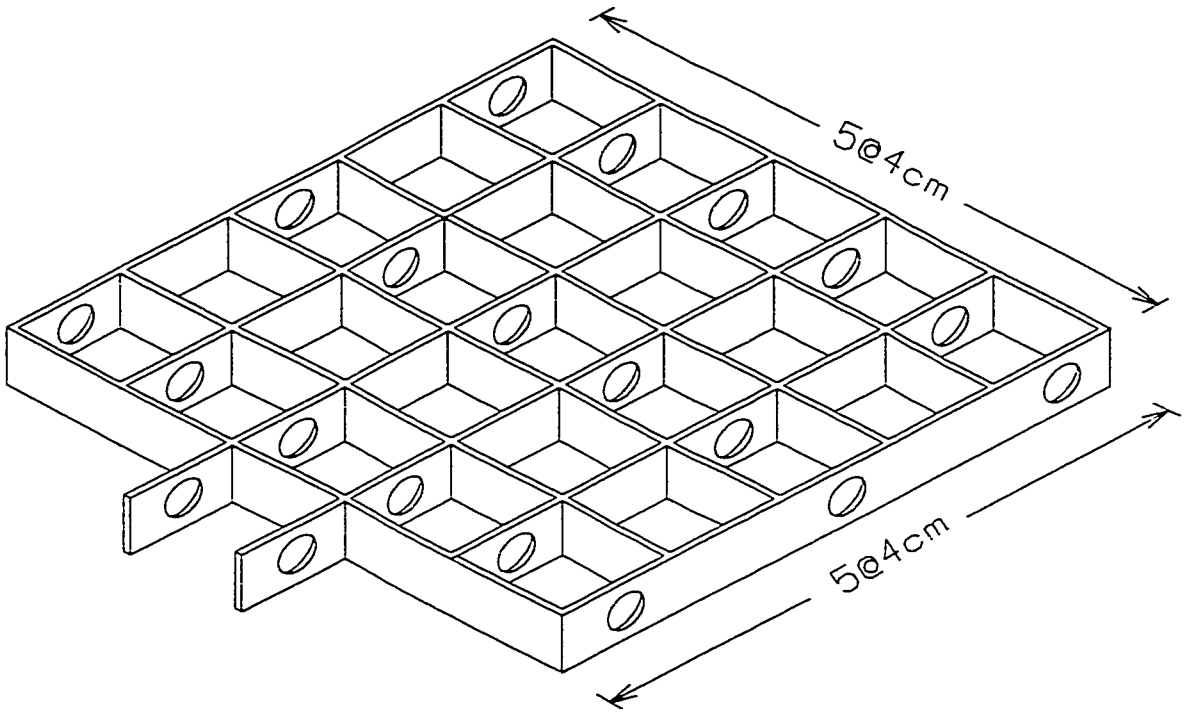

b) Three Dimensional View

Figure 3.8: Pile Group Top Cap.

3.4.9 Bottom Cap

In order to completely restrict the movement of the piles at their bottom, a cap having openings with the same spacing as the top cap was constructed at KFUPM research workshop. As shown in Figure 3.9, the cap consists of a set of steel plates fixed together through long screws. In between these plates openings of slightly less than 40mm diameter were created so that the movement and rotation of each pile is completely restricted in all directions. The cap was designed so that it can be used for single pile, four pile group, and nine pile group.

The cap was fixed against movement and rotation by steel bracing screwed in the cap plates. These bracings were fixed by extending them to the tank walls. In addition to the steel bracing, the weight of the sand above the cap assists in fixing the pile cap. The pile cap and the bracing is shown in figure 3.9.

The bottom cap was fixed at 100mm distance from the bottom of the tank. This will simulate the condition that the piles are driven into a stiff clay layer where the piles will be completely fixed at that level.

3.4.10 LVDT's and LVDT Holder

The Linear Variable Differential Transformer (LVDT) is an electrical device that is used for precise measurement of linear displacement. It consists of a transformer with outer coil and

BOTTOM CAP

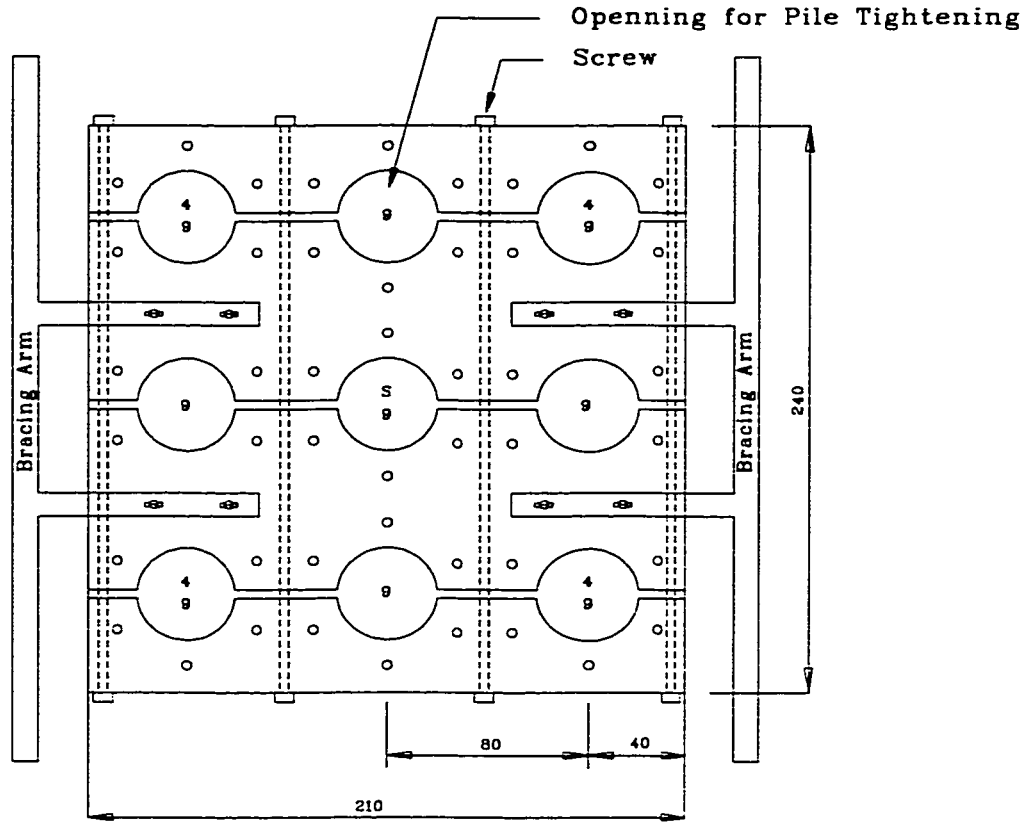

Note :
All Dimensions in mm
S = Used for Single Pile
4 = Used for Four Pile Group
9 = Used for Nine Pile Group

Figure 3.9: Pile Group Bottom Cap (Piles Fixed End)

a movable central core. As the core is moved due to a structural displacement, it produces an electrical signal that can be recorded remotely and continuously, for both static and dynamic response. LVDTs vary in core length such as 10mm and 50mm, which affect the maximum measured displacement. In this research three LVDTs were used at the top of the pile. Two 50mm LVDTs were fixed at a distances of 50mm and 100 mm from the top of the pile. The third is a 30mm LVDT and was used at a distance of 150mm from the top of the pile. These LVDTs were adjusted to measure forward and backward movements.

Special LVDT holders were fabricated at Civil Engineering workshop. Each of these holders can be easily rotated and moved in any direction independent of the other by means of tightening and loosing screws. Three of these holders are fixed on a steel frame, which is bolted to the ground. Figure 3.10 shows the complete setup for the LVDTs frame holders.

3.4.11 Loading Device

3.4.11.1 Introduction

It is very essential in studying the behavior of laterally loaded piles to simulate the actual lateral load that the piles are subjected to. Figure 3.11 shows a typical loading wave on an offshore platform structures. A lateral loading system was designed and constructed to produce a loading wave on the pile group as shown figure 3.12. The system consists of two parts namely:

a) Mechanical air pressure system; and

b) Time controlling electronic circuit unit.

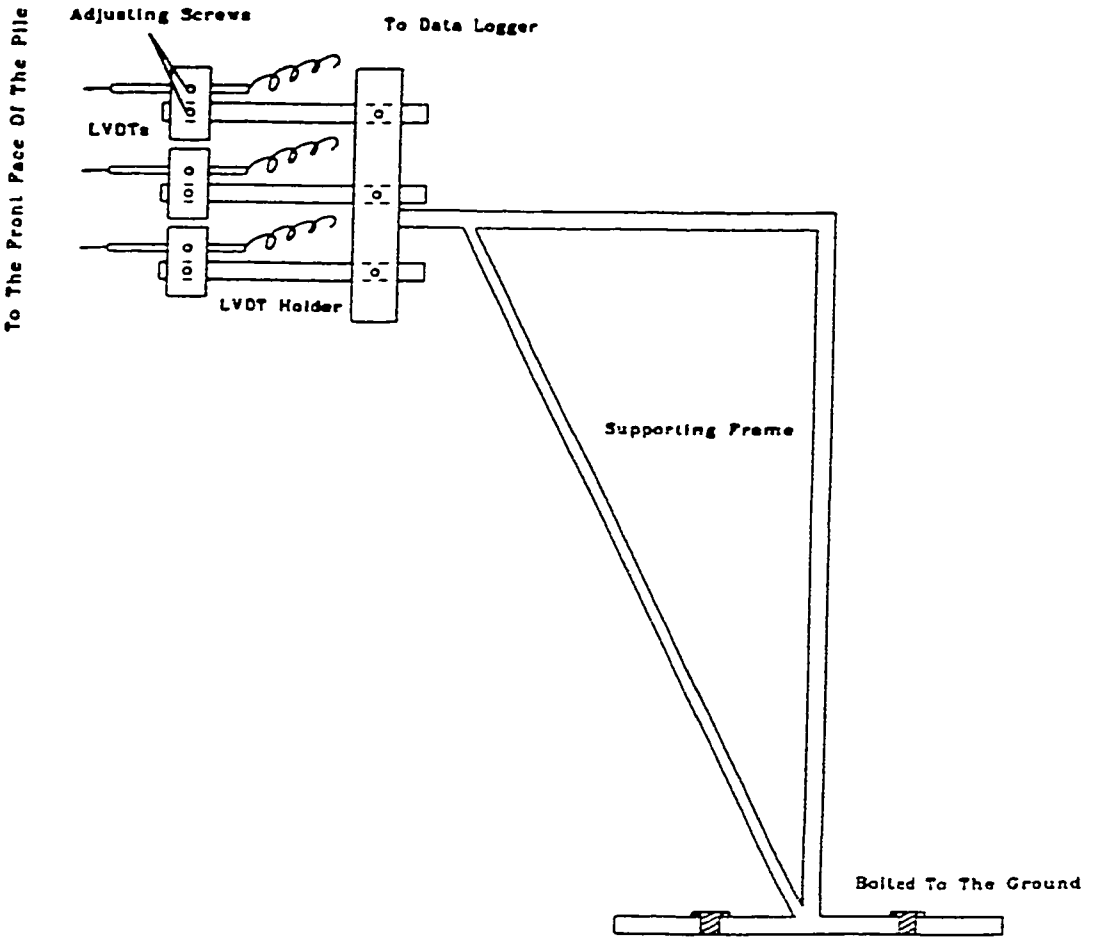

Figure 3.10: LVDTs Holders.

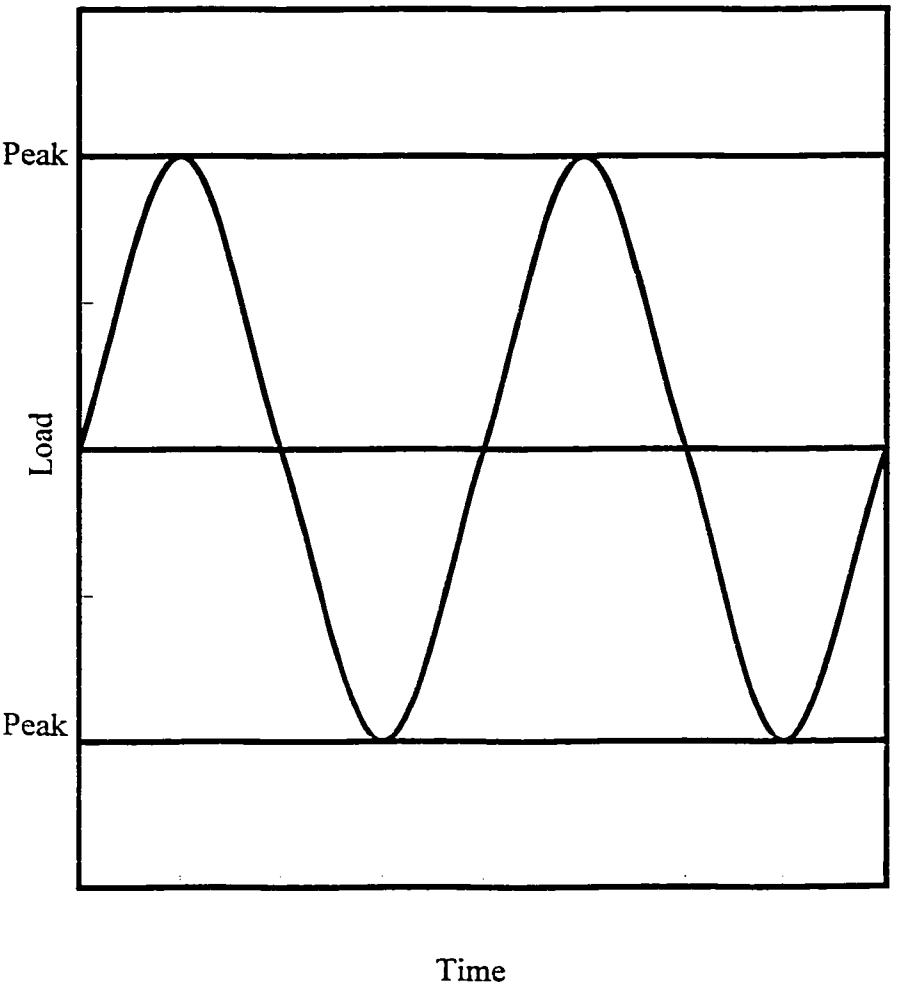

Figure 3.11: Lateral Cyclic Loading Pattern.

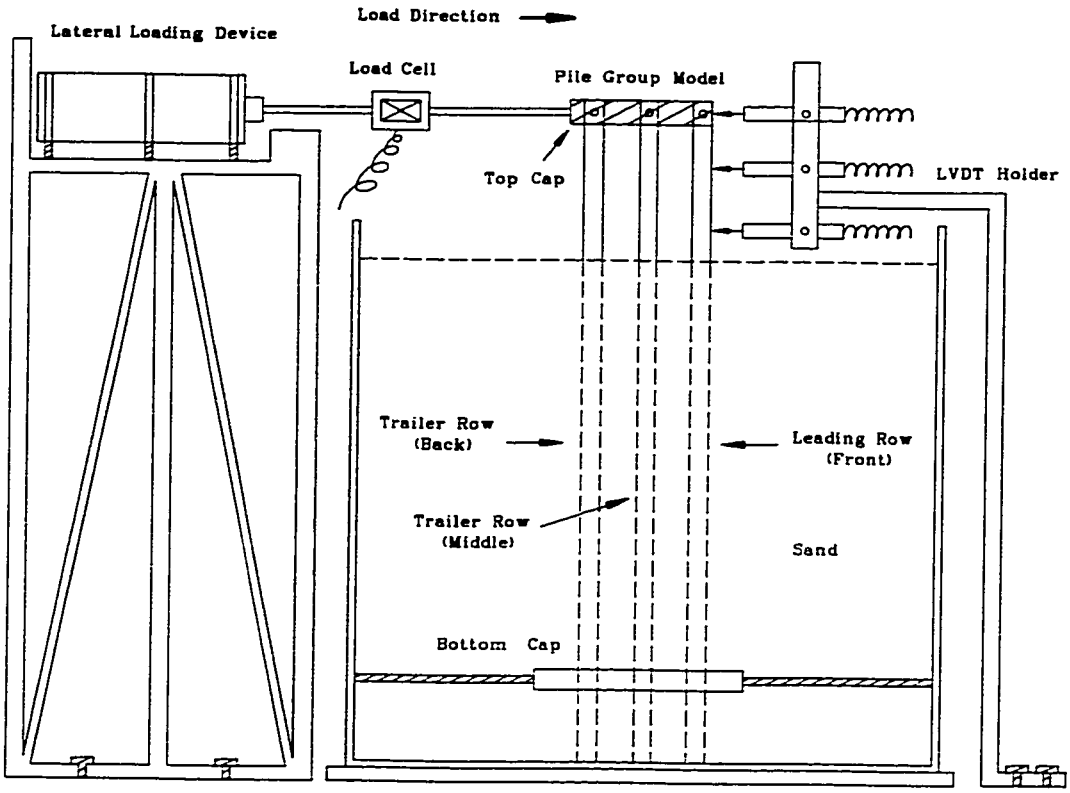

Figure 3.12: Schematic Setup Sectional View.

3.4.11.2 Dry Air Pressure System

The cyclic loading was applied to the piles laterally via an actuator operated by air pressure system. The actuator was designed and fabricated at the Research Workshop at KFUPM after several trials on different sizes and designs. This device is capable of applying both static and completely reversible cyclic loading. The actuator consists of several parts as shown in Figure 3.13, which are:

a) tension-compression Load Cell

b) a cylinder containing piston

c) static pressure gage

d) static pressure valve

e) air cylinder

f) static pressure regulator

g) two solenoid valves

h) two secondary air cylinders

i) four one-way pressure joint (check valve)

j) steel plate on stand bolted firmly to the ground.

The load cell was mounted between the piston rod and the top pile cap to measure precisely the load applied directly on the piles. The whole system is completely restricted against movement and rotation by bolting the system on the steel plate bolted on a stand that is fixed to ground.

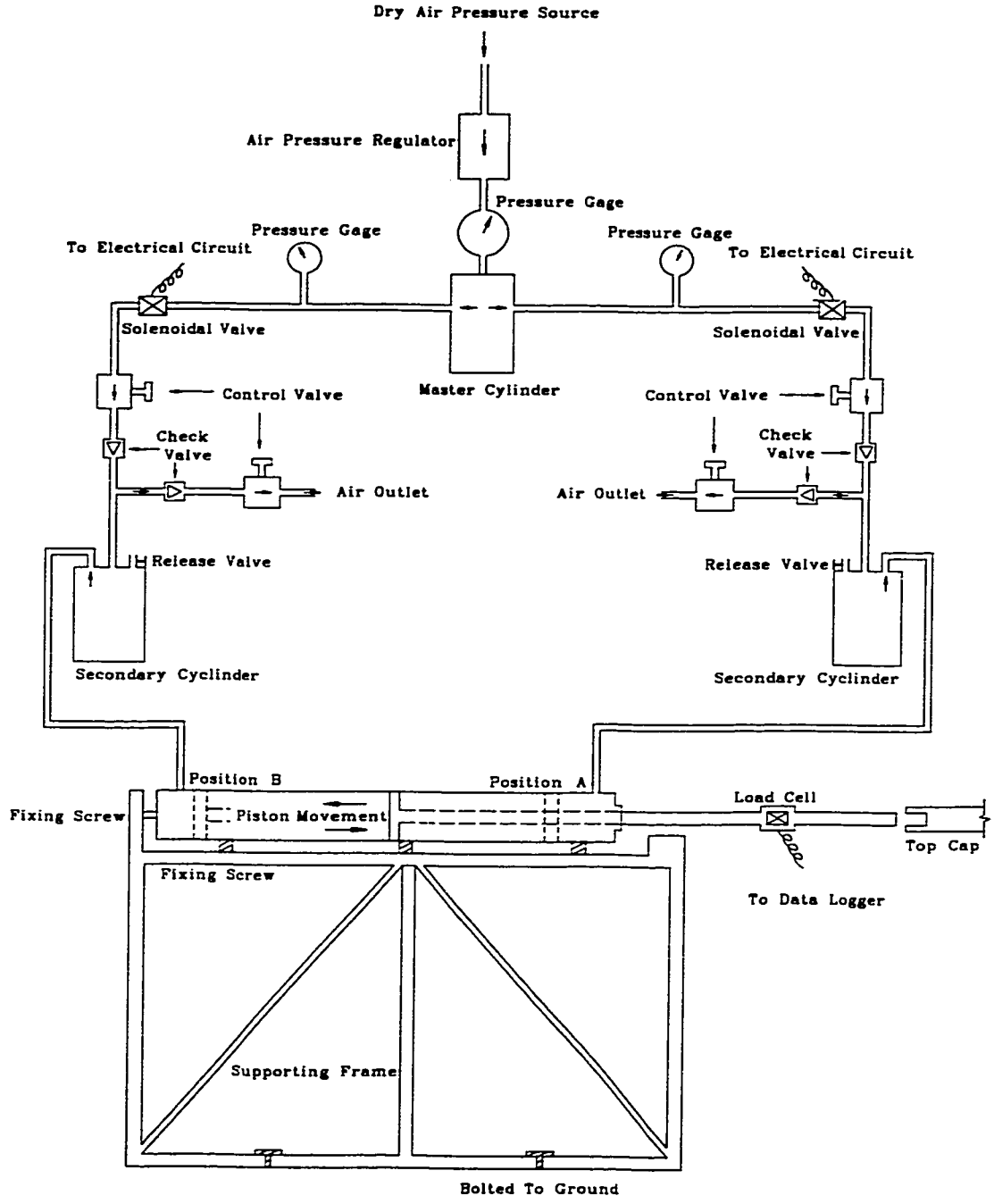

Figure 3.13: Dry Air Pressure System for Cyclic Loading.

The loading is achieved by applying air pressure on the piston. This pressure forces the piston to move forward and backward depending on the pressure direction, which in turn moves the piie top forward or backward, as required.

In case of the static loading, the hose for forward loading is connected to the forward static loading valve. This valve is set open and the pressure is increased gradually by means of the static pressure regulator. For the case of cyclic loading, the pressure application in each direction is controlled by the solenoid valves at different time intervals. The solenoid valves are connected to a specially designed electronic circuit that controls the timing of pressure application in each direction. Moreover, the load peak and the pattern of loading have to be calibrated and preset before each cyclic loading test.

3.4.11.3 Automatic Switch Circuit for Cyclic Loading

In order to control the pressure inlet and outlet from each solenoid valve by certain time intervals, an automatic switch was developed. Figure 3.14 shows the time interval required to control each solenoid valve and figure 3.15 shows the electronic circuit used. This circuit consists of integrated circuits (ICs), resistors, capacitor, led and relays. Each solenoid valve was operated by electric power that was controlled by the circuit through the relays outlet wires. The circuit was developed by Mr. Khalil Aryan (Student at University of Bahrain), Mr. Abdullah Najem (Electronic Technician), and Mr. AbdullMajeed Shakeeb (KFUPM Student).

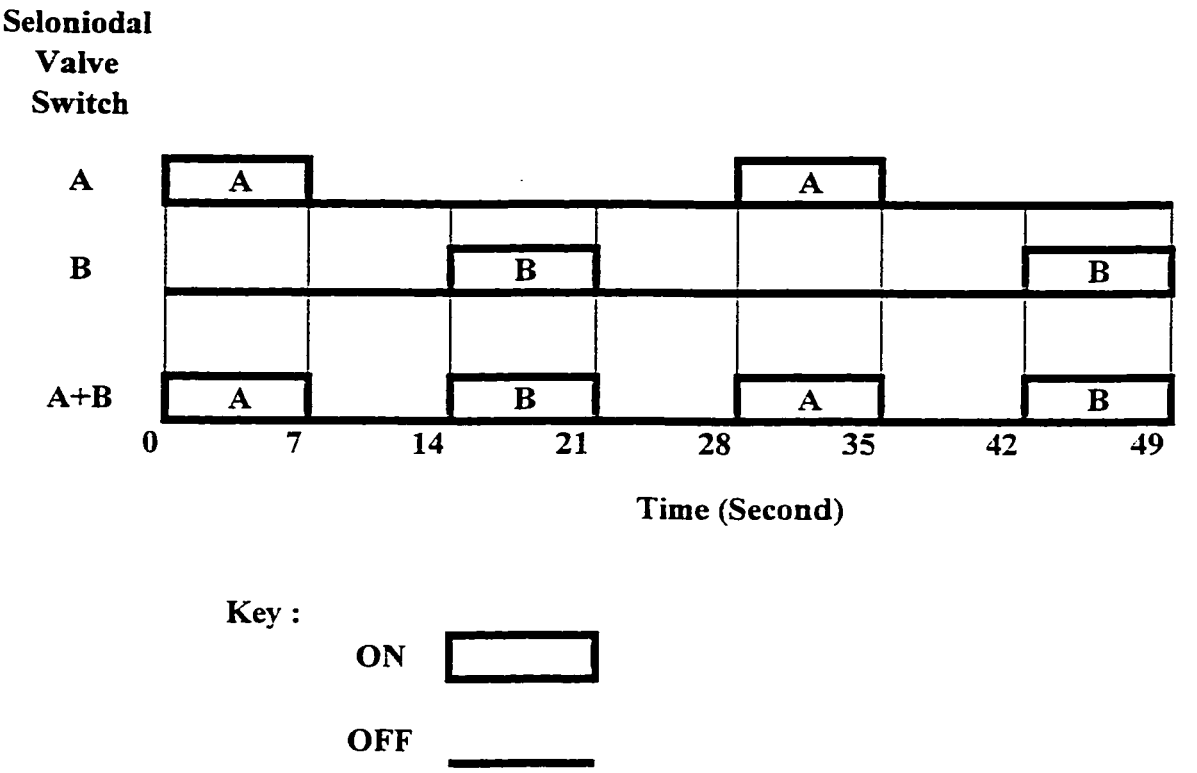

Figure 3.14 Time Intervals of the Solenoid Valves.

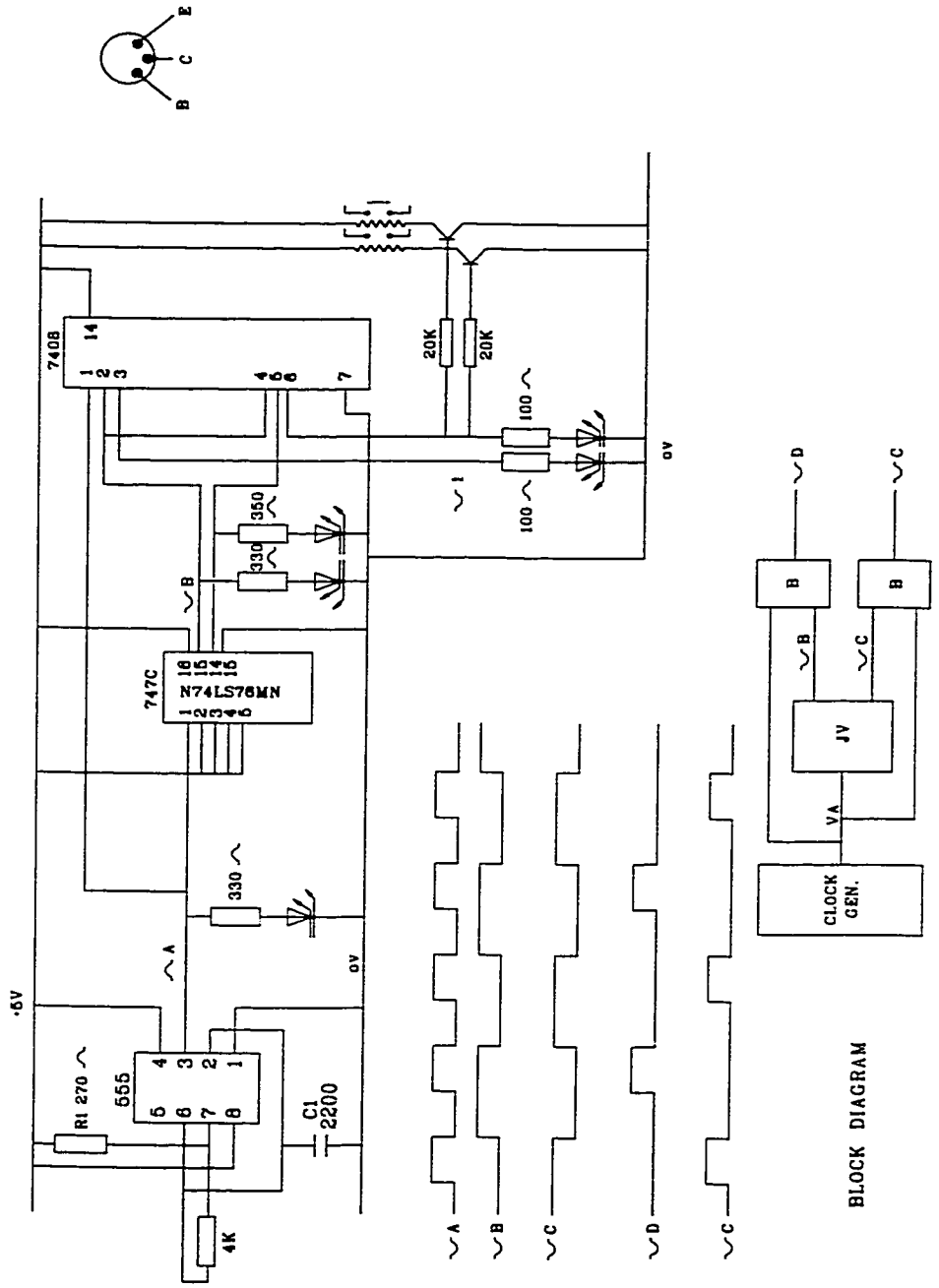

Figure 3.15: Automatic Switch Circuit for Cyclic Loading.

The circuit works as follows:

a) By closing the relative relay outlet switch (i.e. closing the circuit) for seven seconds it will open each solenoid valve independently for seven seconds to compress the air into the secondary cylinders, which will in turn move the piston.

b) By releasing the relay outlet switch (opening the relay circuit) to close each solenoid valve for 21 seconds independently, which will release the pressure exerted previously.

c) The time delay between closing each relay outlet switch, and hence opening each solenoid valve relatively, is 14 seconds.

Thus complete cycle duration is 28 seconds (i.e. loading cycle period is 28 seconds).

3.4.11.4 Static Loading

Static loading was generated by connecting the forward pressure hose to the static loading valve and the valve was left open. Then the pressure was released gradually by turning the static regulator valve in the clockwise direction. This pressure produced forward movement of the piston exerting a force on the piles, which was recorded by a load cell connected to a data logger.

For the static loading tests, load is increased gradually at small load intervals until excessive deflection above the sand surface is reached. Load, deflection and strains readings are recorded at each load level.

3.4.11.5 Cyclic Loading

To produce a completely reversible cyclic loading the forward pressure and the backward pressure hoses must be connected to the appropriate solenoidal valves. The static regulator is turned clockwise to produce a preselected pressure which will be indicated on the pressure gage. Then the Electronic circuit will be switched on and after that the solenoidal valves will be opened and closed automatically according to the pattern shown previously in figure 3.9. During cyclic loading, fine adjustments on the pressure control valves must be carried out to achieve the best cyclic loading pattern.

It is necessary to produce the same load level at both peaks (forward and backward loading). However, the best loading pattern is reached by adjusting the peaks load level to be exactly at the end of the open intervals in both directions. Therefore, it is important to run the load calibration test before each cyclic loading test in order to have uniformity in loading level and pattern through each test and through all tests. The load is recorded during the test by personnel computer connected to the data logger.

For cyclic loading tests, the dynamic loading previously calibrated (calibration procedure is discussed in the following section) was applied for two hours to achieve approximately 200 cycles. At each cycle, readings are recorded every second (roughly 28 readings per cycle). Load, deflections, and strains readings are recorded in every reading.

3.4.12 Calibration for Cyclic Loading

In a quest to calibrate the cyclic loading setup, the sand was gradually poured into the tank till the desired level is obtained. It was essential to fill the gap between the test tank and bottom cap with sand, in order to restrict any sand movement from top to bottom; during the loading process. Therefore, at the bottom pile cap it was important to fill the bottom most layer. The cyclic loading must be applied in a systematic consistent level of loading throughout all loading cycles. Furthermore, the setting of load level must be applied on the same pile deflection condition as pile deflection directly affects the loading levels.

The loading device was then fixed to the top piles cap and trial loading starts. The required loading pattern and level was reached after some time by adjusting the pressure valves. Finally, the sand above the bottom piles cap was removed to deposited uniformly for the actual testing as discussed in the next section. The layer of sand below the bottom cap was not removed because it has no effect on the behavior of the piles due to fixity point at the level of bottom cap.

CHAPTER FOUR

BEHAVIOR OF PILE MODELS UNDER STATIC LATERAL LOAD

4.1 Introduction

In this chapter, the behavior of the pile group models subjected to lateral static load is studied and discussed. The tests on pile models were carried out under both dry and submerged sand conditions. The pile models used were: single pile; four pile group; and nine pile group. The static loading was applied using the loading system discussed earlier. Simple beam theory is applied to calculate the bending moment along the pile length from the measured strains. A BASIC computer program applying the conjugate beam method was developed and used to calculate the deflection along the pile length. The soil pressure along pile length was obtained by differentiating a seventh degree polynomial equation fitted to the calculated moments.

The experimental setup mentioned earlier was also used to study the effect of submergence on the behavior of the model piles and group effect. Comparison between single pile model and both four and nine pile group models were studied in accordance with the following parameters:

1. the spacing of the piles (depends on the number of piles in a group: one, four and nine),
2. the rows location within a group (front, middle, back), and
3. the normalized moment.

4.2 Calculation of Bending Moments and Deflections Along The Pile

From the strain gages readings, bending moments along the pile length were calculated using simple beam theory:

$$M = \varepsilon \frac{EI}{r} \qquad 4.1$$

where

M = Bending moment (kN.mm)

ε = Measured strain (mm/mm)

E = Modulus of elasticity for aluminum pipes (kN/mm^2)

I = Moment of inertia of the pipe section (mm^4)

r = Outside radius of the pipe (mm)

The deflection along the pile is calculated by conjugate beam method. Therefore, a BASIC computer programs was developed utilizing the moments along the pile and the top three deflections above the ground surface to calculate the deflections along the pile. Since the pile is completely fixed at the bottom there will be, theoretically, zero deflection and zero slope. However, practically there will be very small slope at the bottom of the pile because the pile diameter is four times the plate thickness which means there is no full fixity against rotation at the bottom. Therefore, the program first calculates the slope at the bottom based on the three top deflections and bending moments; then it starts calculating the deflection along the pile from bottom to top. Copy of the program is shown in appendix B.

4.3 Procedure for Obtaining p - y Curves

As discussed in Chapter 2, the following well known equations:

$$p = \frac{d^2M(x)}{dx^2} \qquad 4.2$$

$$y = \iint \frac{M(x)}{EI} dx \qquad 4.3$$

can be used to calculate the soil response (pressure) p and pile deflection y along length of the pile (p-y curves). The measured moment along the pile length was fitted with a seven degree polynomial equation as suggested by Ting (1987). Ting assumes conditions which truncate the first four terms of the polynomial equation. However, in our case the only applicable condition is that the soil response at the ground surface is negligible (i.e. Zero) which is a true assumption since the soil used is purely fine sand. Moreover, the moment at the bottom of pile will have some value because the pile is fixed.

Therefore the seven degree polynomial used in this study is as follows:

$$M(x) = a_0 + a_1x^1 + a_2x^2 + a_3x^3 + a_4x^4 + a_5x^5 + a_6x^6 + a_7x^7 \qquad 4.4$$

Where M = Moment along the pile,

a_0 to a_7 = Constant coefficients,

x = Depth from the pile cap.

In order to find out the soil response the above equation will be differentiated twice leading to the following equation.

$$P(x)=\frac{d^2M(x)}{dx^2}=2a_2+6a_3x^1+12a_4x^2+20a_5x^3+30a_6x^4+42a_7x^5 \qquad 4.5$$

In order to compute the constants in equation (4.4) the least square method was applied. Therefore, the error Φ is:

$$\text{Error}=\Phi=\sum_{k=1}^{m}\ (M(x)-M(k))^2 \qquad 4.6$$

By letting the partial derivative of Φ with each constant equal to zero, the following equations will result:

$$\begin{aligned}
&a_0 m + a_1\sum x + a_2\sum x^2 + a_3\sum x^3 + a_4\sum x^4 + a_5\sum x^5 + a_6\sum x^6 + a_7\sum x^7 = \sum M(x)\\
&a_0\sum x + a_1\sum x^2 + a_2\sum x^3 + a_3\sum x^4 + a_4\sum x^5 + a_5\sum x^6 + a_6\sum x^7 + a_7\sum x^8 = \sum M(x).x\\
&a_0\sum x^2 + a_1\sum x^3 + a_2\sum x^4 + a_3\sum x^5 + a_4\sum x^6 + a_5\sum x^7 + a_6\sum x^8 + a_7\sum x^9 = \sum M(x).x^2\\
&a_0\sum x^3 + a_1\sum x^4 + a_2\sum x^5 + a_3\sum x^6 + a_4\sum x^7 + a_5\sum x^8 + a_6\sum x^9 + a_7\sum x^{10} = \sum M(x).x^3\\
&a_0\sum x^4 + a_1\sum x^5 + a_2\sum x^6 + a_3\sum x^7 + a_4\sum x^8 + a_5\sum x^9 + a_6\sum x^{10} + a_7\sum x^{11} = \sum M(x).x^4 \quad \text{.... (4.7)}\\
&a_0\sum x^5 + a_1\sum x^6 + a_2\sum x^7 + a_3\sum x^8 + a_4\sum x^9 + a_5\sum x^{10} + a_6\sum x^{11} + a_7\sum x^{12} = \sum M(x).x^5\\
&a_0\sum x^6 + a_1\sum x^7 + a_2\sum x^8 + a_3\sum x^9 + a_4\sum x^{10} + a_5\sum x^{11} + a_6\sum x^{12} + a_7\sum x^{13} = \sum M(x).x^6\\
&a_0\sum x^7 + a_1\sum x^8 + a_2\sum x^9 + a_3\sum x^{10} + a_4\sum x^{11} + a_5\sum x^{12} + a_6\sum x^{13} + a_7\sum x^{14} = \sum M(x).x^7
\end{aligned}$$

Solving these seven equations simultaneously can be achieved easily by converting the equations into a matrix form:

$$[X]\bullet[A]=[M] \qquad 4.8$$

where

$$[X]=\begin{bmatrix} m & \sum x & \sum x^2 & \sum x^3 & \sum x^4 & \sum x^5 & \sum x^6 & \sum x^7 \\ \sum x & \sum x^2 & L & L & L & L & \sum x^7 & \sum x^8 \\ \sum x^2 & L & L & L & L & \sum x^7 & L & \sum x^9 \\ L & L & L & L & \sum x^7 & L & L & \sum x^{10} \\ L & L & L & \sum x^7 & L & L & L & \sum x^{11} \\ L & L & \sum x^7 & L & L & L & L & \sum x^{12} \\ \sum x^6 & \sum x^7 & L & L & L & L & L & \sum x^{13} \\ \sum x^7 & \sum x^8 & L & L & L & L & L & \sum x^{14} \end{bmatrix}, [A]=\begin{bmatrix} a_0 \\ a_1 \\ a_2 \\ a_3 \\ a_4 \\ a_5 \\ a_6 \\ a_7 \end{bmatrix}, [M]=\begin{bmatrix} \sum M(x) \\ \sum M(x).x \\ \sum M(x).x^2 \\ \sum M(x).x^3 \\ \sum M(x).x^4 \\ \sum M(x).x^5 \\ \sum M(x).x^6 \\ \sum M(x).x^7 \end{bmatrix}$$

Furthermore, the boundary condition at and above the ground surface level must be considered. Therefore, the locations for moment and soil response above the ground surface were not excluded from the matrix. At the ground surface the soil response is forced to be zero by applying lagrangian multiplier method (Swokowski).

Hence, at ground surface (x = 210mm)

$$p(210) = 2a^2 + 6(210)a_3 + 12(210)^2a_4 + 20(210)^3a_5 + 30(210)^4a_6 + 42(210)^5a_7 \qquad 4.9$$

Therefore, the resulted matrix is

$$\begin{bmatrix} m & \sum x & \sum x^2 & \sum x^3 & \sum x^4 & \sum x^5 & \sum x^6 & \sum x^7 & 0 \\ \sum x & \sum x^2 & L & L & L & L & \sum x^7 & \sum x^8 & 0 \\ \sum x^2 & L & L & L & L & \sum x^7 & L & \sum x^9 & 2 \\ L & L & L & L & \sum x^7 & L & L & \sum x^{10} & 6(210) \\ L & L & L & \sum x^7 & L & L & L & \sum x^{11} & 12(210)^2 \\ L & L & \sum x^7 & L & L & L & L & \sum x^{12} & 20(210)^3 \\ \sum x^6 & \sum x^7 & L & L & L & L & L & \sum x^{13} & 30(210)^4 \\ \sum x^7 & \sum x^8 & L & L & L & L & L & \sum x^{14} & 42(210)^5 \\ 0 & 0 & 2 & 6(210) & 12(210)^2 & 20(210)^3 & 30(210)^4 & 42(210)^5 & 0 \end{bmatrix} \bullet \begin{bmatrix} a_0 \\ a_1 \\ a_2 \\ a_3 \\ a_4 \\ a_5 \\ a_6 \\ a_7 \\ \lambda \end{bmatrix} = \begin{bmatrix} \sum M(x) \\ \sum M(x).x \\ \sum M(x).x^2 \\ \sum M(x).x^3 \\ \sum M(x).x^4 \\ \sum M(x).x^5 \\ \sum M(x).x^6 \\ \sum M(x).x^7 \\ 0 \end{bmatrix}$$

4.10a

Where λ = lagrangian multiplier

or in short form

$$[X'] \bullet [A] = [M] \qquad 4.10b$$

Calculating $[X']^{-1}$ and multiplying both sides of equation (4.10b) with the inverse will give the following:

$$[A] = [X']^{-1} \bullet [M] \qquad 4.11$$

Hence, the unknowns a_0 to a_7 can be found from matrix $[A]$. An example of calculating the values of a_0 to a_7 is shown in Appendix A. By knowing these values, equation (4.5) can be solved to determine soil pressure at different depths for the same pile load level. Therefore, the above procedure must be worked out at different pile load levels in order to obtain sufficient number of soil responses (p) at selected depths.

The corresponding deflection (y values) at selected pile load levels and depths are obtained from the BASIC computer program. This calculates the deflection along the pile from the known measured pile top deflection and bending moment by applying the conjugate beam theory.

4.4 Test Results and Discussion

4.4.1 Single Pile

The first two tests were carried out for single pile under static lateral load for dry and submerged sand conditions. The incremental static load was applied at a very slow rate allowing the pile to achieve equilibrium at each level and to have sufficient time to record load, top deflections and strains gages readings along the pile length.

Top deflection

Figure 4.1 depicts lateral load versus top deflection for both dry and submerged conditions. It clearly shows that for the same load level the top deflection is slightly higher in the case of submerged sand condition. This is due to the reduction in the soil resistance, which is directly proportional to the soil effective density (γ). In case of submerged sand condition, the effective soil density was approximately half the effective soil density in case of dry condition.

$$\gamma_{sat} = \gamma - \gamma_{water} \qquad 4.13$$

The top deflection difference between the dry and the submerged condition increases as load level increases, since deflection is load dependent. At low load level the difference is negligible while at high load level the difference is clearly noticeable. This is also noticed by other researchers (Reese 1984). Also, it can be observed that the slopes of the curve is reducing with the increase in load level. This means that as the load level is increased the

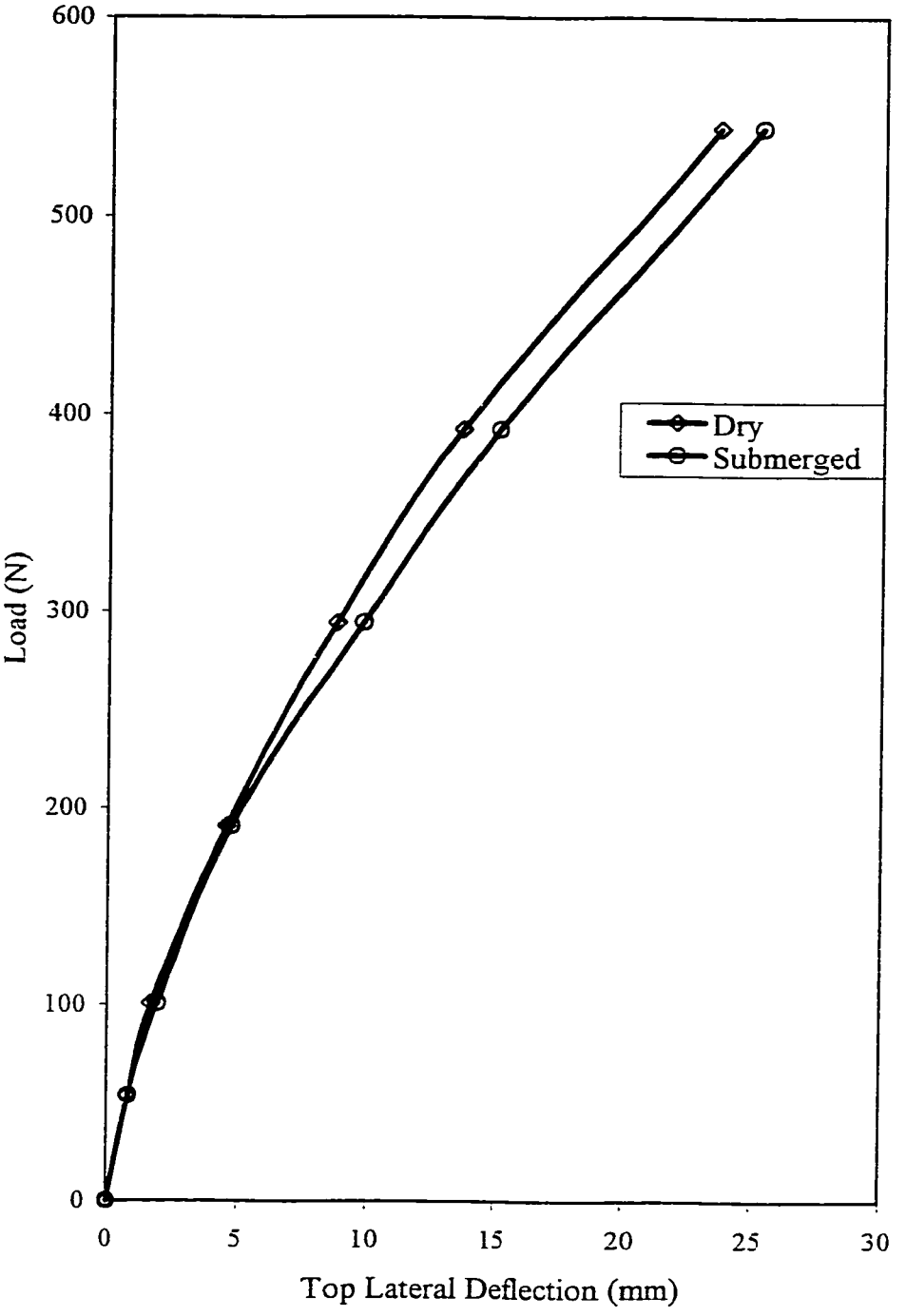

Figure 4.1: Top Lateral Deflection of Single Pile Subjected to Static Load

soil resistance increases, but at a slower rate, which produces accordingly higher deflection at a higher load levels.

Moment diagram

Moment values were obtained from feeding equation (4.1) with strain gage readings, sample calculation is shown Appendix A. Figures 4.2 and 4.3 present the moment diagrams at different load levels for a single pile subjected to static load for dry and submerged sand conditions, respectively. The figures clearly show that an increase in the load level causes an increase in moment and deflection along the pile. These figures also show that the maximum moment location is shifted down as the load level increases. Full scale testing by Brown et al. (1988) have also shown similar behavior.

The top portion of the moment diagram shows a cantilever beam behavior, with a straight-line moment curve starting from value at the free end (pile top). After crossing the ground surface the soil starts to resist the movement of the pile and hence producing an opposite reaction since the soil behaves as Winkler springs foundation. Even-though the soil resisted the pile movement, the curvature and therefore the moment continue increasing but at a smaller increment. At this stage, the curvature of the moment diagram between the ground surface and the maximum moment increased. The final stage in the moment diagram is falling between the maximum moment and the fixed end of the pile. The fixed end at the pile bottom will represent a condition in which the pile is embedded in a stiff hard soil. The values of the moments diagram start to decrease as approaching the fixity point. During this stage the soil starts to overcome the pile movement which will reduce its curvature and

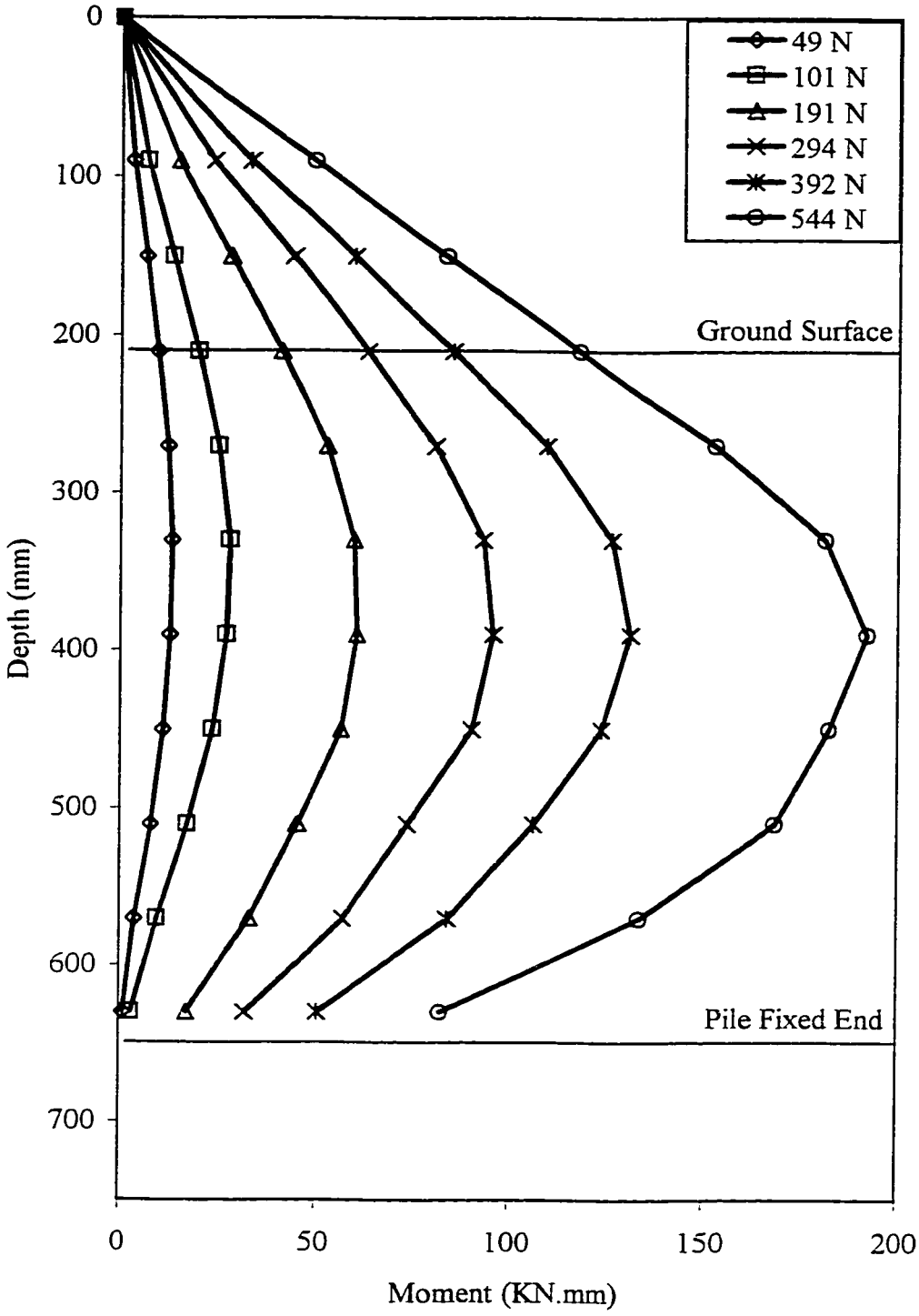

Figure 4.2: The Variation of Moment with Depth for Single Pile in Dry Sand Subjected to Static Loading.

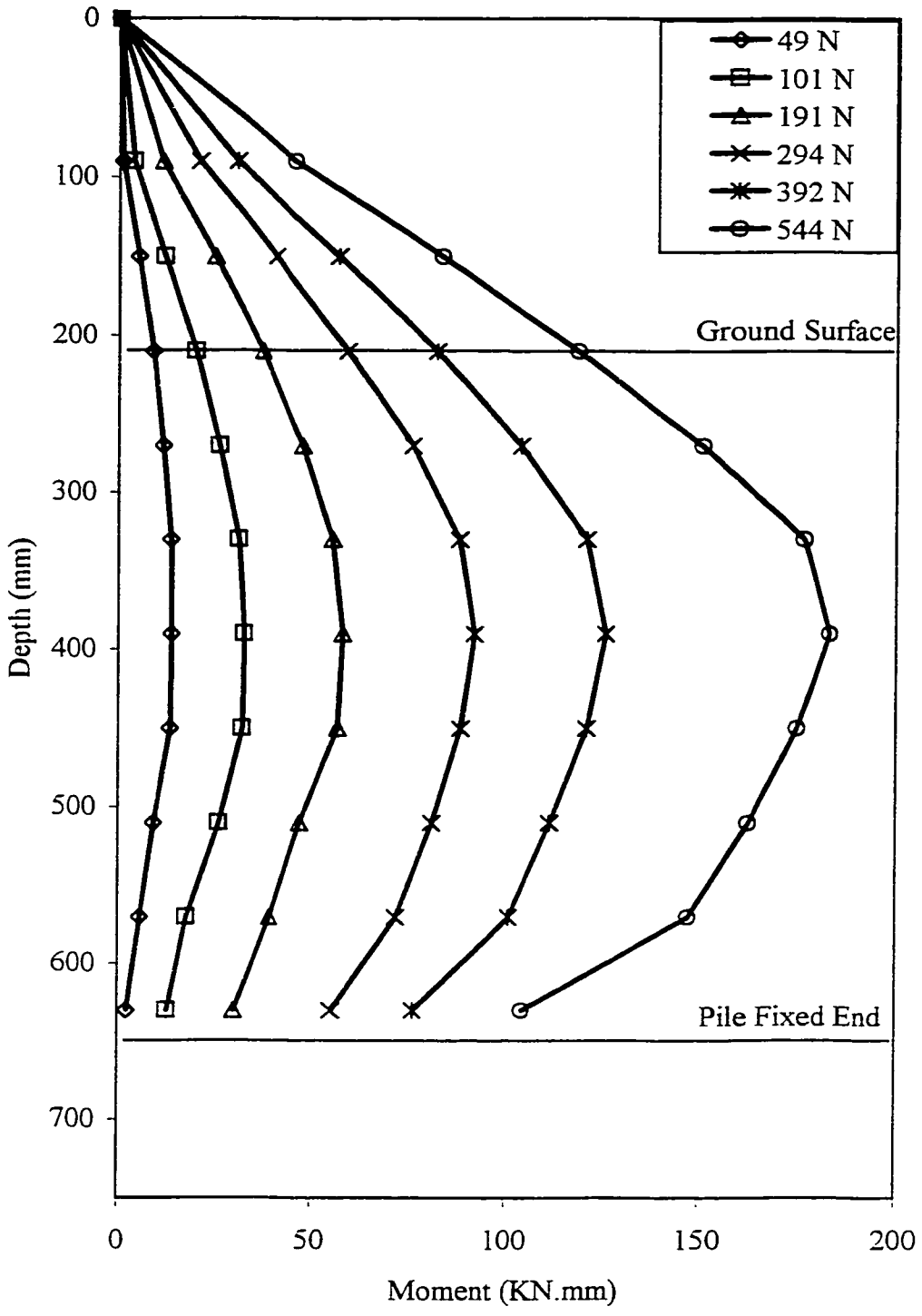

Figure 4.3: The Variation of Moment with Depth for Single Pile in Submerged Sand Subjected to Static Loading.

hence the moment decreases till it reaches the fixed end (stiff soil layer) where the pile movement is restricted by that layer.

The comparison of the moment diagrams for dry and submerged sand conditions is shown in Figure 4.4, at two load levels for namely 101 and 392 N. At the load level of 101 N, the pile embedded in submerged sand shows more moment than in dry condition due to the increase in pile curvature which is caused by reduction in soil response. The percentage difference in maximum moment at this load level is 10.3%. As the load level increases, the percentage difference between the maximum dry and maximum submerged moments starts to decrease (for 392 N, percentage difference is 5.6%). At high load levels (490 N), the maximum bending moments for both sand conditions are almost identical and at the same location. In conclusion, at high load levels the sand resistance was relatively reduced and the stiff layer (at the fixed end of the pile) was absorbing most of the resistance. Observing figure 4.4 shows that the bending moments at the fixed end were higher in case of submerged sand condition reflecting less sand resistance.

Deflection Along the Pile Length

Deflections along the pile length were obtained by feeding the computer program shown in Appendix B with the calculated moments and the deflections at the top of the pile measured at three different locations simultaneously. Figure 4.5 shows the deflected shape of single pile under static load for both dry and submerged sand conditions. The curves shown are for 392 and 495 N load levels, respectively. It proves that the deflection of the pile increases directly with the increase in the load level. To signify the effect of reducing the soil

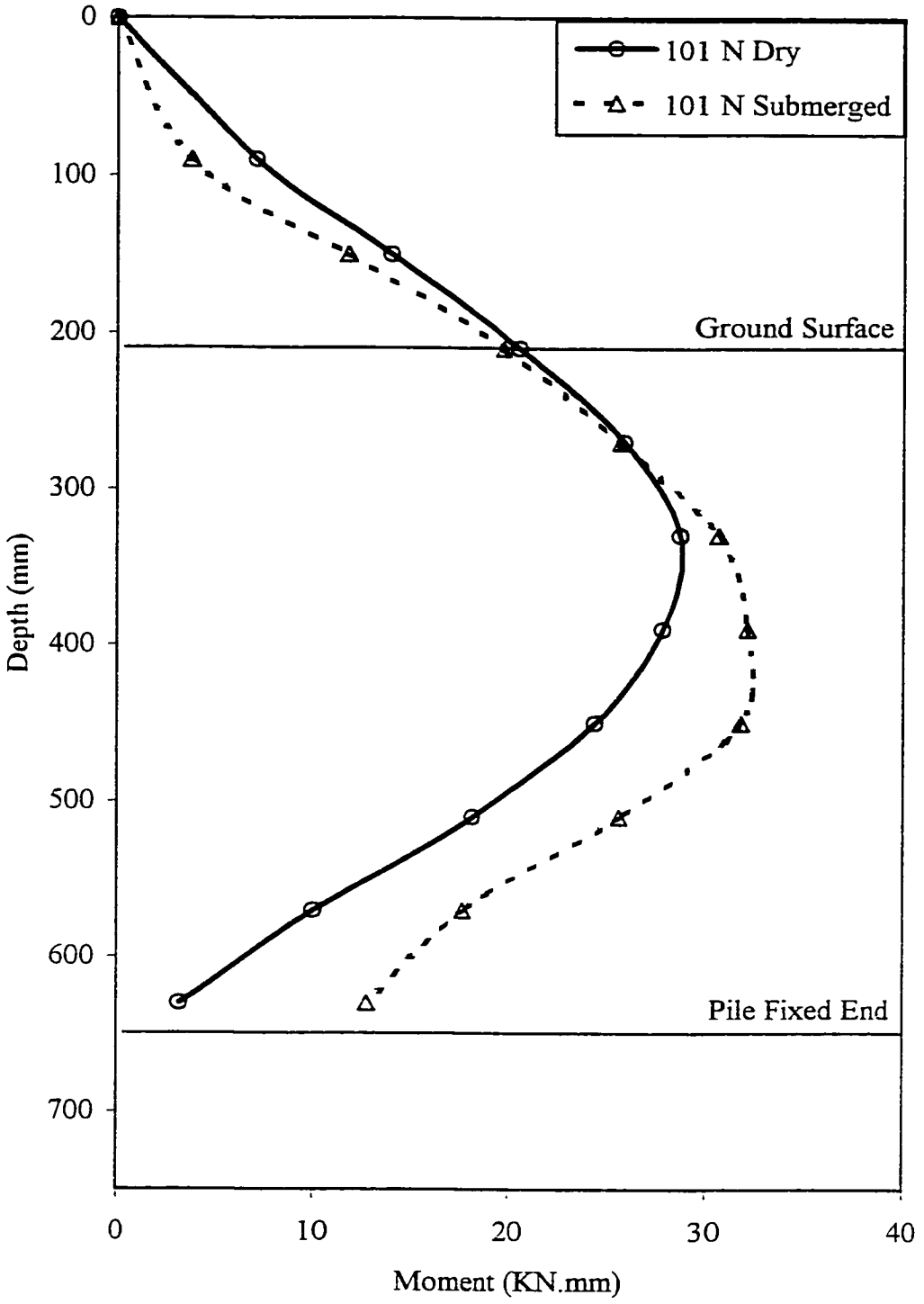

Figure 4.4a: Comparison of Moment Variation with Depth for Single Pile Between Dry and Submerged Sand Conditions at 101N Load Level.

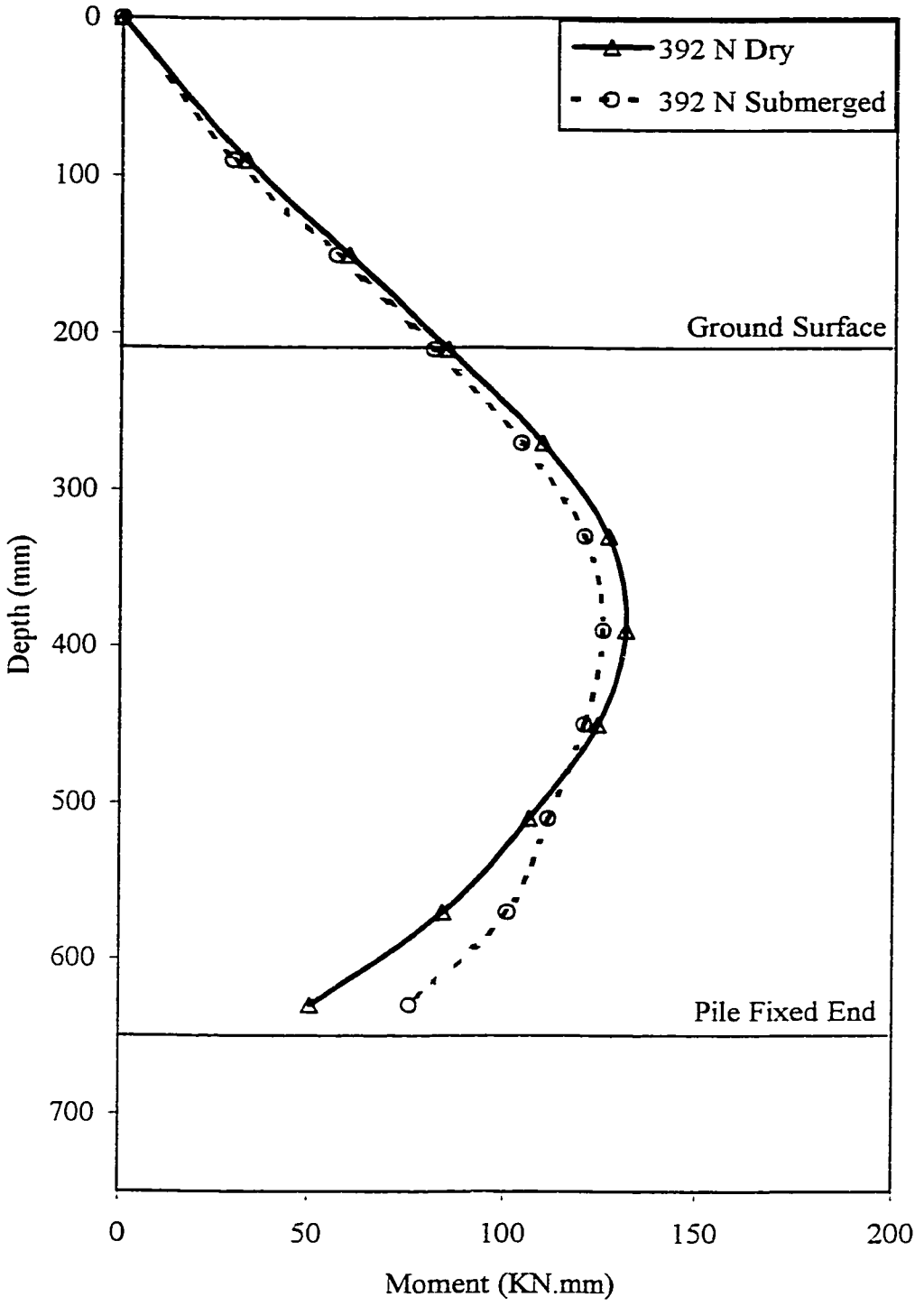

Figure 4.4b: Comparison of Moment Variation with Depth for Single Pile Between Dry and Submerged Sand Conditions at 392N Load Level.

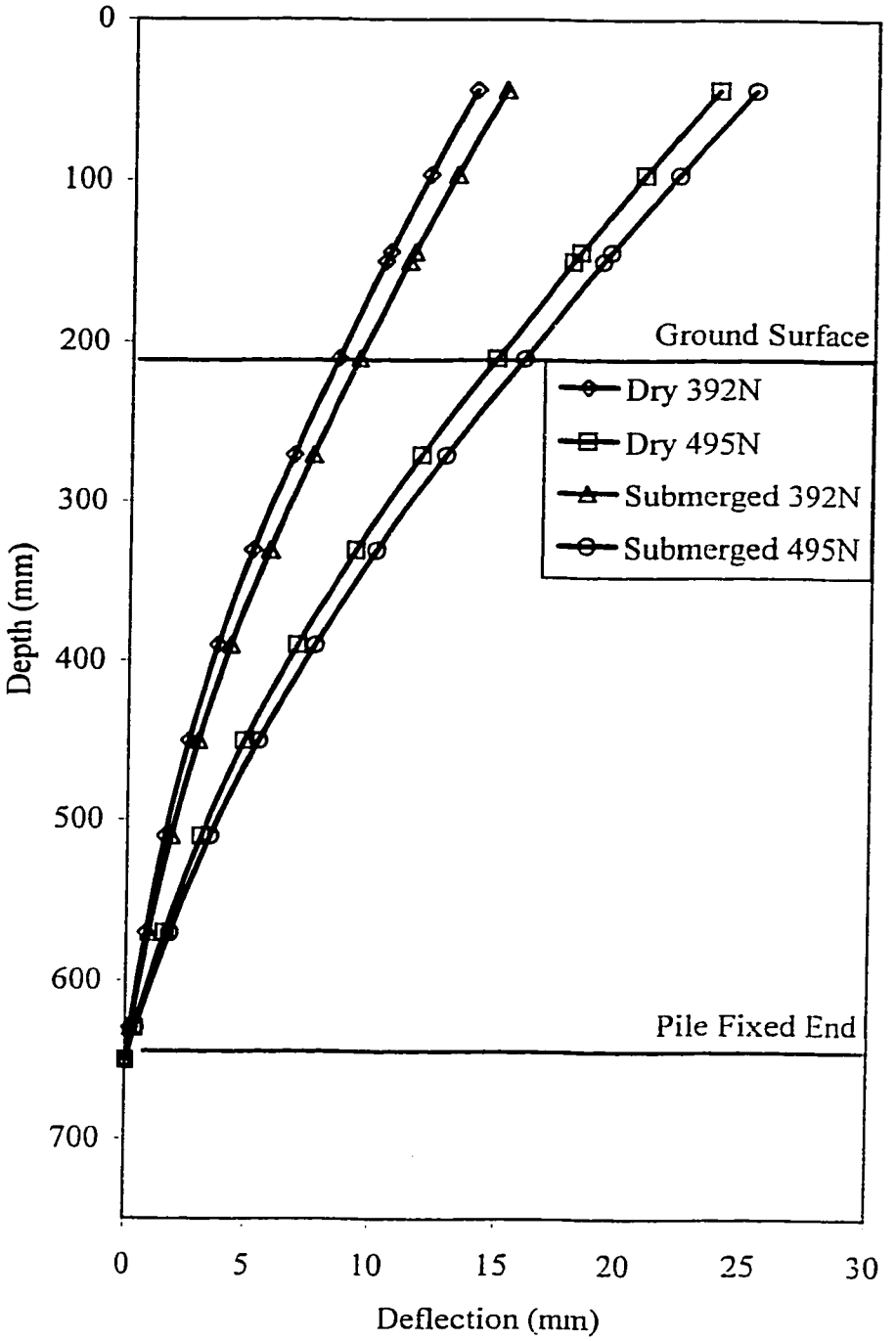

Figure 4.5: The Variation of Deflection with Depth for Single Pile Subjected to Static Lateral Load.

resistance due to submergence, the figure shows that the curvature along the length of the pile increases directly with load level, and that piles embedded in submerged soil deflects more than that embedded in dry soil for all load levels.

The deflection curve in all cases can be divided into two parts. First, the part above the ground surface, where the deflection can be represented by straight line. Second, the part below the ground surface, where deflected shape is not linear due to the effect of soil resistance. At the bottom of the pile the deflection will be diminished due to the forced fixity point (i.e. the slope of the moment curve is decreasing towards reaching the bottom pile cap).

p - y Curves

Figure 4.6 shows the best fit using the seventh degree polynomial presented in equation 4.5 for the moment diagram at dry sand condition. The values of the parameters (a_0 to a_7) for dry and submerged conditions and detailed calculations are shown in Appendix A. Deflection (y) along the pile were obtained from the conjugate beam method, while the soil resistance (p) were obtained from differentiating the moment polynomial equation twice. The soil resistance curves at different load levels for dry and submerged conditions are presented in figures 4.7 and 4.8, respectively. The sand is showing a higher resistance in the dry case than in the submerged case. This is an expected results because the effective soil density is higher in the former case and the soil resistance is directly proportional to the effective soil density as presented in equations 2.5 and 2.6. In other words, as the effective

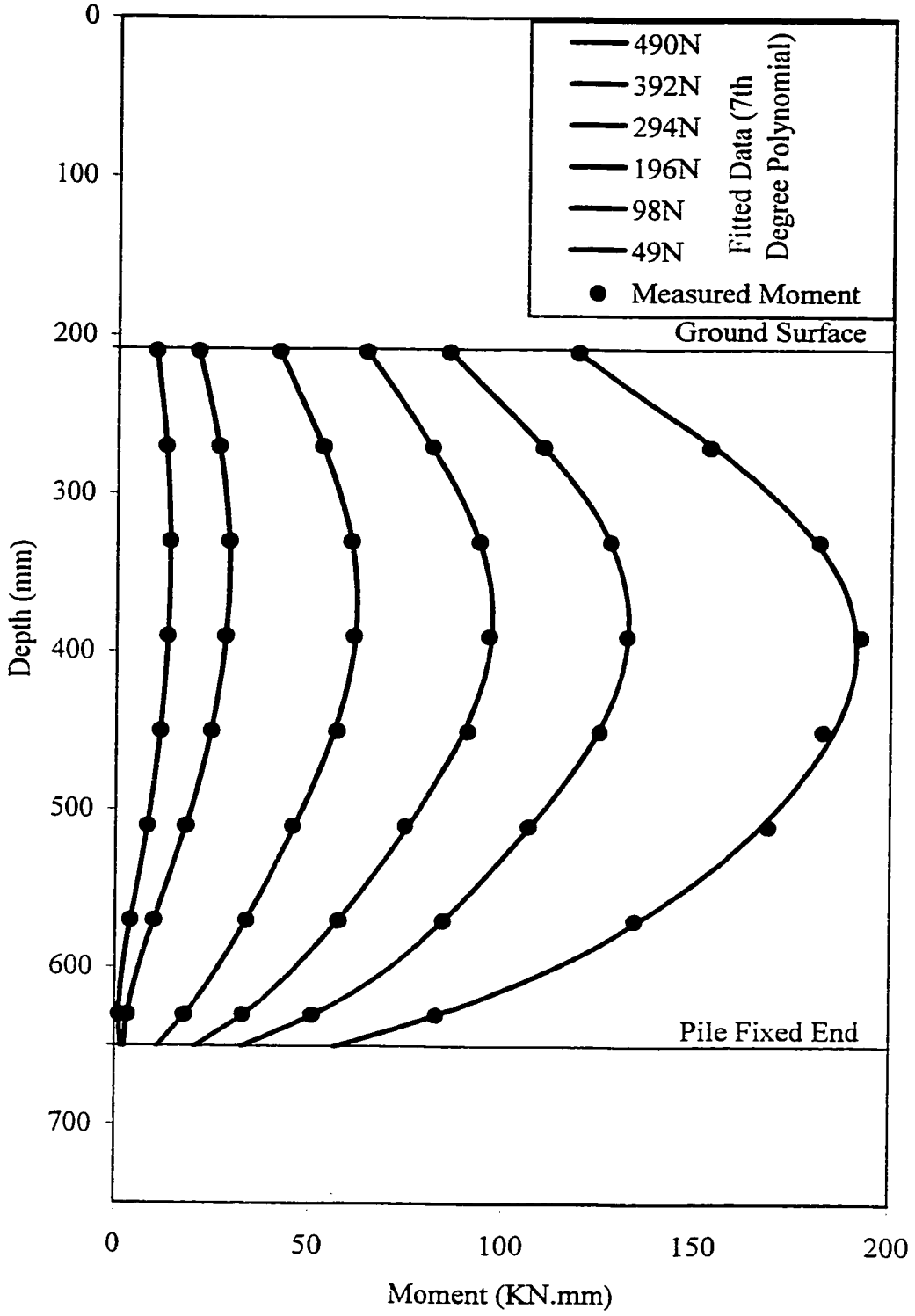

Figure 4.6: Moment Regression Curve for Single Pile in Dry Sand Subjected to Static Lateral Load.

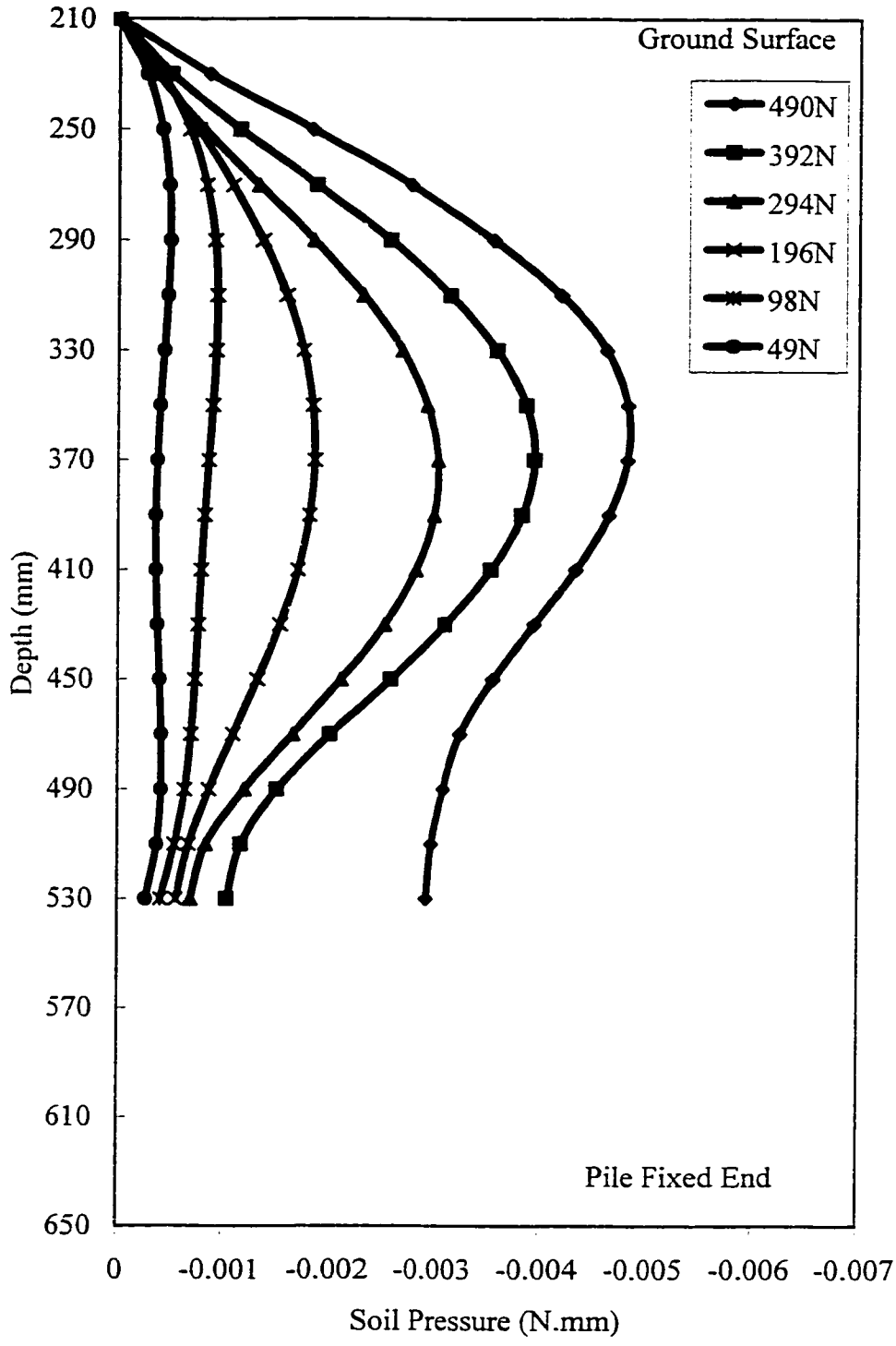

Figure 4.7: Soil Pressure for Single Pile in Dry Sand Subjected to Static Lateral Load.

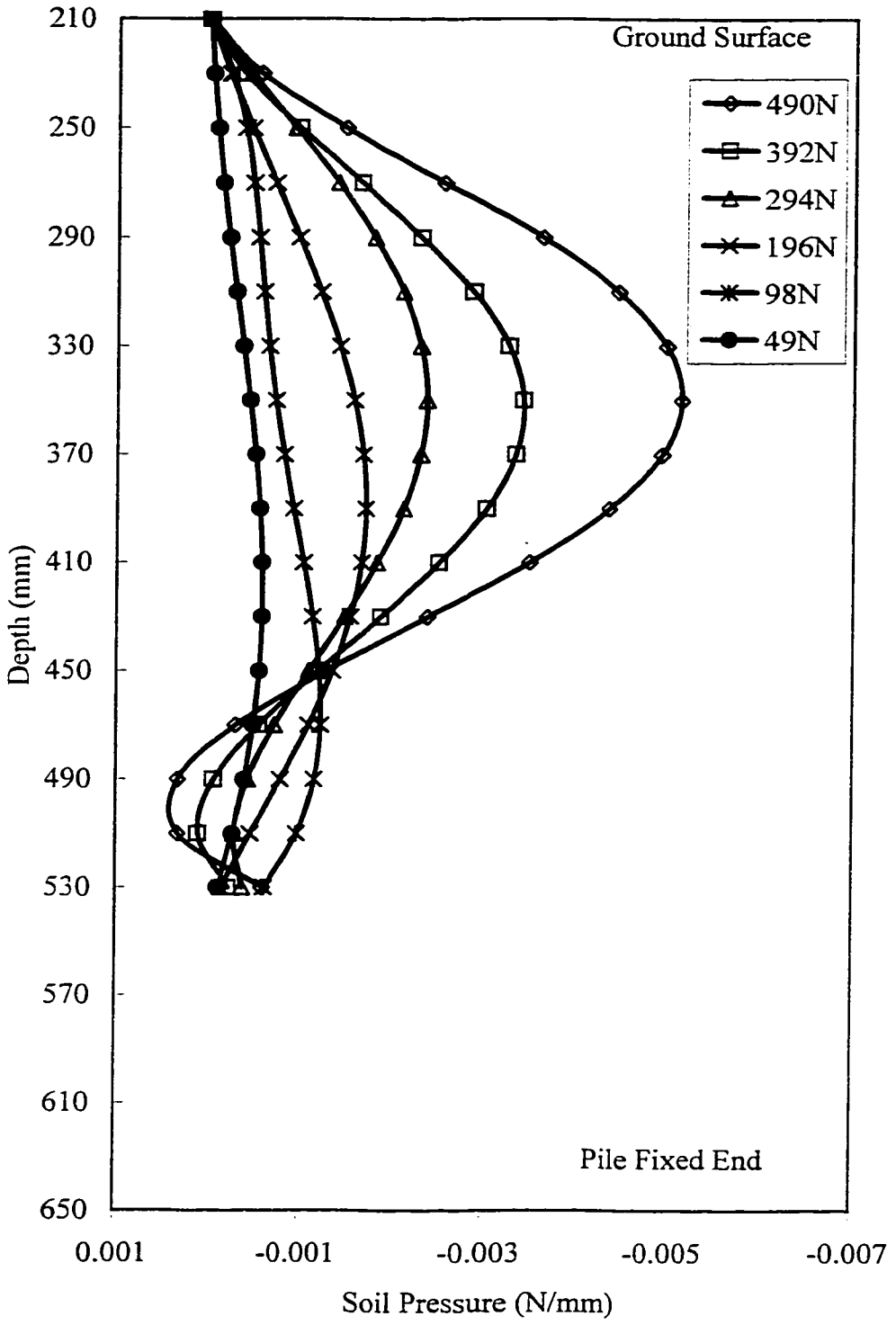

Figure 4.8: Soil Pressure for Single Pile in Submerged Sand Subjected to Static Lateral Load.

soil density increase the soil resistance increase accordingly. Moreover, the peak soil resistance occurs at a lower depth in the case of submerged sand condition due to the increase in soil confinement with depth for small load levels i.e. 49, 98, 196 N, while it occurs at almost the same depth for higher load levels. On the other hand and as indicated before, both the dry and the submerged conditions tend to behave almost the same at higher load levels. This is because the small submergence effect is at higher load levels. In comparing the lower parts of both figures, it is obvious that higher soil resistance is produced by the dry sand. Furthermore, higher bending moments, deflection and consequently greater pile curvature were produced in the submerged sand, where the soil resistance started to reduce gradually with increase in load level. Accordingly, at high load level opposite resistance was produced to counter-act the pile tendency to change its curvature to the opposite direction at the pile bottom. The p-y curves are presented in figures 4.9 and 4.10 for dry and submerged sand conditions, respectively. These curves present the soil pressure at three different depths i.e. 270, 330 and 390mm from the top of the pile. The figures show an increase in soil pressure due to an increase in both depth and pile top deflection. The soil pressure increases with the depth since the soil confinement increases with depth according to equation (2.2). Finally, the soil resistance values were always smaller in the submerged sand due to saturation, when considering them at the same depth, load level and deflection.

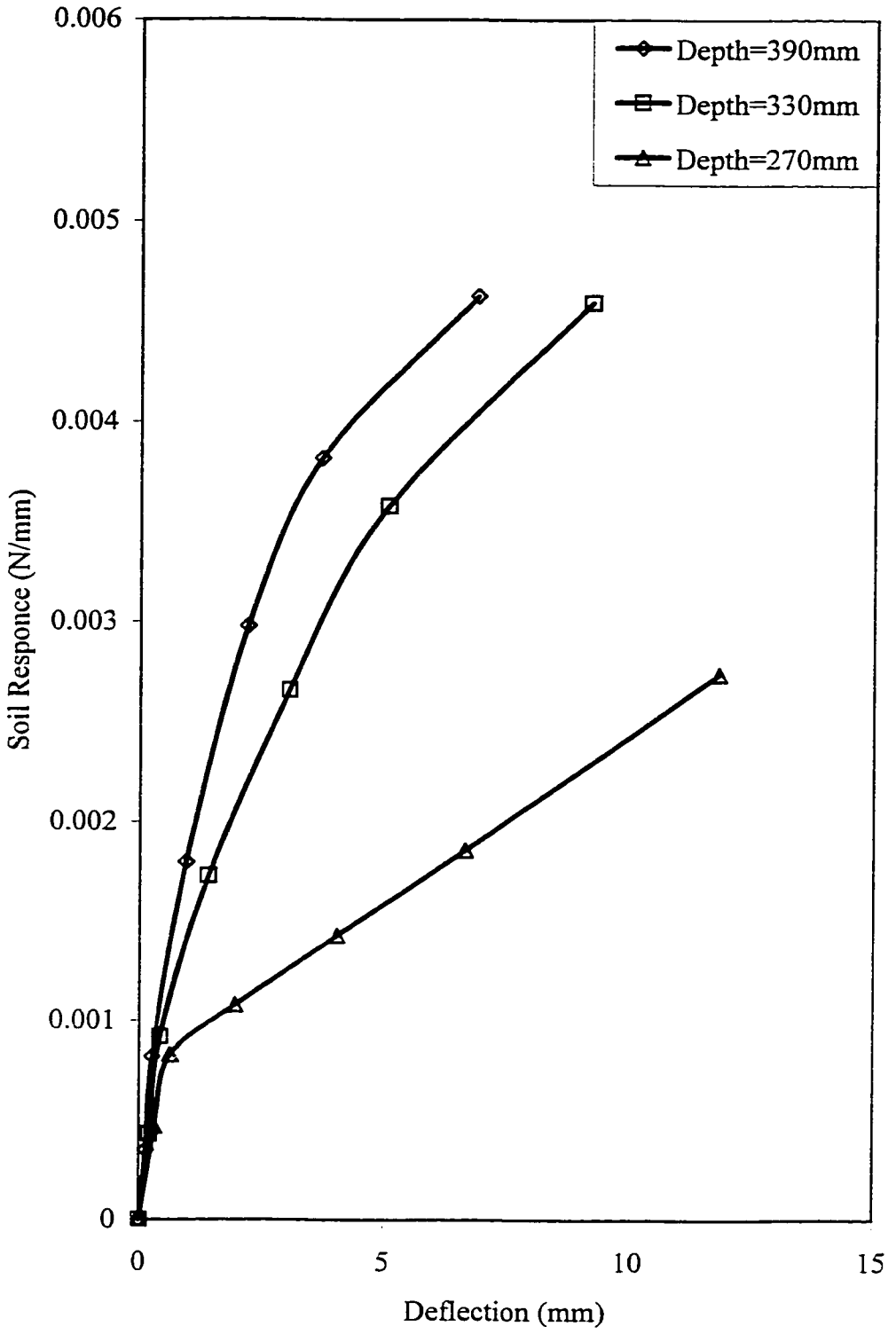

Figure 4.9: p-y Curves for Single Pile in Dry Sand Condition Subjected to Static Lateral Load.

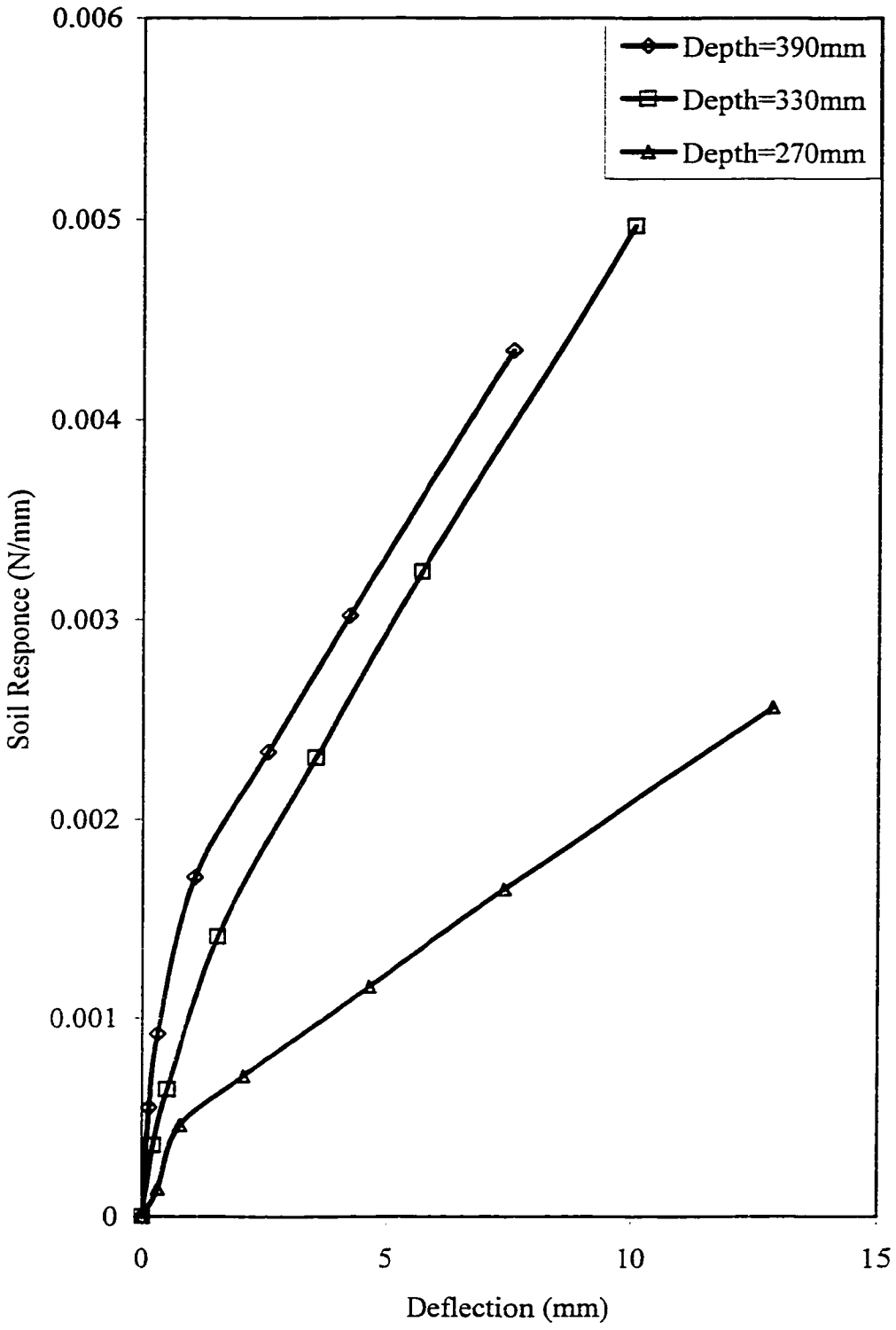

Figure 4.10: p-y Curves for Single Pile in Submerged Sand Condition Subjected to Static Lateral Load.

4.4.2 Four Pile Group

Piles usually are constructed in practice to form of a groups capped together to form one structural unit. In this section, a four pile group model was studied. This pile group consists of four model piles capped at the top and fixed at the bottom. The piles were arranged into two rows each containing two piles. They were spaced equally by a distance equivalent to four times the diameter of the pile center to center in both direction. The pile arrangement in the group is shown in figure 4.11. The piles were subjected to the load by the loading device via the top cap.

Top Deflection

Figures 4.12 and 4.13 depicts the pile head lateral load versus top deflection of front and back rows for both dry and submerged conditions. The figures represent the effect of submergence and row position on the pile top deflection according to pile head load. Figures 4.13a and 4.13b show the effect of the pile row position. It clearly shows that for the same pile head load level, the deflection is higher for the back row piles. This indicate that the group behavior is significantly associates with "Shadowing"; where the soil resistance of a pile in the back row is reduced due to the presence of the pile ahead of it. This is due to the fact that the back row resists less amount of sand pressure, which is laying between the two pile rows, and the deflection of the front pile will result in reducing the sand confinement. In other words, the pile in the front row takes up higher loads due to higher soil resistance and the pile attracts less load level at the back row due to less soil resistance. Moreover, the figure shows for piles embedded in submerged sand

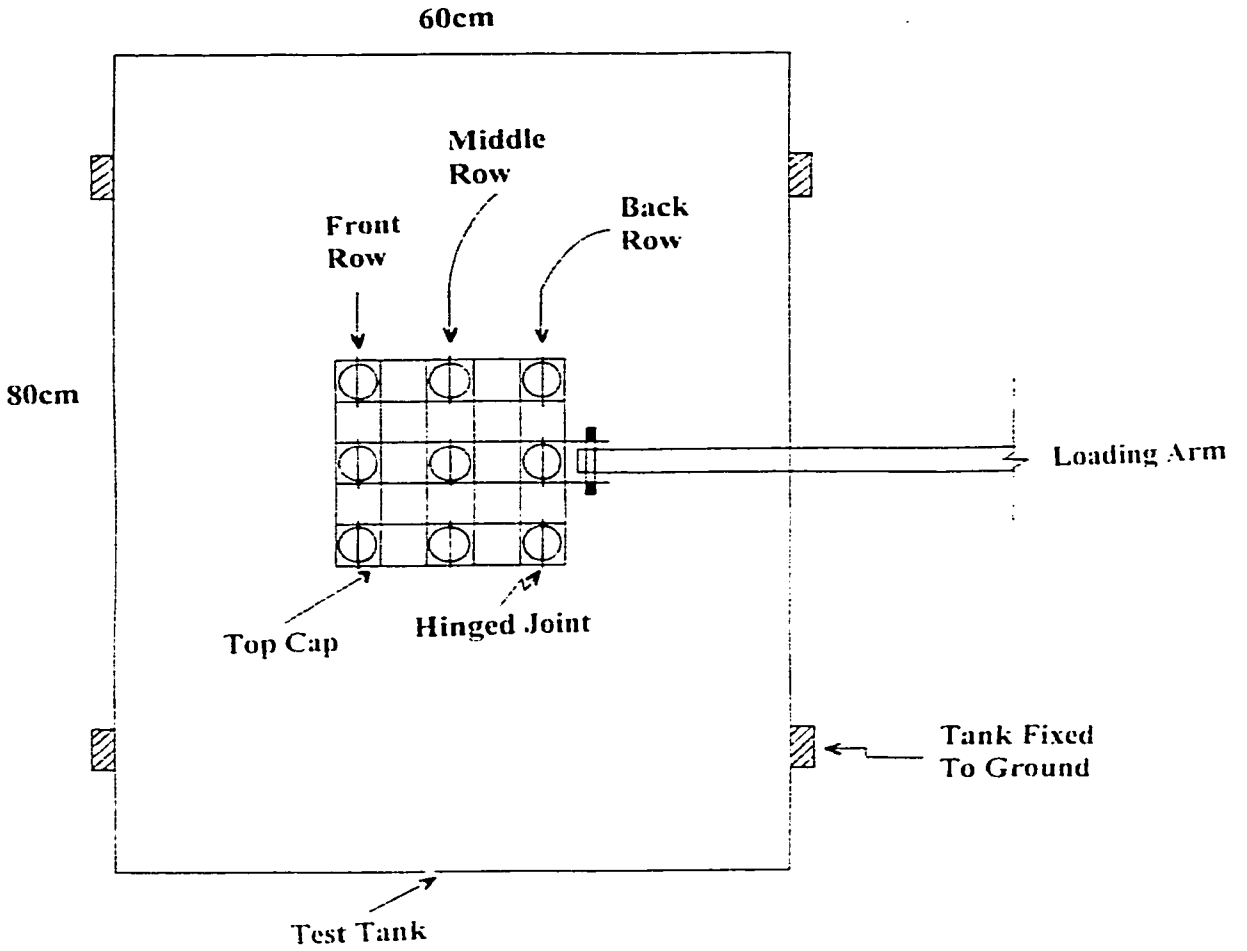

Test Setup Top View

Figure 4.11: Test Setup Top View.

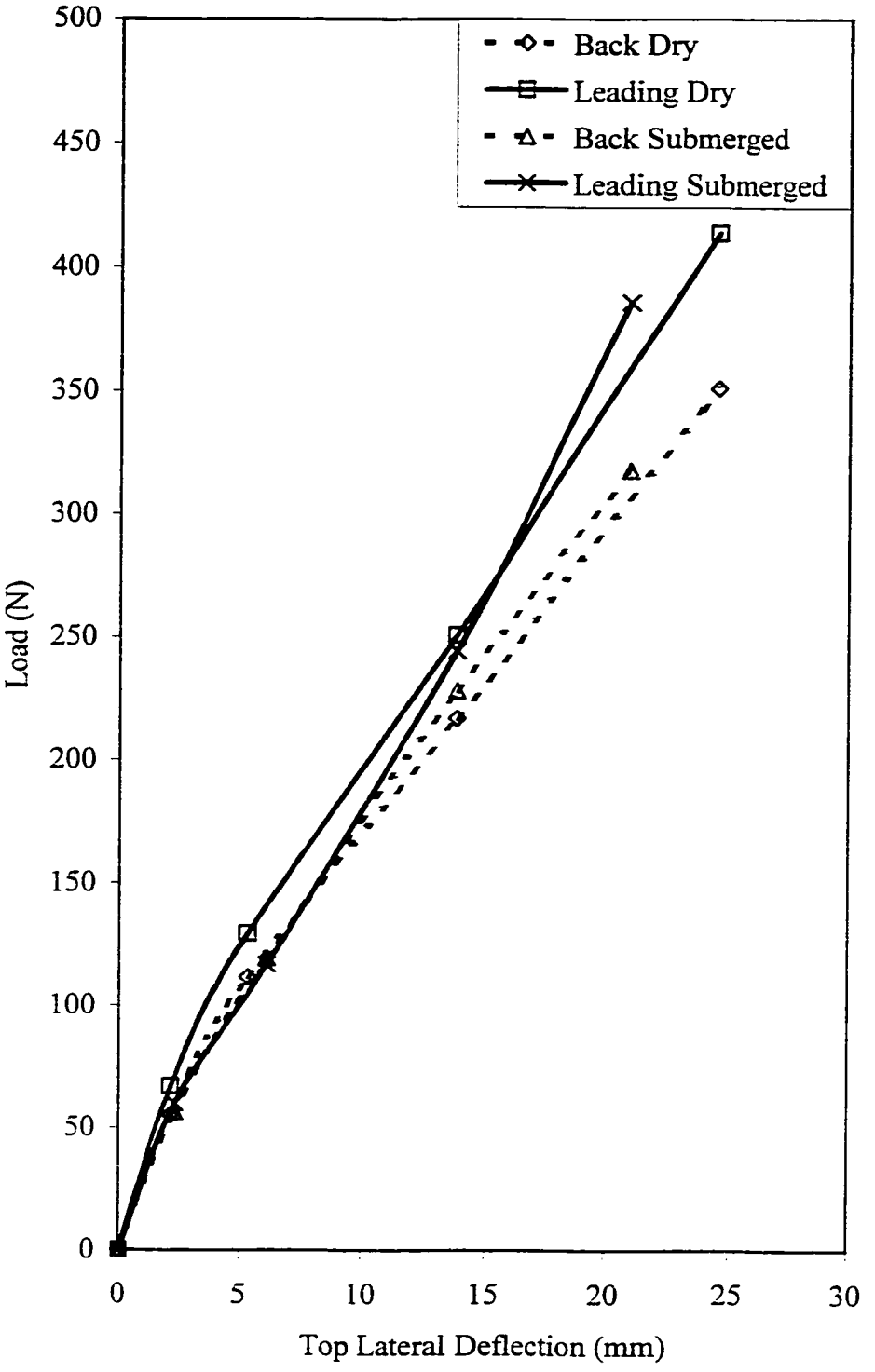

Figure 4.12: Load Deflection Curve for Four Pile Group Subjected to Static Lateral Load.

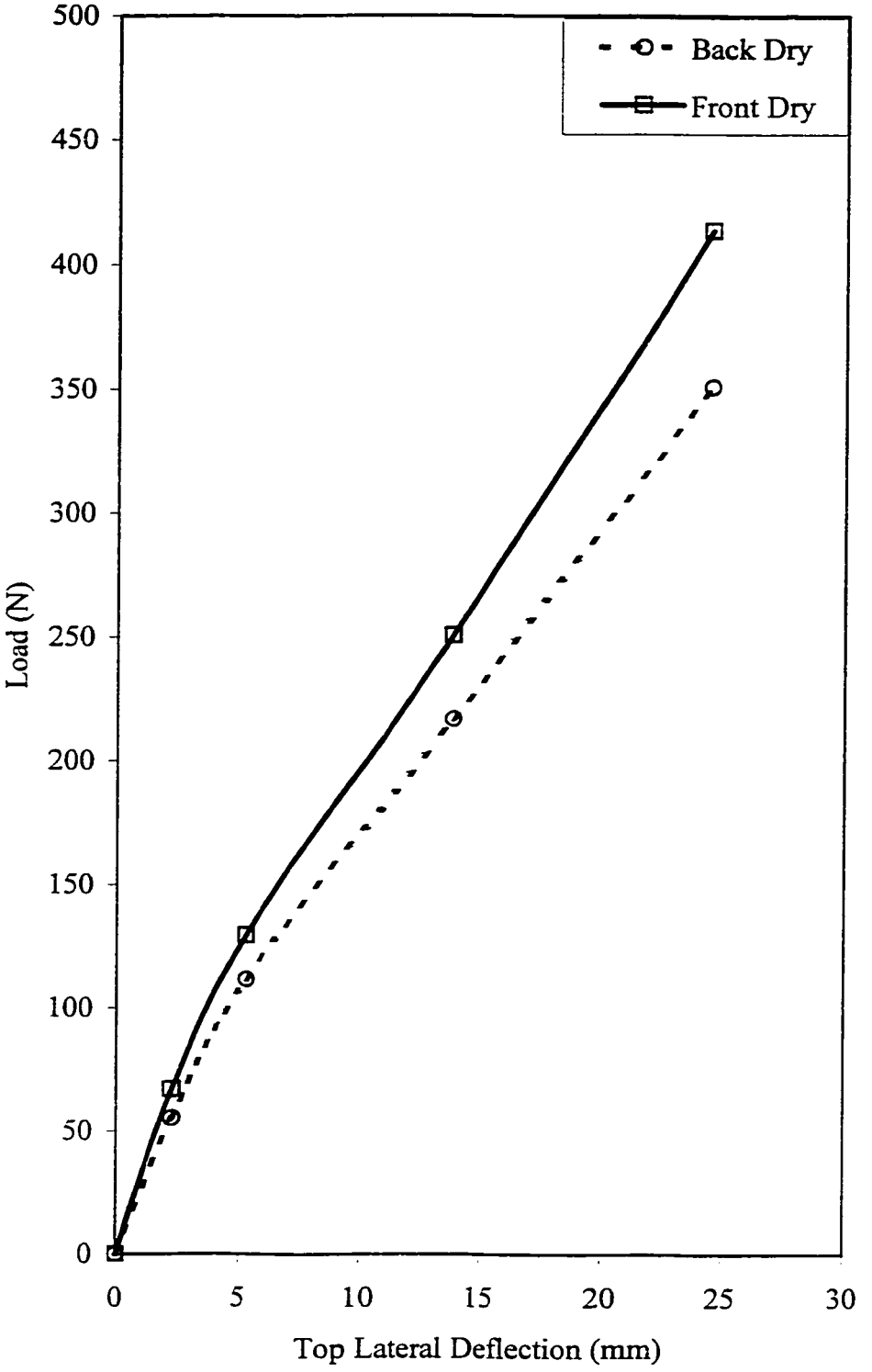

Figure 4.13a: Comparison of Load Deflection Curve for Four Pile Group Between Front and Back Row Piles in Dry Sand Subjected to Static Lateral Load.

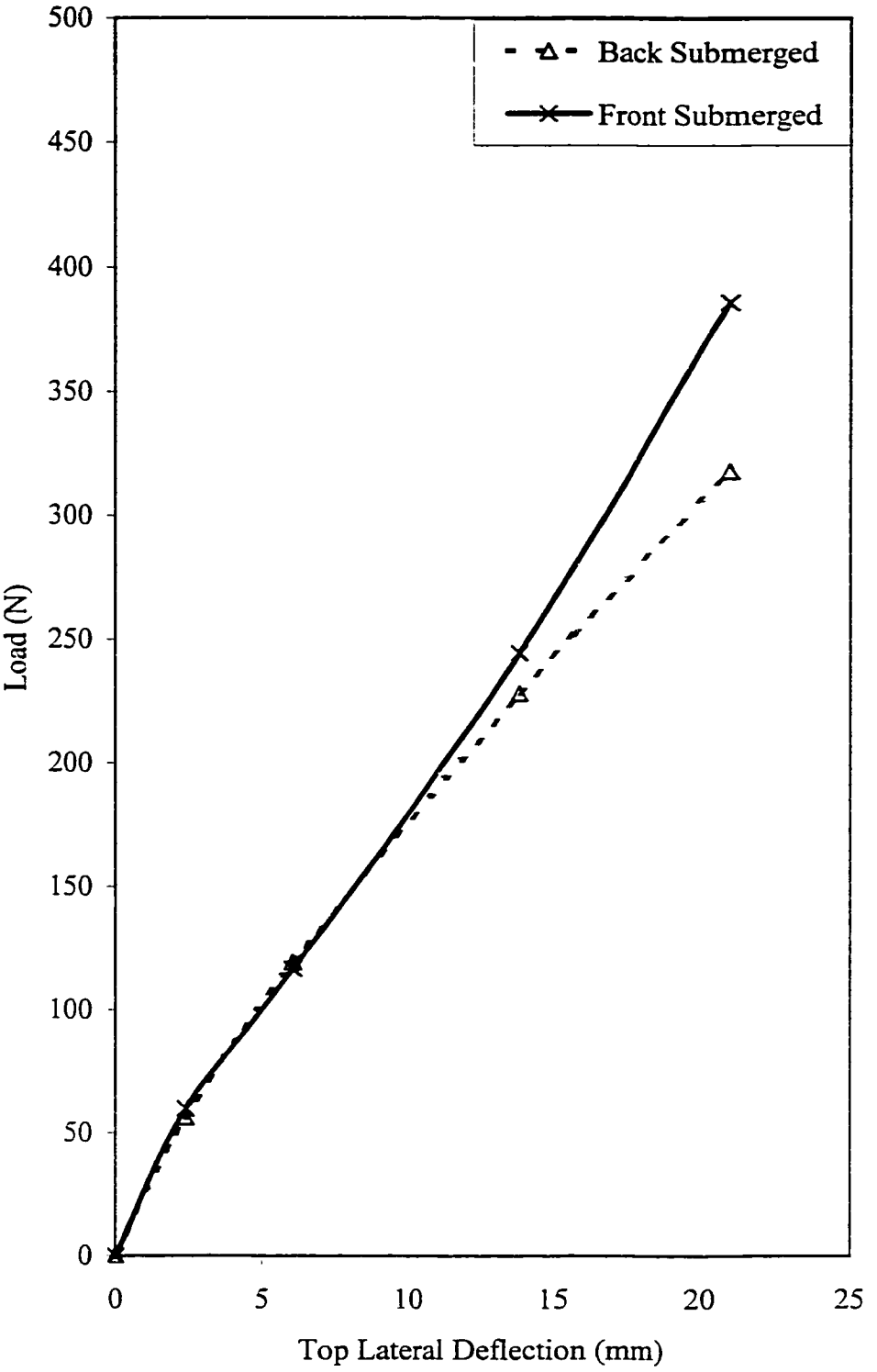

Figure 4.13b: Comparison of Load Deflection Curve for Four Pile Group Between Front and Back Row Piles in Submerged Sand Subjected to Static Lateral Load.

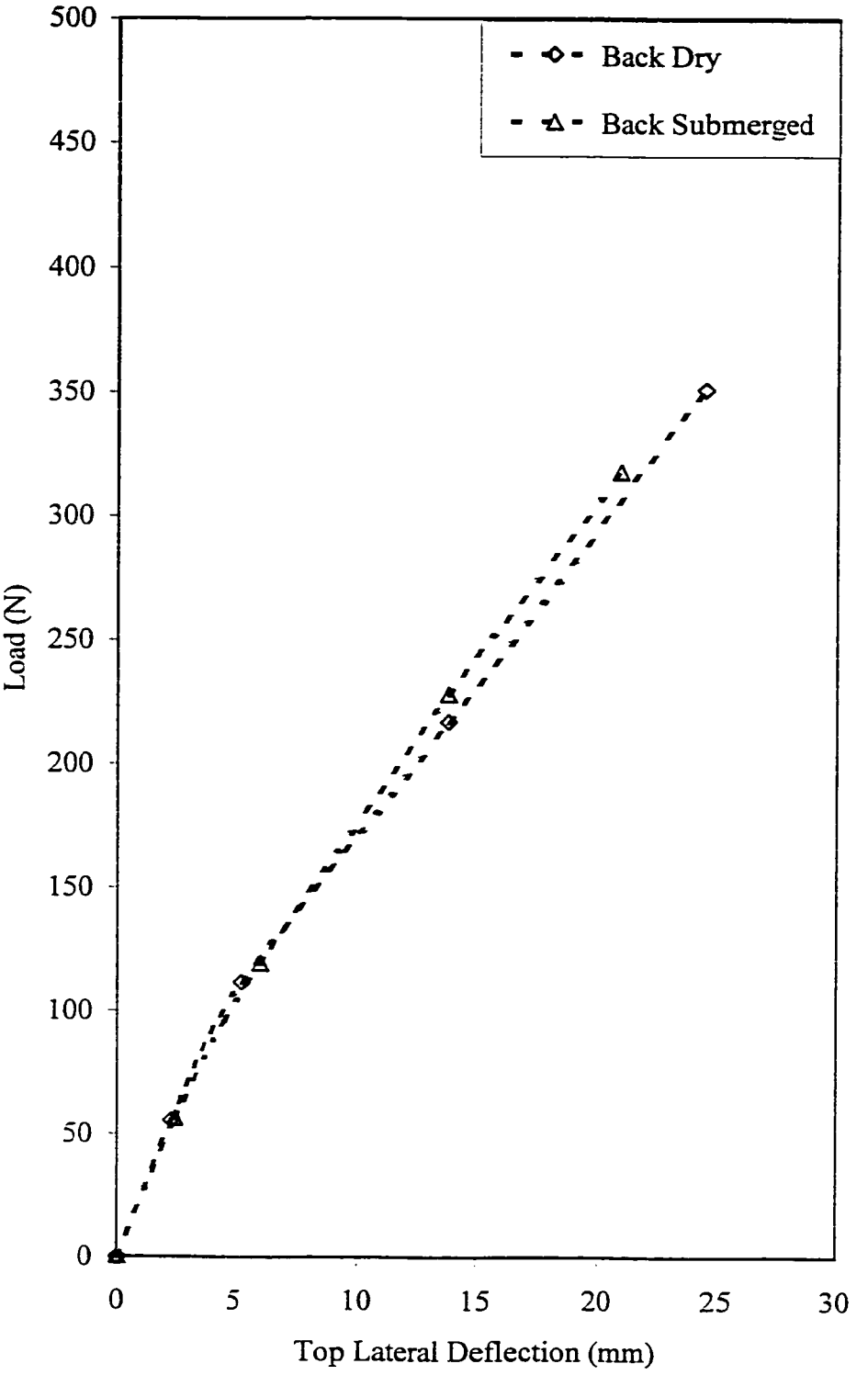

Figure 4.13c: Comparison of Load Deflection Curve for Four Pile Group Between Dry and Submerged Sand Conditions for Back Row Piles Subjected to Static Lateral Load.

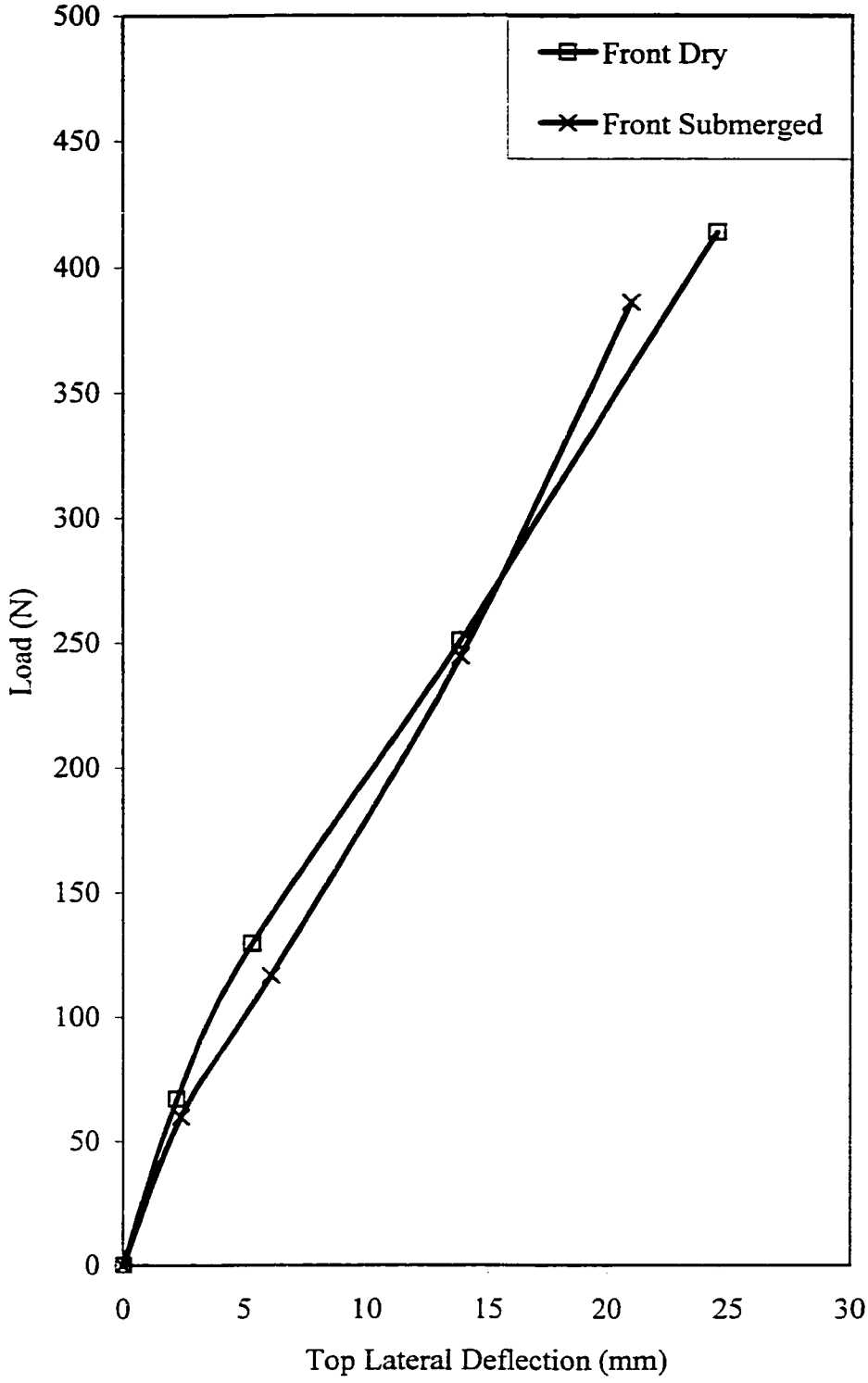

Figure 4.13d: Comparison of Load Deflection Curve for Four Pile Group Between Dry and Submerged Sand Conditions for Front Row Piles Subjected to Static Lateral Load.

that the difference in top deflection for the same load level is very small at low load level and increases as the load level increases. This is due to the effect of submergence that reduces the soil resistance.

Figures 4.13c and 4.13d show the effect of submergence on the group behavior for each row. The differences between the dry and submerged conditions for both front and back row were found negligible. It is concluded that the effect of submergence on four pile group is negligible for the case of top deflection. However, the behavior of the front row is the same as the single pile behavior, as it does not have any effect from sand shadowing which is greatly affecting the trailer (back) rows.

Moment Diagram

Moments diagram for pile group was obtained by the same procedure used previously for single pile. Figures 4.14 and 4.15 present the moment diagrams at different load levels for four pile group subjected to static load for dry and submerged sand conditions, respectively. The figures clearly show that the front row pile are attracting higher moments while the back row pile are attracting lower moments. This is because the front row attracts more pile head load due to higher soil resistance while the back row piles attracts less due to the shadowing effect of the sand as mentioned before. Figure 4.15 shows that the lower part of the piles attract more moments which means that the effect of shadowing is decreasing with depth in the case of submerged sand condition. This was due to reduction in soil resistance which is directly proportional to the effective density.

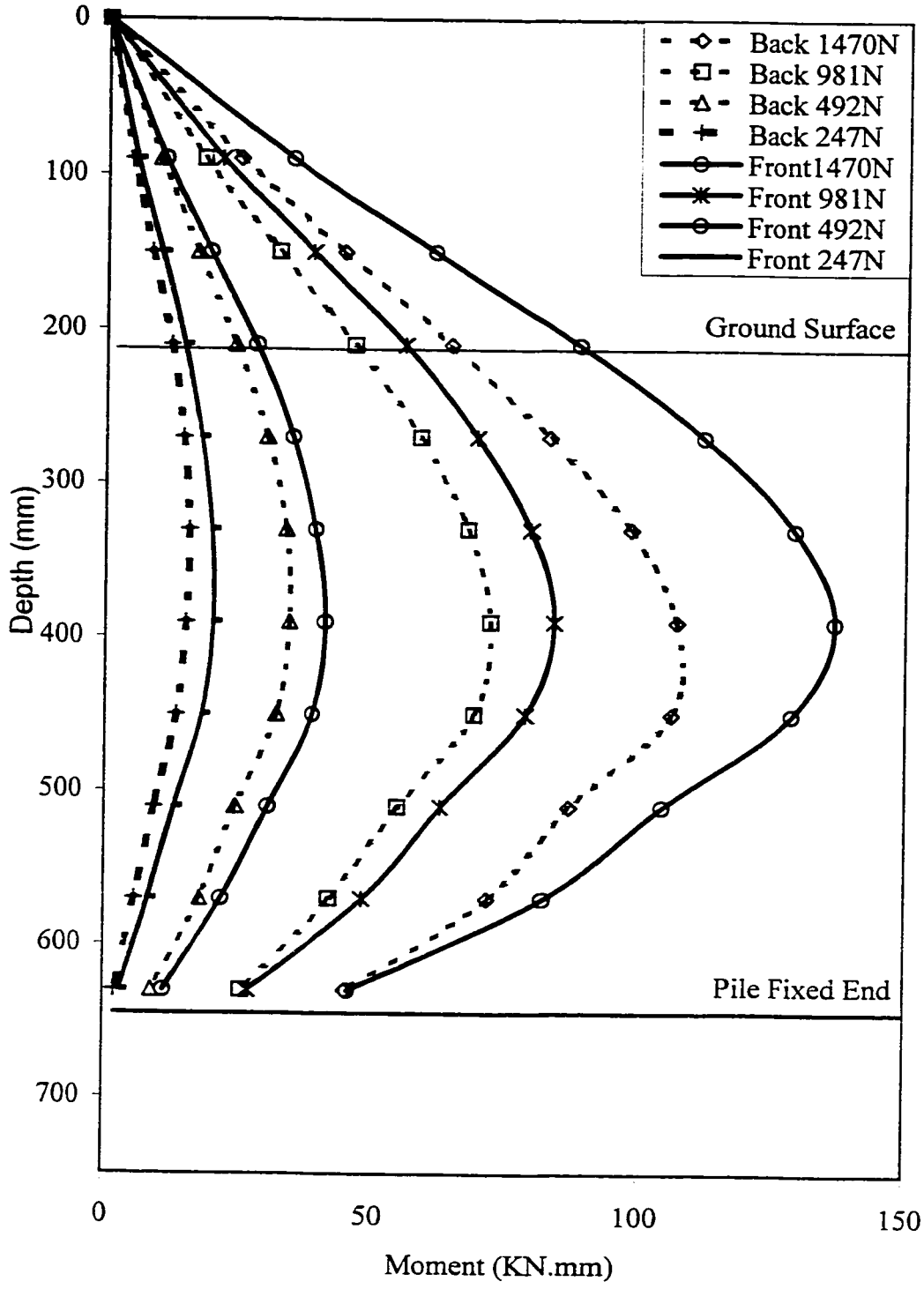

Figure 4.14: The Variation of Moment with Depth for Four Pile Group in Dry Sand Subjected to Static Lateral Load.

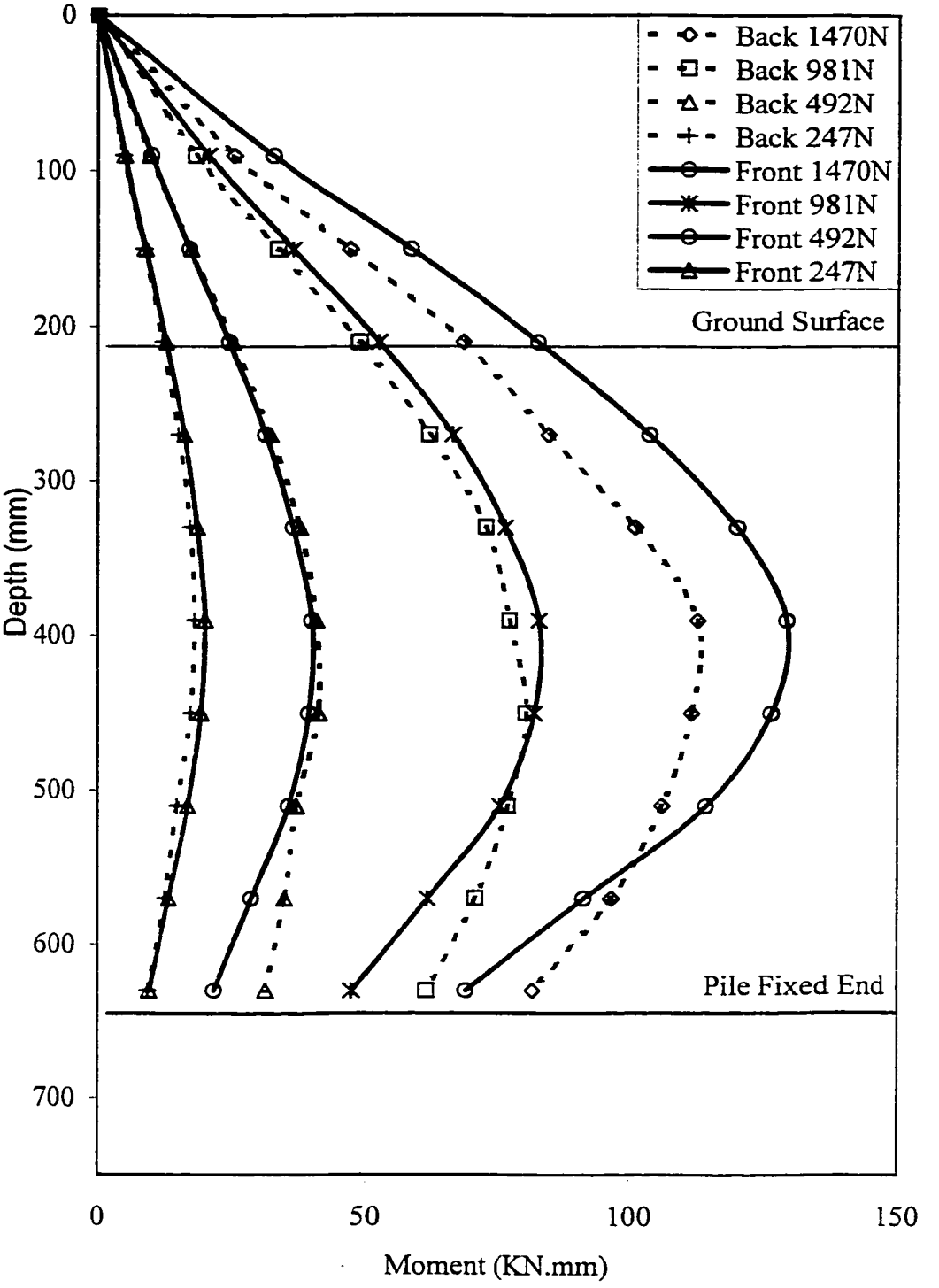

Figure 4.15: The Variation of Moment with Depth for Four Pile Group in Submerged Sand Subjected to Static Lateral Load.

From both figures, it is clear that as the load level increases, the difference in the moment between the front and the back row piles increases accordingly. Moreover, this difference in the submerged condition is smaller than that in the dry one. The percentage difference in maximum moment is presented clearly in figure 4.16, for each load level. This may reflect that due to submergence the difference in the amount of load level per pile head sustained by front and back row is lower on the piles embedded in submerged sand.

Figures 4.17 and 4.18 show a comparison between the dry and submerged sand conditions and their effect on the front and back rows. Figure 4.17 shows that for the same pile cap load level, the moment is higher in the front piles embedded in the dry sand. This is mainly because the moment is compared against the total cap load level applied to the pile and not against the pile head load level, since the piles in the front row in the dry sand sustain more load than the one in submerged sand. Therefore, front row pile embedded in dry sand attracts higher pile head load level for the same pile cap load level (group load level) due to shadowing effect, which is reduced due to submergence. In other words, the comparison must be taken on the normalized moment diagrams which will be discussed later. On the other hand, the back row case (figure 4.18) does not contradict the front row case, since the back row piles get higher share of the piles group load in the case of submergence as discussed before.

As the load level increases the percentage difference in the maximum moment due to submergence is decreasing as shown in figure 4.19. Even though the figure presents

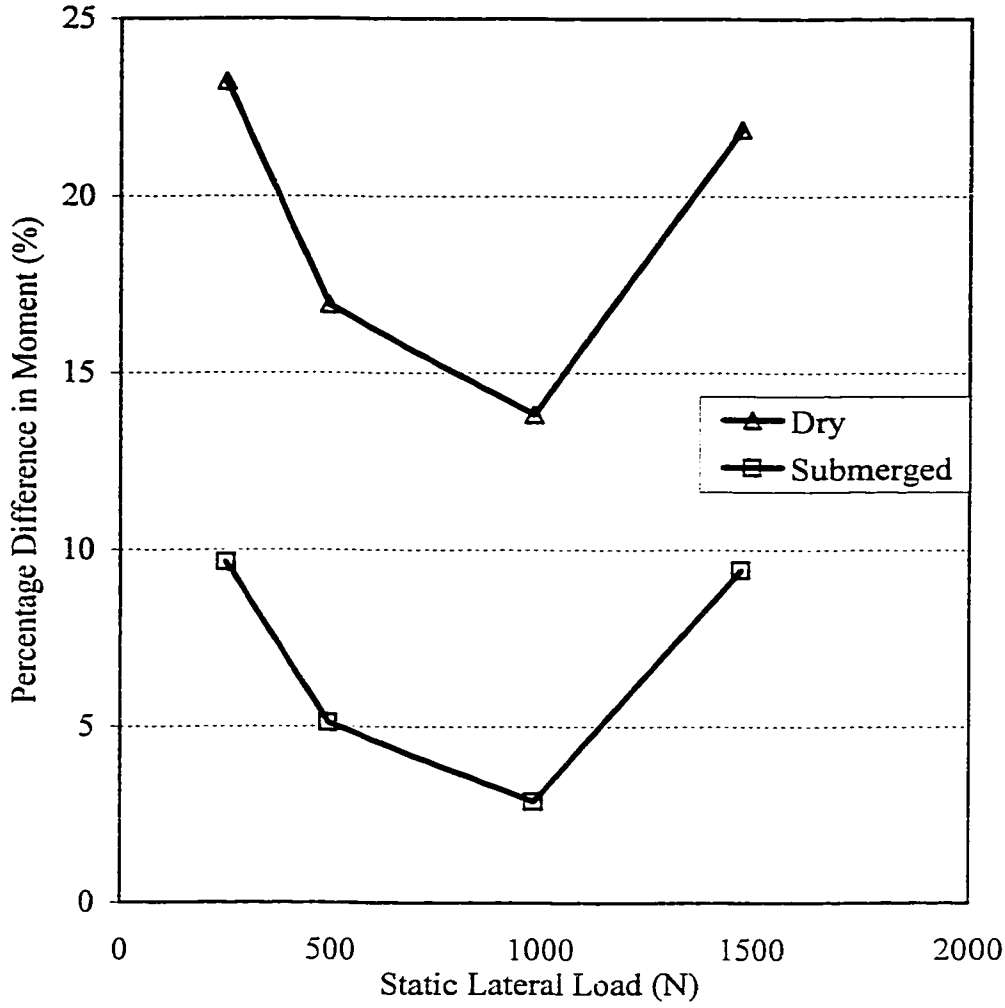

Figure 4.16: The Variation in Percentage Difference in Moment Between Front and Back Row Piles for Four Pile Group Subjected to Static Lateral Load.

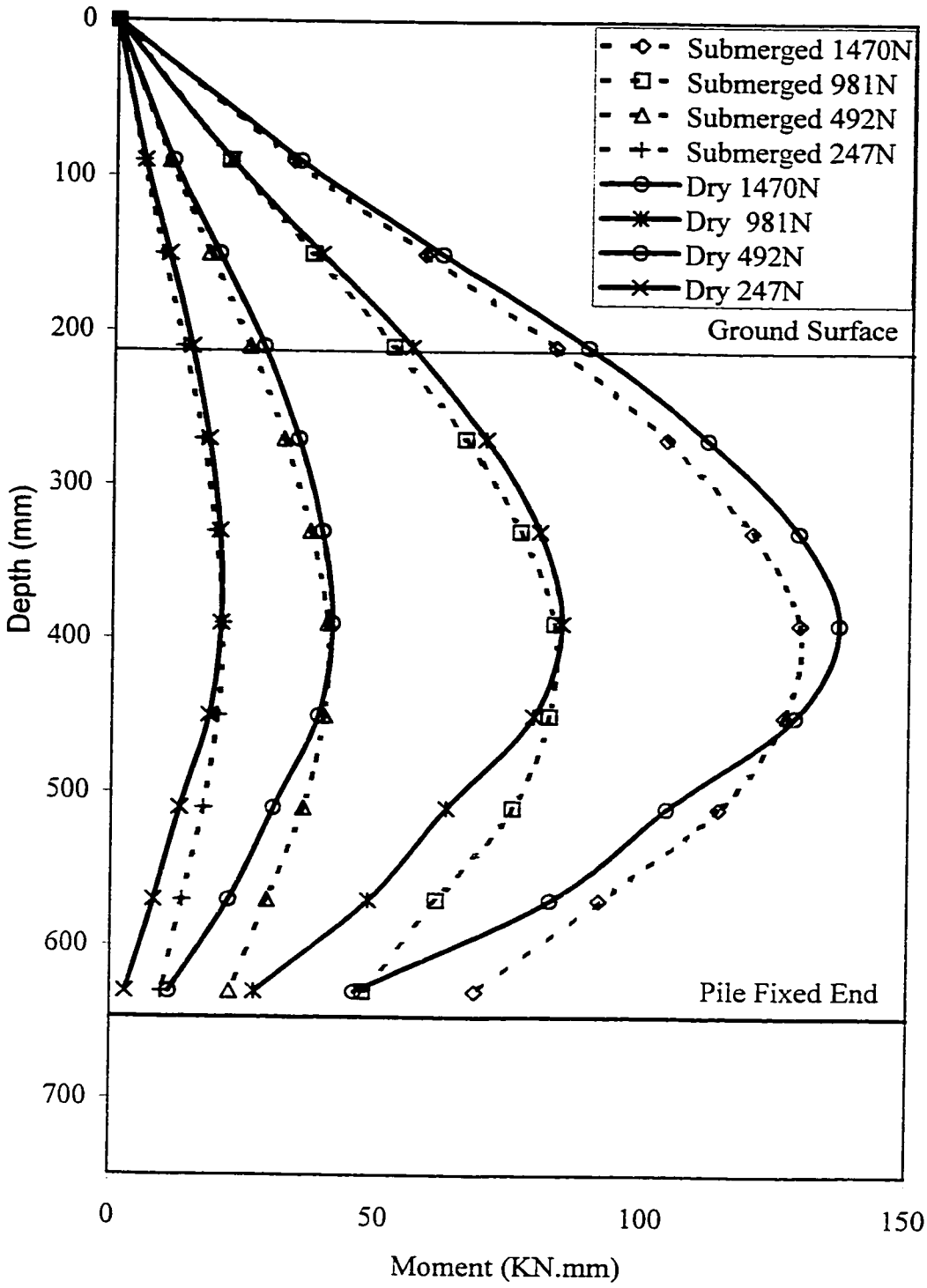

Figure 4.17: The Variation of Moment with Depth for Front Row Piles in Four Pile Group Subjected to Static Lateral Load.

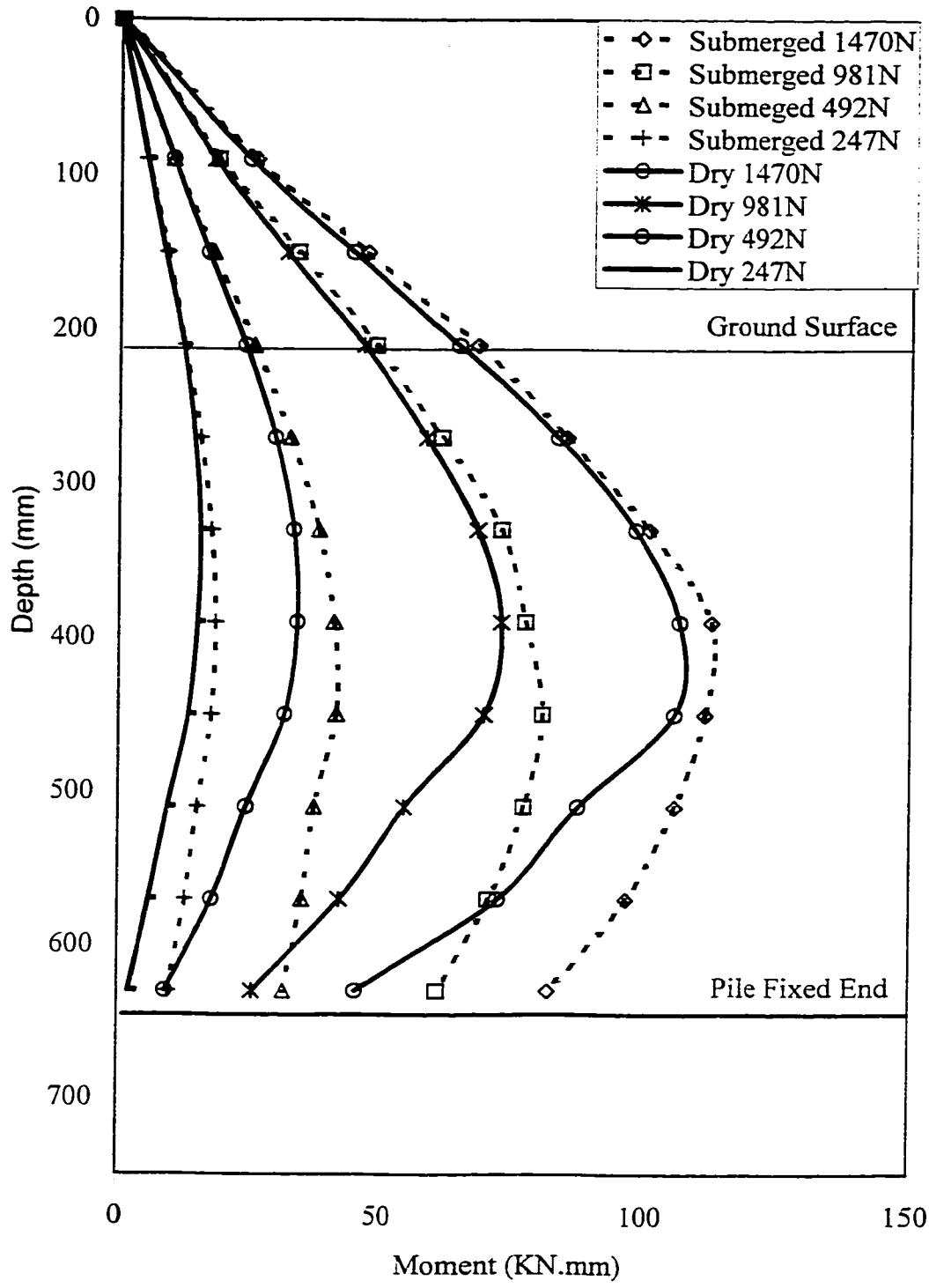

Figure 4.18: The Variation of Moment with Depth for Back Row Piles in Four Pile Group Subjected to Static Lateral Load.

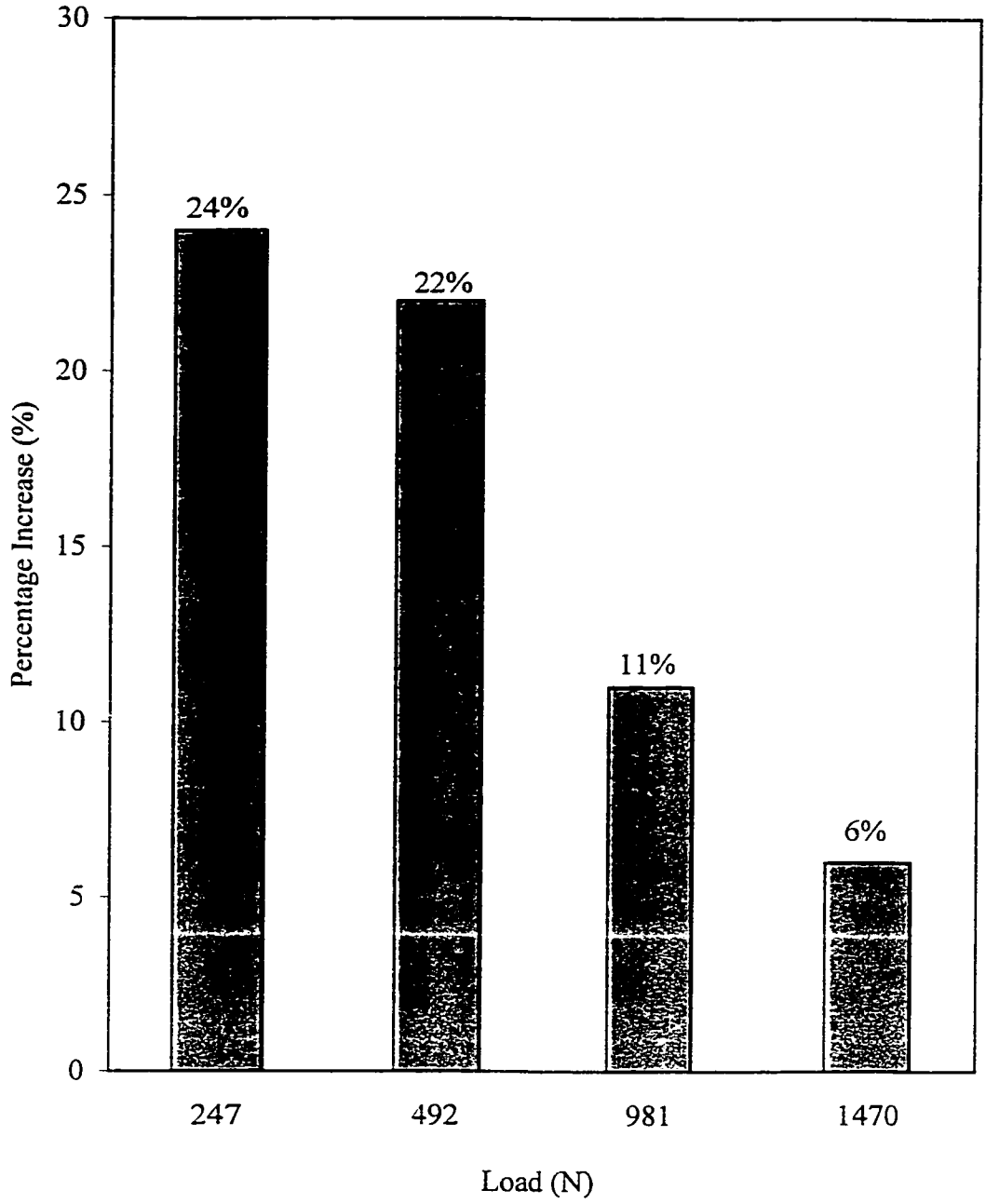

Figure 4.19: The Percentage Increase in Maximum Moment Due to Submergence for Back Row Piles in Four Pile Group Subjected to Static Lateral Load.

resistance in the case of the back row, the condition applied to the front row. This is occurring as the load level increases the effect of sand on the piles decreases accordingly since the piles movement is greatly governed by the pile group movement.

Normalized Moment:

It is necessary to unify the moment diagram (normalize the moment) as it is difficult to discuss the effect of the pile group on each isolated pile. Here the load is unevenly distributed with respect to row location. Since the changing factor here is the load per pile head, it is convenient to normalize the moments according to a unit load. Therefore, all moments diagram values were considered per their pile head load. Sample calculation for producing normalized moment is presented in Appendix A. Figures 4.20 and 4.21 present typical normalized moment diagrams comparing the front and back pile rows, and the percentage difference for both pile groups embedded in dry and submerged sand, respectively. The figures depict that the maximum moment is always greater for the back rows piles when normalized. However, the non-normalized maximum moments for a given group load are greater in the piles of the front rows. Furthermore, the maximum moment in the piles of the back rows occurs at greater depth compared to that on the front row piles, due to the reduction in the load transfer near the sand surface. This conclusion was also found by Reese et al (1983).

Figures 4.20 and 4.21 present that at small load increments piles behaves just like the single isolated pile due to the very small soil resistance and hence, negligible shadowing

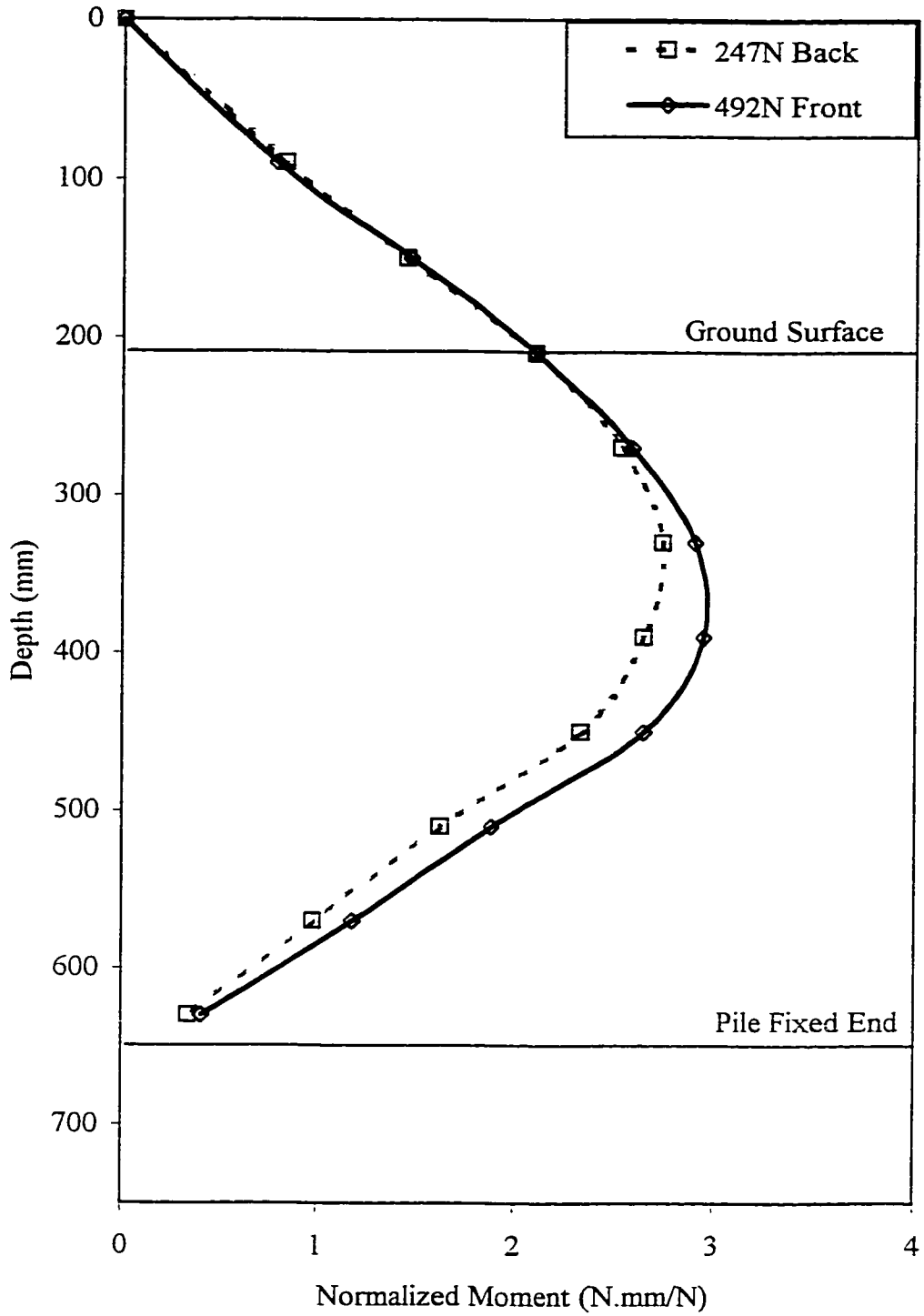

Figure 4.20a: Comparison of Normalized Moment Variation with Depth for Four Pile Group Between Front and Back Row Piles in Dry Sand Subjected to 247N Static Lateral Load Level.

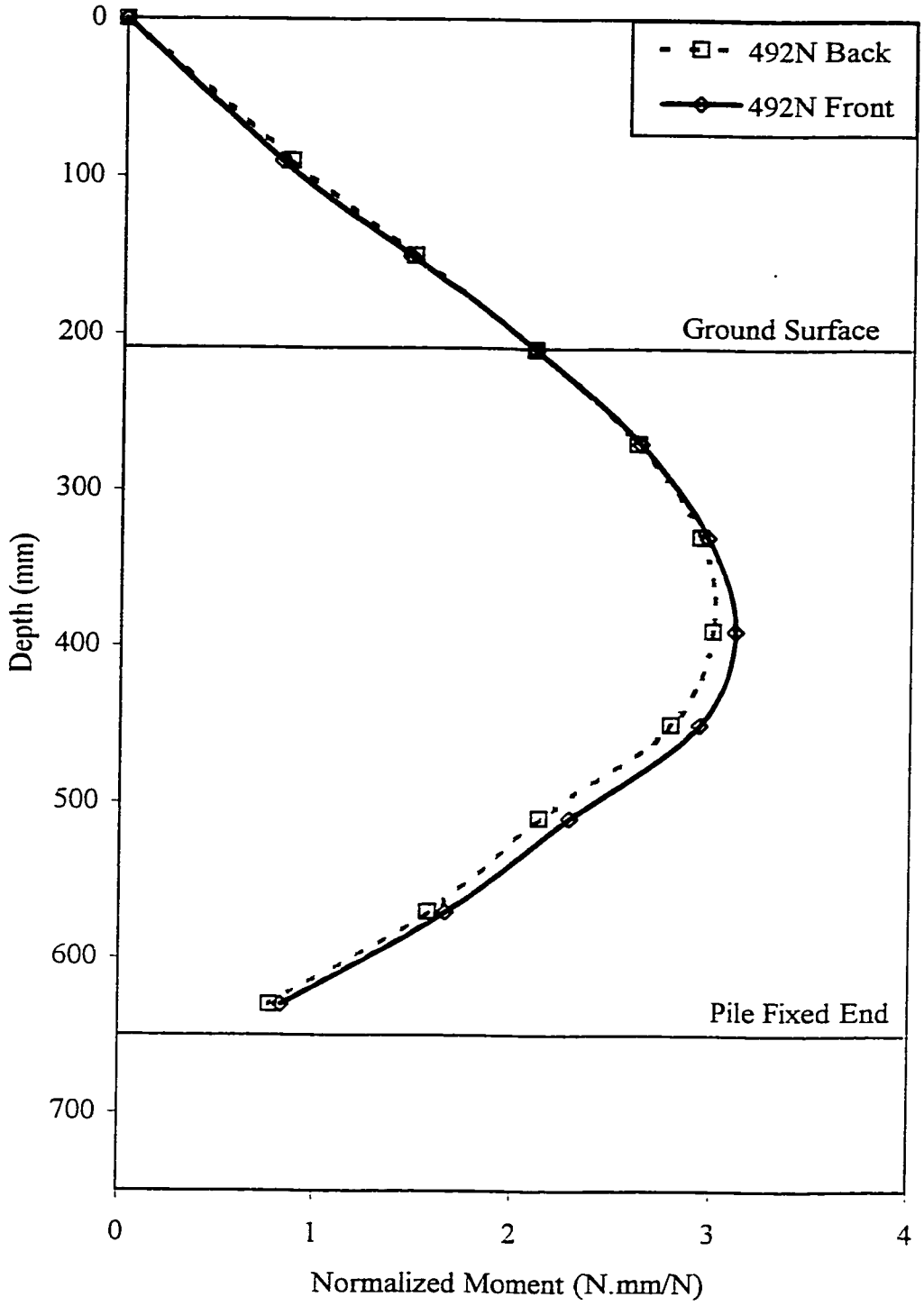

Figure 4.20b: Comparison of Normalized Moment Variation with Depth for Four Pile Group Between Front and Back Row Piles in Dry Sand Subjected to 492N Static Lateral Load Level.

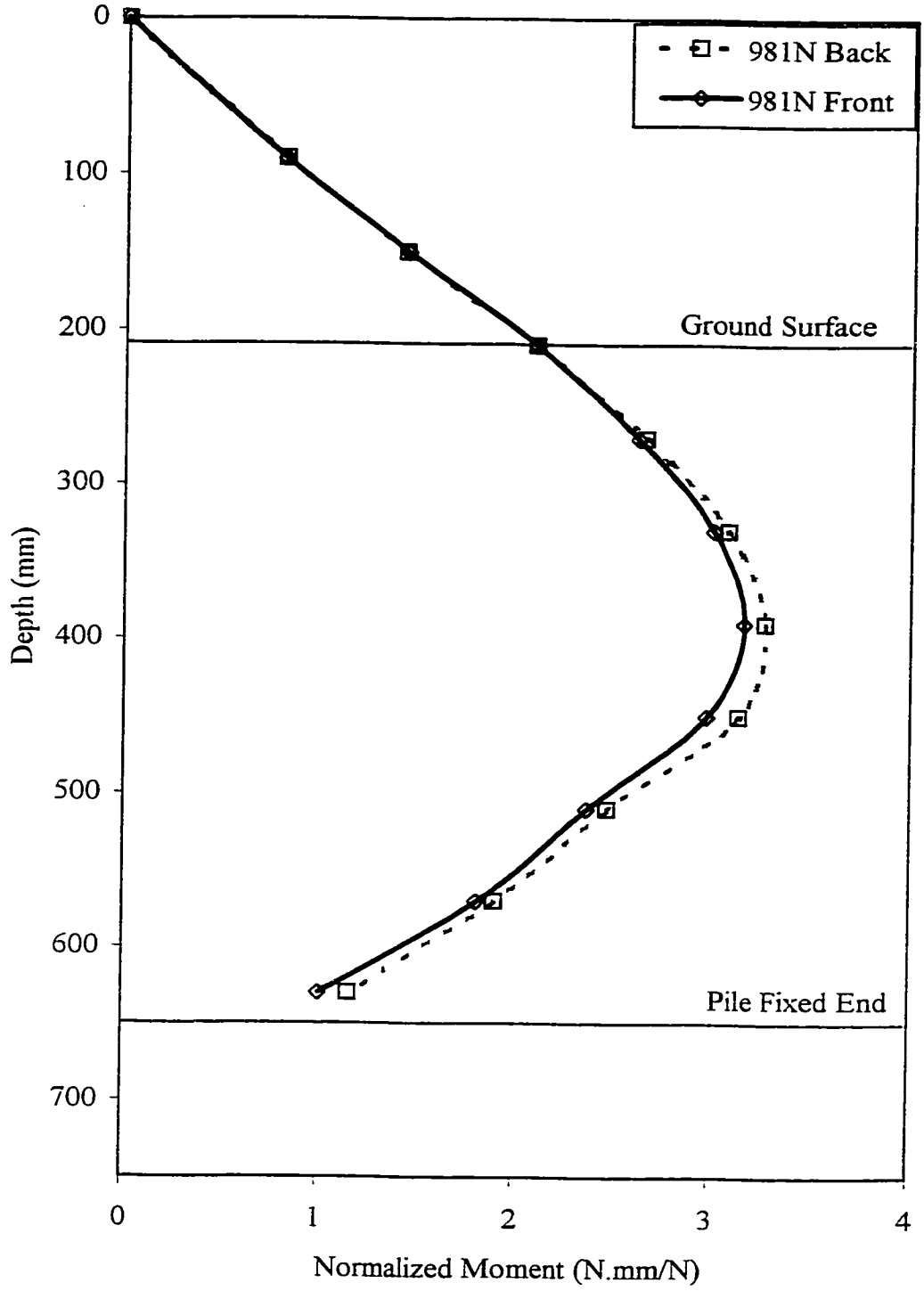

Figure 4.20c: Comparison of Normalized Moment Variation with Depth for Four Pile Group Between Front and Back Row Piles in Dry Sand Subjected to 981N Static Lateral Load Level.

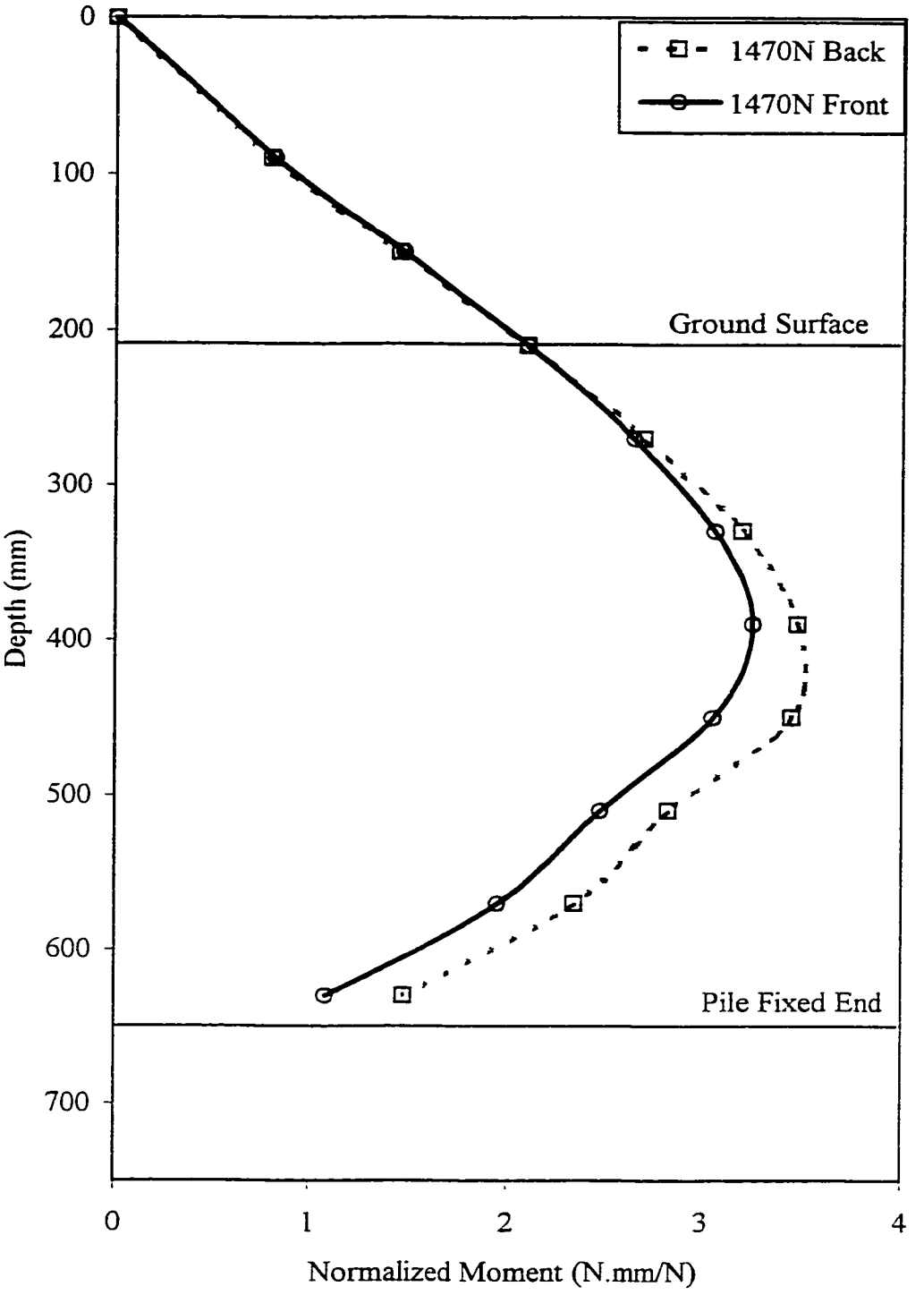

Figure 4.20d: Comparison of Normalized Moment Variation with Depth for Four Pile Group Between Front and Back Row Piles in Dry Sand Subjected to 1470N Static Lateral Load Level.

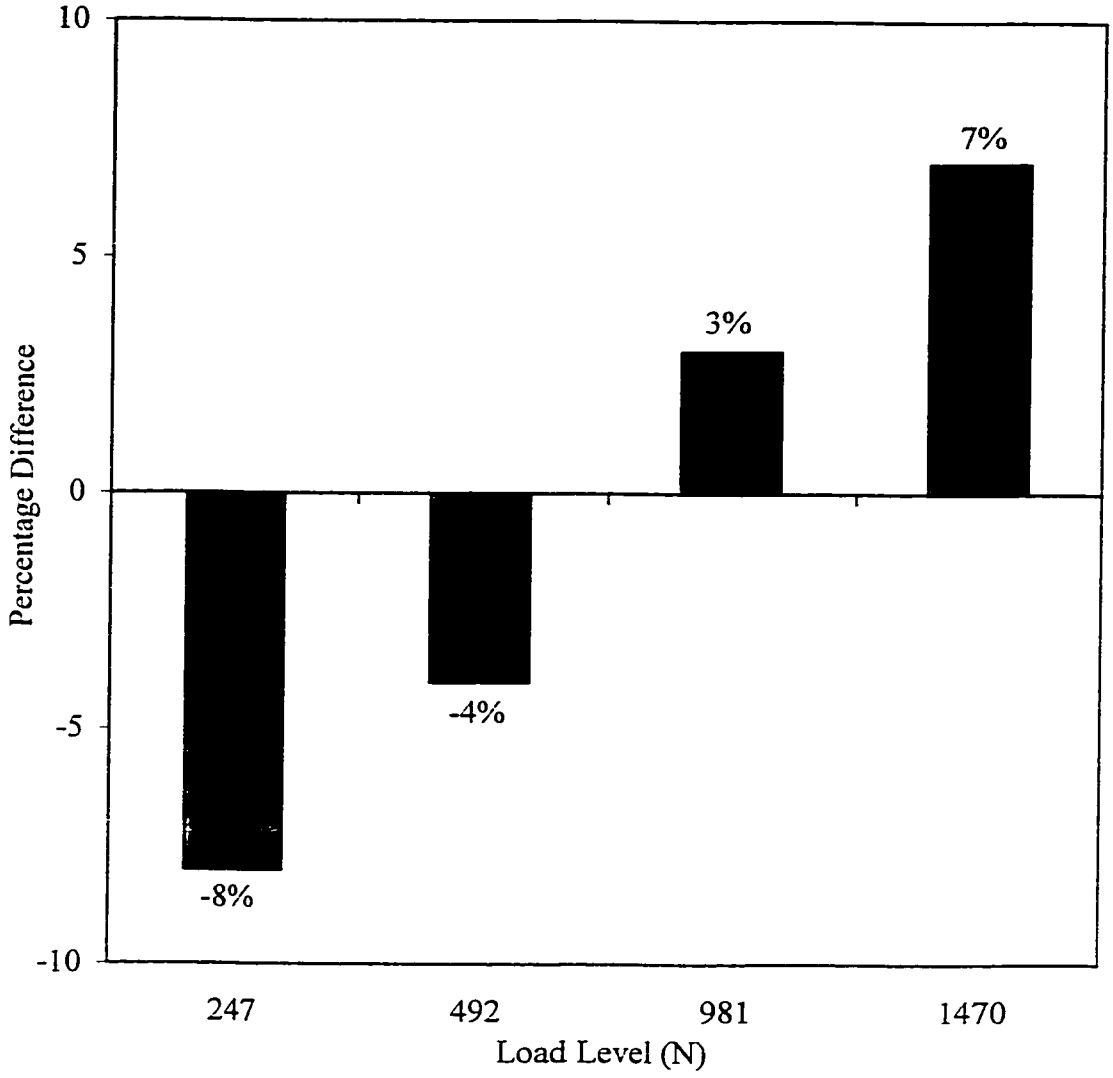

Figure 4.20e: Percentage Difference of Normalized Moment Variation with Depth for Four Pile Group Between Front and Back Row Piles in Dry Sand Subjected to Static Lateral Load Level.

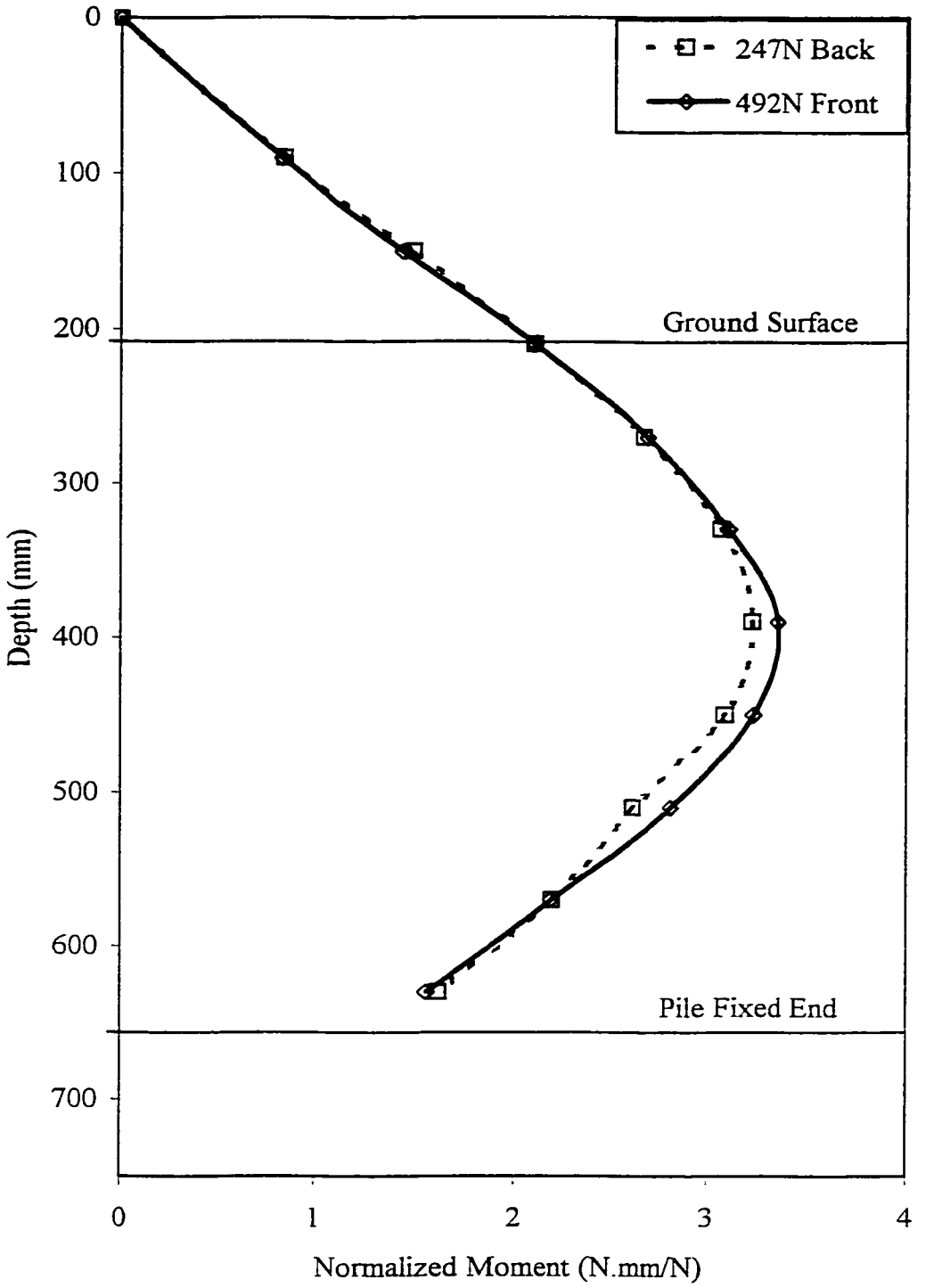

Figure 4.21a: Comparison of Normalized Moment Variation with Depth for Four Pile Group Between Front and Back Row Piles in Submerged Sand Subjected to 247N Static Lateral Load Level.

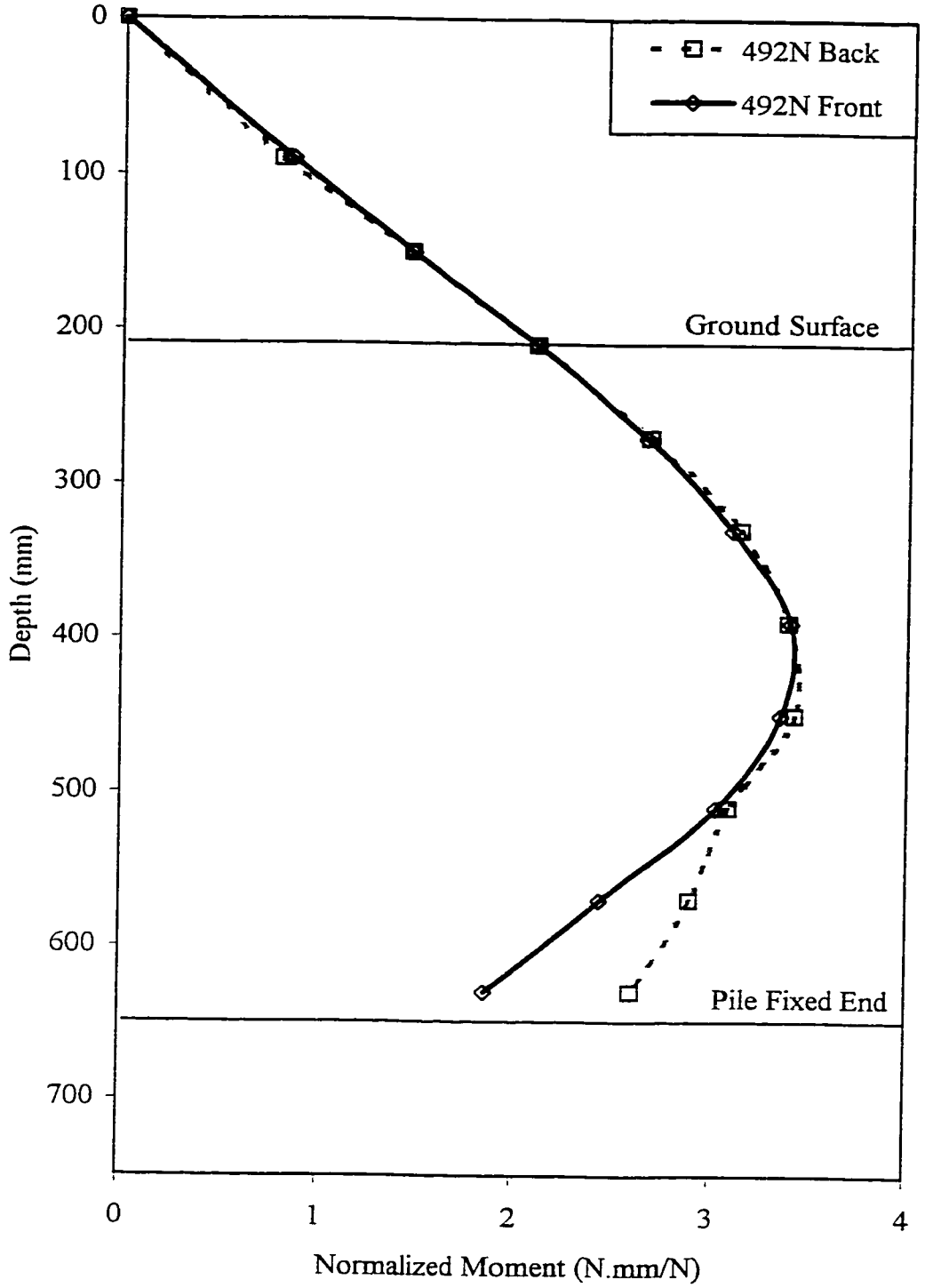

Figure 4.21b: Comparison of Normalized Moment Variation with Depth for Four Pile Group Between Front and Back Row Piles in Submerged Sand Subjected to 492N Static Lateral Load Level.

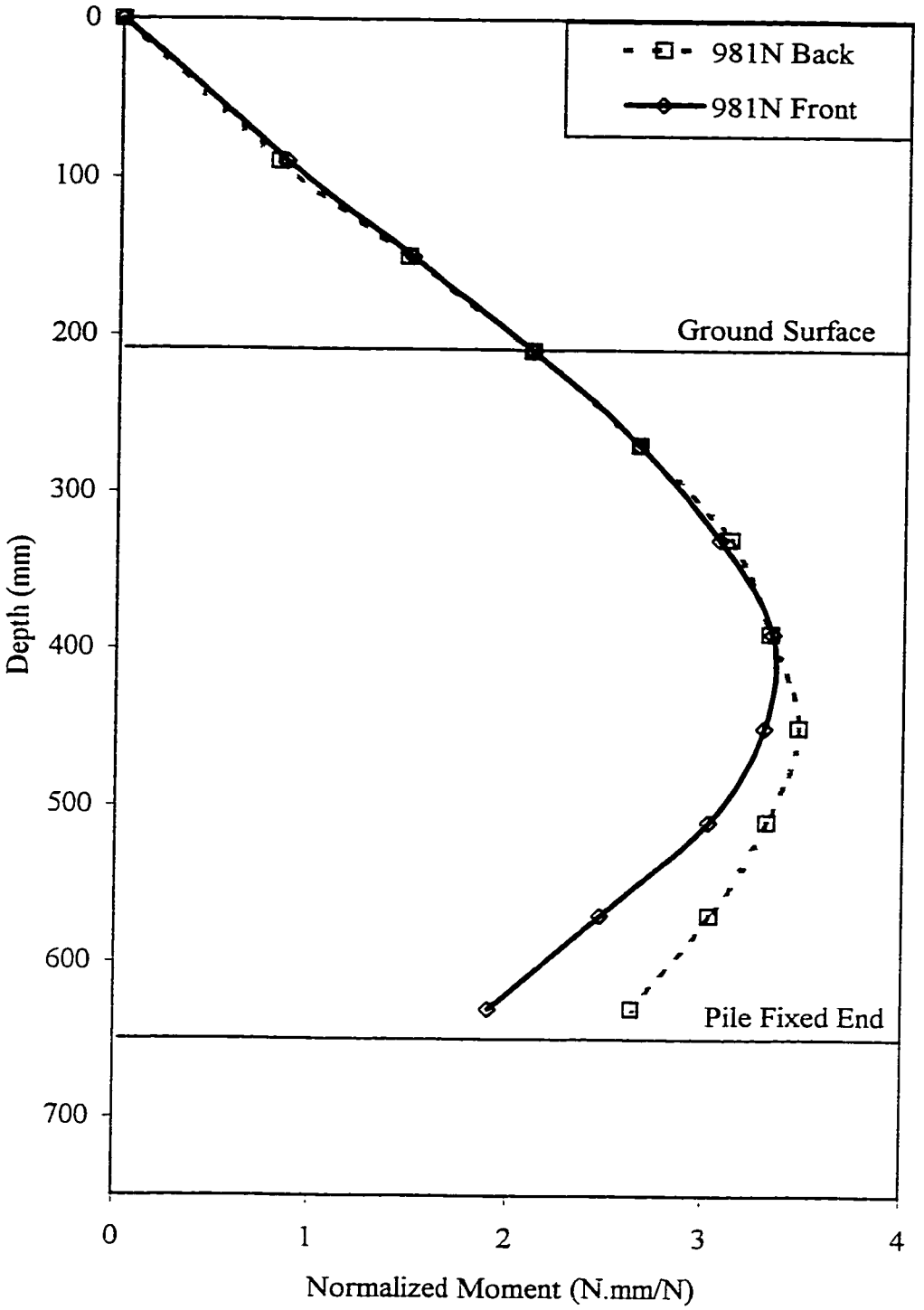

Figure 4.21c: Comparison of Normalized Moment Variation with Depth for Four Pile Group Between Front and Back Row Piles in Submerged Sand Subjected to 981N Static Lateral Load Level.

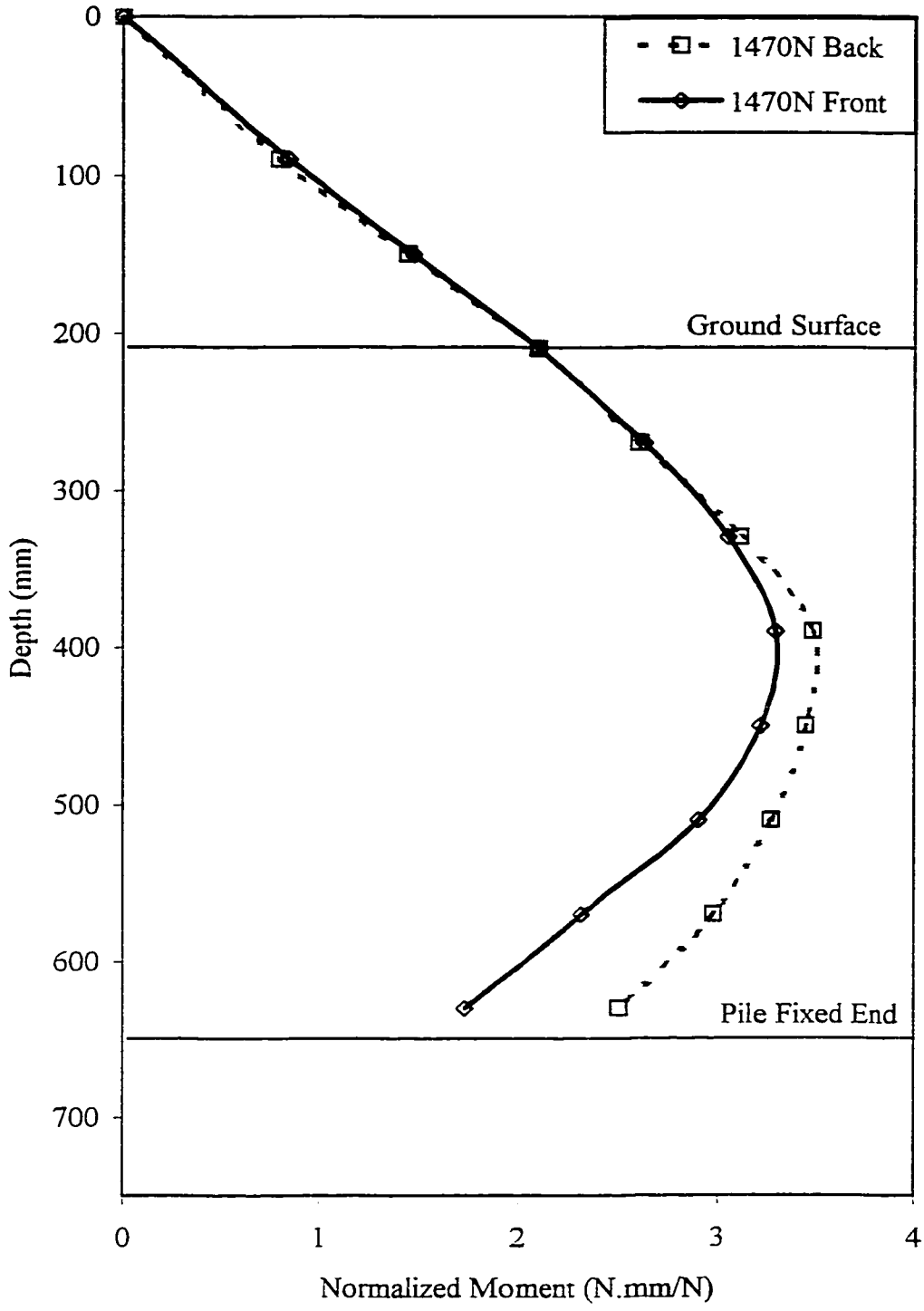

Figure 4.21d: Comparison of Normalized Moment Variation with Depth for Four Pile Group Between Front and Back Row Piles in Submerged Sand Subjected to 1470N Static Lateral Load Level.

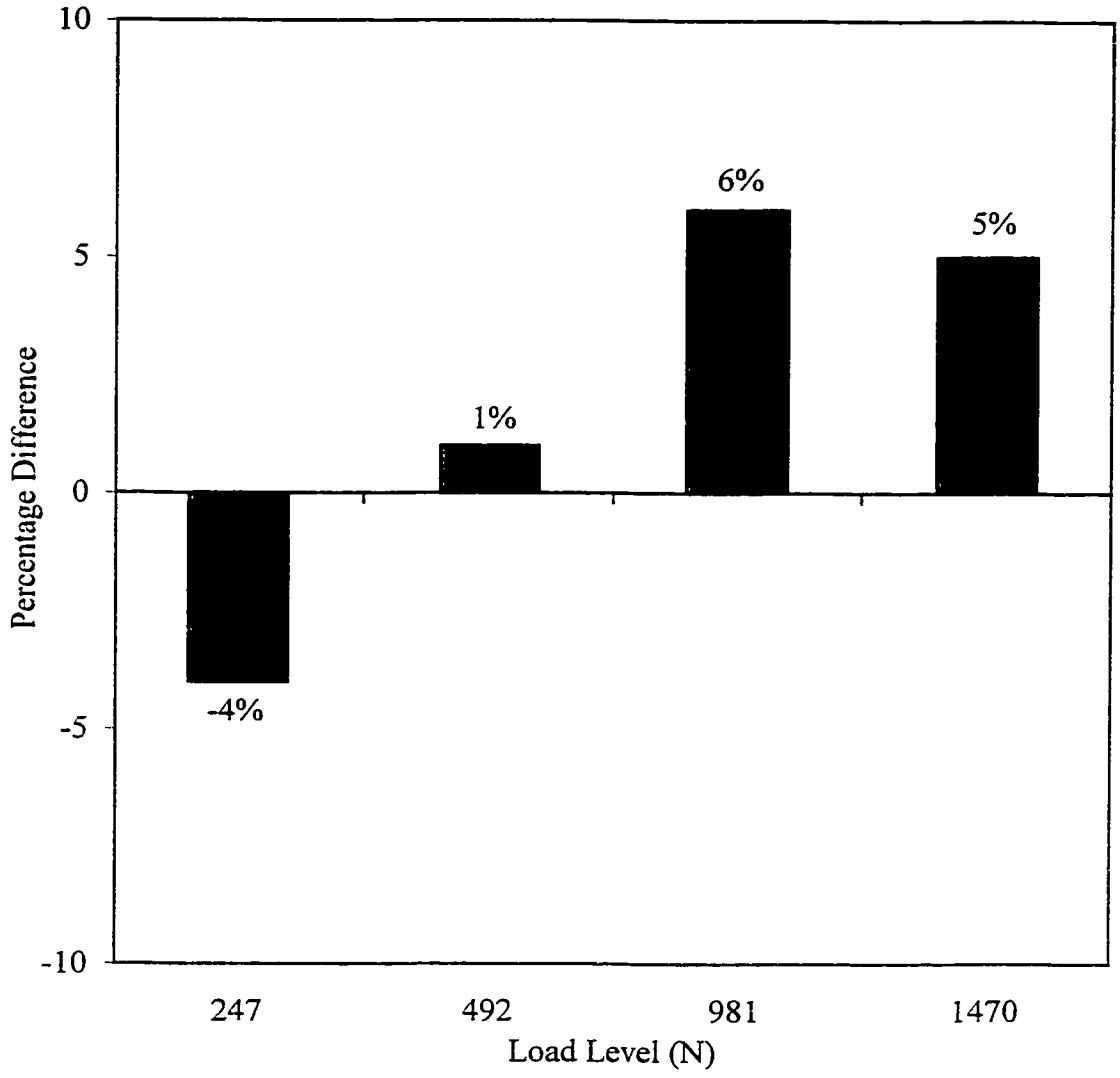

Figure 4.21e: Percentage Difference of Normalized Moment Variation with Depth for Four Pile Group Between Front and Back Row Piles in Submerged Sand Subjected to Static Lateral Load Level.

sand effect. However, while increasing the load level, the soil resistance increases and as a result the shadowing effect appears clearly in distributing the loads to the piles. This is presented in the percentage difference diagram in Figures 4.20e and 4.21e. The transfer from isolated piles behavior to group behavior occurs at faster rate for piles embedded in the submerged sand due to the reduction in the soil density. Moreover, for both sand conditions, the percentage difference between the front and back rows increase as load level increases whereas it is a load dependent in the absolute moment with no specific trend as shown in figure 4.16.

Deflection along the pile

The pile group behavior is clearly significant at high load levels. The two load levels which were selected to present the deflection along the piles in the group are 981 N and 1470 N. Deflection diagrams for pile group were produced using the same procedure for single pile explained earlier. In figure 4.22, the pile deflections are presented for piles in the front and back rows as well as for dry and submerged sand condition. The deflection along the pile and the pile curvature are increasing as the load level increases. The figure reflects the same results found earlier, that is the front row always get the higher share of load distribution, which in turn deflect relatively more than the back row piles. Even though, the top deflection is the same on both rows. In the single pile case, the piles embedded in submerged sand tends to deflect more than the piles embedded in the dry sand for the same load level. But figure 4.22 dictates that deflection is more in the dry sand condition due to the effect of shadowing as discussed earlier. This is due to the effect

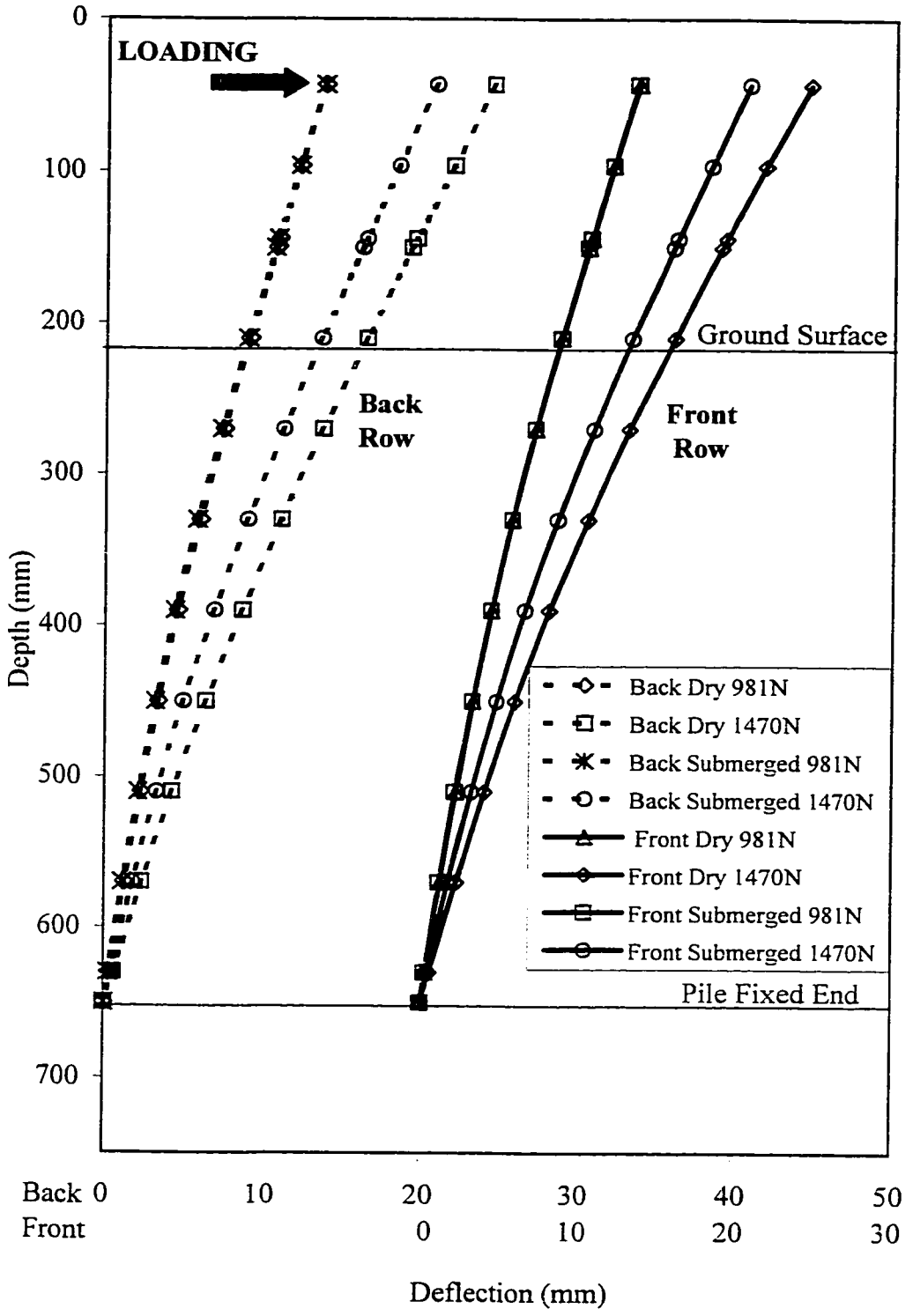

Figure 4.22: The Variation of Deflection with Depth for Four Pile Group Subjected to Static Lateral Load.

of shadowing which allow the front pile to sustain more load level per pile head. Again the distribution of the load level to the piles in the front row is higher for the dry sand condition, which definitely resulted in higher deflection along the pile.

4.4.3 Nine Pile Group:

The two changing parameters in this set of tests are the number of piles per group (nine piles) and the equal spacing between them. Naturally, due to the increase in the number of piles the group can sustain higher load level than the four pile group. In other words, for the same group deflection, the load level is higher for the nine pile group than the four pile group. Similarly, the sand shadowing effect exists which affect the behavior of the piles in the middle and back rows. The following paragraphs discuss in detail the behavior of the nine pile group embedded in dry and submerged sand under lateral static load.

Top Deflection:

Figures 4.23 and 4.24 present the top deflection versus pile group load level for piles embedded in dry and submerged sand conditions, respectively. The top deflection pattern is very much similar to the four pile group case. However, the number of rows affected by shadowing here is two, whereas it was only one for the four pile group case. The figures show that for the same pile head load, the top deflection is higher in the back row followed by the middle row and finally the front row. Comparing the behavior of piles embedded in dry and submerged sand, it can be noticed that the front row piles attracts higher head load level in the submerged sand condition. This means that the front row in

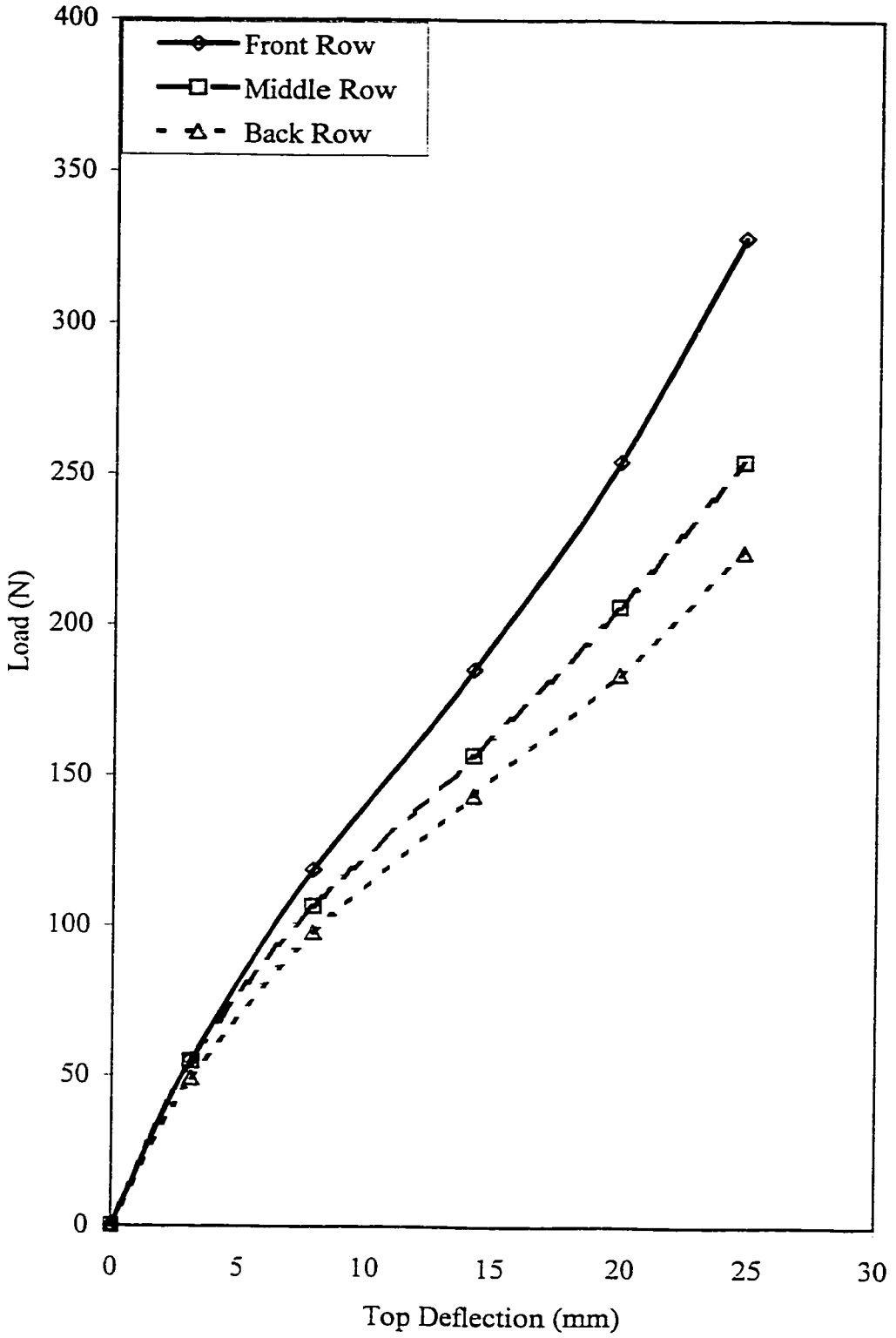

Figure 4.23: Load Deflection Curve for Nine Pile Group in Dry Sand Subjected to Static Lateral Load.

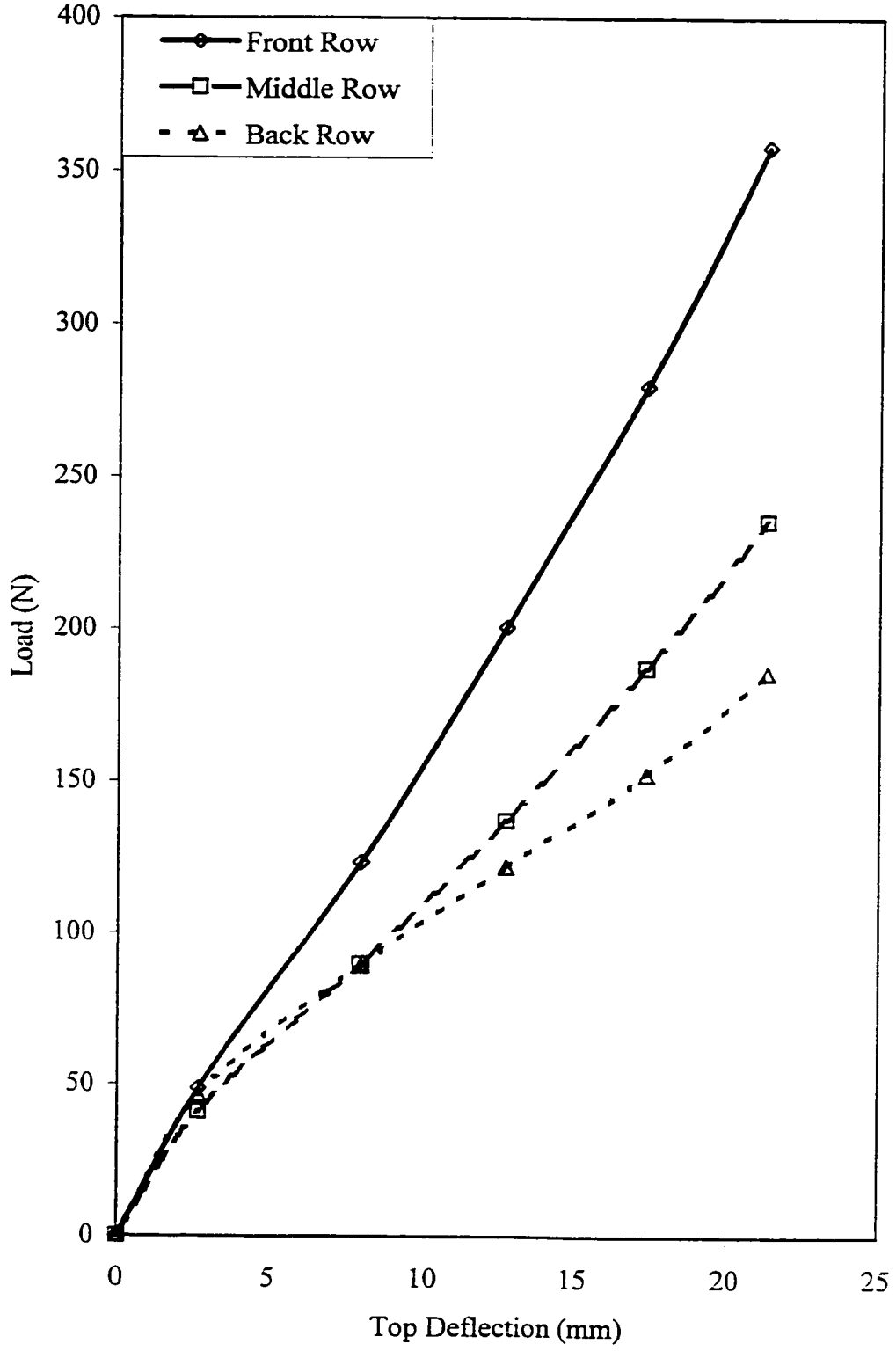

Figure 4.24: Load Deflection Curve for Nine Pile Group in Submerged Sand Subjected to Static Lateral Load.

the submerged case can sustain higher load levels and hence higher moment. This is due to the distribution of load level to the piles head by the sand shadowing.

For the piles in the middle row, the difference between the dry and submerged condition is almost negligible. Therefore, the behavior of the middle row under both conditions is considered the same. Finally, for the back row, the piles behave in the opposite way of the front piles, that is the head load level is higher in piles embedded in the dry sand for the same top deflection. In short, the top deflection of the piles according to the pile head load level is affected greatly by the sand shadowing. The load level distributed to piles depends on the pile position in the rows. Furthermore, the shadowing depends on the sand density which in turn depends on the sand condition whether it is dry or submerged.

Finally, comparing the two figures, the slope change rate of the curves is higher in the submerged case due to the reduction in density discussed earlier. Therefore, it can be concluded that the behavior of top deflection versus load in the nine pile group case is similar to the four pile group case.

Moment Diagram:

Moments diagram for pile group was obtained by the same procedure used previously for single pile and four pile group. The moment diagrams for the nine pile group are shown in figures 4.25 and 4.26, for piles embedded in dry and submerged sand, respectively. As presented earlier, the difference in moments at low load level (i.e. 492 N) is minimal due to the increase in the pile group stiffness (by increasing the number of piles) which

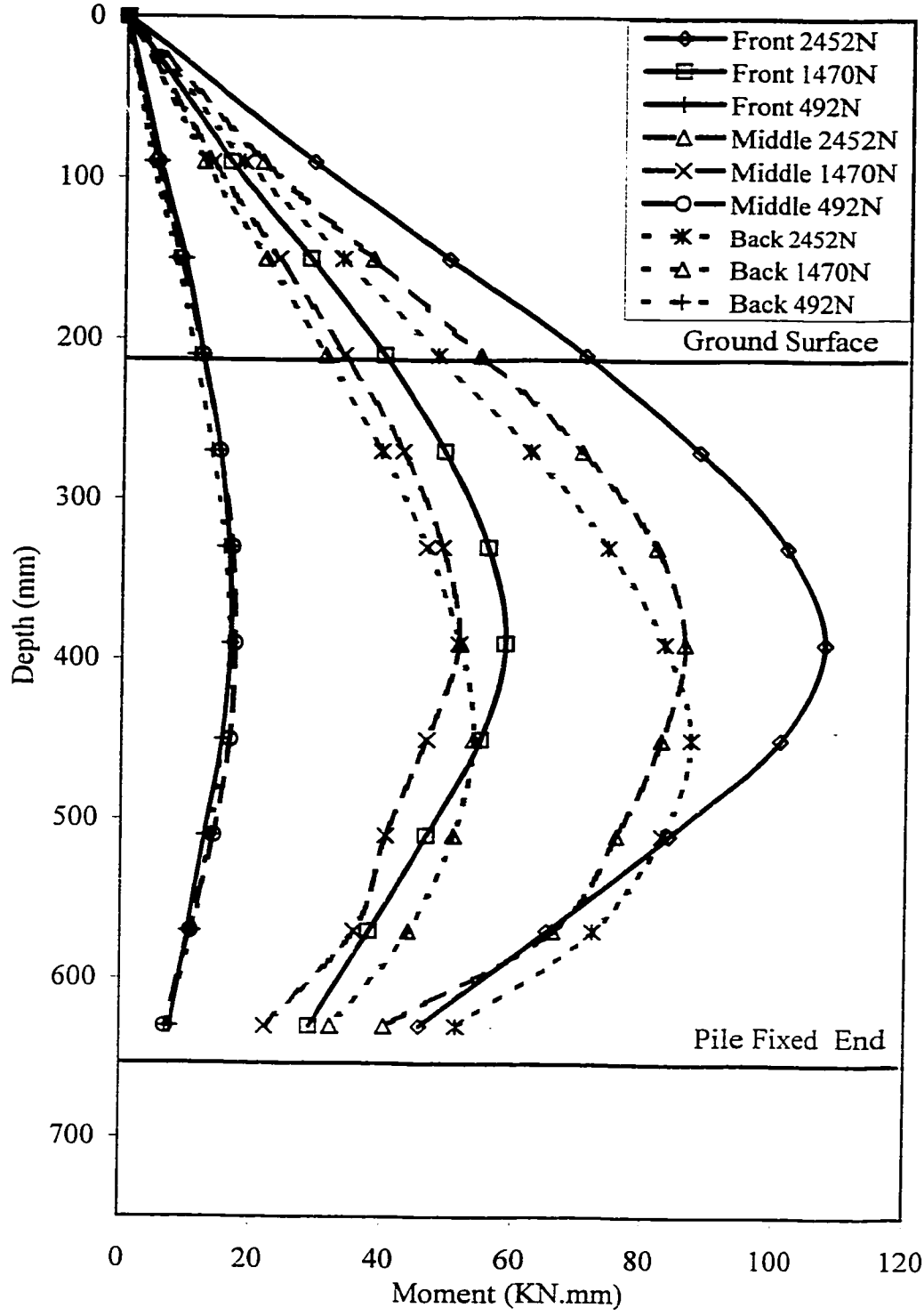

Figure 4.25: The Variation of Moment with Depth for Nine Pile Group in Dry Sand Subjected to Static Lateral Load.

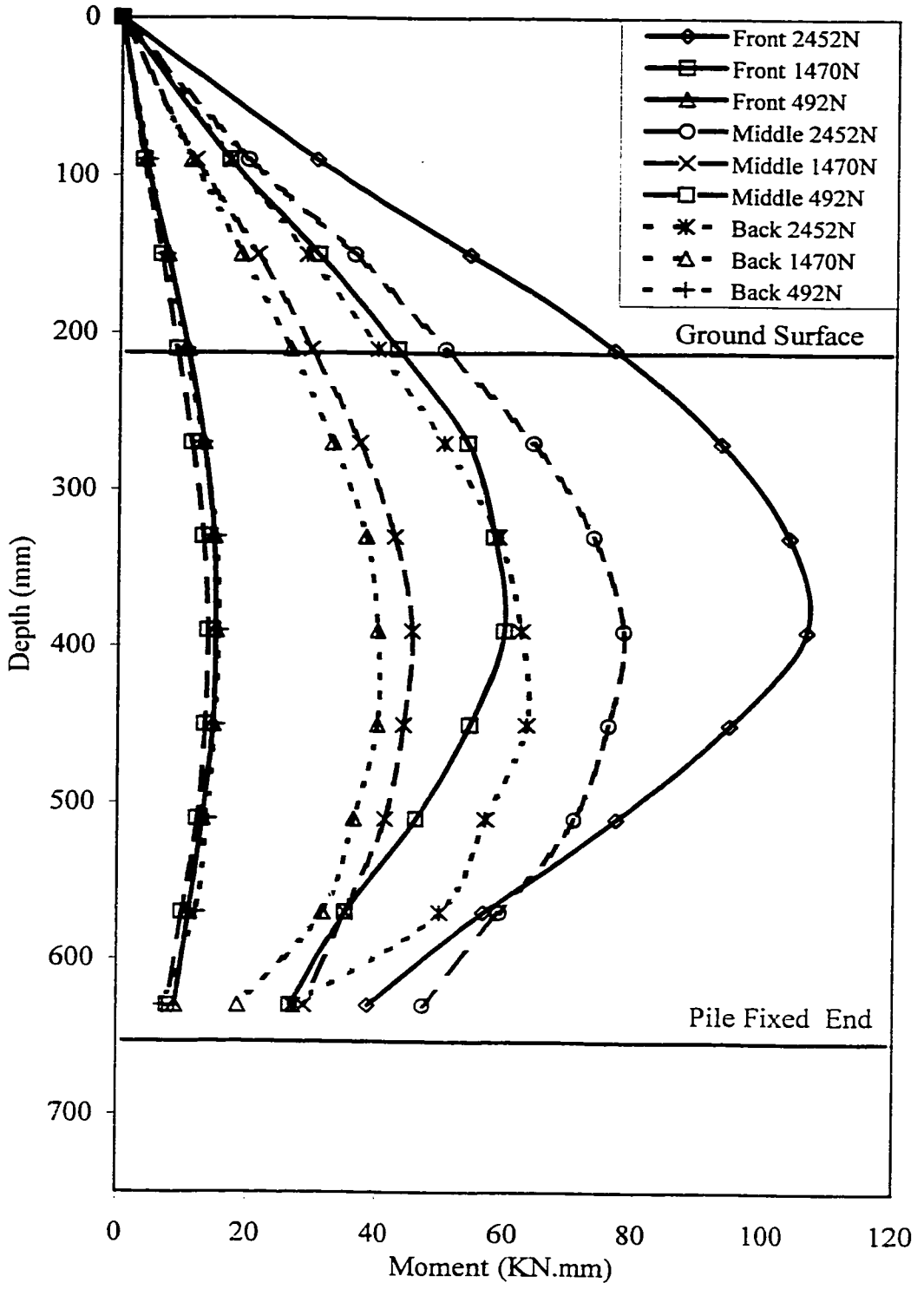

Figure 4.26: The Variation of Moment with Depth for Nine Pile Group in Submerged Sand Subjected to Static Lateral Load.

resulted in the reduction in piles top deflection and hence the moment difference. This finding is applicable for piles embedded in dry and submerged sand conditions. Similar to the four pile group discussed earlier, the figures show that the front rows always attract more moment and hence more pile head load level due to shadowing effect. The piles in the front rows resists the sand with its full capacity, while in the trailing rows (i.e. middle and back) the shadowing effect tends to cause reduction in soil resistance. Therefore, the maximum bending moment for a given load on the pile group tends to be in the front row pile. The maximum moment for the piles in the middle and back row occurs at a greater depth, because of the reduction in the load transfer near the surface. This was also found by other researchers, Reese (1983). Moreover, the figures depicts that as the group load level increases the difference in moments for the piles in the front, middle and back rows increase accordingly. The difference in the moment between the piles according to their row positions is greater in the case of submerged sand as shown in figure 4.26. This is due to the reduction in soil resistance. Furthermore, in both sand conditions the figure shows that the difference in moment between the piles in the front row and the piles in the middle row is greater than the ones between the piles in the middle row and the piles in the back row. This is mainly because both the middle and the back rows were affected by shadowing while the front row was not. In other words, the piles in the middle row were affected by shadowing from the piles in the front row while the piles in the back row were affected by shadowing from piles in the middle and front rows. Therefore, the effect of sand shadowing is greater on the back, since it is effected by the two leading rows.

For the purpose of presenting the effect of submergence on the nine pile group subjected to lateral static load, the piles in the front row are selected, as presented in figure 4.27. It shows that the submerged piles attract slightly higher level of moment at all load levels which reflect the same behavior of the single pile subjected to lateral static load. This is because the pile head load level depends on the proportion of load distributed by the sand shadowing, as discussed in the case of four pile group earlier.

Normalized Moment

The group load is distributed via the sand shadowing to each pile according to pile row location. Therefore, the individual behavior of each pile in the group must be studied according to the head load level which is applied to. Hence, its necessary to normalize the moment diagram by dividing the moments by individual piles head load, similar to the procedure used earlier for four pile group. Figures 4.28 and 4.29 present the normalized moment diagrams for nine pile group embedded in dry and submerged sand, respectively. The figures show the normalize moment for the following load group levels 492, 981, 1470 and 2452 N to show the variations as the load level increases. The maximum moment of the piles in the middle and back rows were greater than the piles in the front row when normalized by their individual pile head load. However, even after normalizing, the maximum moment for the piles in the back rows occurs at a greater depth as discussed earlier.

From the figures, it can be realized that as the load level increases the differences in normalized moment between front, middle and back row piles increases. At small load

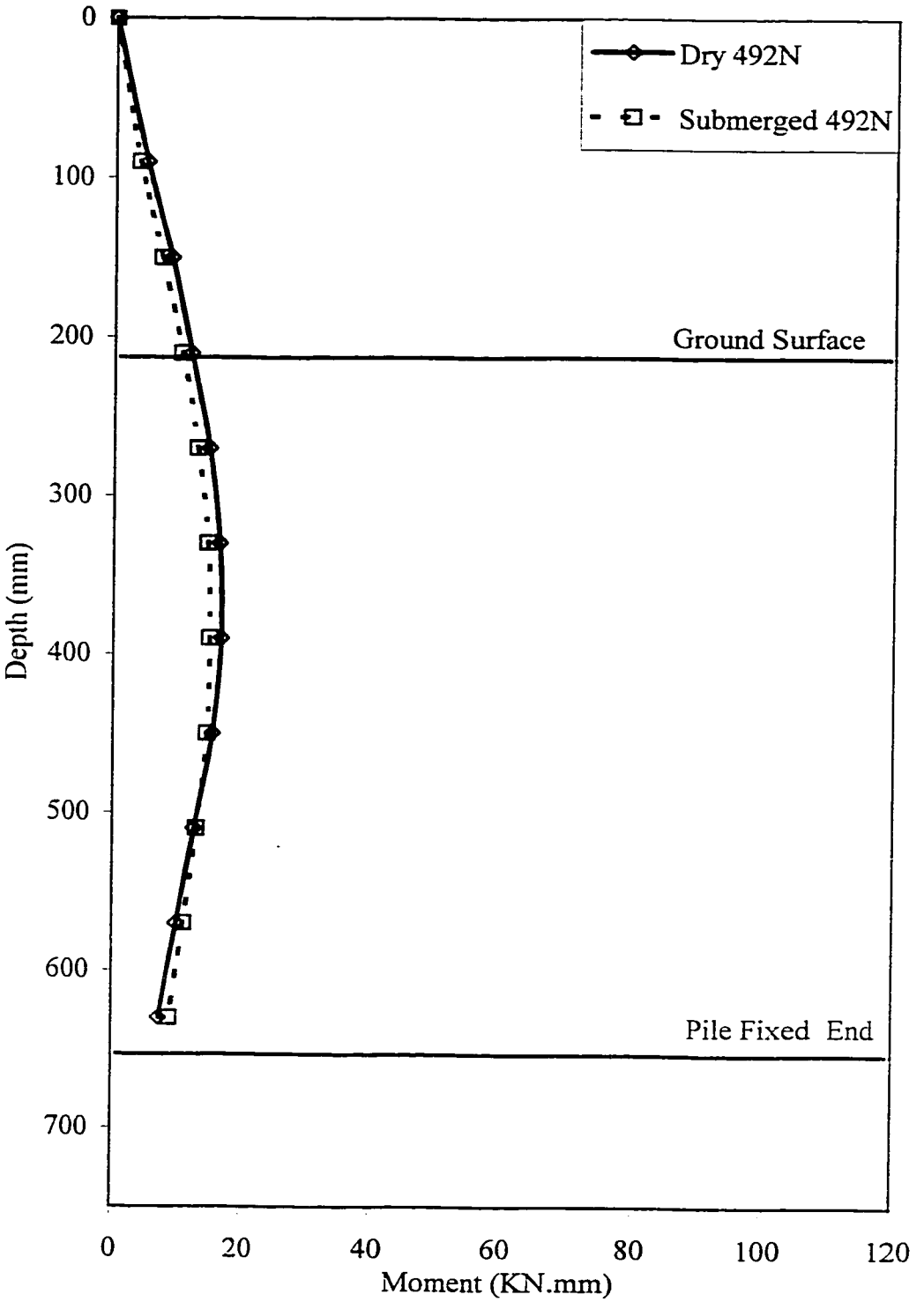

Figure 4.27a: Comparison of Moment Variation with Depth for Front Row Piles in Nine Pile Group Between Dry and Submerged Sand Conditions Subjected to 492N Static Lateral Load.

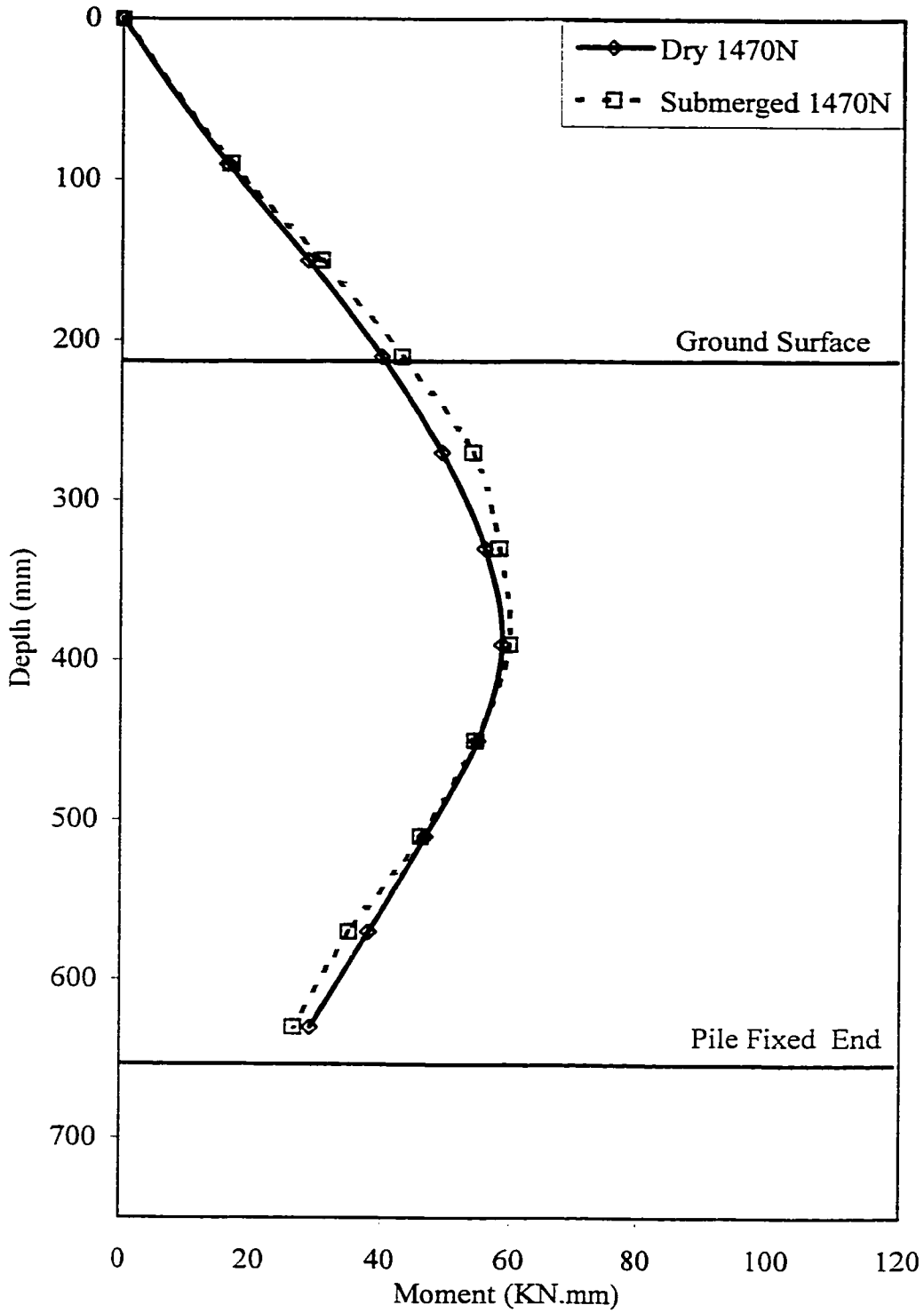

Figure 4.27b: Comparison of Moment Variation with Depth for Front Row Piles in Nine Pile Group Between Dry and Submerged Sand Conditions Subjected to 1470N Static Lateral Load.

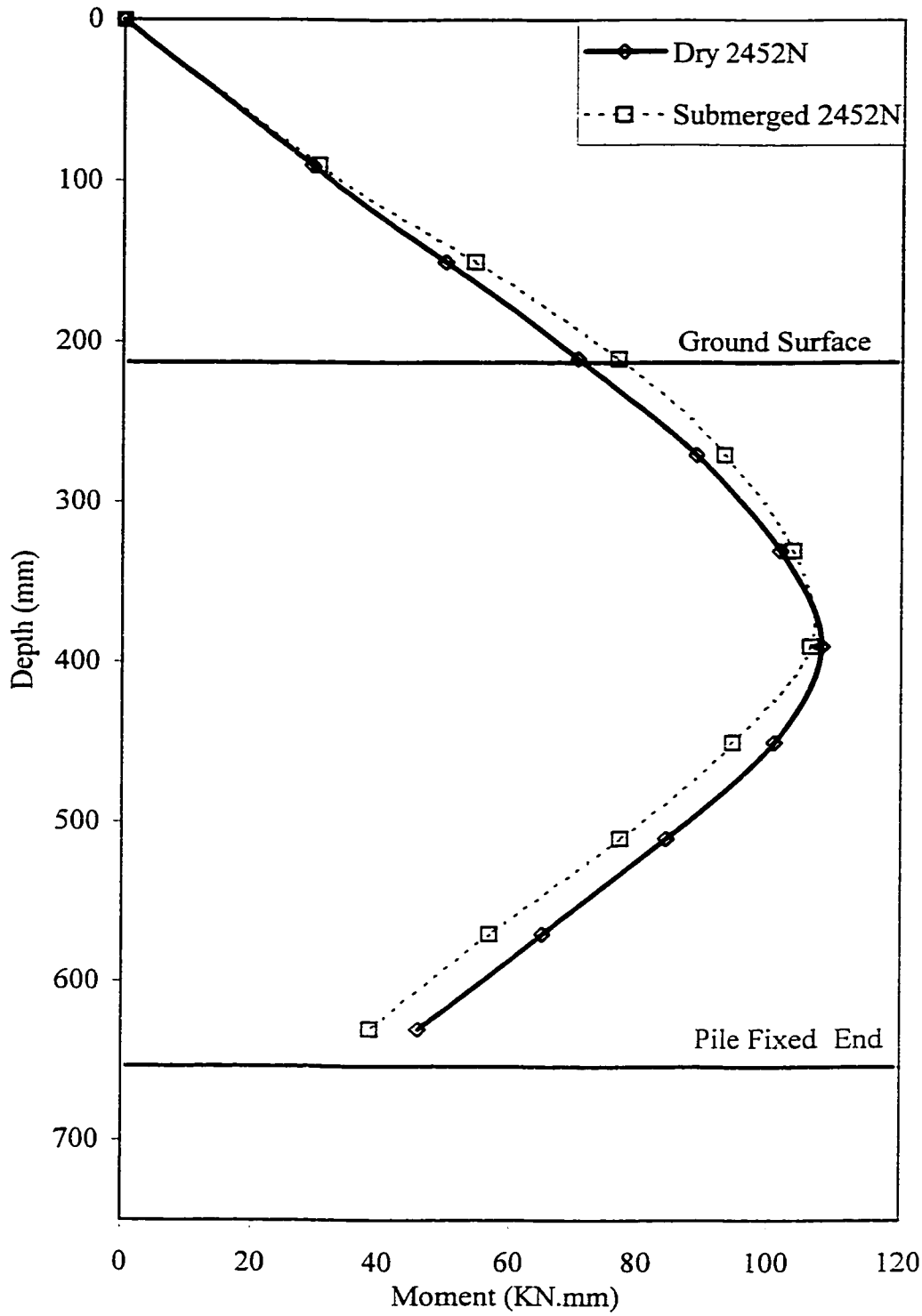

Figure 4.27c: Comparison of Moment Variation with Depth for Front Row Piles in Nine Pile Group Between Dry and Submerged Sand Conditions Subjected to 2452N Static Lateral Load.

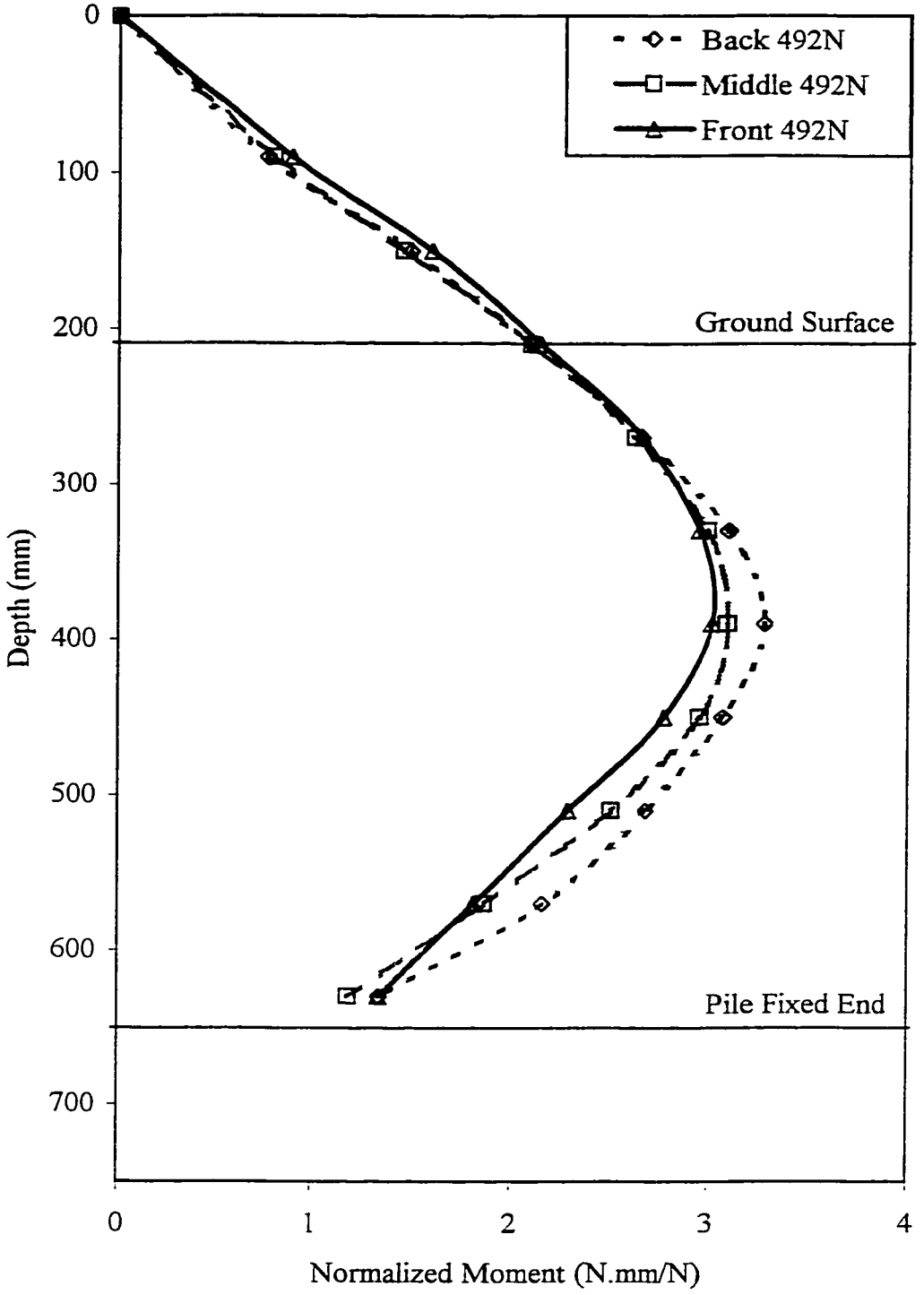

Figure 4.28a: Comparison of Normalized Moment Variation with Depth for Nine Pile Group Between Front, Middle and Back Row Piles in Dry Sand Subjected to 492N Static Lateral Load.

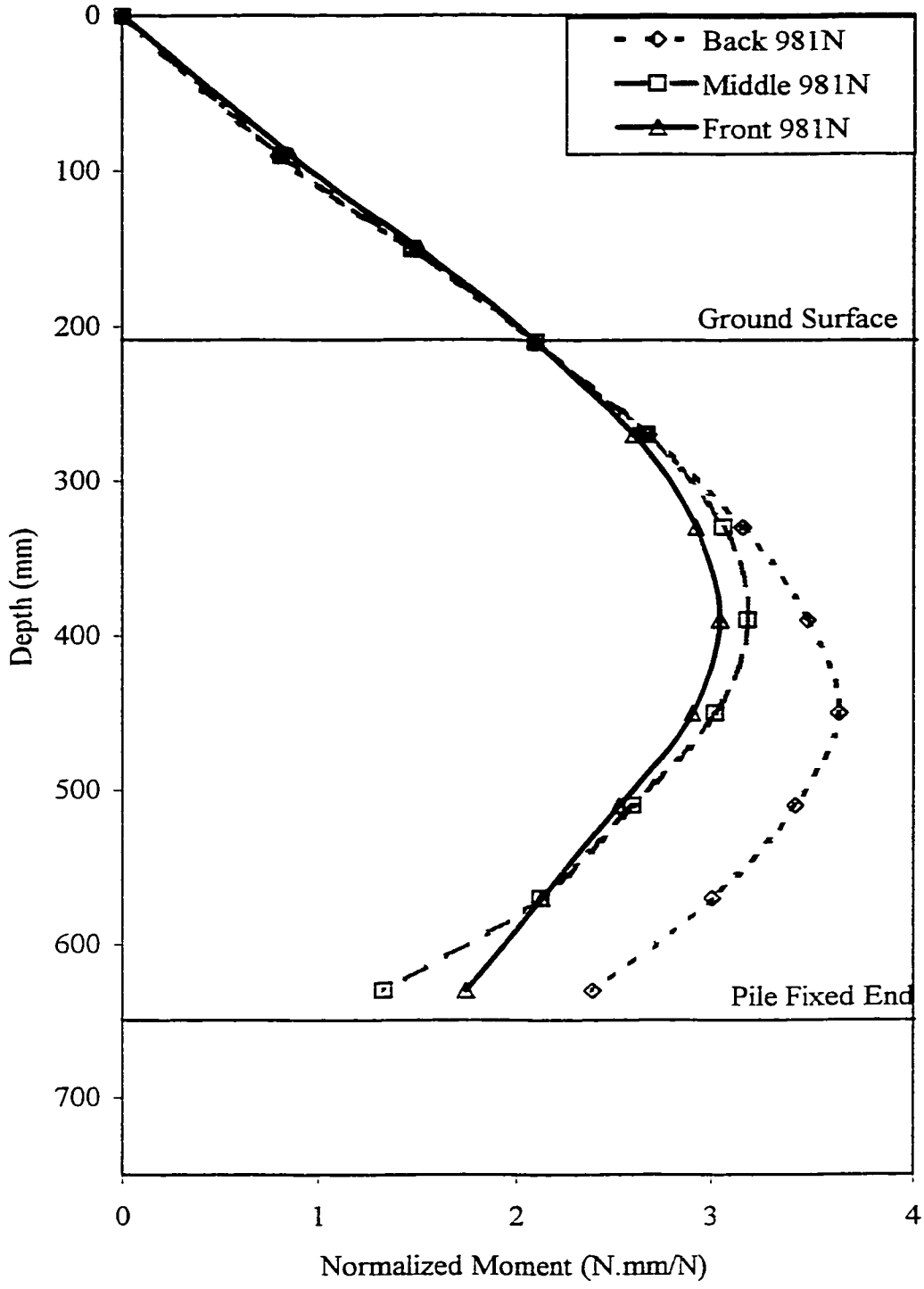

Figure 4.28b: Comparison of Normalized Moment Variation with Depth for Nine Pile Group Between Front, Middle and Back Row Piles in Dry Sand Subjected to 981N Static Lateral Load.

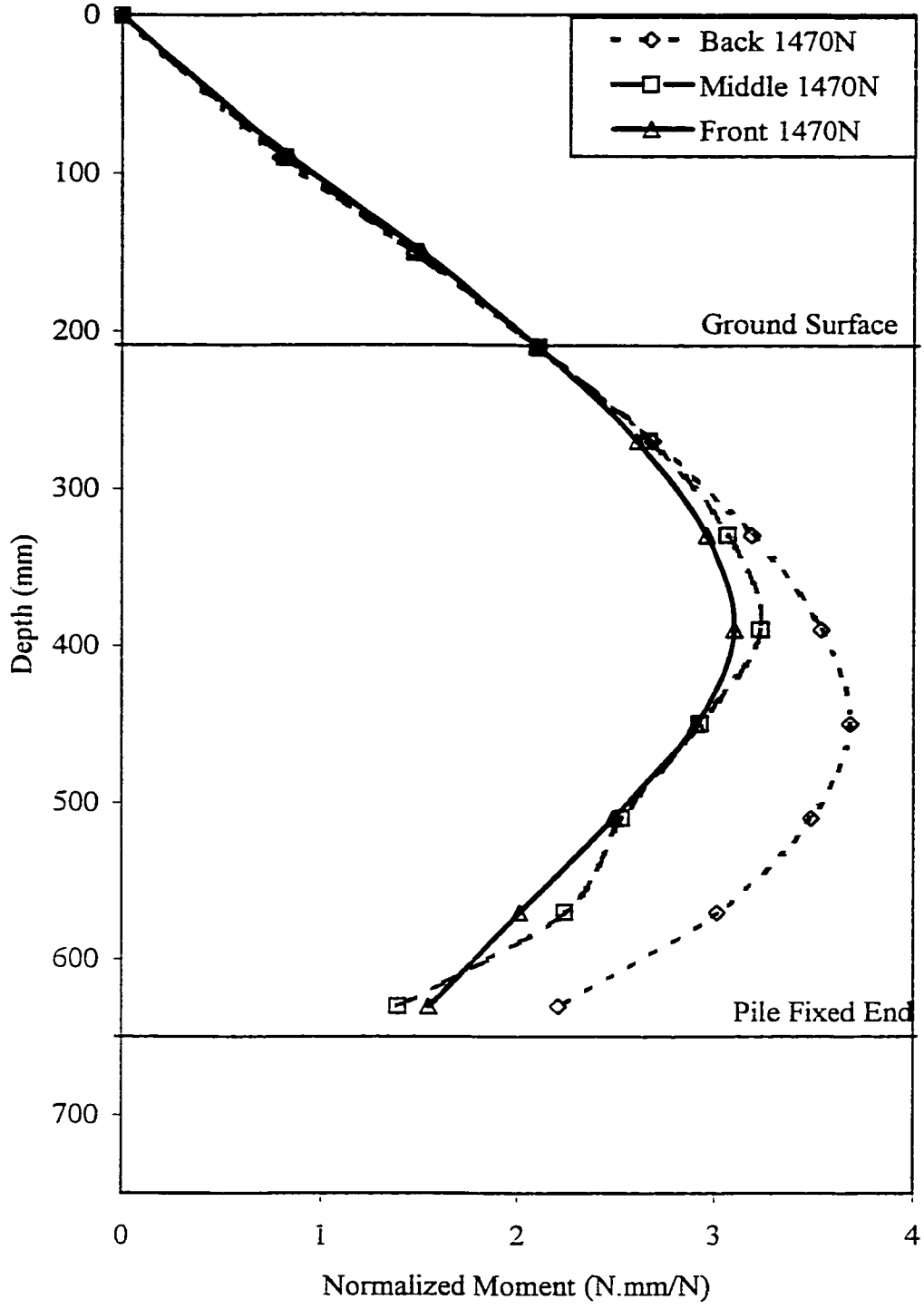

Figure 4.28c: Comparison of Normalized Moment Variation with Depth for Nine Pile Group Between Front, Middle and Back Row Piles in Dry Sand Subjected to 1470N Static Lateral Load.

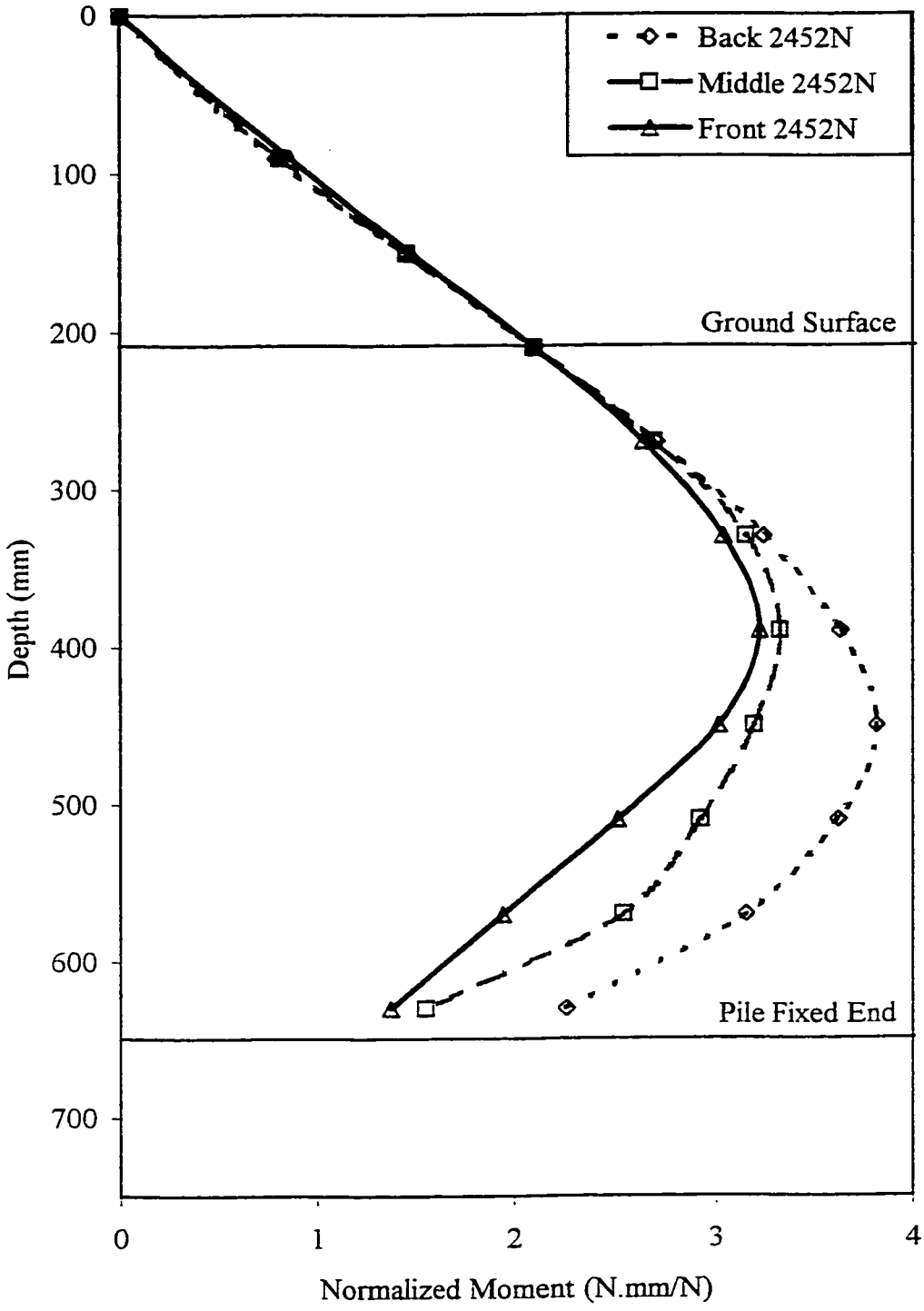

Figure 4.28d: Comparison of Normalized Moment Variation with Depth for Nine Pile Group Between Front, Middle and Back Row Piles in Dry Sand Subjected to 2452N Static Lateral Load.

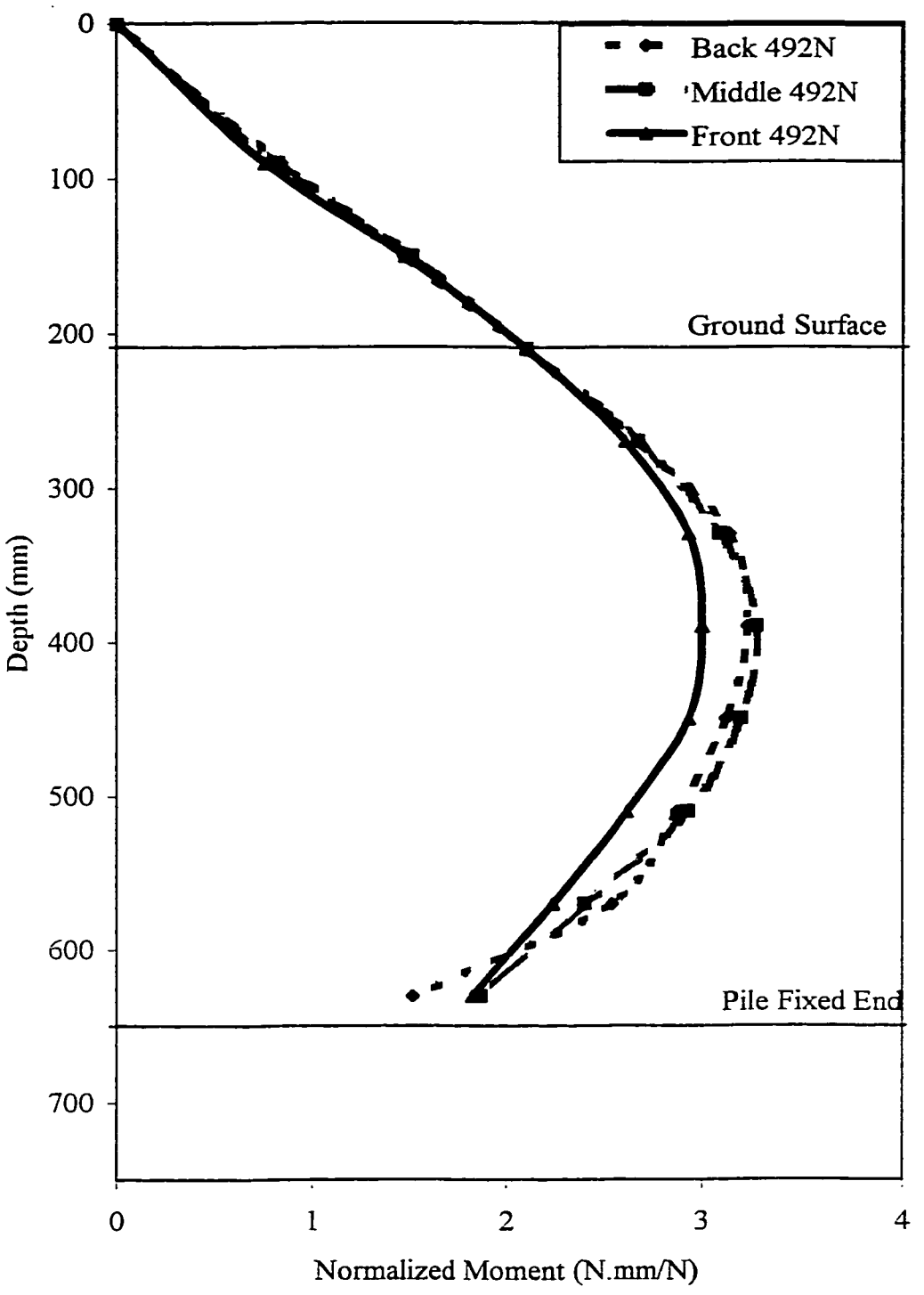

Figure 4.29a: Comparison of Normalized Moment Variation with Depth for Nine Pile Group Between Front, Middle and Back Row Piles in Submerged Sand Subjected to 492N Static Lateral Load.

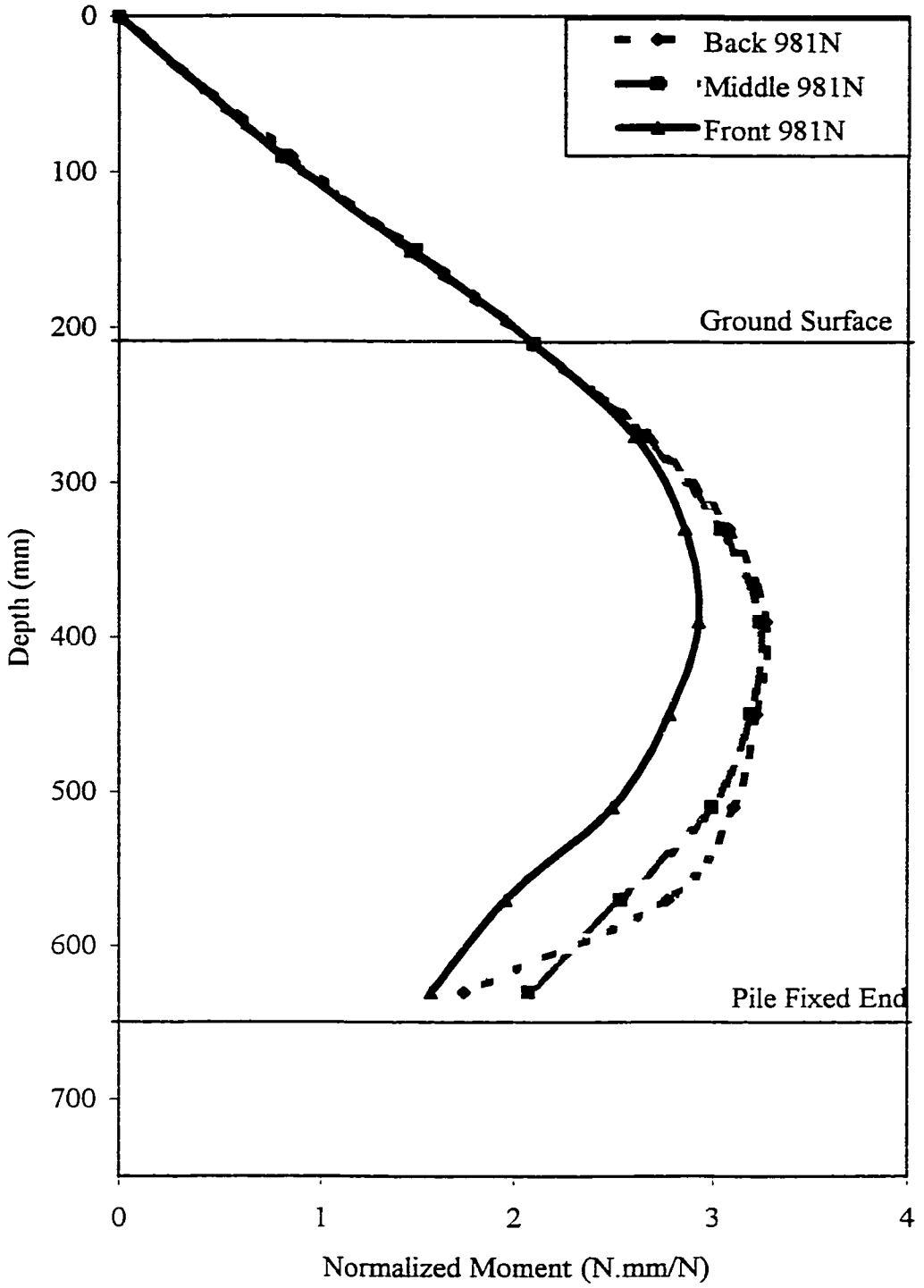

Figure 4.29b: Comparison of Normalized Moment Variation with Depth for Nine Pile Group Between Front, Middle and Back Row Piles in Submerged Sand Subjected to 981N Static Lateral Load.

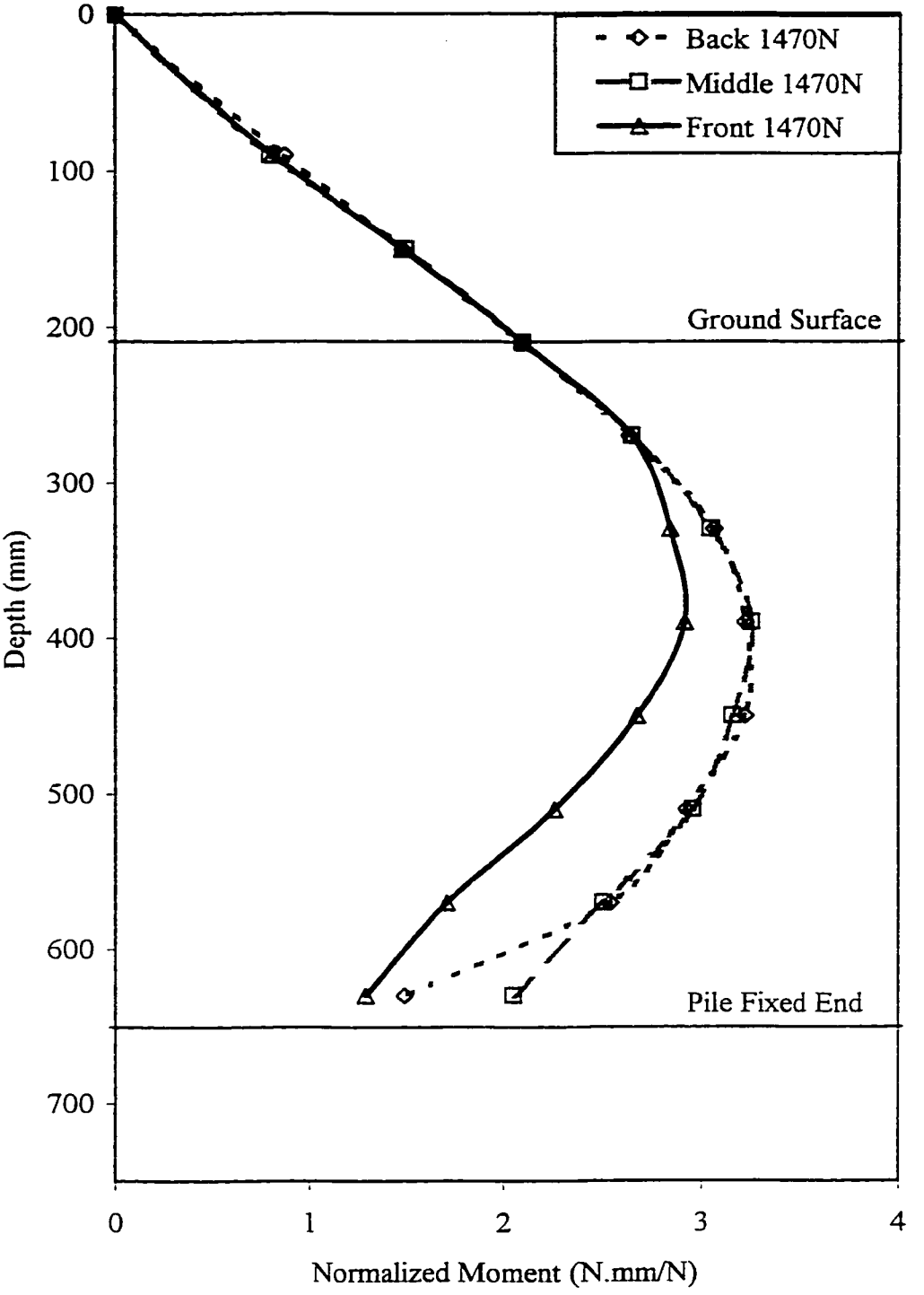

Figure 4.29c: Comparison of Normalized Moment Variation with Depth for Nine Pile Group Between Front, Middle and Back Row Piles in Submerged Sand Subjected to 1470N Static Lateral Load.

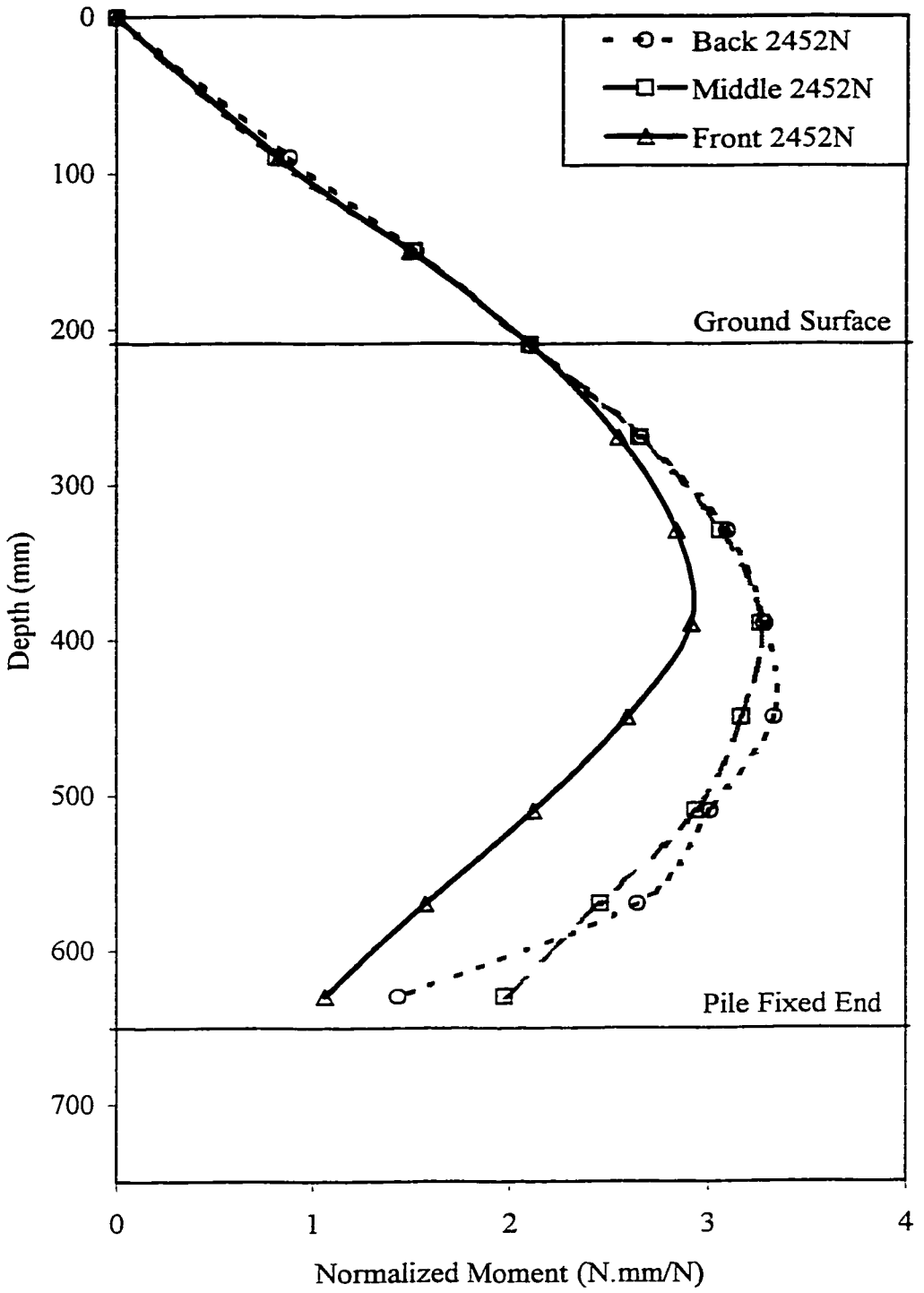

Figure 4.29d: Comparison of Normalized Moment Variation with Depth for Nine Pile Group Between Front, Middle and Back Row Piles in Submerged Sand Subjected to 2452N Static Lateral Load.

level, the differences are minor and the piles behave as single isolated pile. At higher load level, the group effect starts to appear and it becomes evident at the highest load level (2452 N). These findings are true for both piles embedded in dry and submerged sand conditions. Comparing the dry and submerged conditions it can be observed that in the dry sand condition the normalize moment trend of the piles in the middle row is very much similar to those in the front row while it is very much similar to the back row in the case of piles imbedded in submerged sand. This is due to the effect of reduction in soil stiffness in the submerged condition which can be clearly seen at high load levels.

Deflection Along the Pile

As discussed earlier the group effect can be clearly noticed at high load levels. Two load levels of 1962 N and 2452 N were selected to study the deflection along the depth of the pile for the nine pile group. Deflection diagrams for pile group were produced using the same procedure for single pile explained earlier. Results are presented in Figures 4.30 and 4.31. Figure 4.30 shows that for the same load level, the deflection along the piles is higher for piles embedded in dry sand than in submerged one. This is due to the effect of load distribution according to the pile location which is greatly affected by shadowing phenomena. Moreover, the soil disturbed more in the case of dry sand due to the shadowing effect which in turn producing more deflection at the top of piles. It is noticeable that the curvature of the deflection curve below the ground surface is more in the front row piles, due to the higher soil resistance which produces higher moment. Figure 4.31 shows comparison for the two load levels for both dry and submerged sand conditions. It shows

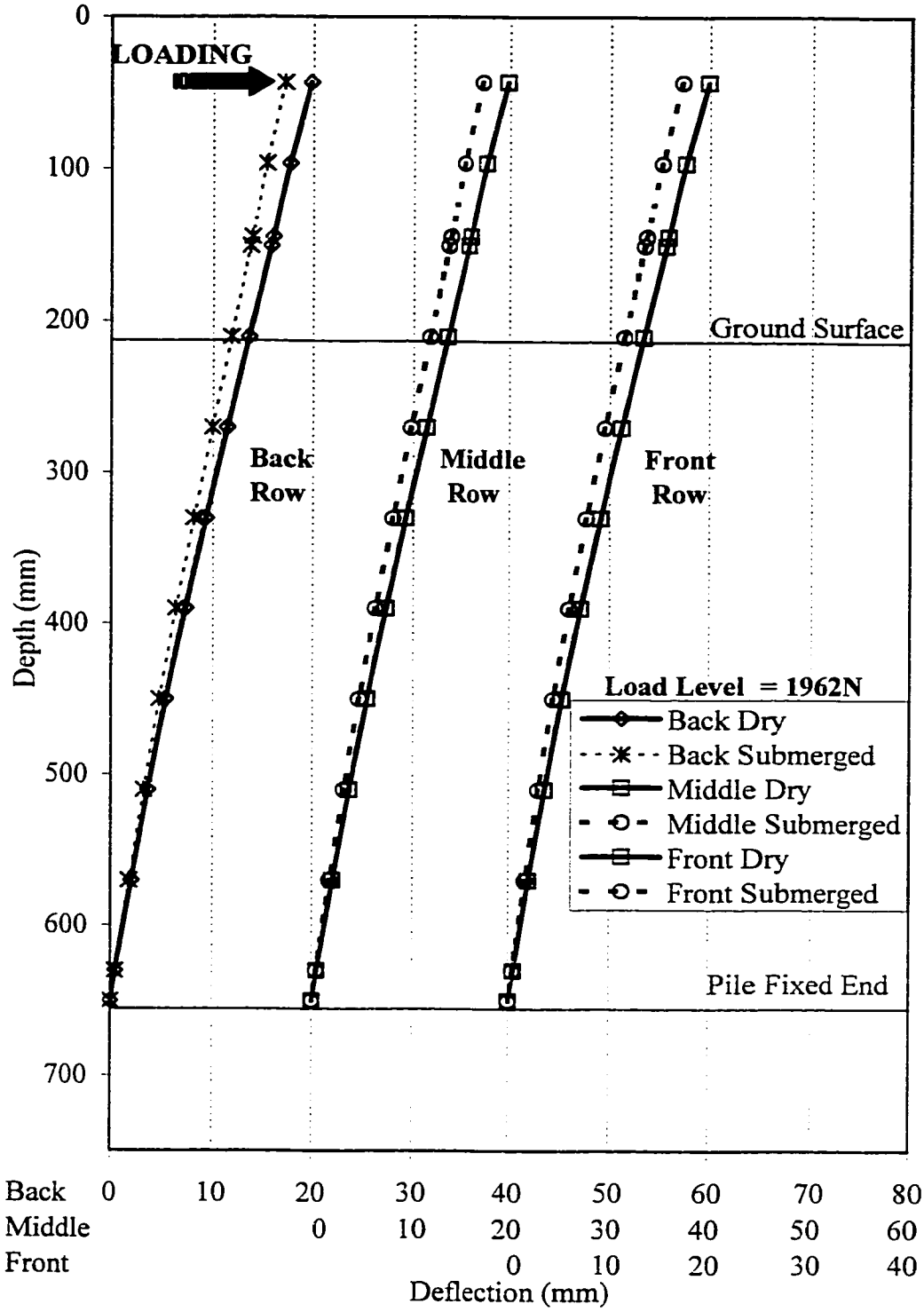

Figure 4.30a: Comparison of Deflection Variation with Depth for Nine Pile Group Between Dry and Submerged Sand Conditions Subjected to 1962N Static Lateral Load.

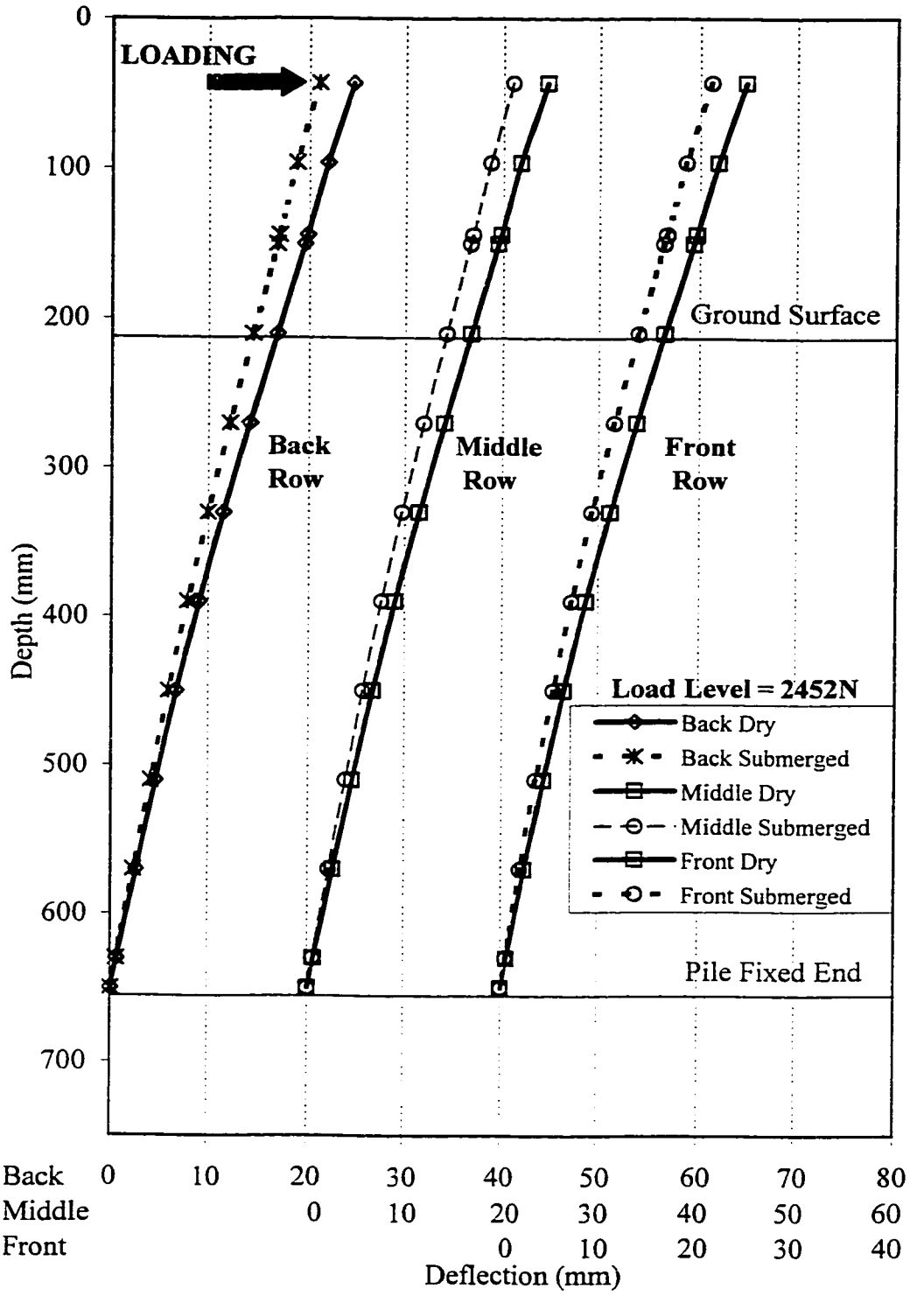

Figure 4.30b: Comparison of Deflection Variation with Depth for Nine Pile Group Between Dry and Submerged Sand Conditions Subjected to 2452N Static Lateral Load.

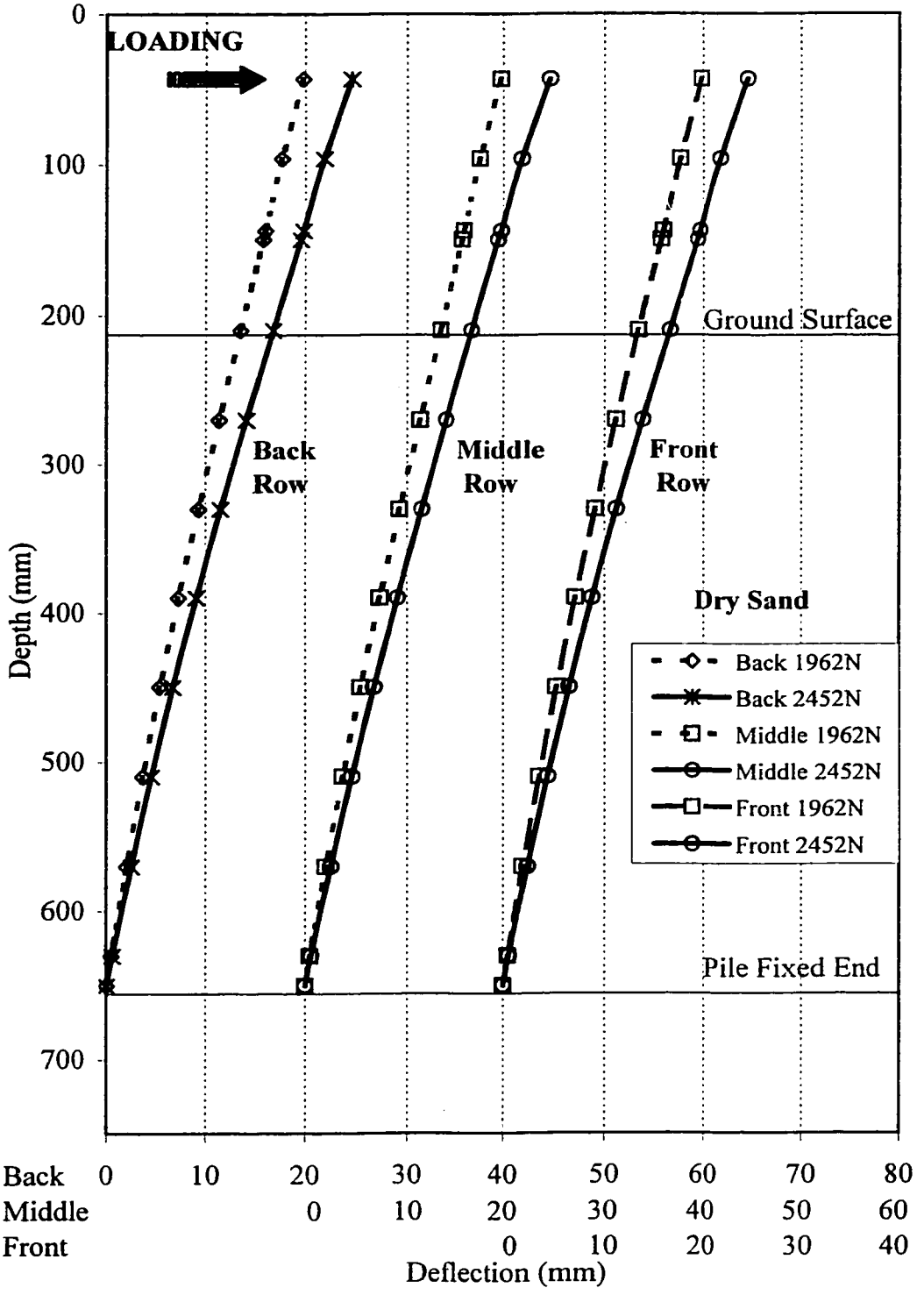

Figure 4.31a: The Variation of Deflection with Depth for Nine Pile Group in Dry Sand Subjected to Static Lateral Load.

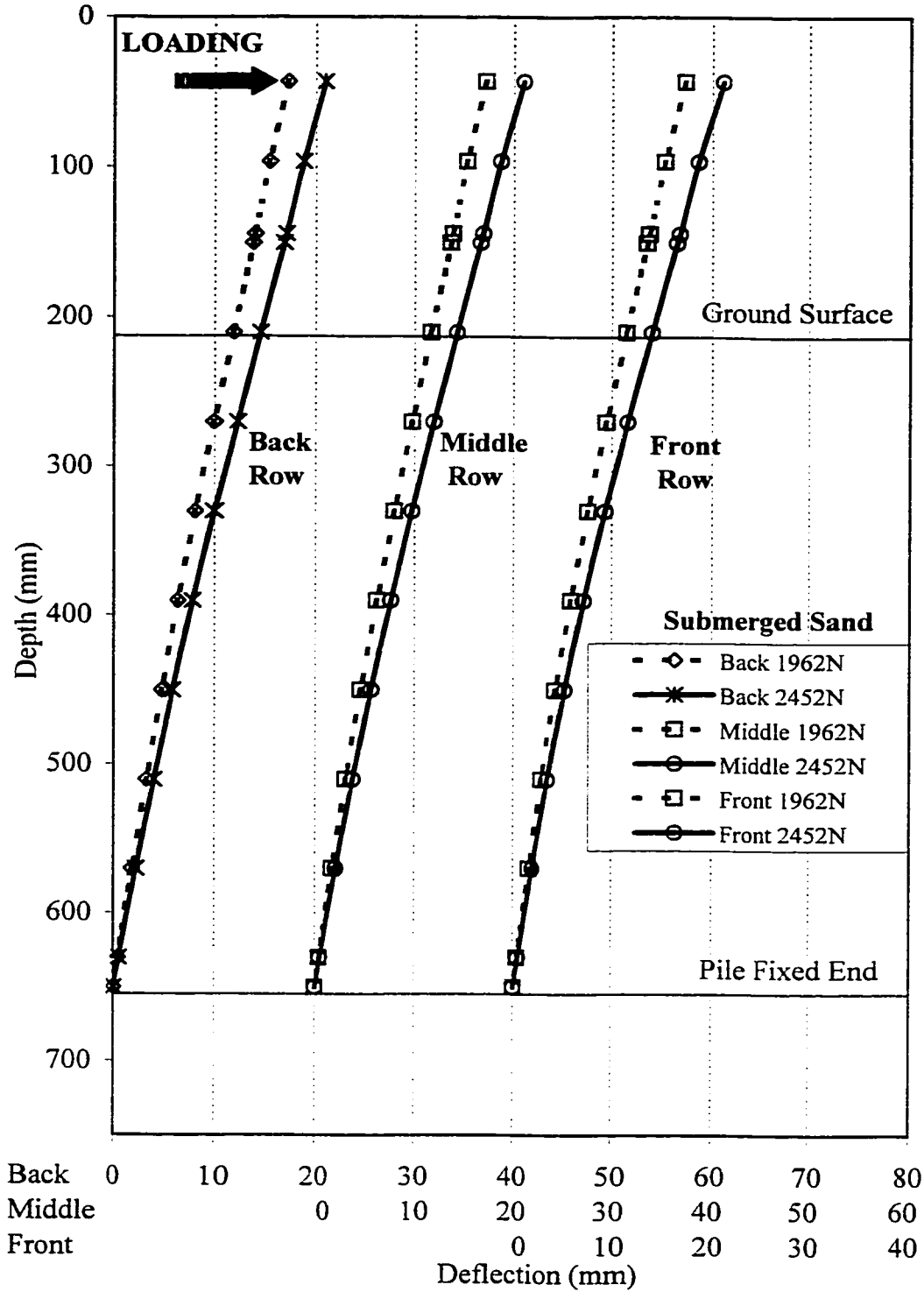

Figure 4.31b: The Variation of Deflection with Depth for Nine Pile Group in Submerged Sand Subjected to Static Lateral Load.

that as the load level increases, the deflection and the curvature along piles increases accordingly for all pile rows positions and in both dry and submerged sand conditions. Hence, it is concluded that the deflection along the piles is affected by the group behavior as discussed earlier.

4.5 Comparison of Experimental and Semi-Empirical Moments and Deflections

The experimental bending moments and deflections were compared with semi-empirical ones using an interactive computer Software. This software was programmed by utilizing the finite difference method to solve equation 2.1 mentioned earlier in chapter two.

Figurers 4.32 and 4.33 represent the comparison between the experimental and theoretical results for the bending moments and deflections, respectively, at static load level of 392N and 554N. It can be clearly seen from figure 4.33 that there is a considerable differences in deflections where the experimental deflections greater than the theoretical ones, if considered at the same depth and for the same load level. Thus, it is reflecting that the semi-empirical p-y curves were stiffer than the experimental ones. Therefore, the pile actually will resists less stiffer soil than expected. This may result in greater experimental moments, which was usually expected. However, as shown in figure 4.32 that the experimental moments were greater along the pile sections except for the middle section which is the most critical part of the pile due to the maximum moment position. The reductions of maximum experimental moments were due to the fixity end of the pile that was producing moments at the bottom of the pile, whereas in the theoretical pile was assumed to have a

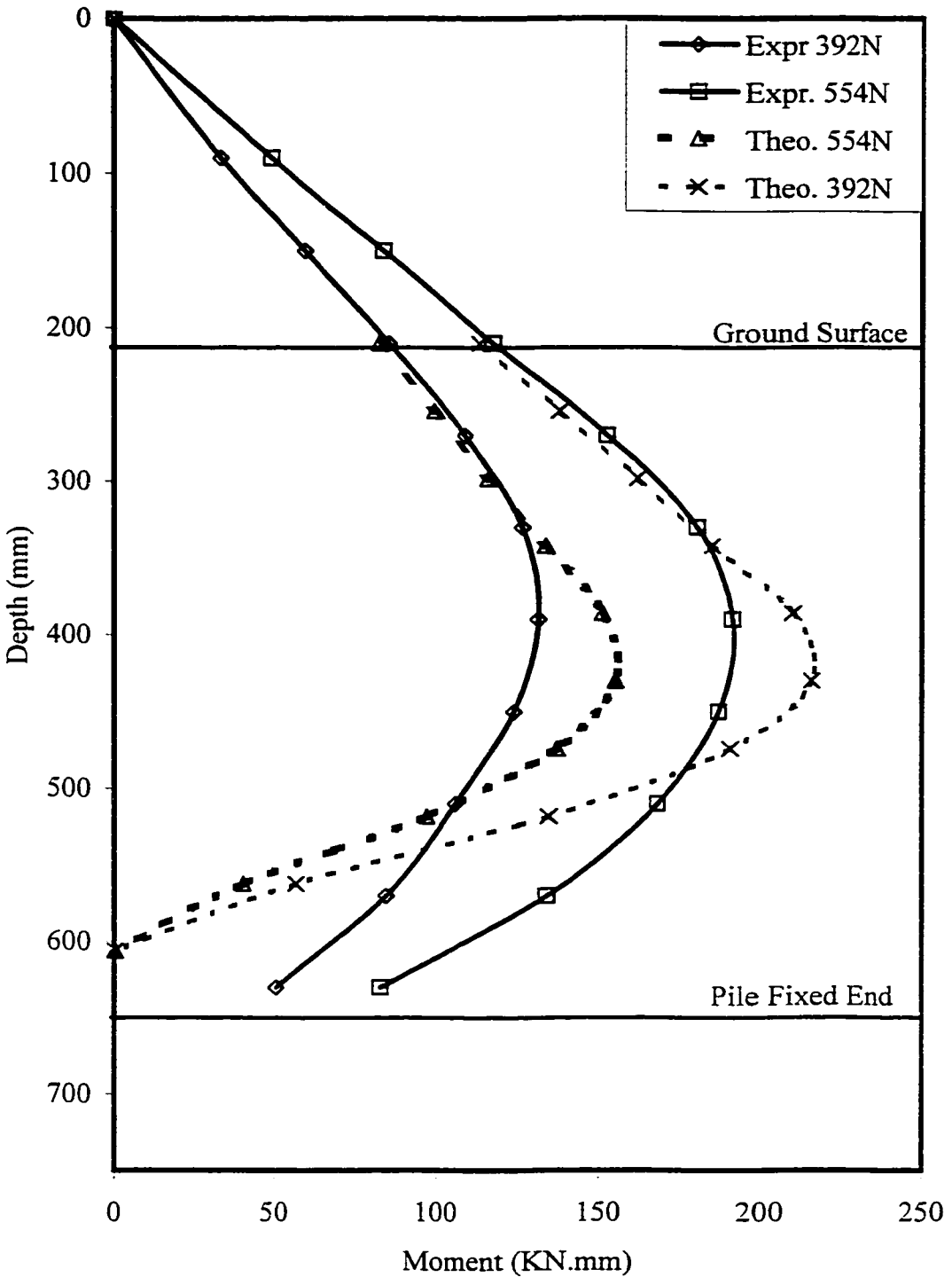

Figure 4.32: Experimental and Theoretical Moment Comparison for Single Pile in Dry Sand Subjected to Lateral Static Load.

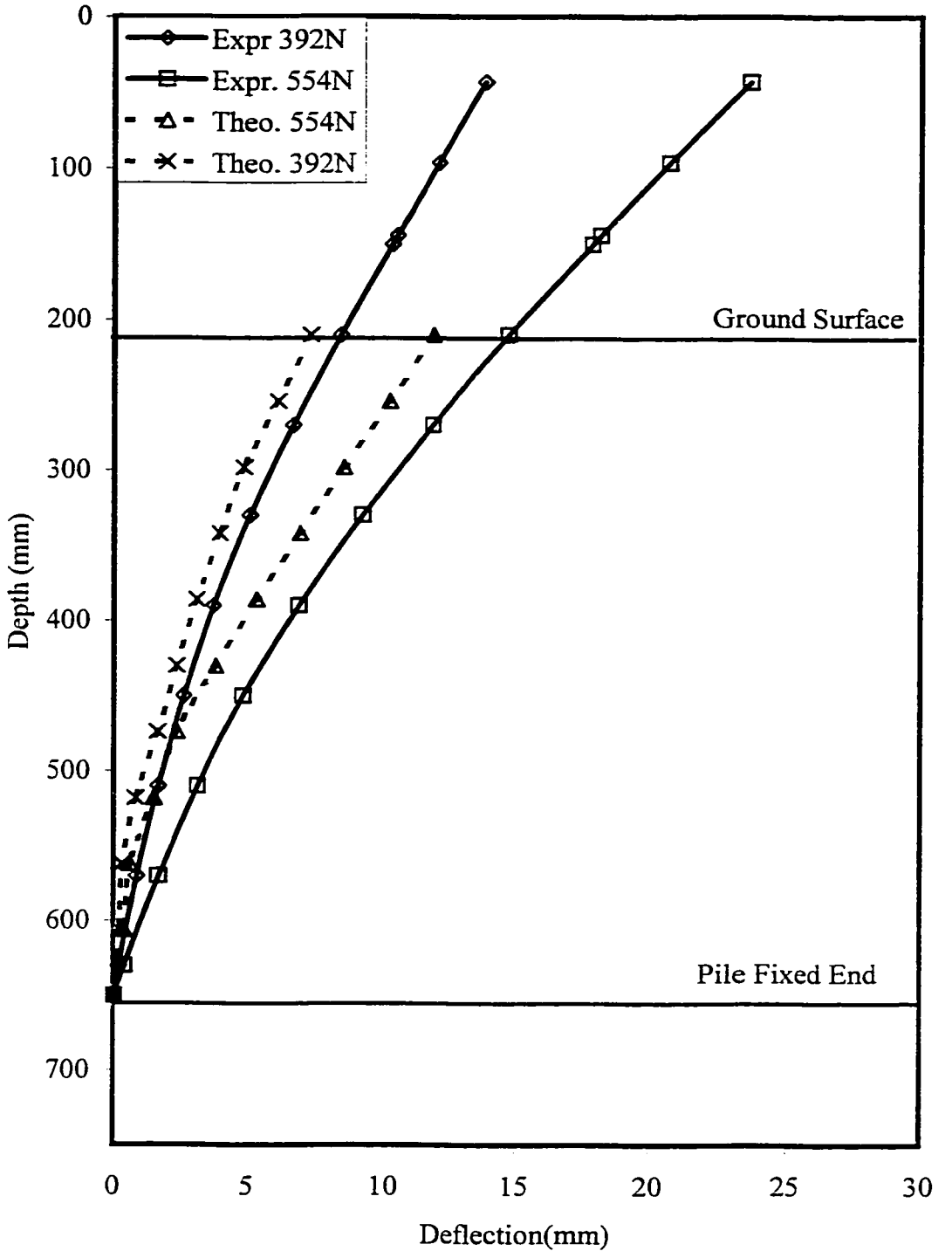

Figure 4.33: Experimental and Theoretical Deflection Along the pile Comparison for Single Pile in Dry Sand Subjected to Lateral Static Load.

free end, which does not produce any moments. In other words, it can be concluded that theoretical solution is more conservative than the actual situation and that the p-y curves is stiffer than the actual.

CHAPTER FIVE

BEHAVIOR OF PILE MODELS UNDER CYCLIC LOAD

5.1 Introduction

Piles for offshore structure are usually subjected to cyclic lateral loads in addition to static loads. The type of loading and hence the movement of piles due to such load has great effect on the soil behavior. Such movement will disturb the soil and may change some of its characteristics and properties. Studying these effects, the piles embedded in the sand were subjected to fully reversible load by controlling and monitoring the load level. The load was initially restrained by means of control valves to one third the maximum static load applied earlier for each type of the pile group. The load level, deflection, and strains were recorded by data acquisition system. At each cycle, an average of twenty readings were recorded, these were analyzed via computer software. Finally, the results were drawn and discussed hereinafter.

5.2 Test Results and Discussion

5.2.1 General Pile Behavior Under Cyclic Loading

It is very important to study the load-deflection curve of piles occurring due to cyclic loading, in order to analyze and understand the behavior of such piles. The analysis will be based on three different pile groups, i.e. single pile, four pile group and nine pile group, in addition to varying the sand condition, i.e. either dry or submerged. Figures 5.1 to 5.6 represent the load-deflection curve for the six cases mentioned above considering the group load and the group deflection.

In order to study the load deflection curves a representative sample was selected for the analysis since all the other pile groups behaved similarly, except for the magnitude of the deflection and the load level. Figure 5.5 represented load-deflection curve of nine piles embedded in dry sand and subjected to lateral cyclic loading. The intention was to measure the load level versus the overall deflection of the group in all experiments, as shown in the figure. It can be noted that the peak load level was almost fixed at both sides and the varying parameter was the deflection, according to the number of cycles. At initial stage the deflection of the group was greater at first cycle in the forward stroke due to the small value of the initial dry density of sand. Following which, the deflection was decreasing as the number of cycles increased due to sand gradual compaction until the sand stabilizes at high cycle number. Hence, the load-deflection curves were overlapping as the movement was stabilized almost beyond ten cycles.

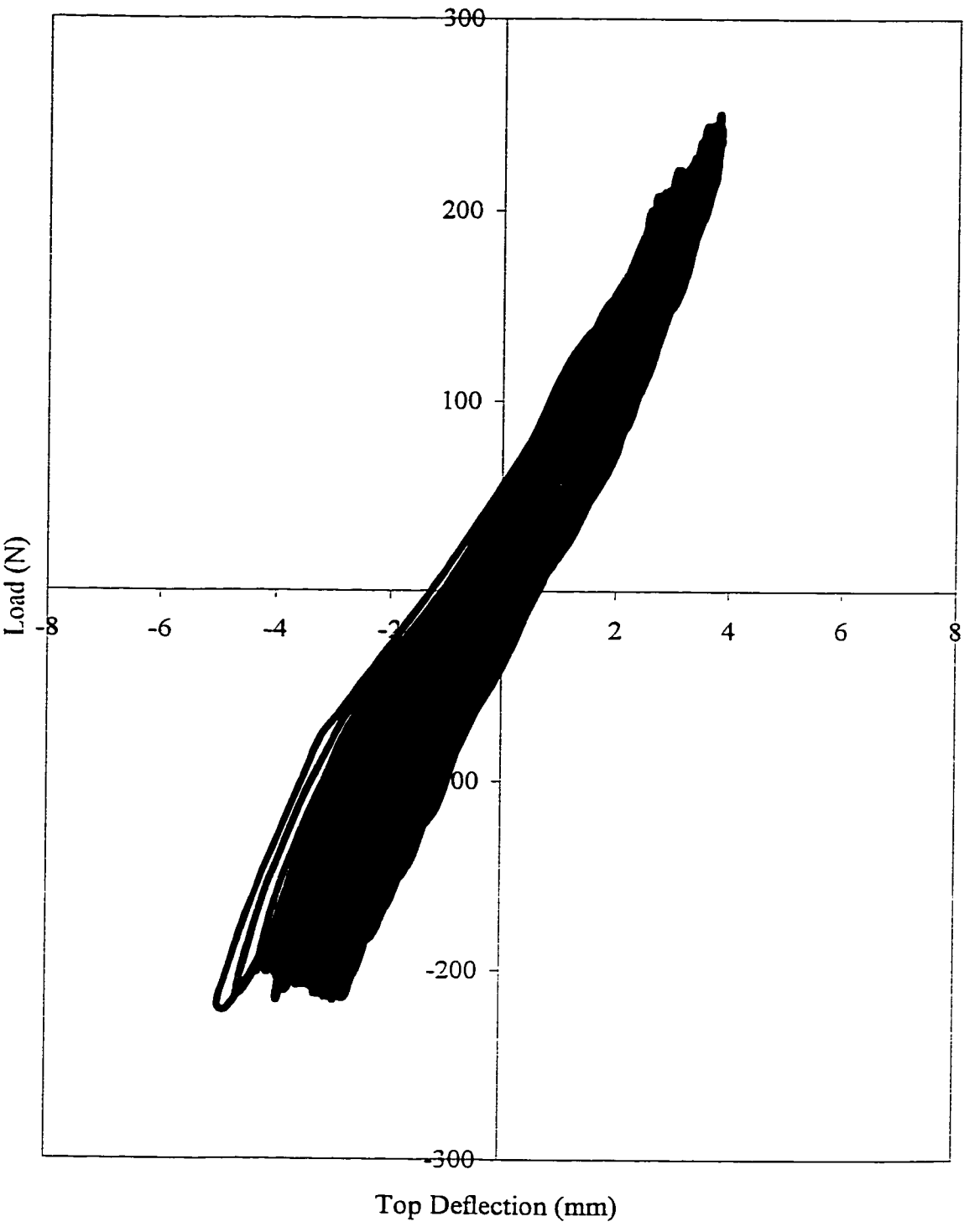

Figure 5.1: Load Deflection Curve for Single Pile in Dry Sand Subjected to Cyclic Lateral Load.

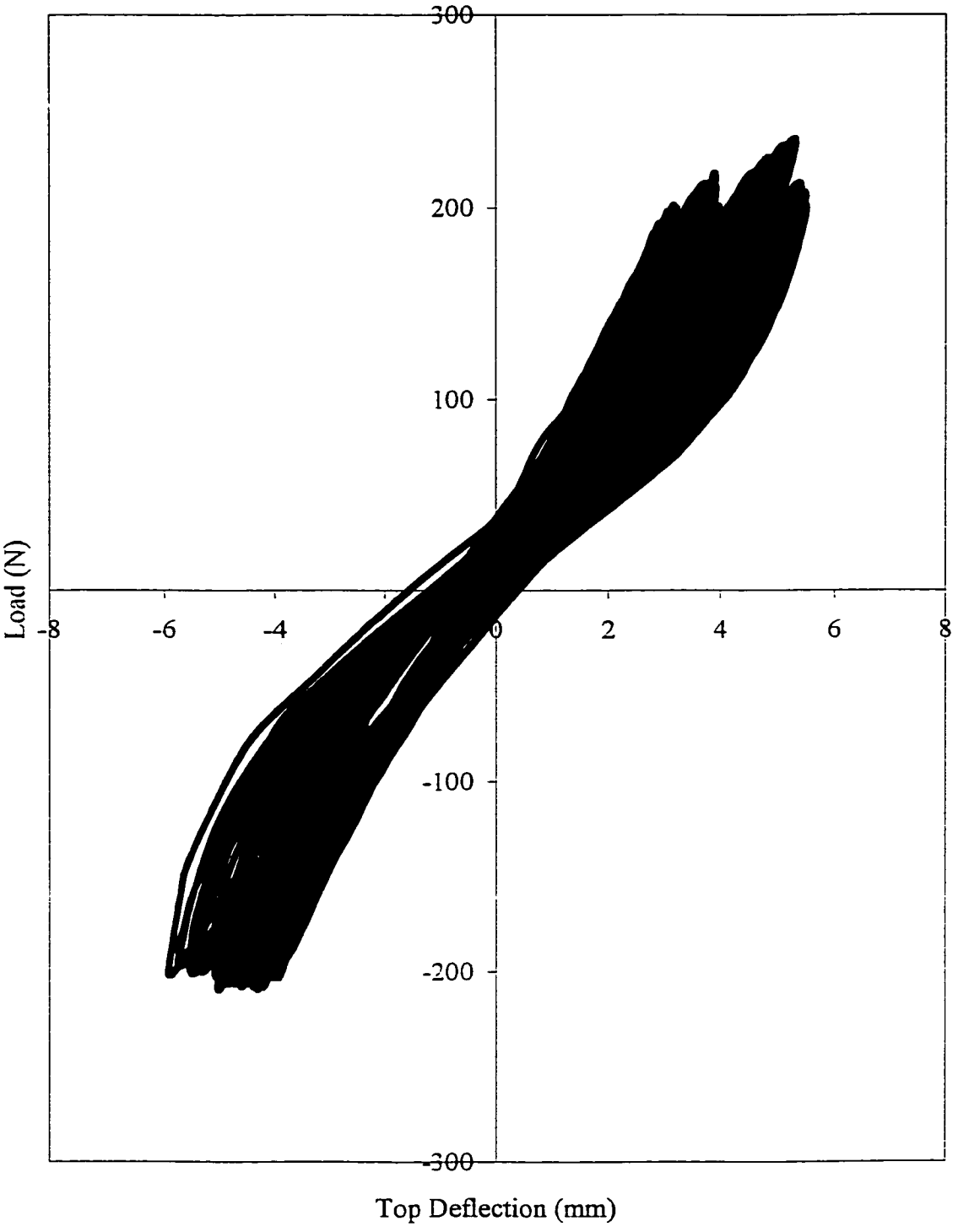

Figure 5.2: Load Deflection Curve for Single Pile in Submerged Sand Subjected to Cyclic Lateral Load.

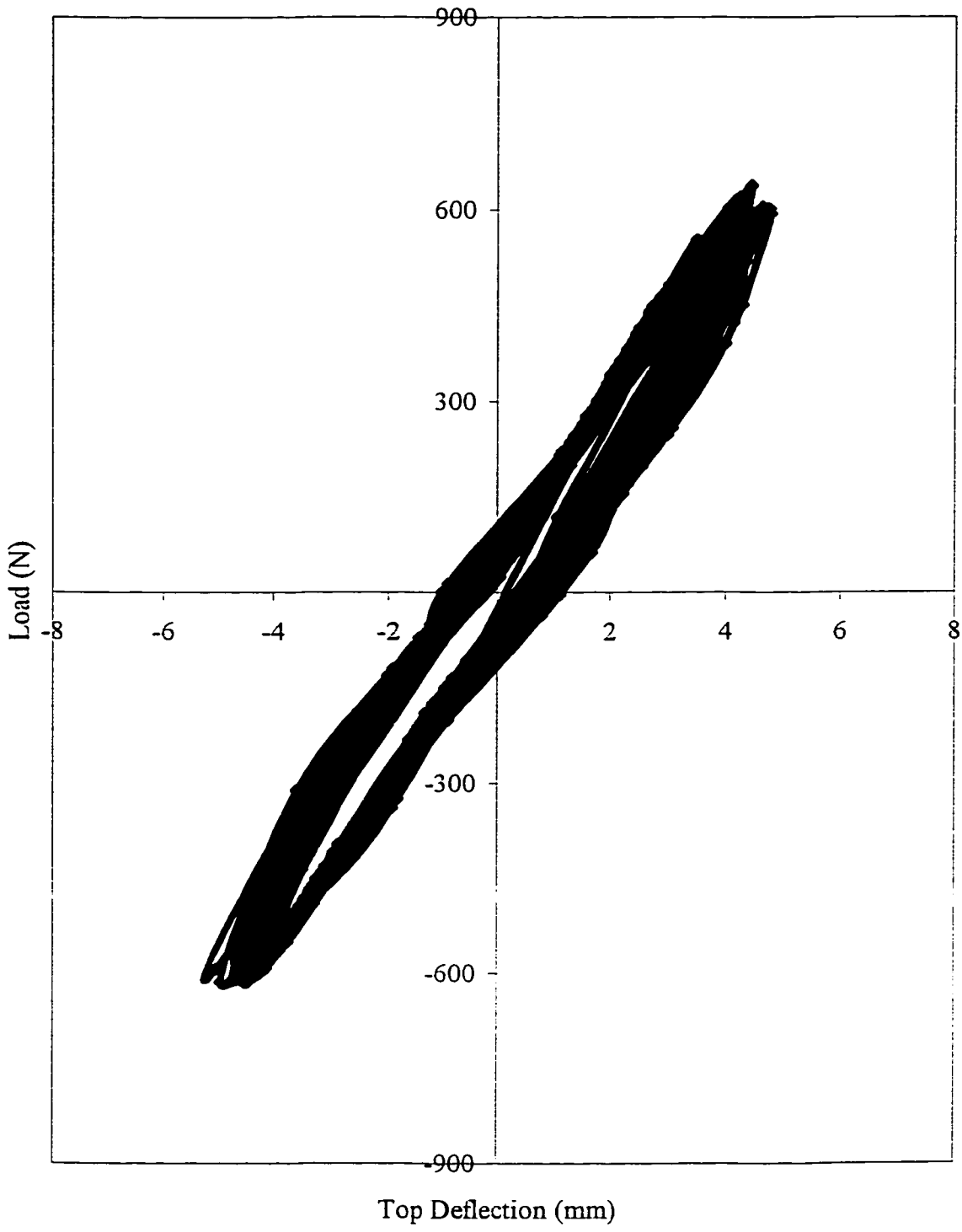

Figure 5.3: Load Deflection Curve for Four Pile Group in Dry Sand Subjected to Cyclic Lateral Load.

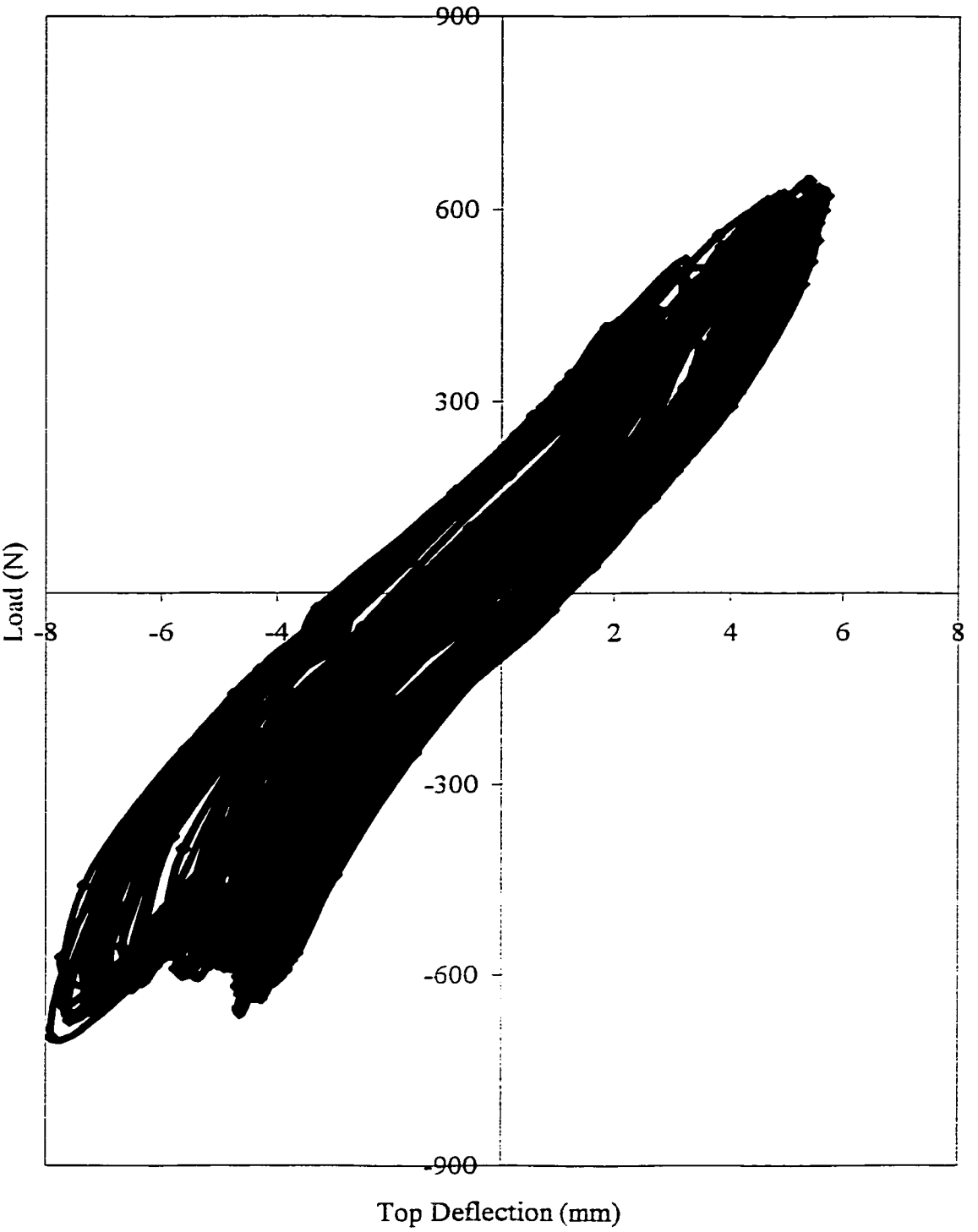

Figure 5.4: Load Deflection Curve for Four Pile Group in Submerged Sand Subjected to Cyclic Lateral Load.

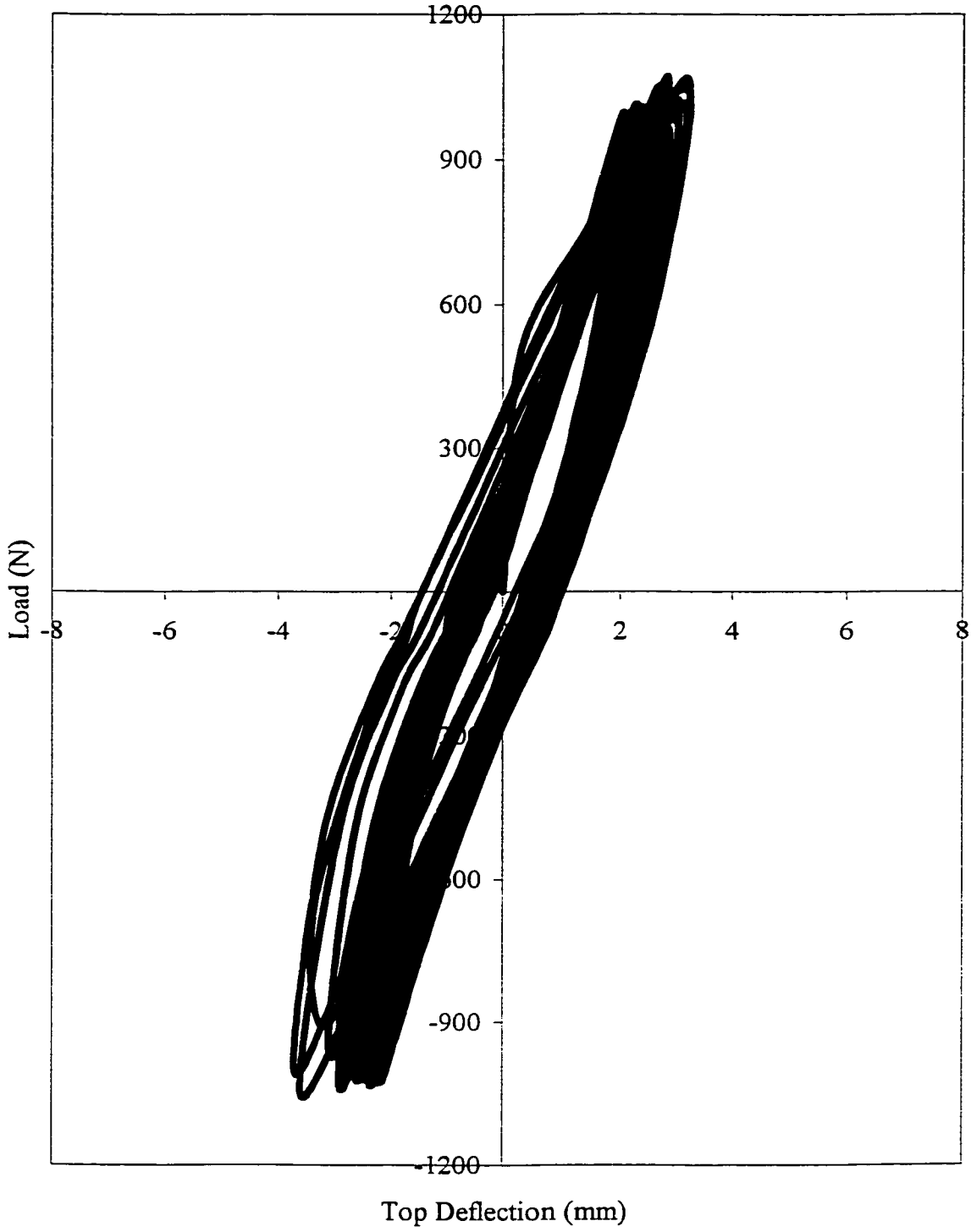

Figure 5.5: Load Deflection Curve for Nine Pile Group in Dry Sand Subjected to Cyclic Lateral Load.

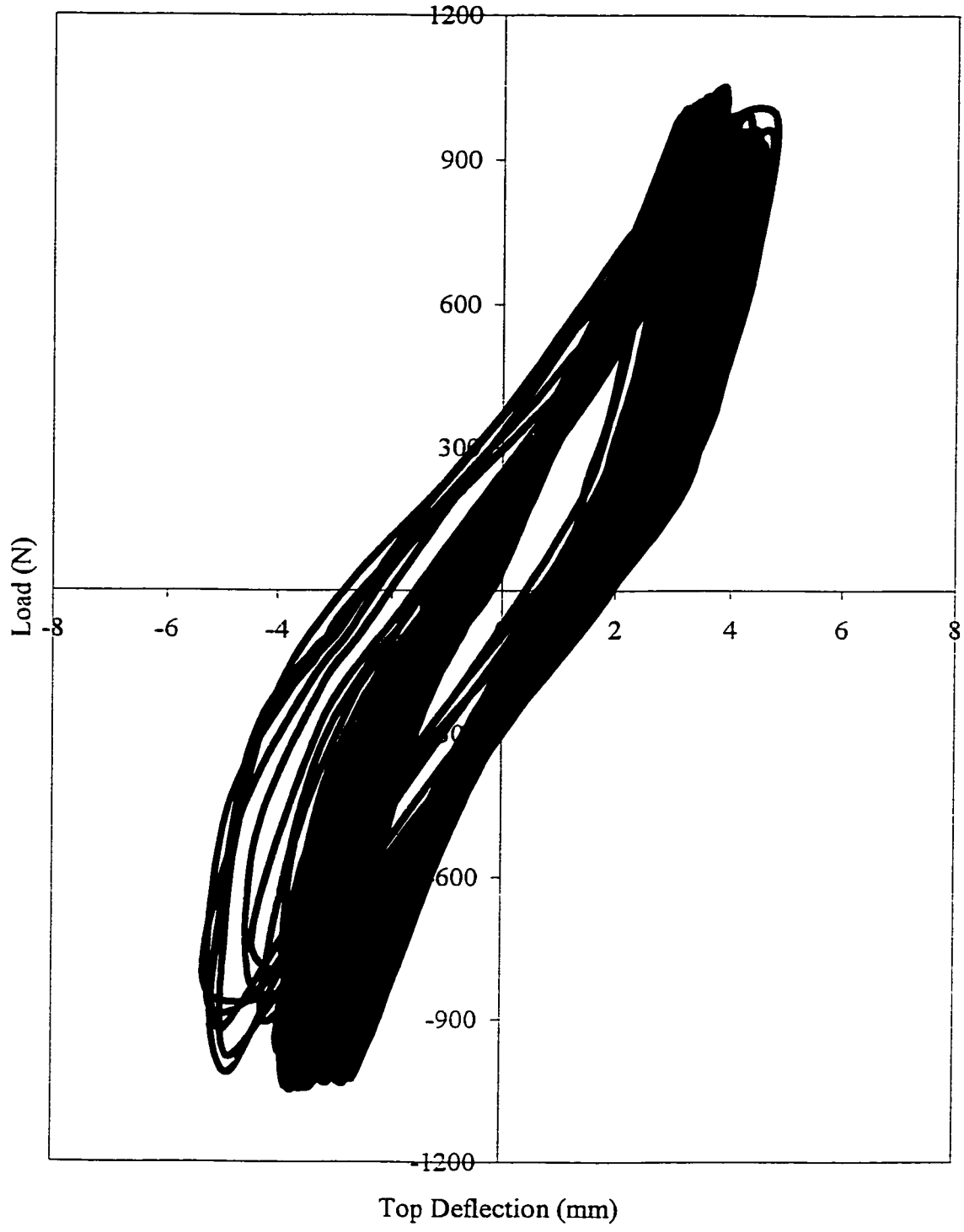

Figure 5.6: Load Deflection Curve for Nine Pile Group in Submerged Sand Subjected to Cyclic Lateral Load.

The figure may not show clearly the phasing of the deflection changes. In order to clearly show this behavior in the load deflection curve three cycles were isolated in separate chart as shown in figure 5.7. The selected cycles were 1, 10 and 200 respectively. The deflection was reduced due to sand compacting as piles movement alters the soil density. The sand was densified due to the following reasons. First, the relatively slow sand vibration which allow for sand compaction. The cycling frequency used in practice usually 0.067 Hz, such as in Reese, et al. (1988) experiments, while the one used in these experiment was 0.036 Hz which is almost half. Secondly, the sand relative density was less than 75% which allows more densification with loading (Woods 1996). The sand density tends to increase with piles movement until it reaches a limiting value corresponding to current load level. Third, the type of cyclic lateral loading on the sand, in which the peak load was constant during the tests, tending to shakedown and confine the sand by filling the voids between sand particles. Contrarily, in most of previous experiments carried out on the same type, the loading depends on the fixed peak deflection which disturbs and loosen the sand by increasing the voids between the sand particles that reduces the confinement, regardless of the load magnitude (Reese, et al. 1988). In fact, the mechanism applied in this study simulates the actual loading criteria in nature, where the load is the governing factor rather than the deflection. Finally, as an evidence to the downward sand particles movement and therefore sand densification the sand area around the piles was moved as shown in plate 5.1.

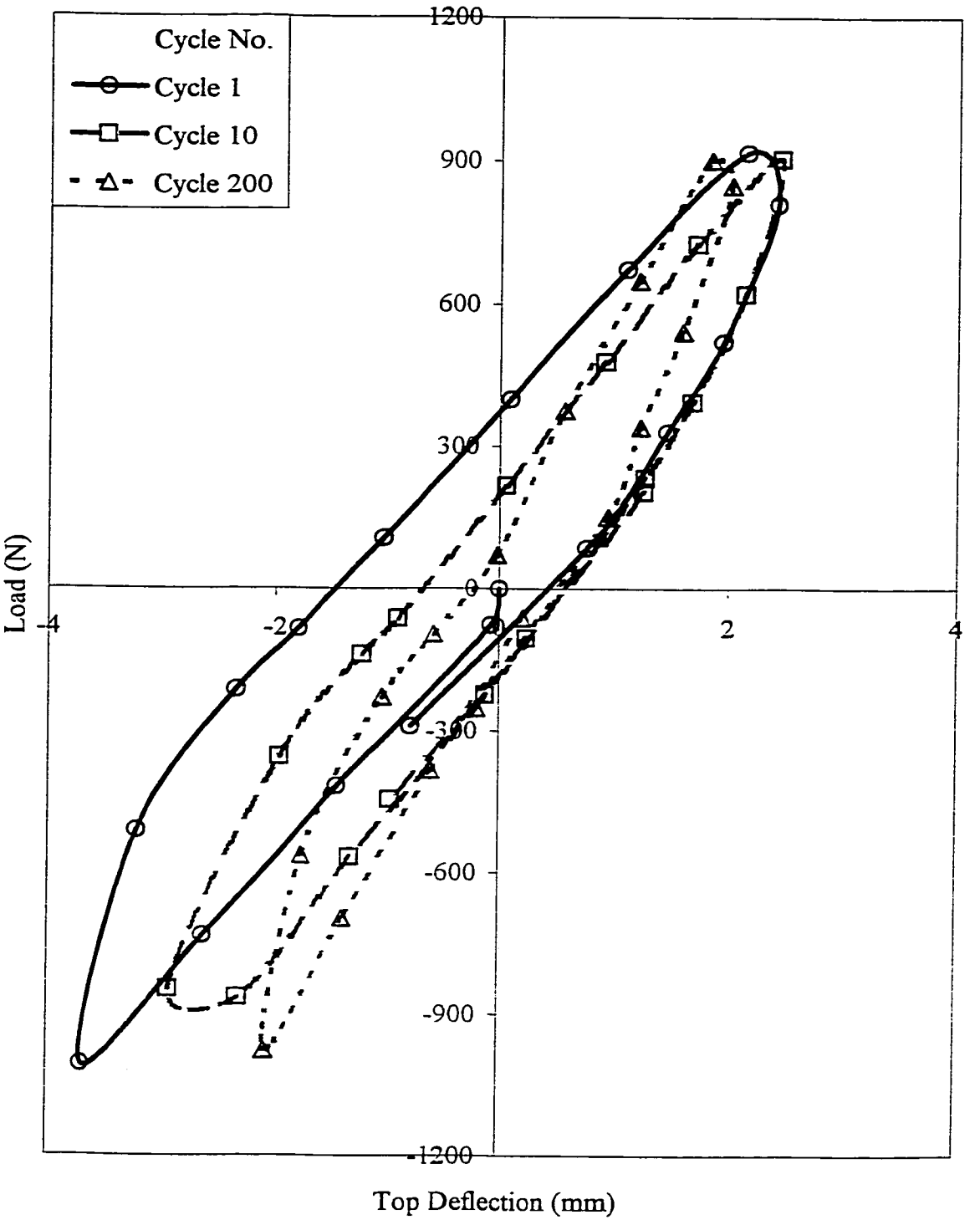

Figure 5.7: Isolated Cycles of Load Deflection Curve for Nine Pile Group in Dry Sand Subjected to Cyclic Lateral Load at Different Cycles.

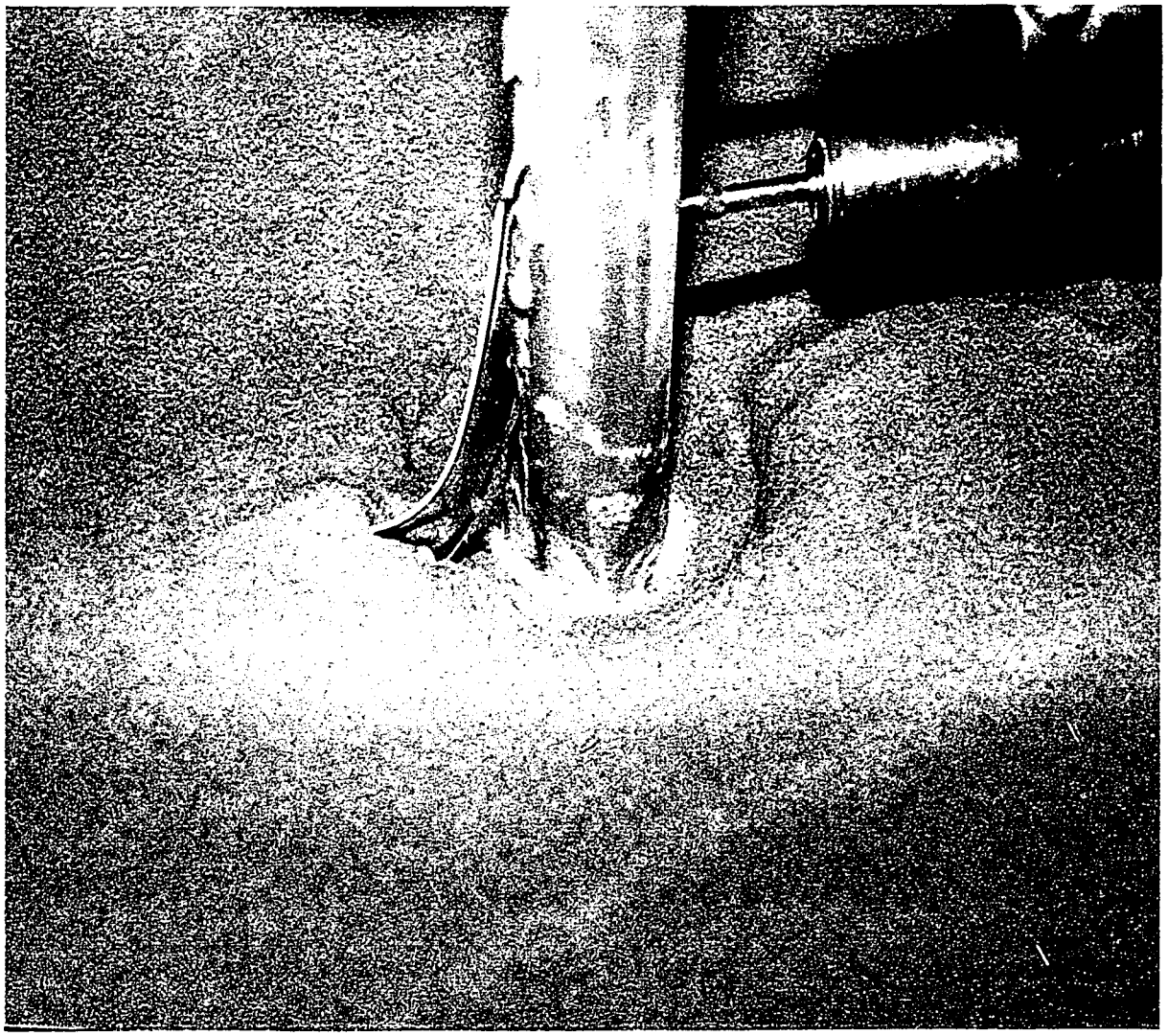

Plate 5.1: Downward Sand Particles Movement Causing Densification.

In conclusion, due to all reasons mentioned above sand densification is likely to occur, and thereafter increasing the soil resistance which cause reduction in deflection and bending moments.

5.2.2 Single Pile

The foundations supporting offshore structures are subjected to vertical axial loads due to facilities on the deck and the self weight of the structure, in addition to lateral cyclic loads due to sea wave action. These foundations are transferring loads from the superstructure to piles constructed below them and then to the surrounding soil. The following paragraphs discuss the effect of lateral cyclic loading on single pile model embedded into both dry and saturated sand. The behavior of the pile will be studied by analyzing the top deflection, moment, deflection along the pile, and p-y curves.

Top Deflection

Figure 5.8 presents the lateral load versus top deflection for single pile embedded in dry sand and subjected to cyclic loading. At the initial stage, after the first few cycles, the deflection decreases with the increase in the number of cycles. After which the deflection tends to stabilize as the number of cycles increase, due to soil densification as a result of pile movement. Hence, as the number of cycles increases the pile will face larger resistance, which will lead to the reduction of top deflection.

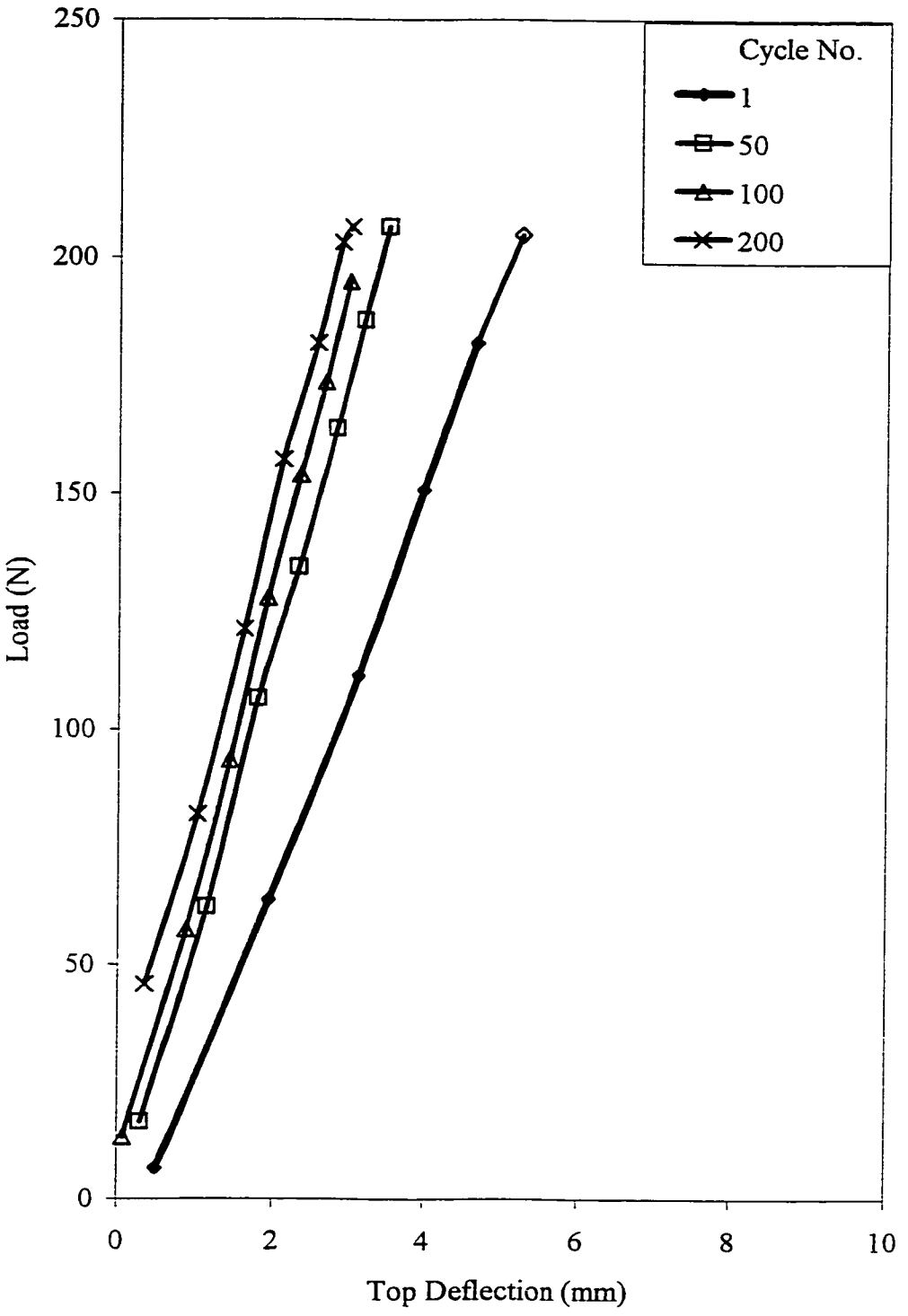

Figure 5.8: Load Deflection Curve for Single Pile in Dry Sand Subjected to Cyclic Lateral Load at Different Cycles.

Similar behavior is shown in figure 5.9 for submerged sand. However, the movements were almost ceased as the number of cycles increase as shown for cycles 50,100 and 200. This is due to the reduction of soil effective density which is directly proportional to soil resistance. The differences between dry and submerged condition increases as the number of cycles increase.

Moment Diagram

The variation of moments along the pile is very important for studying the behavior of pile foundation, as it is needed for the structural design of the pile (i.e. pile section). Moments diagram for pile group was obtained by the same procedure used previously in chapter four for single pile, four pile group, and nine pile group. Figures 5.10 and 5.11 presents moment distribution along the pile for different load cycles under dry and submerged sand conditions, respectively. The figures clearly shows that an increase in number of cycles causes the pile curvature to decrease which in turn causes a decrease in both moment and deflection along the pile.

As discussed in the static loading, the top portion of the moment diagram reflects a cantilever type of behavior. However, in the second portion, moment increases but at a slower rate due to soil resistance until it reaches its maximum moment. Finally, the moment starts to decrease in a nonlinear manner until it reaches the fixed end of the pile. Therefore, the behavior of moment at each cycle is similar to the static loading behavior but at different load level per pile head. Figure 5.12 shows a comparison of maximum moment for a

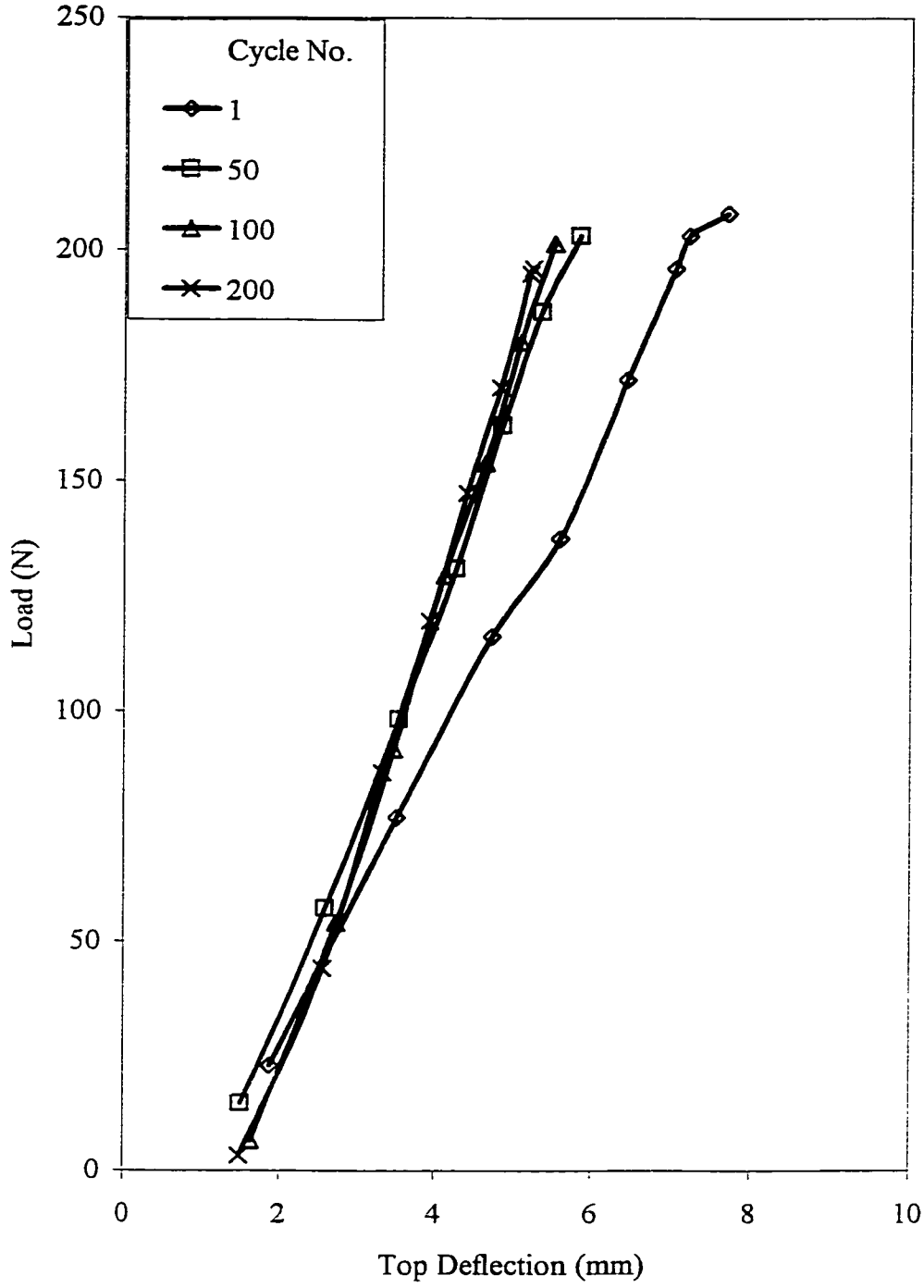

Figure 5.9: Load Deflection Curve for Single Pile in Submerged Sand Subjected to Cyclic Lateral Load at Different Cycles.

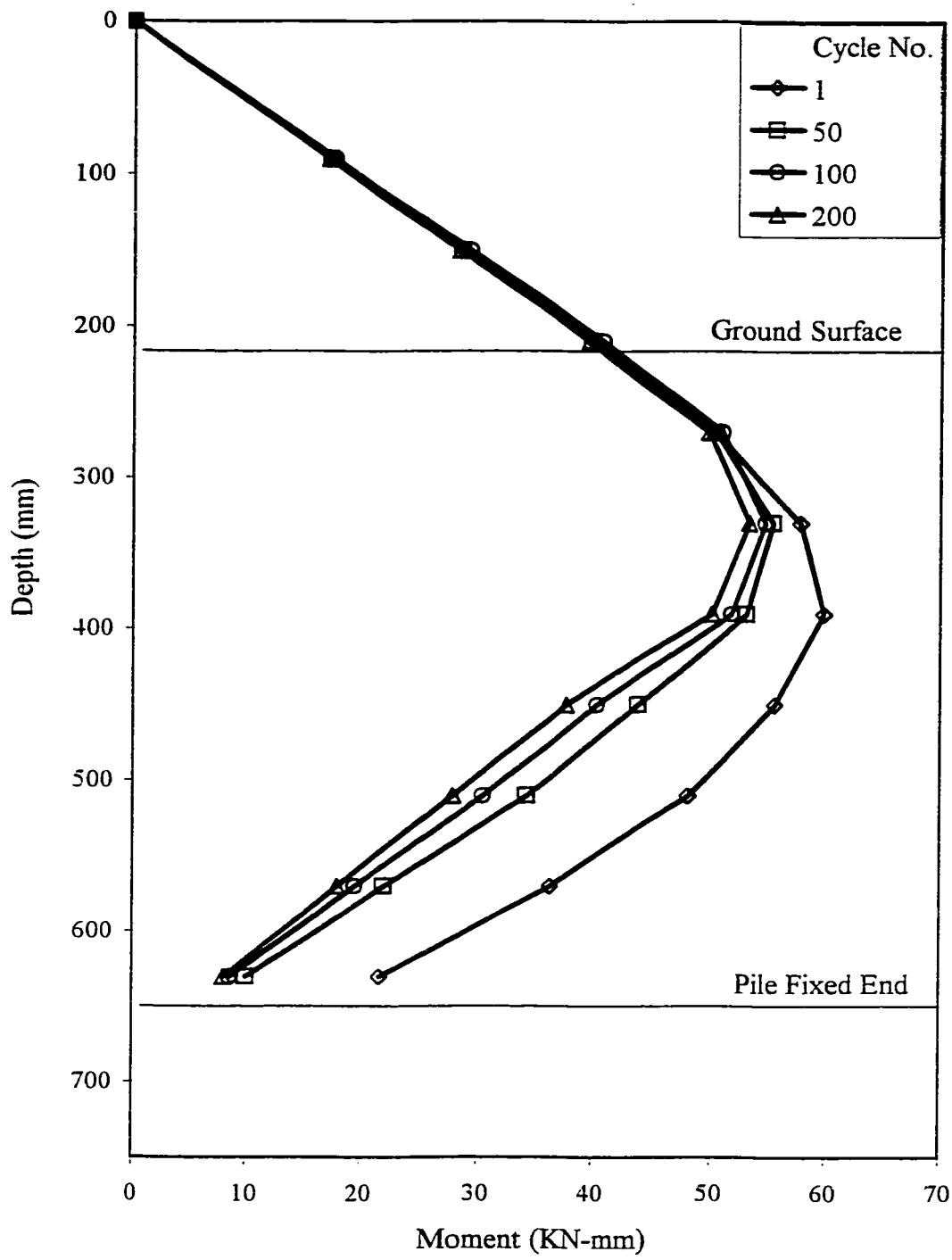

Figure 5.10: The Variation of Moment with Depth for Single Pile in Dry Sand Subjected to Cyclic Lateral Load.

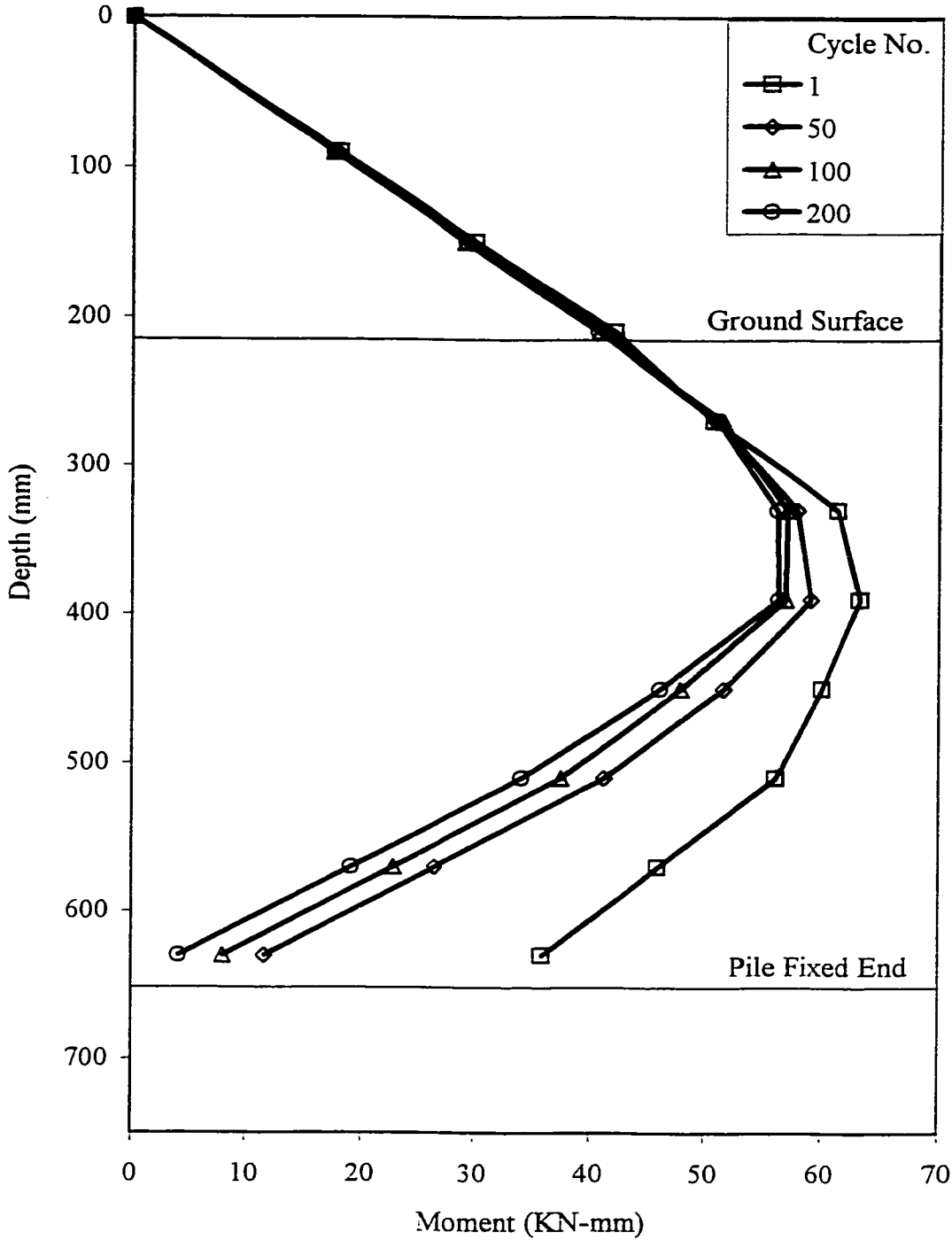

Figure 5.11: The Variation of Moment with Depth for Single Pile in Submerged Sand Subjected to Cyclic Lateral Load.

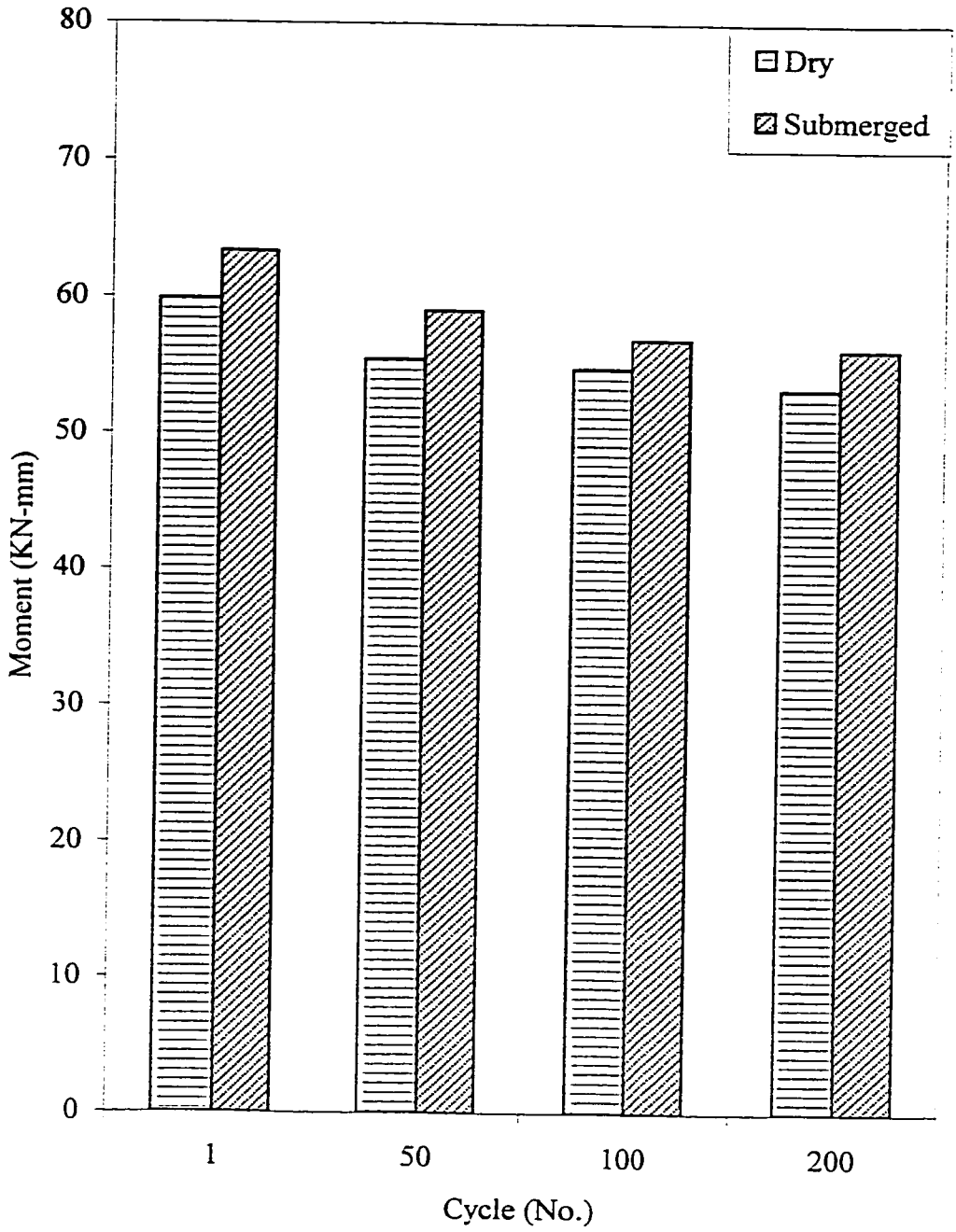

Figure 5.12: Comparison Between Maximum Moment for Dry and Submerged Sand Conditions for Single Pile Subjected to Cyclic Lateral Load.

selected load cycles for both dry and submerged sand condition. It depicts that the maximum moment decreases with the increase in the number of cycles. In addition, it shows that at all cycles, the maximum moment for submerged condition is higher than the dry one, due to the reduction in soil resistance. Figure 5.13 show that the difference mainly occurs below the soil surface (mud line).

Deflection Along Pile Length

Deflection diagrams were produced using the same procedure explained earlier in chapter four for single pile, four pile group, and nine pile group. Figures 5.14 and 5.15 show the deflected shape of a single pile under cyclic load for both dry and submerged sand conditions, respectively. The curves shown are for cycles 1, 50, 100 and 200 at a maximum load level of 20 Kgf. The figures clearly indicated that the deflection of the pile decreases as the number of cycles increase. Figure 5.16 signifies the effect of reducing the soil resistance due to submergence effect where the curvature along the pile is higher for pile embedded in submerged sand than the pile embedded in dry sand. In other words, the deflection is always greater in the submerged sand condition. Furthermore, the curvature of the pile decreases with the increase in number of cycles. This is due to increase in initial slope which is affected by the increase in soil resistance as mentioned earlier. At the bottom of the pile the deflection diminishes due to the fixity condition.

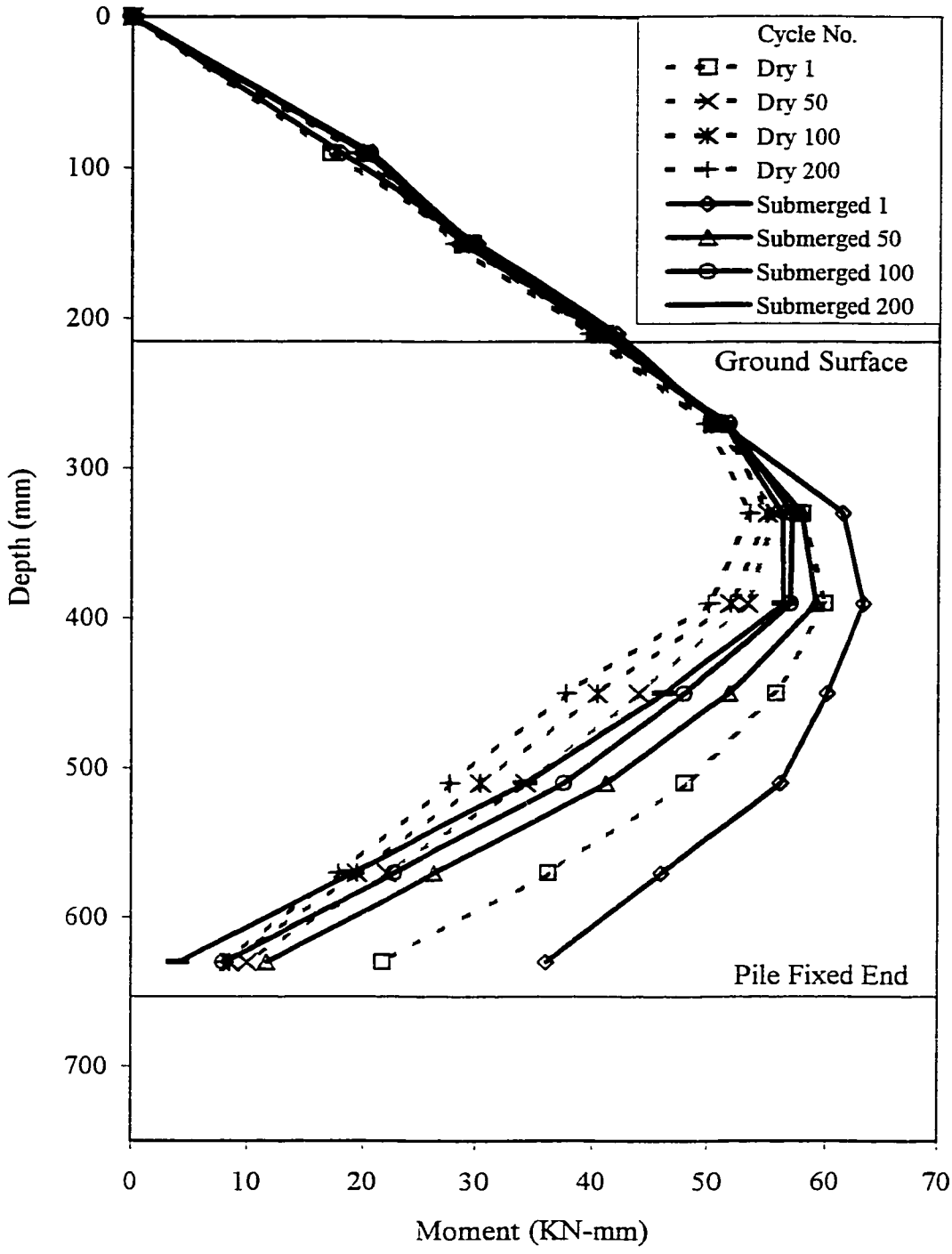

Figure 5.13: Comparison of Moment Variation with Depth Between Dry and Submerged Sand Conditions for Single Pile Subjected to Cyclic Lateral Load.

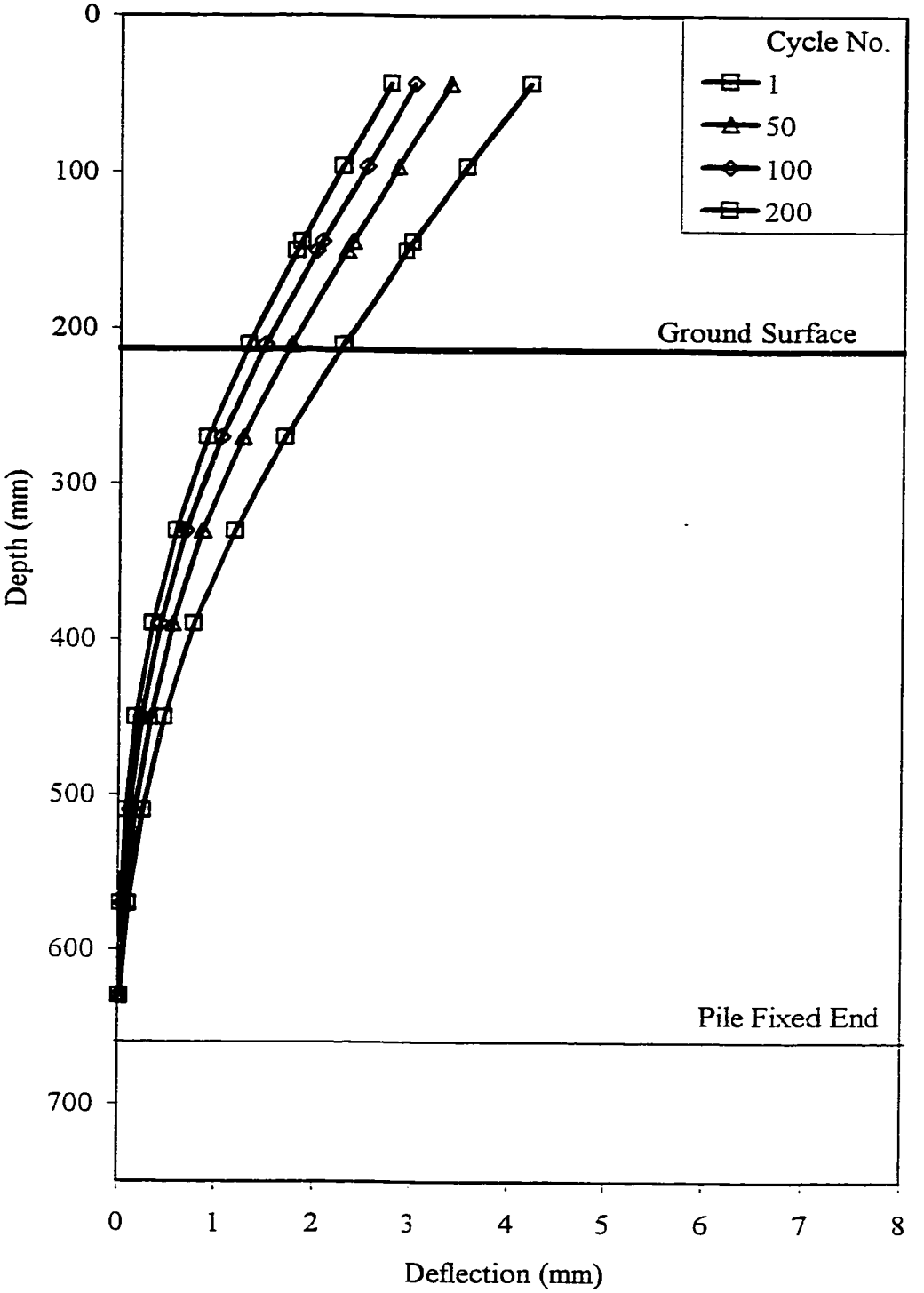

Figure 5.14: The Variation of Deflection with Depth for Single Pile in Dry Sand Subjected to Cyclic Lateral Load.

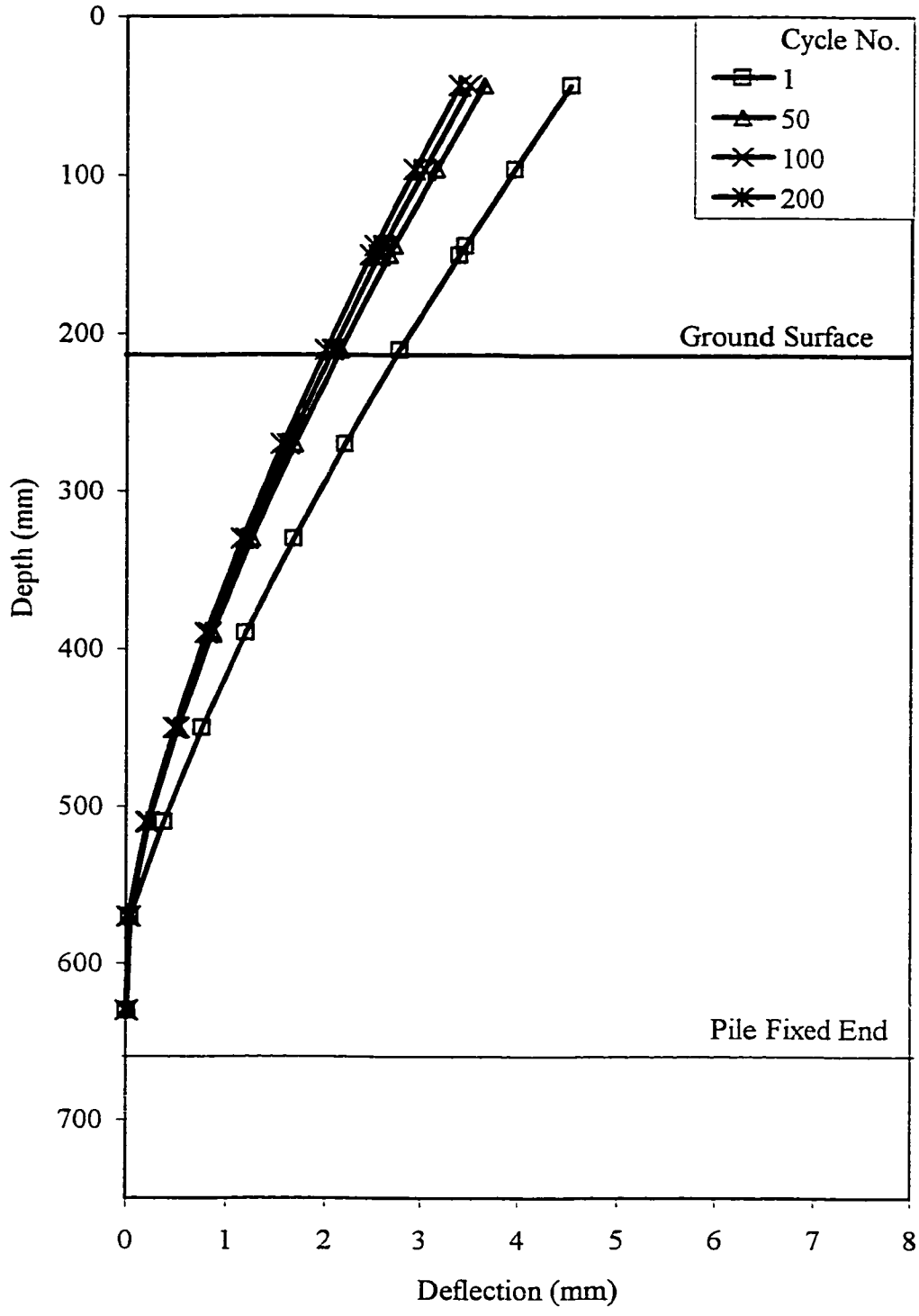

Figure 5.15: The Variation of Deflection with Depth for Single Pile in Submerged Sand Subjected to Cyclic Lateral Load.

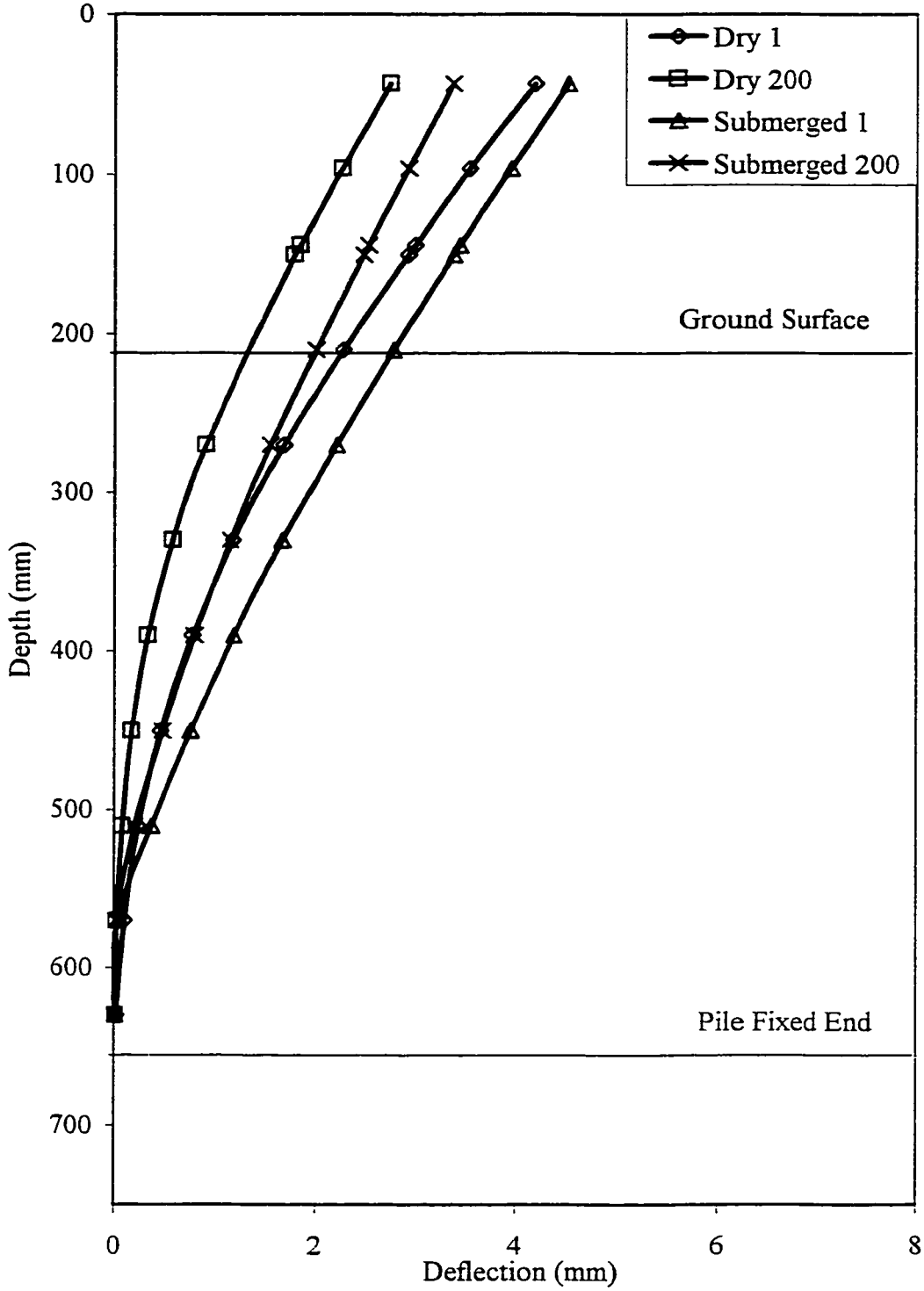

Figure 5.16: Comparison of the Variation of Deflection with Depth for Single Pile Between Dry and Submerged Sand Conditions Subjected to Cyclic Lateral Load.

p-y Curves

The same procedure used in chapter four earlier was applied in this section, to obtain the required soil resistance and p-y curves. The soil resistance was obtained by differentiating the best fit seventh polynomial moment equation twice, while the deflection along the pile was calculated by the conjugate beam method. The soil resistance curves for single pile embedded in dry sand are presented in figure 5.17 for different load cycles. The figure shows that the soil resistance increases with cycles due to the densification in sand discussed earlier (i.e. increase in density). Furthermore, reduction in bending moments and deflection occurred for high number of cycles, while an increase in soil resistance took place with increase in number of cycles. At higher cycles, opposite resistance was produced to counter-act the pile tendency to changes its curvature at pile bottom.

The p-y curves are presented in figure 5.18 for single pile embedded in dry sand and subjected to cyclic load. The measurements were taken at 330mm pile depth. The figure shows the p-y curves for three different cycles i.e. 1, 100 and 200. The figure depicts an increase in soil resistance for the same pile deflection due to increase in number of load cycles. The difference between the first cycle and cycle number 100 is more significant than between that cycle100 and cycle 200. This indicates that the densification process mainly has taken place in the initial load cycles.

5.2.3 Four Pile Group

Four pile group model was also subjected to cyclic lateral load in quest to study the effect of wave action on the row position of the pile group. Piles arrangement was similar to those

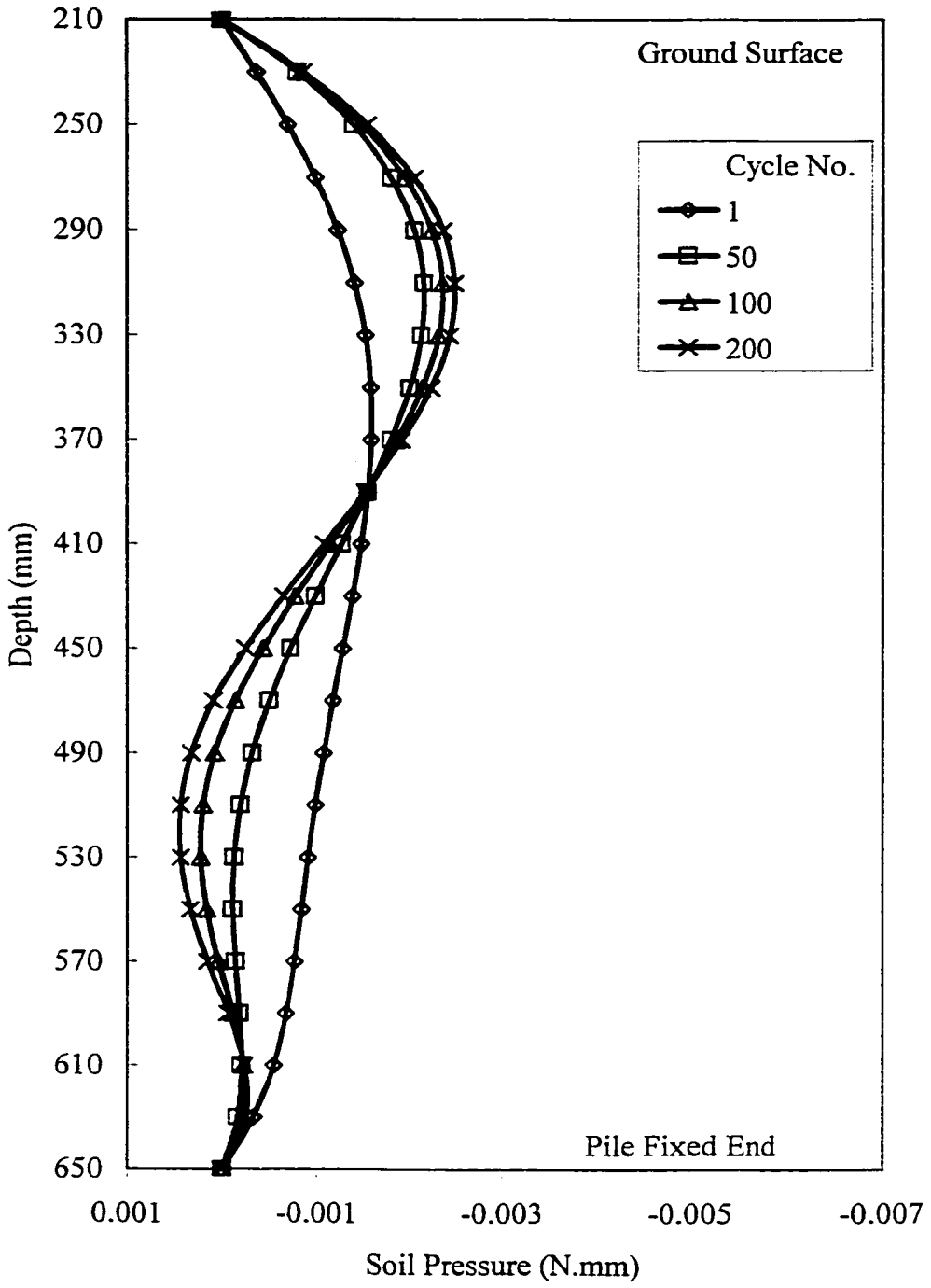

Figure 5.17: Soil Pressure Variation with Depth for Single Pile in Dry Sand Subjected to Cyclic Lateral Load.

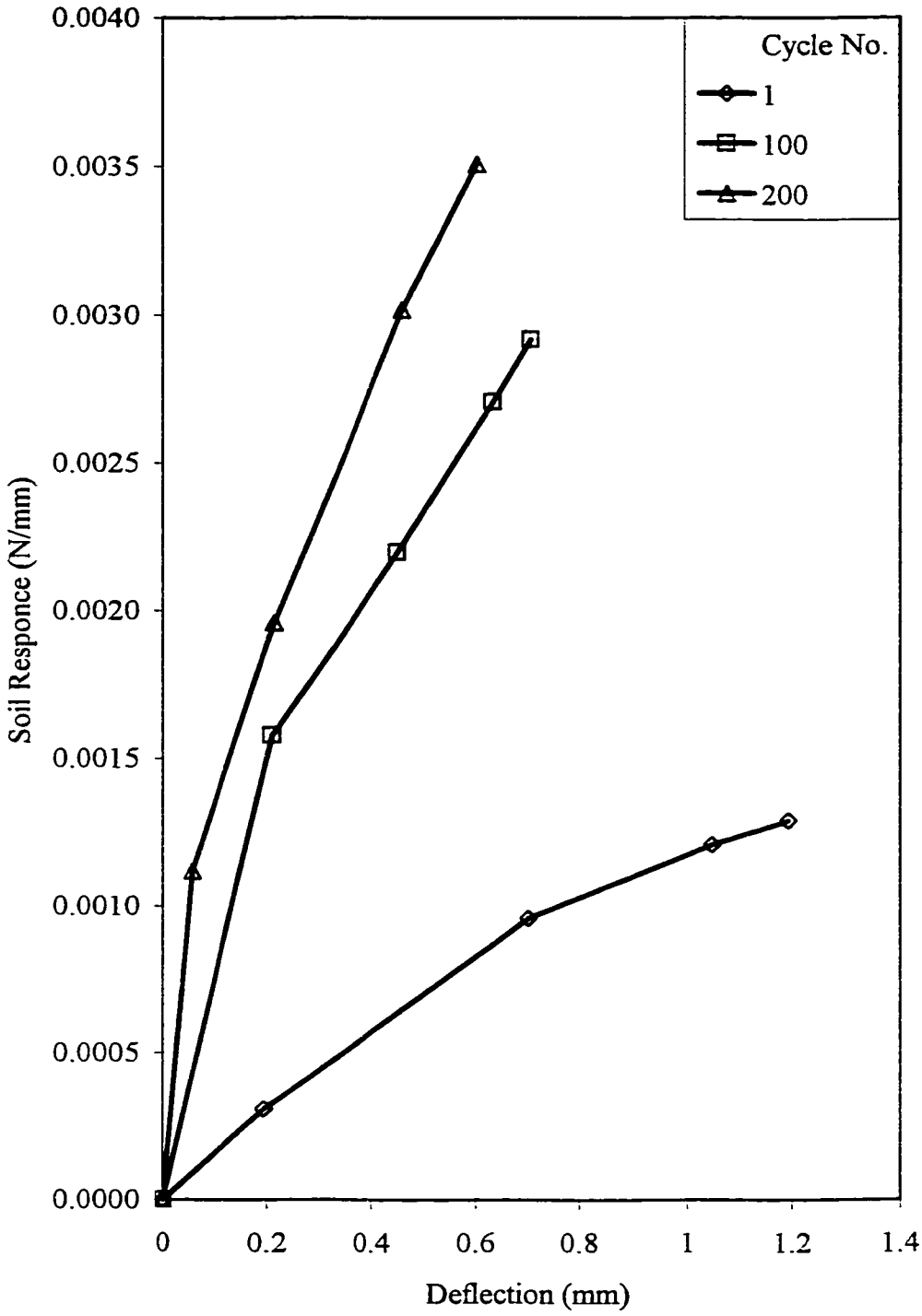

Figure 5.18: p-y Curves for Single Pile in Dry Sand Subjected to Cyclic Lateral Load at Depth of 330mm.

used in static loading. Two tests were carried out; the first one was under dry sand condition while the second was under submerged sand condition. The load at the top of each pile is calculated by the same procedure used previously in chapter four for the static loading case.

Top Deflection

Figure 5.19 depicts the pile head load versus top deflection of the front pile embedded in dry sand for different load cycles. The figure, in general, reflects the same behavior observed for the single pile. At higher load level, the deflection at the top of the pile decreases with the increase in number of cycles. This means that the sand stiffness is increasing with number of cycles. At high number of cycles (e.g. 100 & 200) the movement at the top of pile has been stabilized. At low load level, the deflection at the pile top is higher in the first cycle, considering the same load level. The reason behind this is that the shadowing effect did not take place. Moreover, each pile behaves as an isolated single pile rather than as a part of the group. Therefor, the shadowing effect for certain group will take effect only after reaching specified load level at the first cycle. Figure 5.20 depicts that the back row behavior is identical to the front row.

At the first cycle the group behavior was similar to the one observed for the static loading case. In order, to study the behavior of group of piles under cyclic loading, it was essential to consider it at high number of cycles such as cycle 200 as shown in Figure 5.21. In this figure, the front row attracted higher pile head load, and consequently deflected more than the back row. This behavior was also predicted earlier in the static loading case. Moreover, the cyclic loading reduced the piles top deflection for all piles located at different rows.

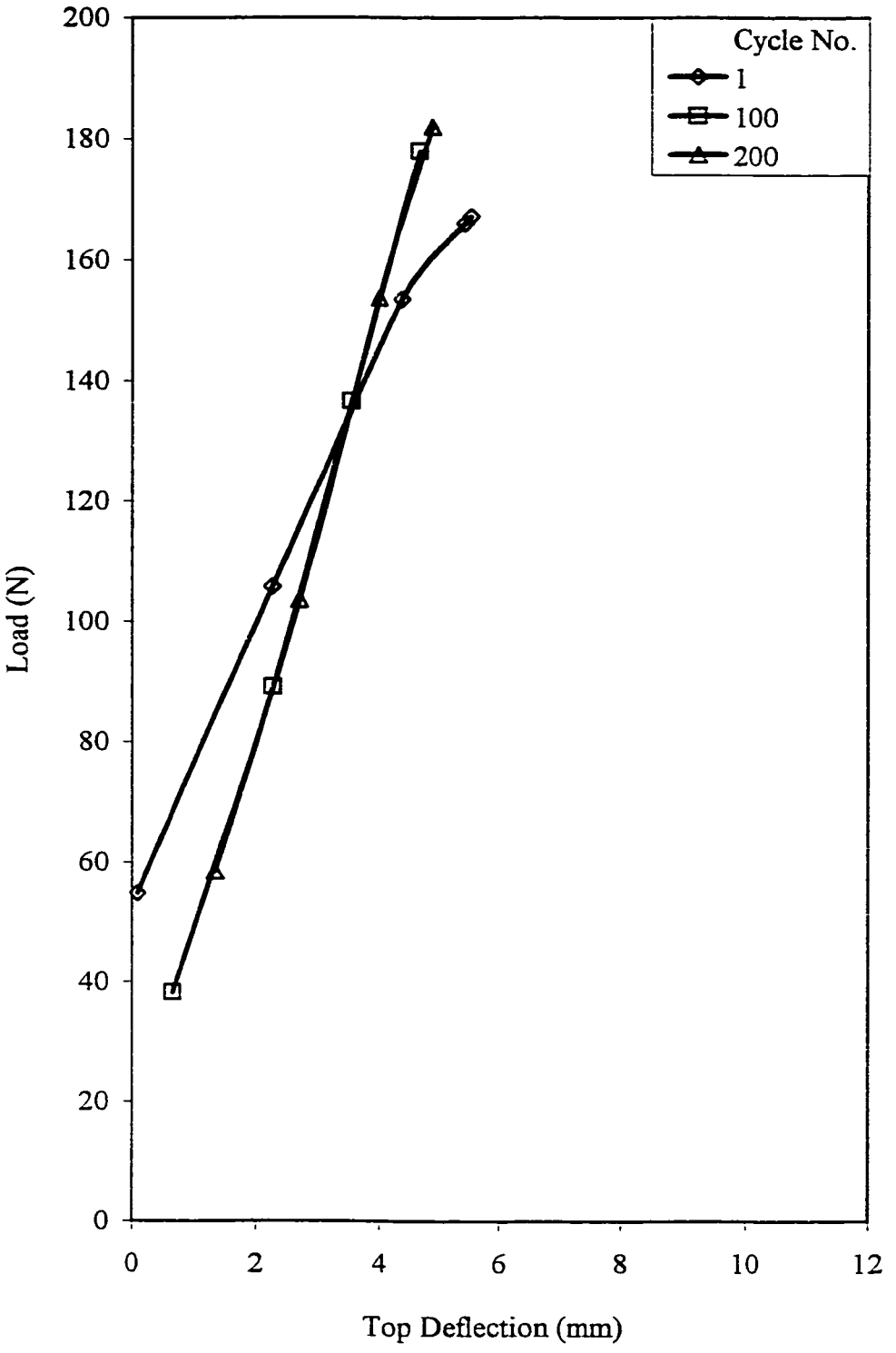

Figure 5.19: Load Deflection Curve for Front Row Pile in Four Pile Group in Dry Sand Subjected to Cyclic Lateral Load.

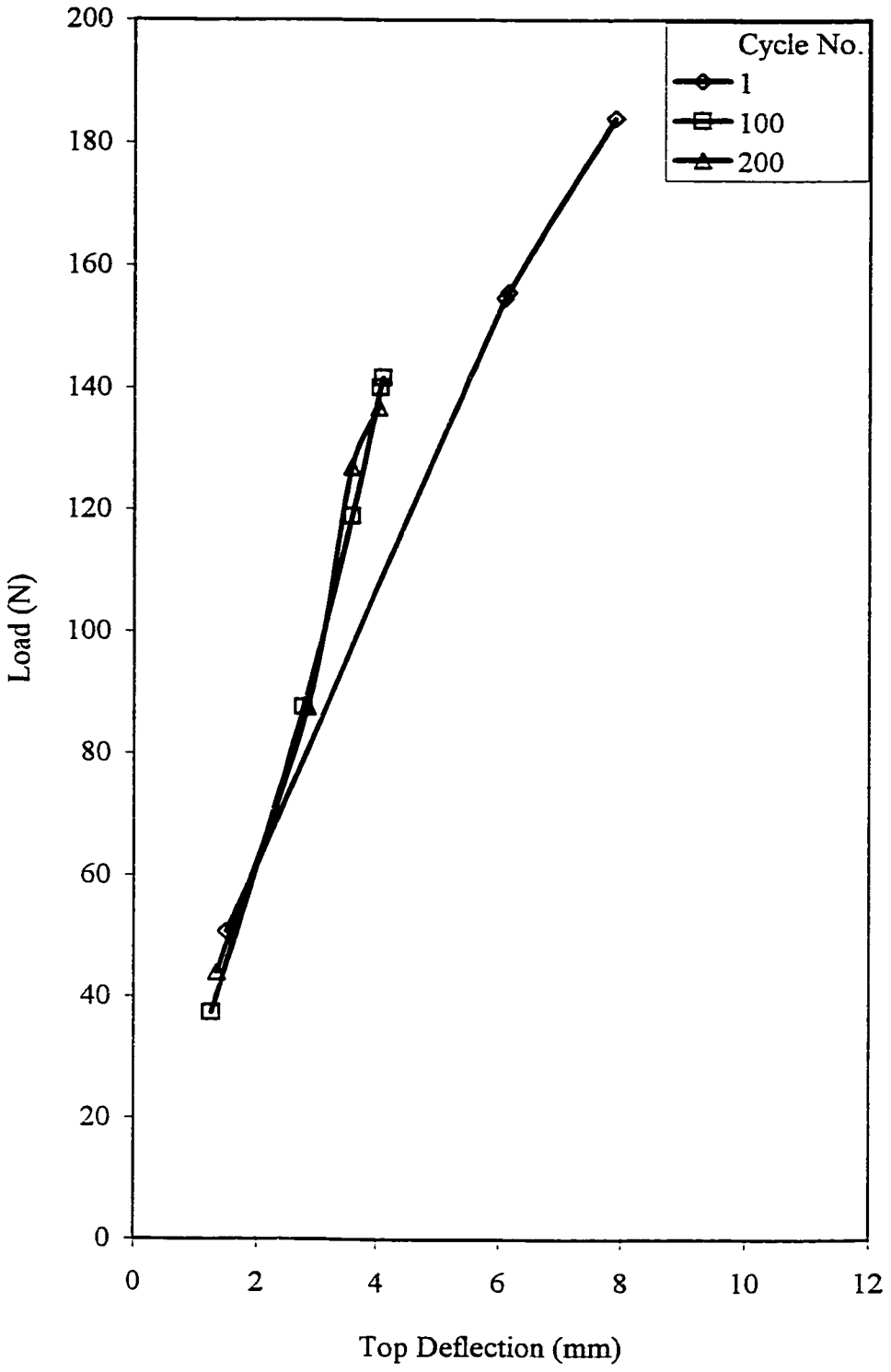

Figure 5.20: Load Deflection Curve for Back Row Pile in Four Pile Group in Dry Sand Subjected to Cyclic Lateral Load.

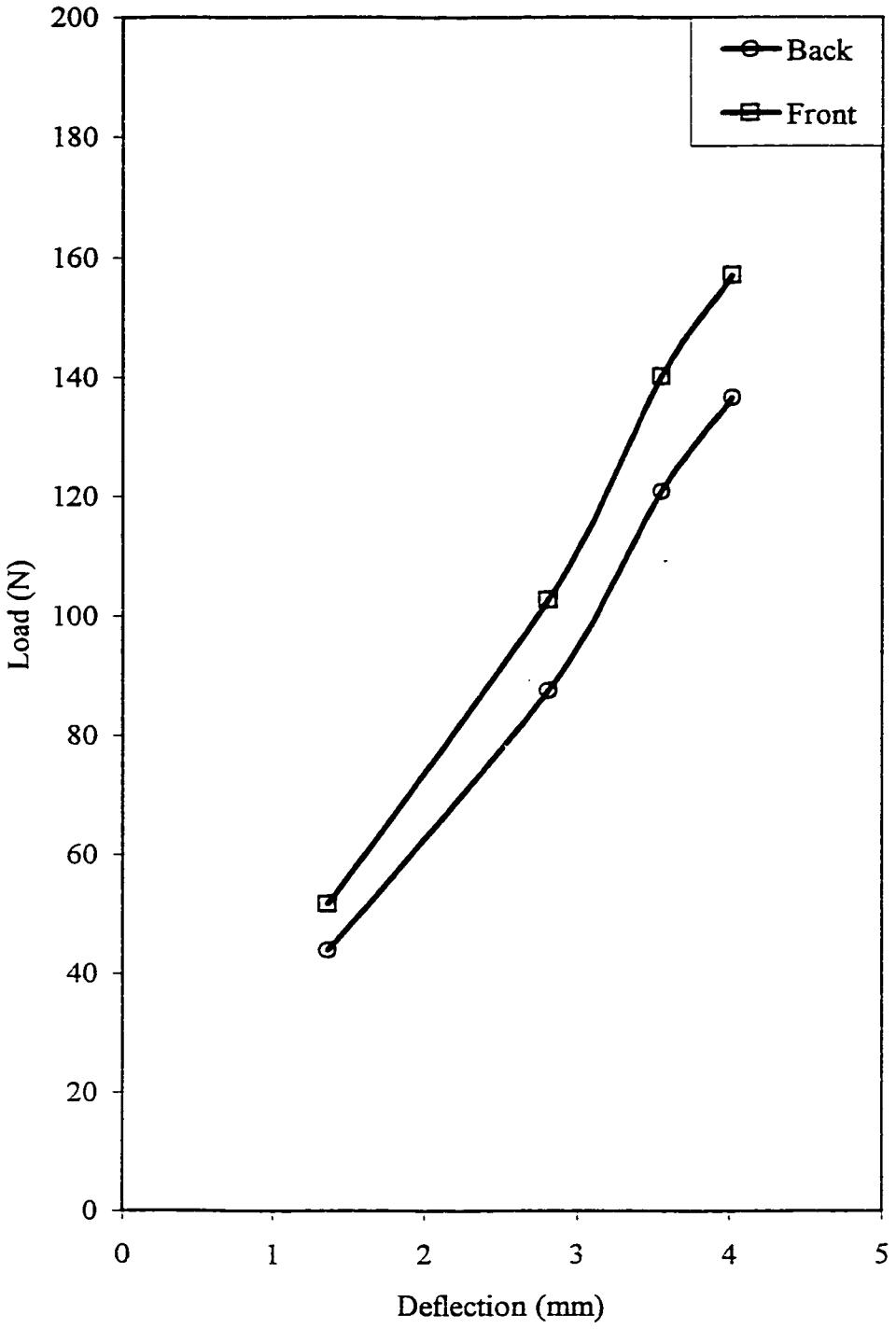

Figure 5.21: Load Deflection Curve for Four Pile Group in Submerged Sand Subjected to Cyclic Lateral Load at Cycle 200.

Moment Diagram

Moments diagram for pile group was obtained by the same procedure used previously in chapter four for single pile, four pile group, and nine pile group. Figures 5.22 and 5.23 present the moment diagrams at peak load level at cycles 1, 50, 100 and 200 for the piles in the front and the back row, respectively. The first figure shows the behavior of piles in the back row embedded in dry sand while the second figure shows the piles in the front row embedded in submerge sand. In both figures, the moments were reduced as the number of load cycles increases. After a certain number of cycles the moments tend to stabilize since the soil reached the maximum possible density due to the effect of pile movement. The behavior is similar to the behavior of single pile. Figure 5.22 shows that back row piles attracts higher moments in the first load cycle and accordingly higher load per pile head, while in the front row piles the moment was almost the same in the upper potion of the pile for all cycles.

In order to study the effect of shadowing, a comparison was made between the front row piles and back row piles, after the application of large number of load cycles. Figure 5.24 represents the moment diagram for the piles in the front and back rows embedded in dry sand at load cycle 200. It depicts that the front row always gained higher load per pile head than the back row piles. This was due to the shadowing effect since the piles in the first row resists stiffer soil. Therefore, pile group effect was also apparent after large number of load cycles. Similar findings were noticed in figure 5.25 which depicts the moment diagram for piles embedded in submerged sand condition at load cycle 200. Furthermore, the difference

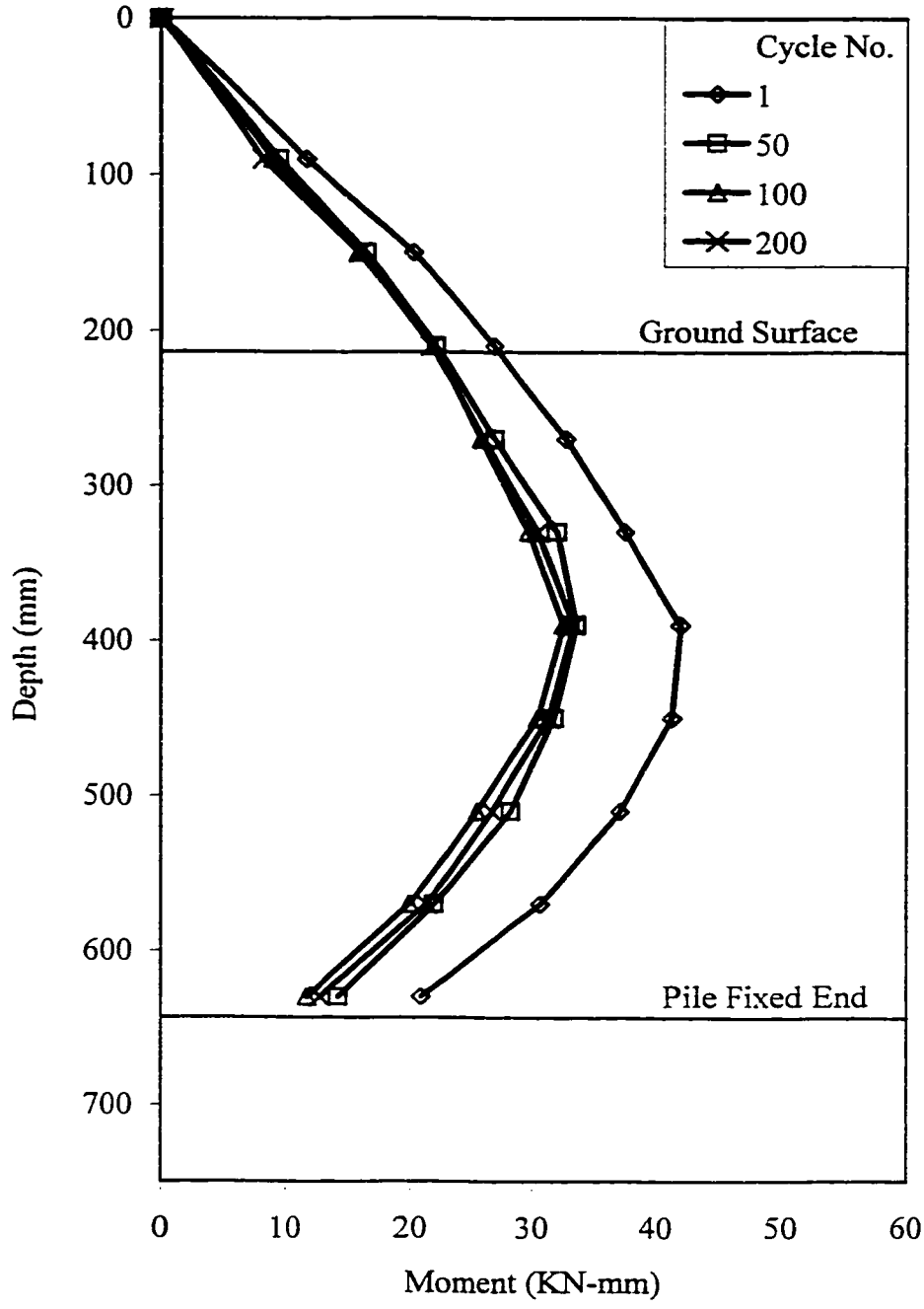

Figure 5.22: The Variation of Moment with Depth for Back Row Pile in Four Pile Group in Dry Sand Subjected to Cyclic Lateral Load.

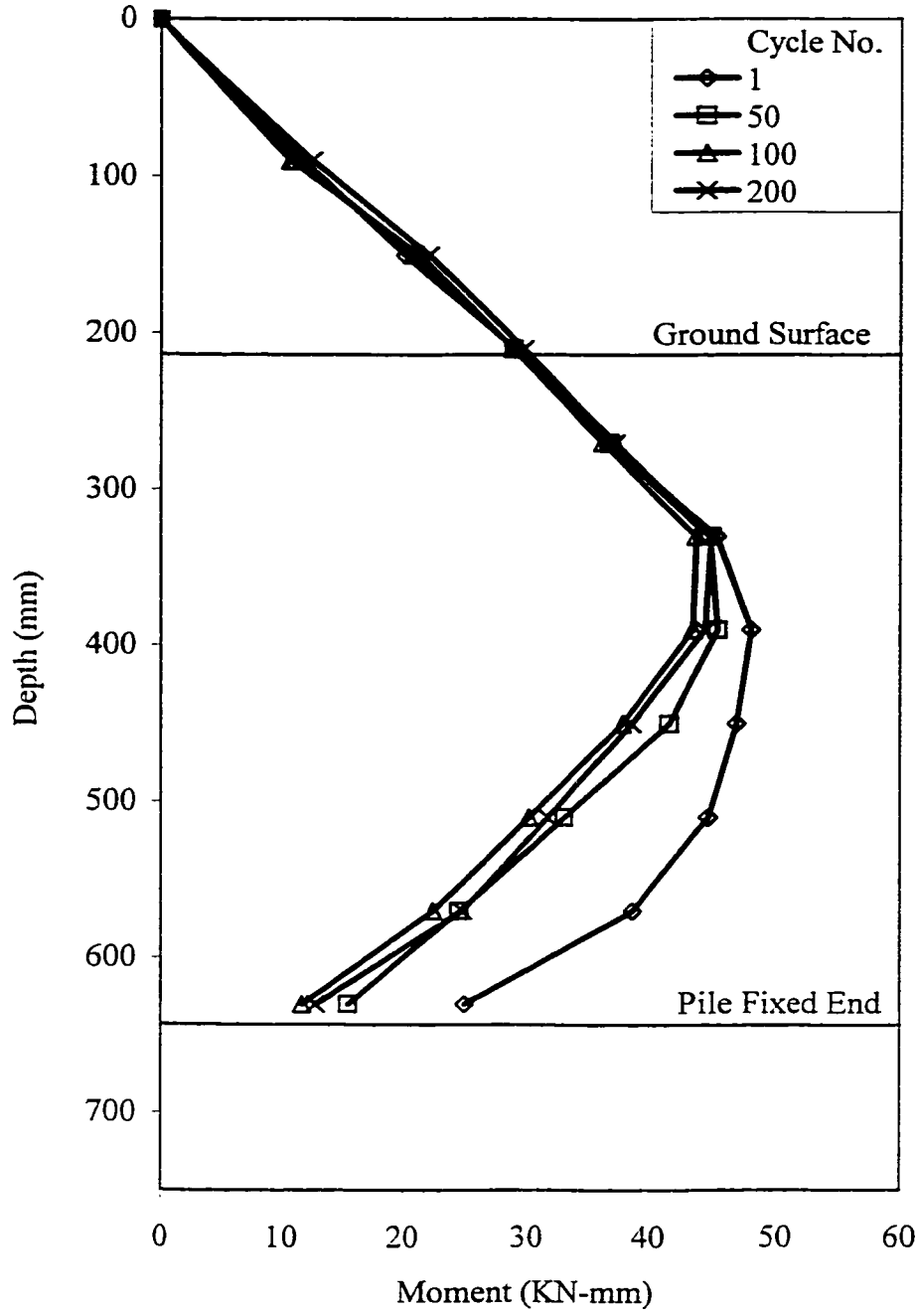

Figure 5.23: The Variation of Moment with Depth for Front Row Pile in Four Pile Group in Submerged Sand Subjected to Cyclic Lateral Load.

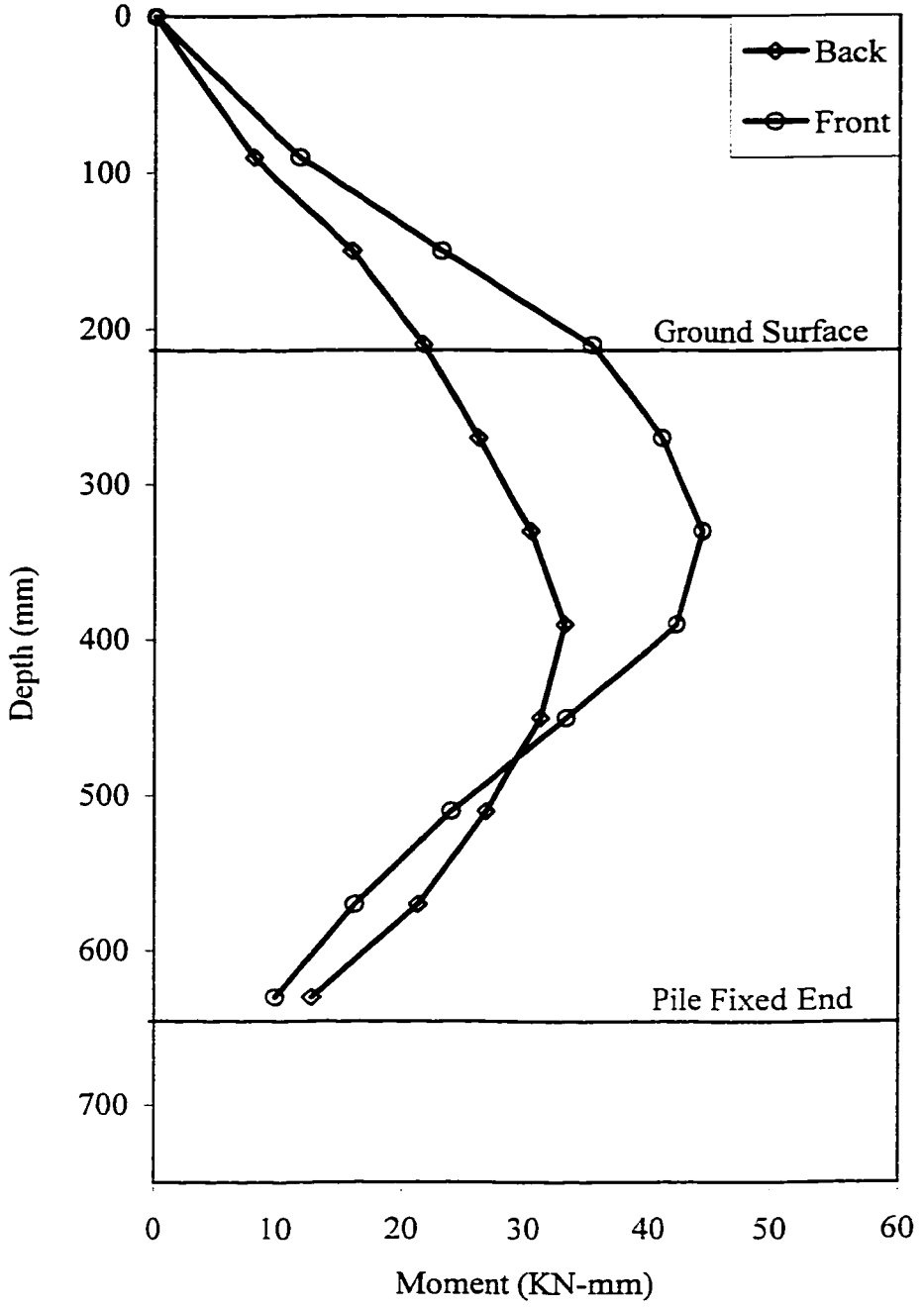

Figure 5.24: The Variation of Moment with Depth for Four Pile Group in Dry Sand Subjected to Cyclic Lateral Load at cycle 200.

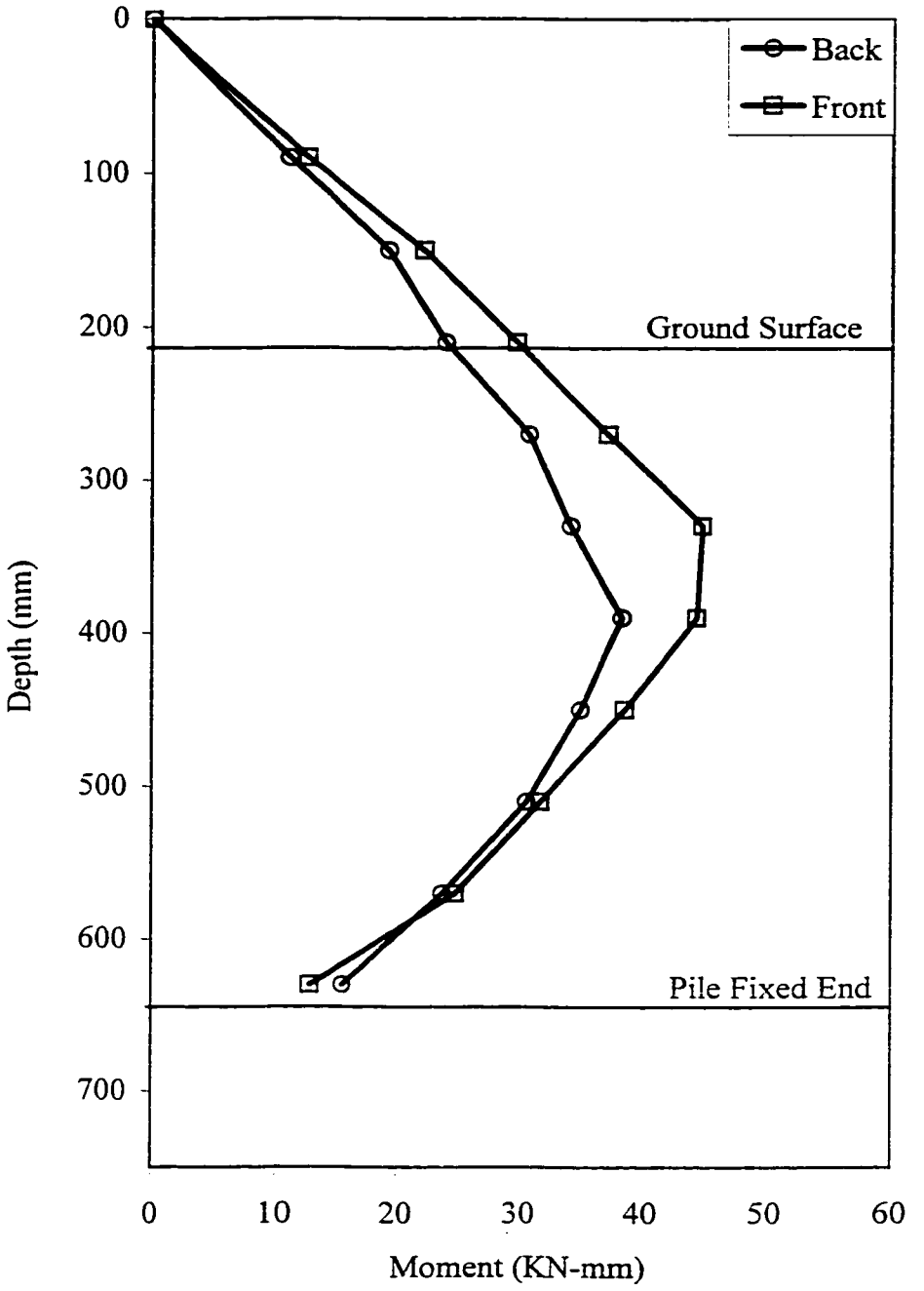

Figure 5.25: The Variation of Moment with Depth for Four Pile Group in Submerged Sand Subjected to Cyclic Lateral Load at cycle 200.

in the pile head load between the piles in the front and back rows was greater in the case of dry sand than the submerge one. The effective soil density was reduced in the submerged condition due to the presence of water which reduced the effective density to approximately half of its value. The submergence effect on the piles was represented in figures 5.26 and 5.27. The figure depict that higher moments were produced in the submerged sand condition due to reduction in soil resistance

Normalized Moment Diagram

Its necessary to normalize the moment diagram by dividing the moments by individual piles head load, similar to the procedure used earlier in chapter four for four pile group and nine pile group. Figure 5.28 shows the normalized moment (moment divided by the pile head load) for front row piles embedded in dry sand. It is clearly indicated that the normalized moment decreases with the number of cycles. Similar behavior was obtained for all cases, both for the back and front row piles under the two different sand conditions. Figures 5.29 and 5.30 depict the normalized moment diagrams for dry sand condition at load cycles of 100 and 200. Both figures reflected similar behavior, where, the back row of piles will be subjected to higher moments for the same unit load applied to piles in both the front and the back rows. The soil resisting the front row of piles was more confined than the one resisting the back row of piles. This is because the soil between the two rows of piles was loosen by the movement, whereas the soil in the front was confined more due to loading. In other words the front piles disturbed the soil between the rows due to shadowing effect.

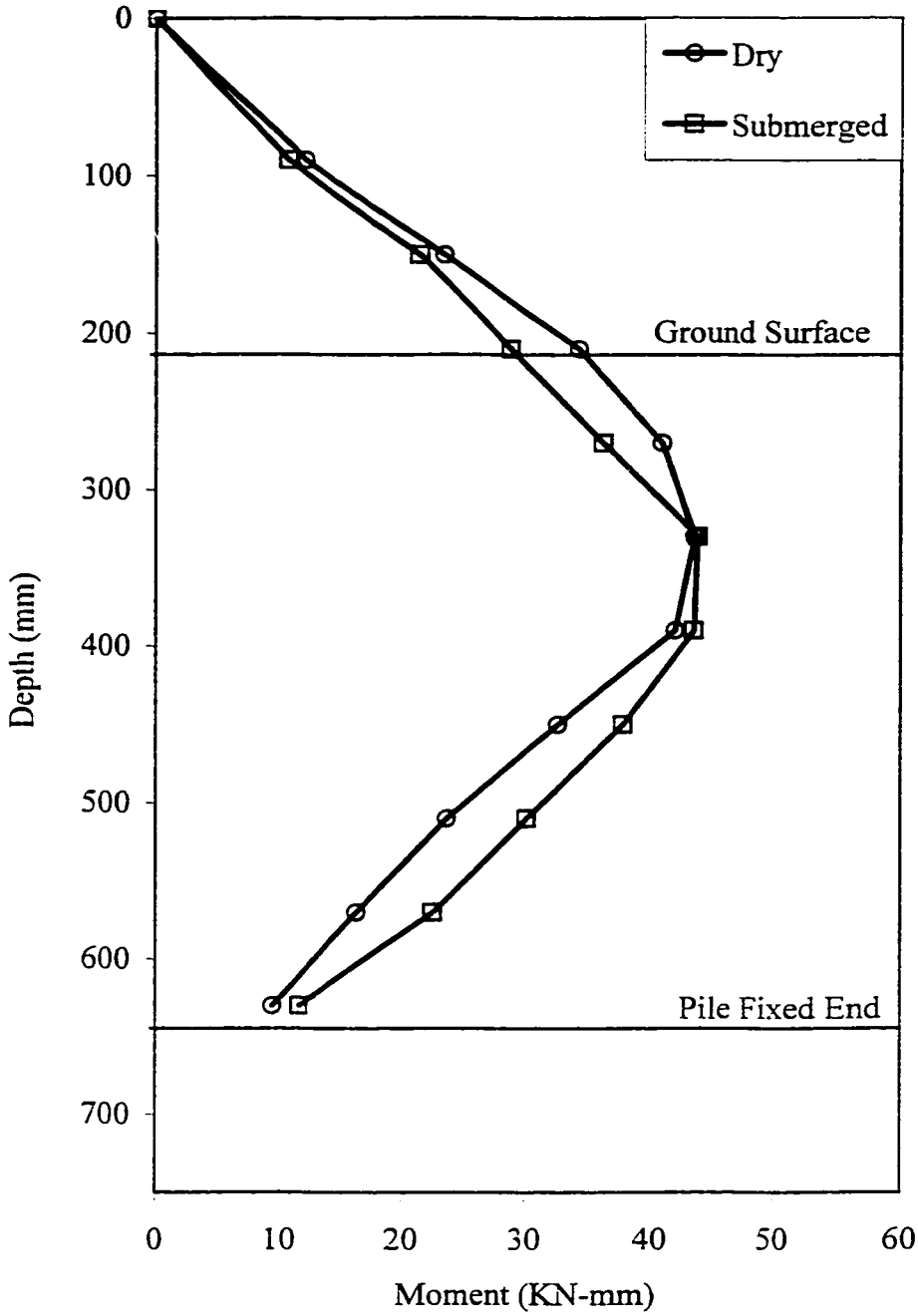

Figure 5.26: The Variation of Moment with Depth for Front Row Pile in Four Pile Group Subjected to Cyclic Lateral Load at cycle 100.

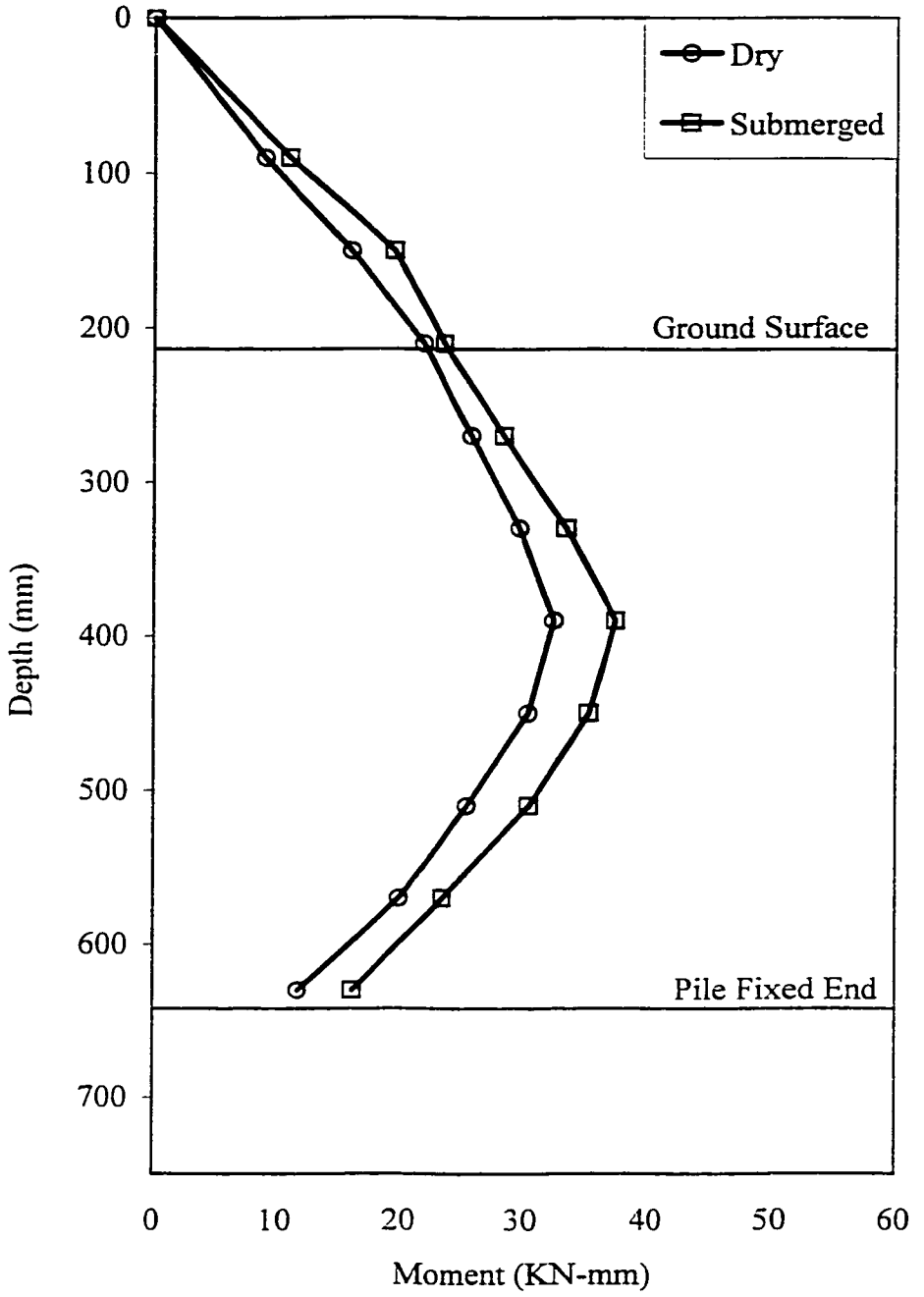

Figure 5.27: The Variation of Moment with Depth for Back Row Pile in Four Pile Group Subjected to Cyclic Lateral Load at cycle 100.

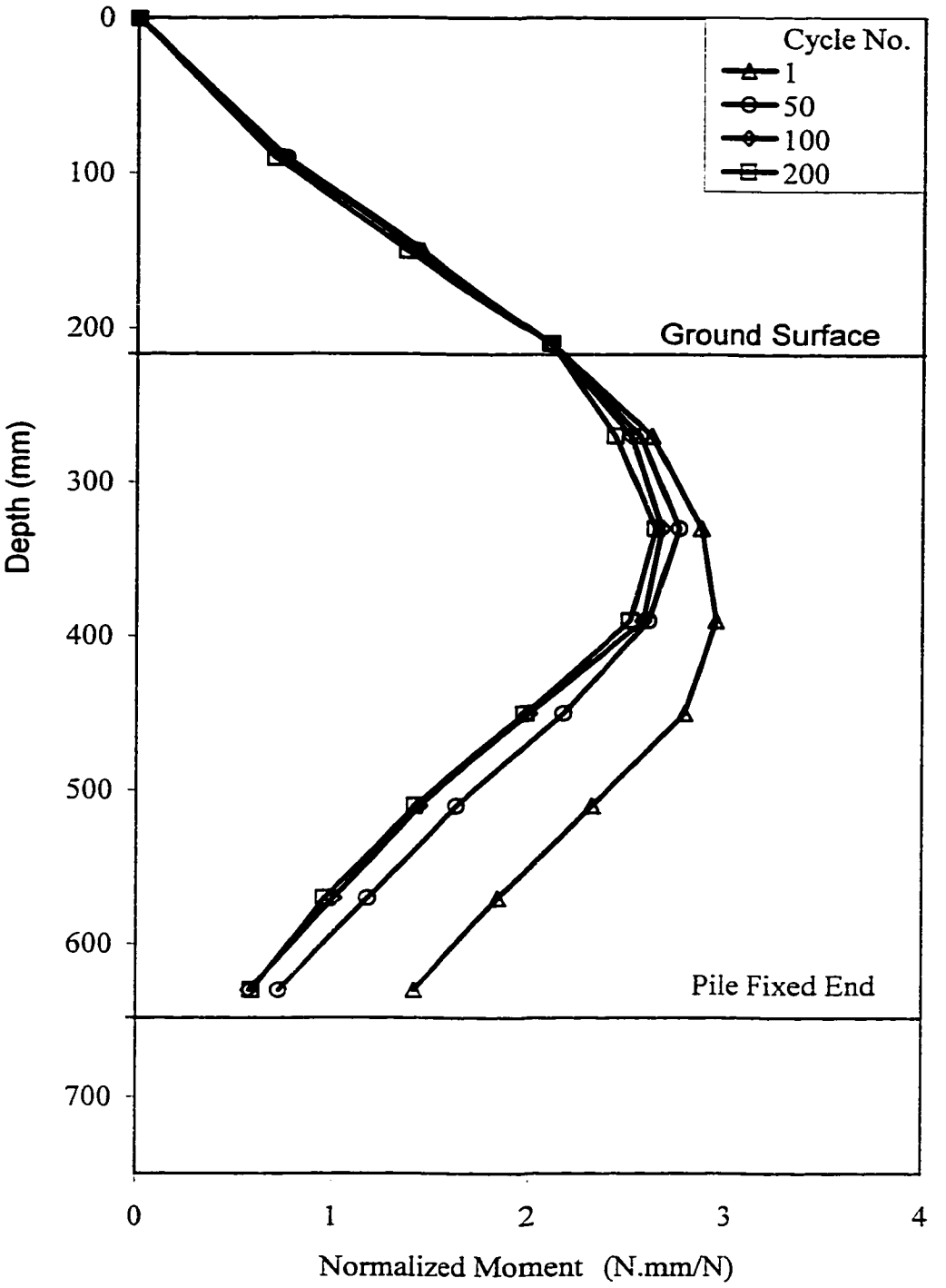

Figure 5.28: The Variation of Normalized Moment with Depth for Front Row Pile in Four Pile Group in Dry Sand Subjected to Cyclic Lateral Load.

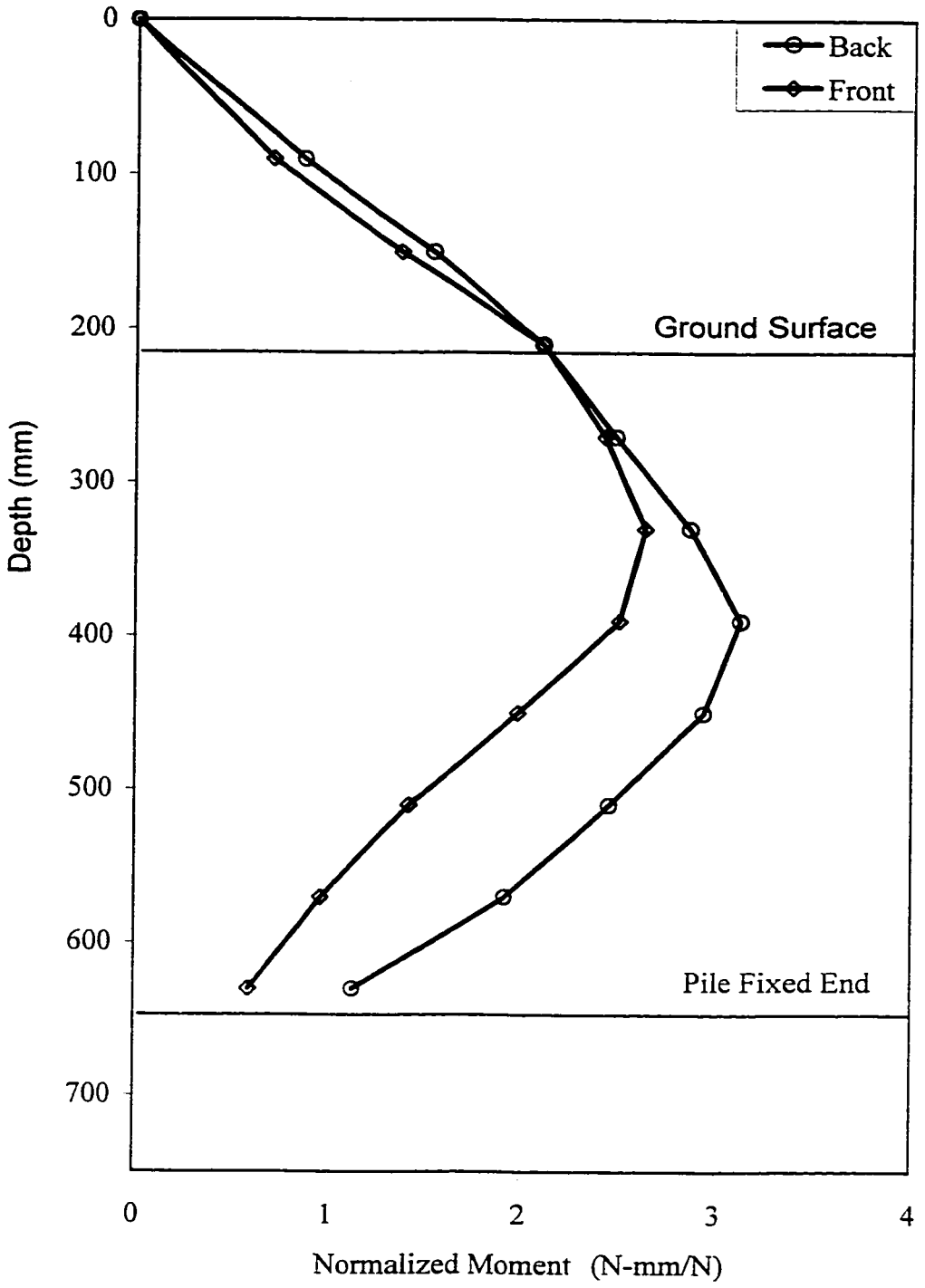

Figure 5.29: The Variation of Normalized Moment with Depth for Four Pile Group in Dry Sand Subjected to Cyclic Lateral Load at Cycle 100.

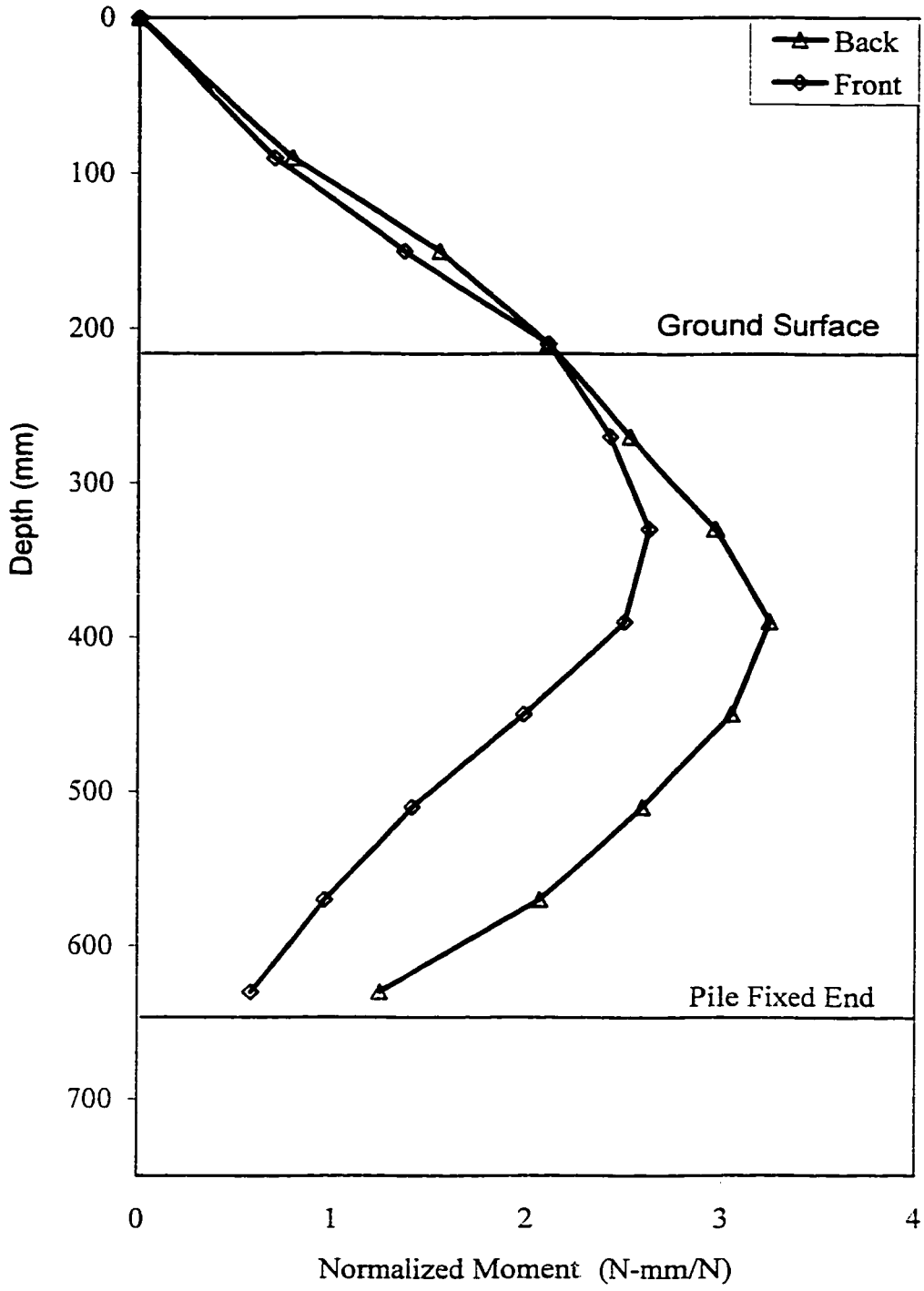

Figure 5.30: The Variation of Normalized Moment with Depth for Four Pile Group in Dry Sand Subjected to Cyclic Lateral Load at Cycle 200.

The effect of submergence was significant in the normalized moment for the piles in the front row. On the other hand, it was insignificant for the piles in the back row. These findings are presented by figures 5.31 and 5.32 respectively. Finally, it can be concluded that piles in the front and back rows behave differently even if they are subjected to the same load level per pile head.

Deflection Along Pile Length

The pile group behavior is similar to single pile when subjected to cyclic load. The four pile group was subjected to a maximum cyclic load level of 60 Kgf. Deflection diagrams were produced using the same procedure explained earlier in chapter four for single pile, four pile group, and nine pile group. Figures 5.33 and 5.34 represent the deflected shapes of the piles at cycles 1,100 and 200 for the piles in front and back rows, respectively. Both figures are for piles embedded in dry sand which is identical for piles embedded in submerged sand but with smaller deflection values. These figures show that the deflection is decreasing as the cycle number increase. Figure 5.35 reflects the same results founded in chapter four earlier: i.e. the front row always get the higher share of load distribution due to shadowing effect, which in turn deflects relatively more than the back row piles, regardless of the top deflection which is almost the same for piles in both rows. This is due to the effect of shadowing which allows the front pile to sustain more load level per pile head. Reduction in deflection in both the front and back rows was decreasing with number of cycle, due to sand compaction. However, the reduction in deflection is significant between cycle 1 and

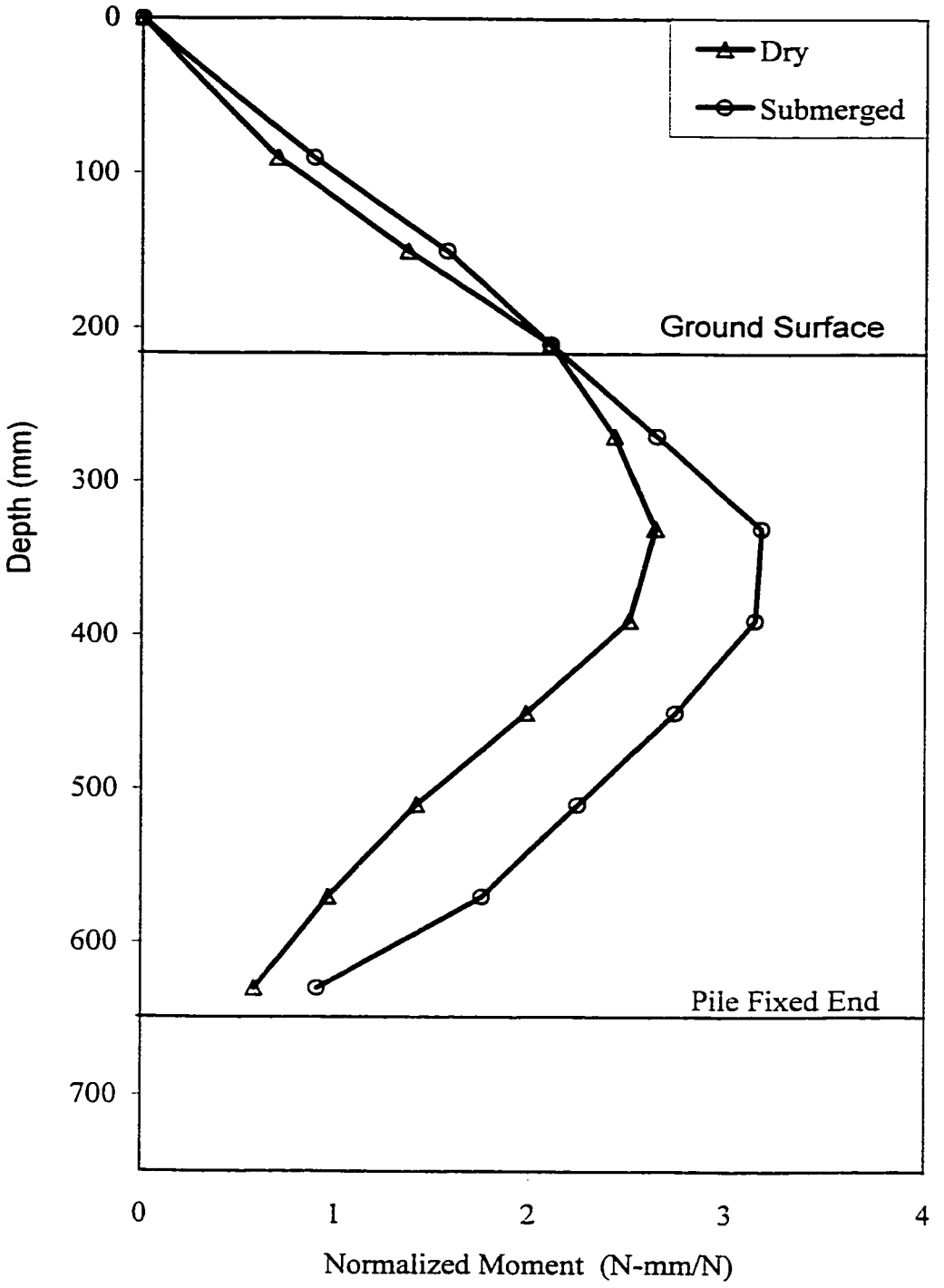

Figure 5.31: The Variation of Normalized Moment with Depth for Front Row Pile in Four Pile Group Subjected to Cyclic Lateral Load at Cycle 200.

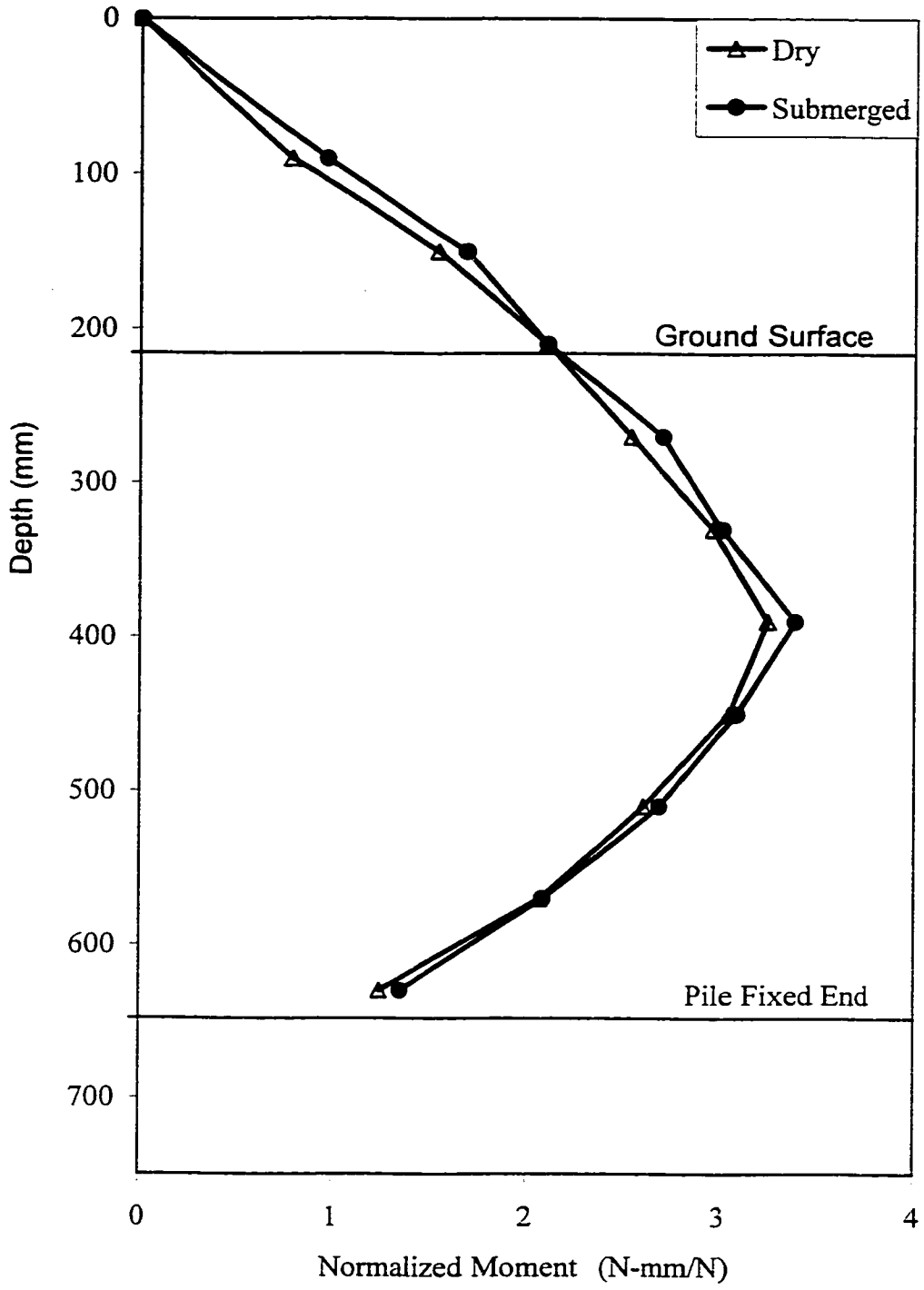

Figure 5.32: The Variation of Normalized Moment with Depth for Back Row Pile in Four Pile Group Subjected to Cyclic Lateral Load at Cycle 200.

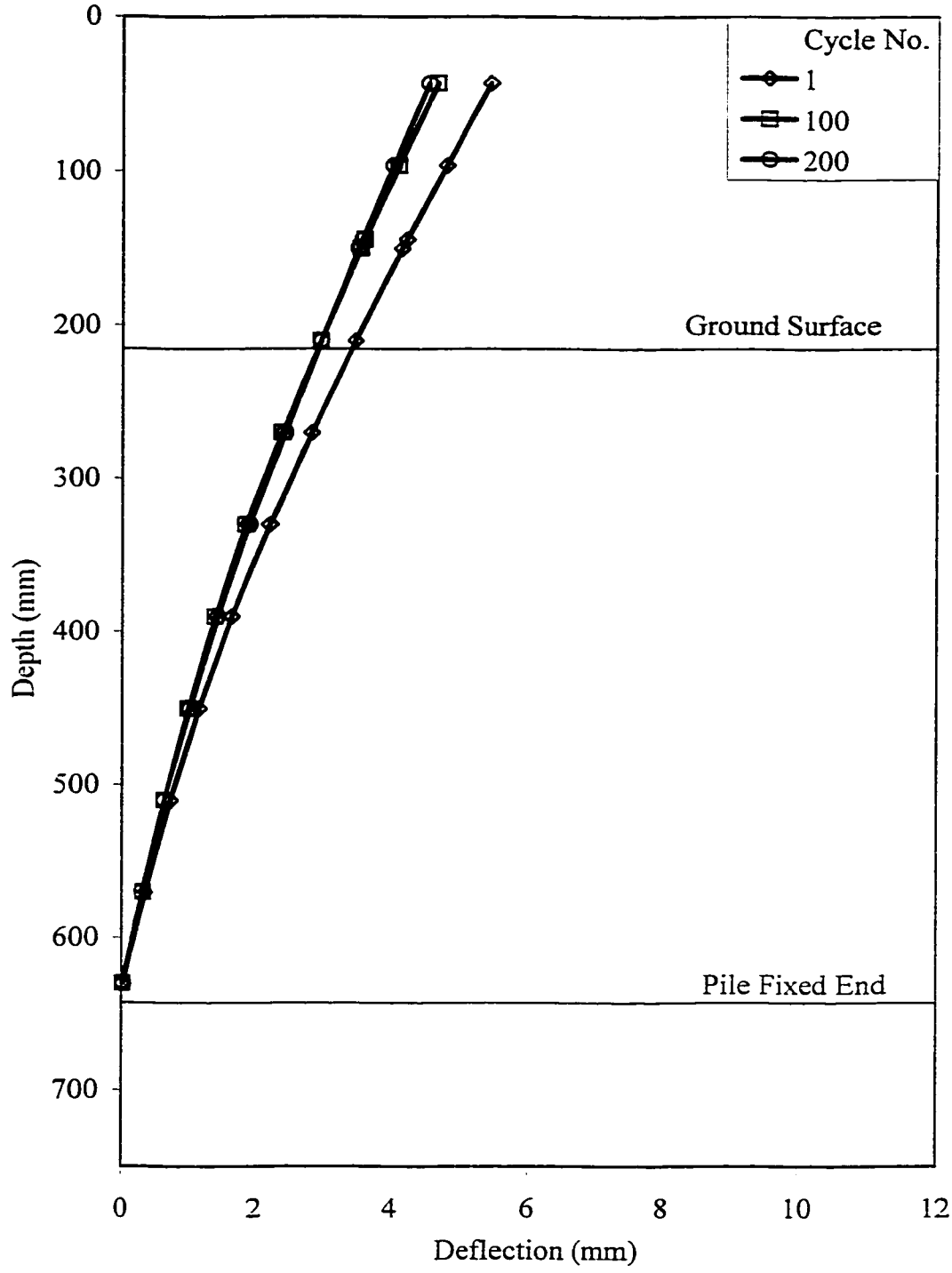

Figure 5.33: The Variation of Deflection with Depth for Front Row Pile in Four Pile Group in Dry Sand Subjected to Cyclic Lateral Load.

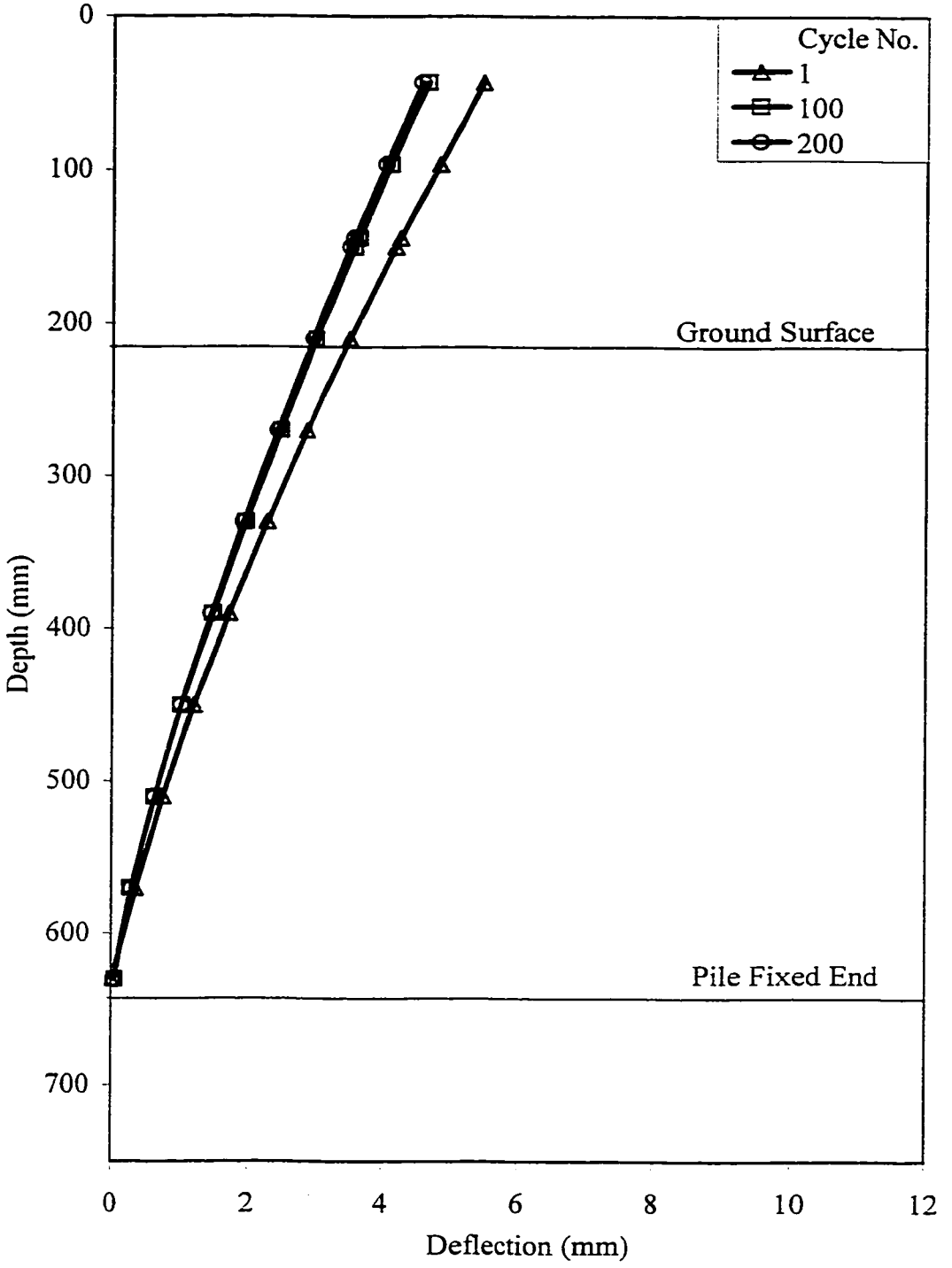

Figure 5.34: The Variation of Deflection with Depth for Back Row Pile in Four Pile Group in Dry Sand Subjected to Cyclic Lateral Load.

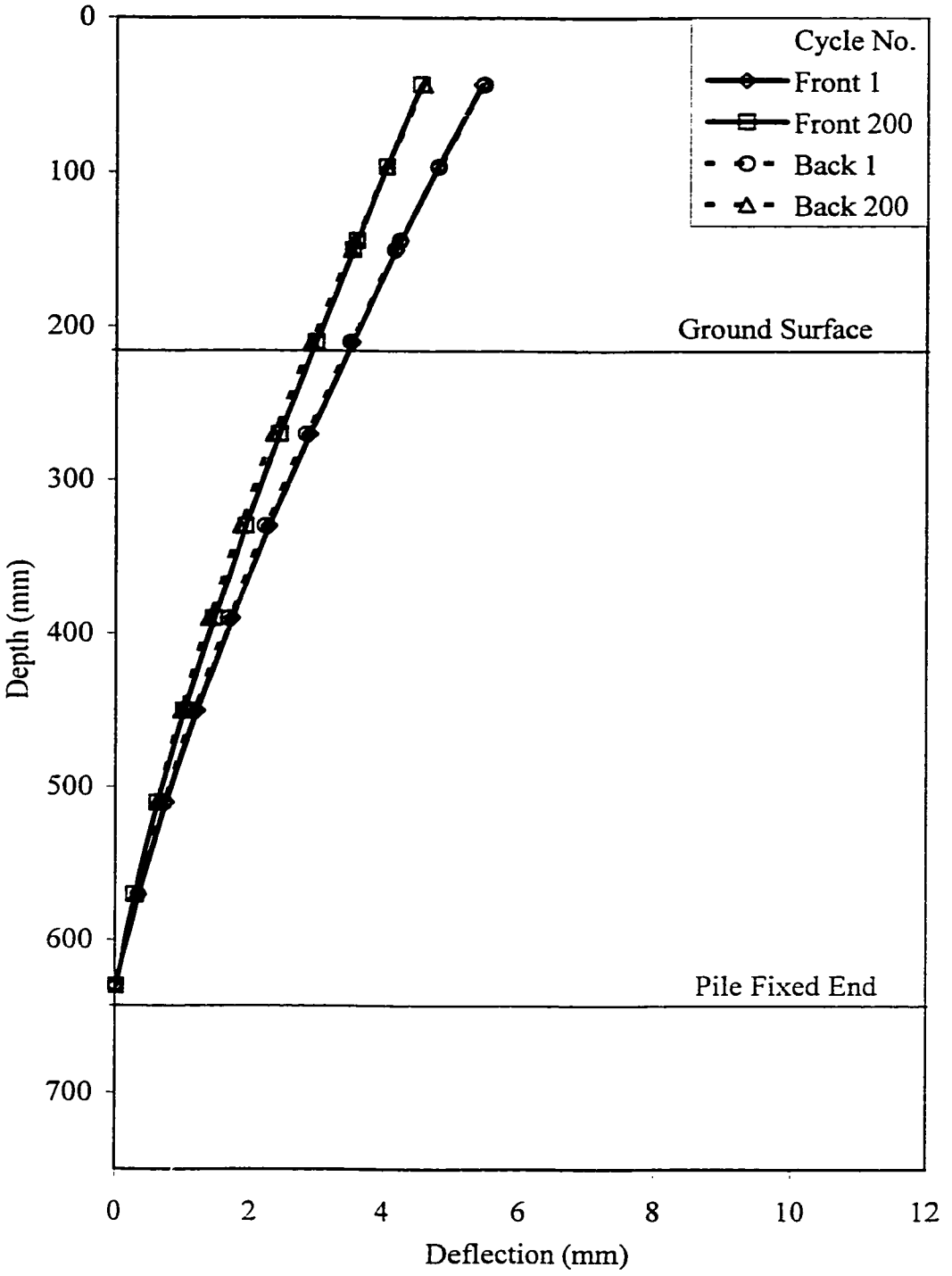

Figure 5.35: Comparison of Variation of Deflection with Depth Between Front and Back Row Piles in Four Pile Group in Dry Sand Subjected to Cyclic Lateral Load.

100, while its is less significant between cycles 100 and 200 due to sand densification action that took place after the first few cycles.

5.2.4 Nine Pile Group

Nine pile group was subjected to cyclic lateral load similar to the four pile group with higher load level compared to the single pile and four pile group in order to study the effect of the closely spaced piles row and their behavior. Pile arrangement was identical to those used in static loading tests. Two tests were carried out, one using piles embedded in dry sand, while the second test using piles embedded in submerged sand. The load at the top of each pile is calculated by the same procedure used in previous section and in chapter four for static loading case. The following paragraphs present the analysis and discuss the behavior of these piles in detail.

Top Deflection

Figure 5.36 depicts the pile head load versus top deflection of piles embedded in dry sand for cycles 1, 50, 100, and 200. The figure reflects the same behavior observed by the single piles and four pile group at high load level. The top deflection of each pile decreases with the increase in number of cycles at the same load level. This behavior was observed for all piles in the group, i.e. front row, middle row and back row. This means that the sand has been densified with increasing number of cycles. As sand reaches its maximum density, the maximum possible confinement, the deflection at the pile top is not affected as the number

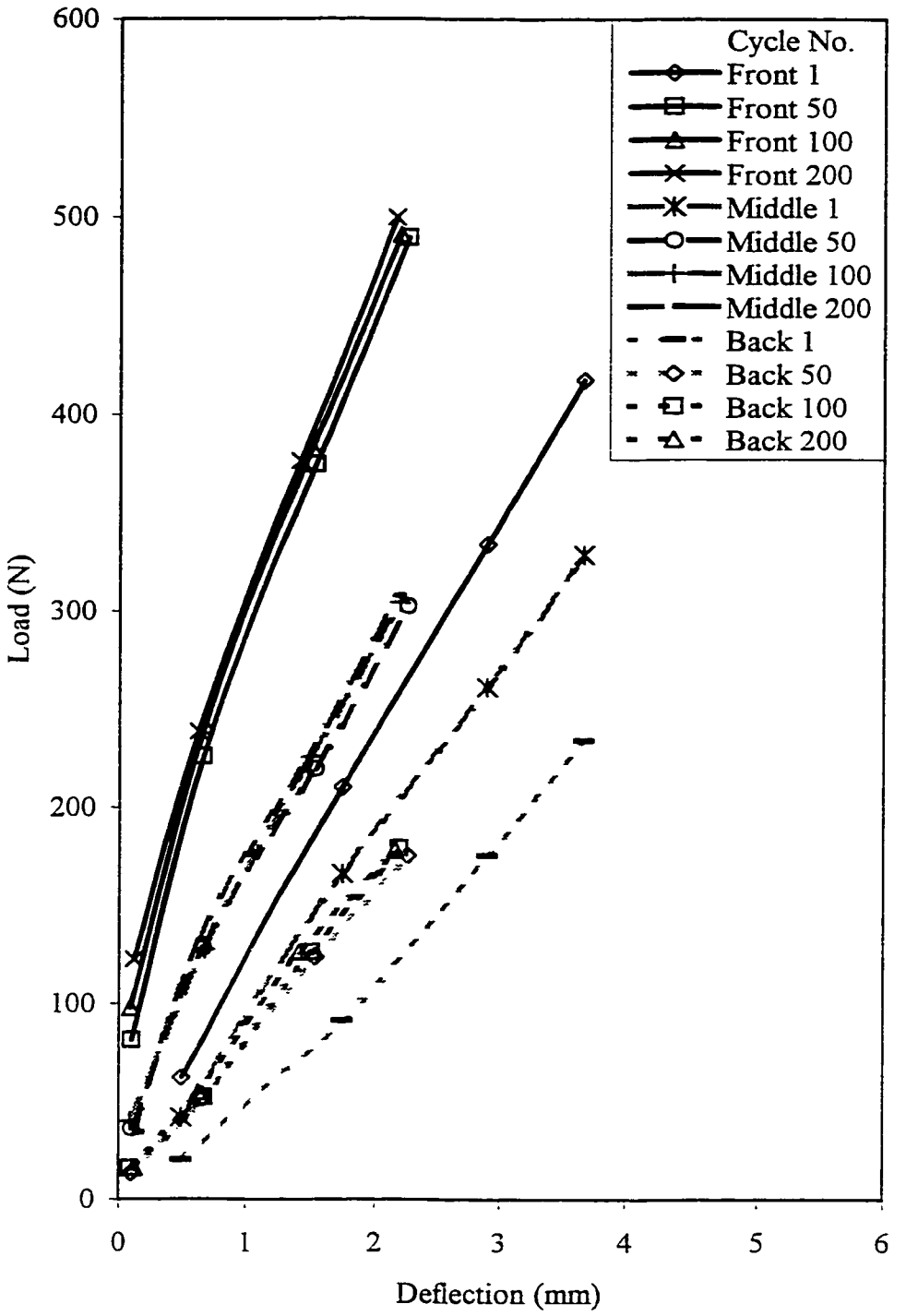

Figure 5.36: Load Deflection Curve for Nine Pile Group in Dry Sand Subjected to Cyclic Lateral Load.

of cycles increases such as for cycles 100 and 200. In other words, the variation of deflection for the same load level at different cycles is insignificant at high cycle numbers.

Unlike four pile group, this behavior is observed even for low load levels which indicates that the shadowing effect takes place at low load level for closely spaced piles. Moreover, at lower load levels each pile in this group behaves as part of the group and not similar to the piles in the four pile group. Hence, the shadowing effect for closely spaced piles will take place at low load levels and from the first cycle. It is clear that the effect of cycling at all load levels is similar for all piles in all rows, i.e. the higher the cycle number the lower the deflection of the pile at that specific load level. Furthermore, due to the shadowing effect the piles in the front rows are always carrying higher load per head followed by piles in the middle rows and then the piles in the back rows.

Similar Behavior was observed for the nine pile group embedded in submerged sand as shown in figure 5.37. Following the discussion and the results drawn in previous sections, the submerged sand tends to be softer than the dry sand, where it produced lower soil resistance. Hence, the top deflection of the piles embedded in submerged sand will be greater than the top deflection of the piles embedded in dry sand at the same load level.

Moment Diagram

Moments diagram for pile group was obtained by the same procedure used previously in chapter four for single pile, four pile group, and nine pile. Figures 5.38 and 5.39 represent

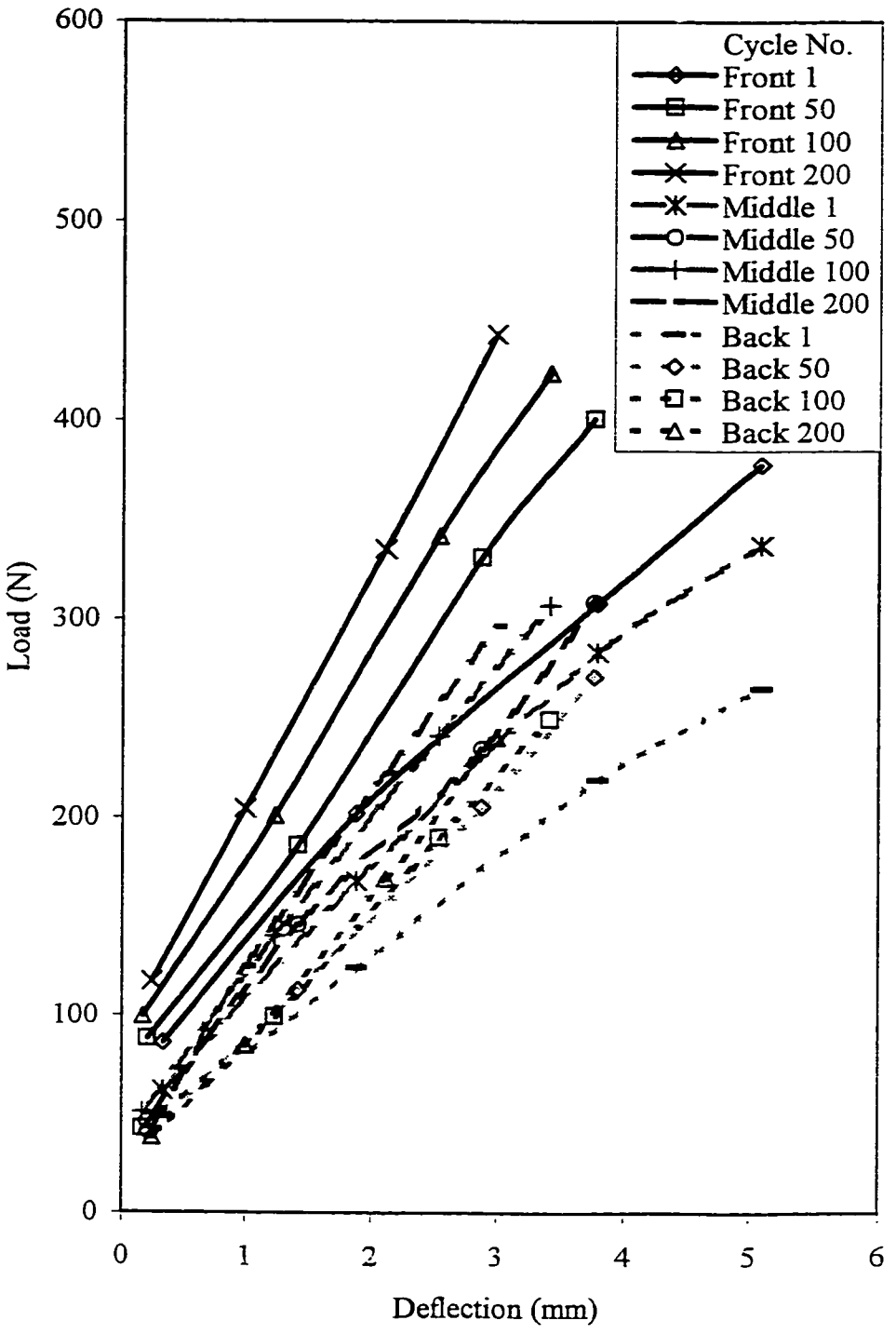

Figure 5.37: Load Deflection Curve for Nine Pile Group in Four in Submerged Sand Subjected to Cyclic Lateral Load.

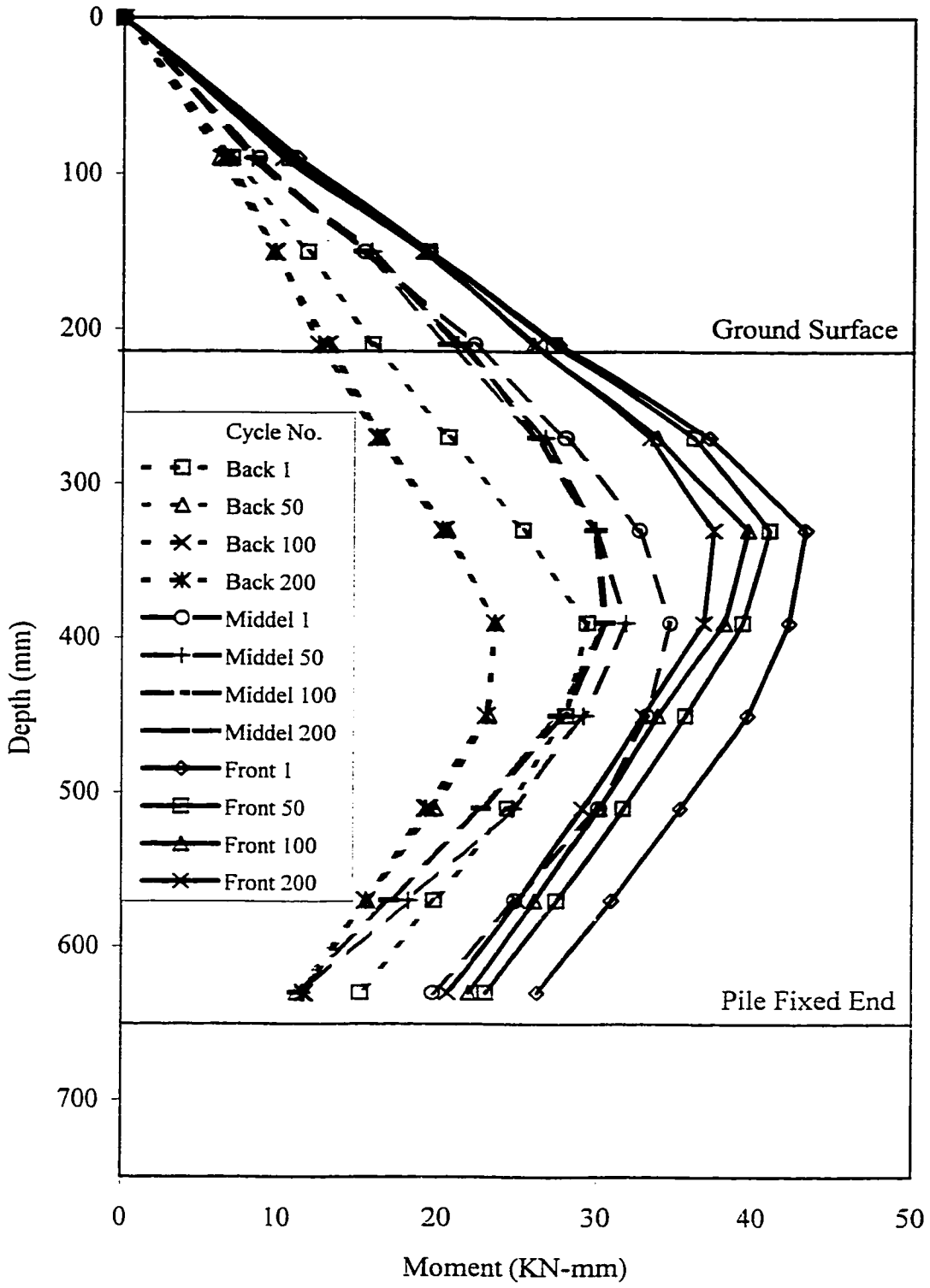

Figure 5.38: The Variation of Moment with Depth for Nine Group in Dry Sand Subjected to Cyclic Lateral Load.

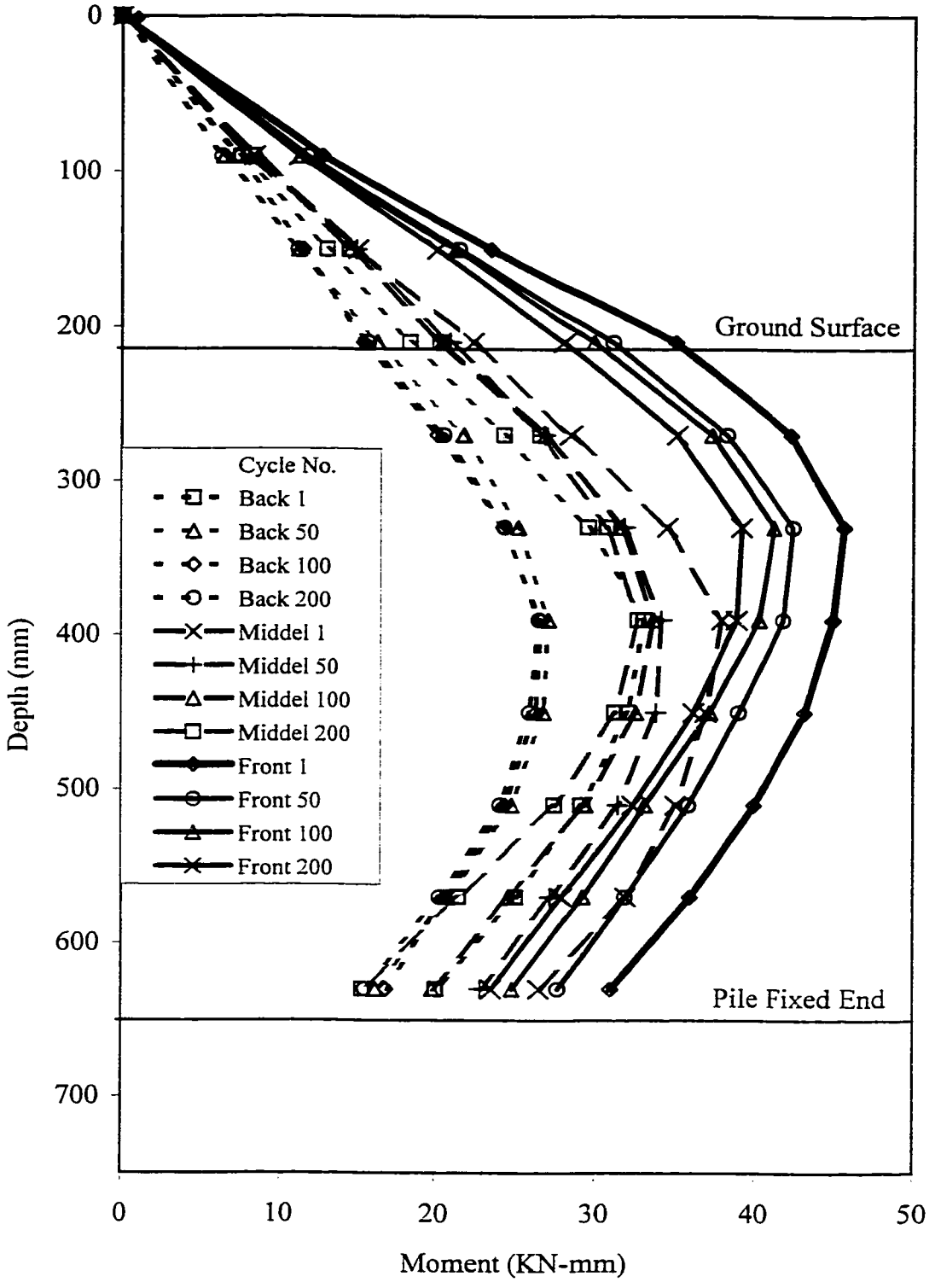

Figure 5.39: The Variation of Moment with Depth for Nine Group in Submerged Sand Subjected to Cyclic Lateral Load.

the moment diagrams at the peak load levels at cycles 1, 50, 100 and 200 for all piles in nine pile group. Figure 5.38 shows the behavior of piles located in the front, middle, and back rows embedded in dry sand; whereas figure 5.39 represents the same pile arrangement embedded in submerged sand. Unlike the behavior of four pile group, the shadowing was observed at the first cycle. This behavior continued with the same trend in all cycles but at different distributions of moment percentages to each row. The figures show that the moments were reduced as the number of load cycles increases. After certain number of cycles, the moment rate of change tends to stabilize since the soil reached its maximum possible density due to effect of pile movement. This movement will densify the sand and reduces the deflection of the piles, which in turn reduces the moments. This behavior is similar to the behavior of the single pile and four pile group drawn in previous sections of this chapter.

Brown, et al. (1988) conducted study on full scale pile group model embedded in sand and subjected to lateral cyclic loading. The piles bottom were embedded in stiff clay to restrict its bottom movement. Similar results were concluded on pile group behavior where the leading row attracts higher bending moment and deflection due to shadowing effect. On the other hand, an opposite behavior was noticed due to the effect of cyclic loading where the movement of the piles tend to loosen the sand with cycling which produced greater pile deflections and bending moments as the load cycle increase. His model was similar to the model used in this study but at larger scale. Another study conducted by Shamem (1988) on small scale single pile model embedded in sand with no restriction at the bottom of pile. It

was concluded that the deflection of the pile and the bending moments increase as the number of load cycle increases due to reduction in sand resistance. This loss in sand resistance occur due loosen of sand with pile movement which reduced the sand confinement around the pile. Both studies were discussed thoroughly in chapter two earlier. Their results are opposite to the findings discussed in the this study for the behavior of pile that is subjected to cyclic lateral load where the deflection of the pile and the bending moments decreases as number of load cycle increases due to sand densification as an effect of pile movement. On the other side, Woods (1996) was expecting piles behavior similar to those found in this study with medium to low relative density of sand. Copy of Woods (1996) fax is shown in Appendix C.

The shadowing phenomena affects the level of moment for piles in each row as load was distributed to piles according to their row position. Opposite behavior was observed for the four pile group, the shadowing effect on the moment took place at the first cycle and continue to the last cycle, but with different percentage distribution of load. This was due to the strengthen of sand as the number of cycles increases, as discussed earlier. This increase tends to increase the percentage difference between the piles in front, middle, and back row, which is clearly noticed in both figures. In general, the piles in the front rows were resisted by stronger soil, which in turn produces higher moments on the piles. Similarly, the piles in middle rows interact with a stronger soil than the piles in the back row.

Figures 5.40, 5.41, and 5.42 depicts the comparison between the nine pile group embedded in dry and submerged sand conditions for front, middle, and back rows, respectively. Generally, as pointed out in previous sections that the piles embedded in submerge sand will be subjected to moments higher than the piles embedded in dry sand. This trend was observed for piles in different row positions. This was a result of reduction in effective density of sand in the submerged condition because of the presence of water that reduced the effective soil density to approximately half its value.

Furthermore, the following can be pointed out from the figures:

- The percentage differences between submerge and dry sand was greater for the piles in the back rows followed by piles in the middle and front rows, respectively.
- The difference in moments between piles in different rows was greater in submerged sand condition case, between piles in the front and middle rows. However, it was greater in the case of dry sand condition, between the piles in the back and middle rows, as well as between the piles in the back and middle rows.

Moreover, the differences in moments between different cycles in the same pile position is greater in the front pile row followed by piles in the middle and back rows, respectively. This finding is true for all load cycles with the exception of the first cycle, which resembles the static load case. As the sand gets densified due to compaction by the cycling effect, it changes the distribution of load per pile head. This led to the reduction on the load level distribution to the piles in the first row with increasing number of cycles.

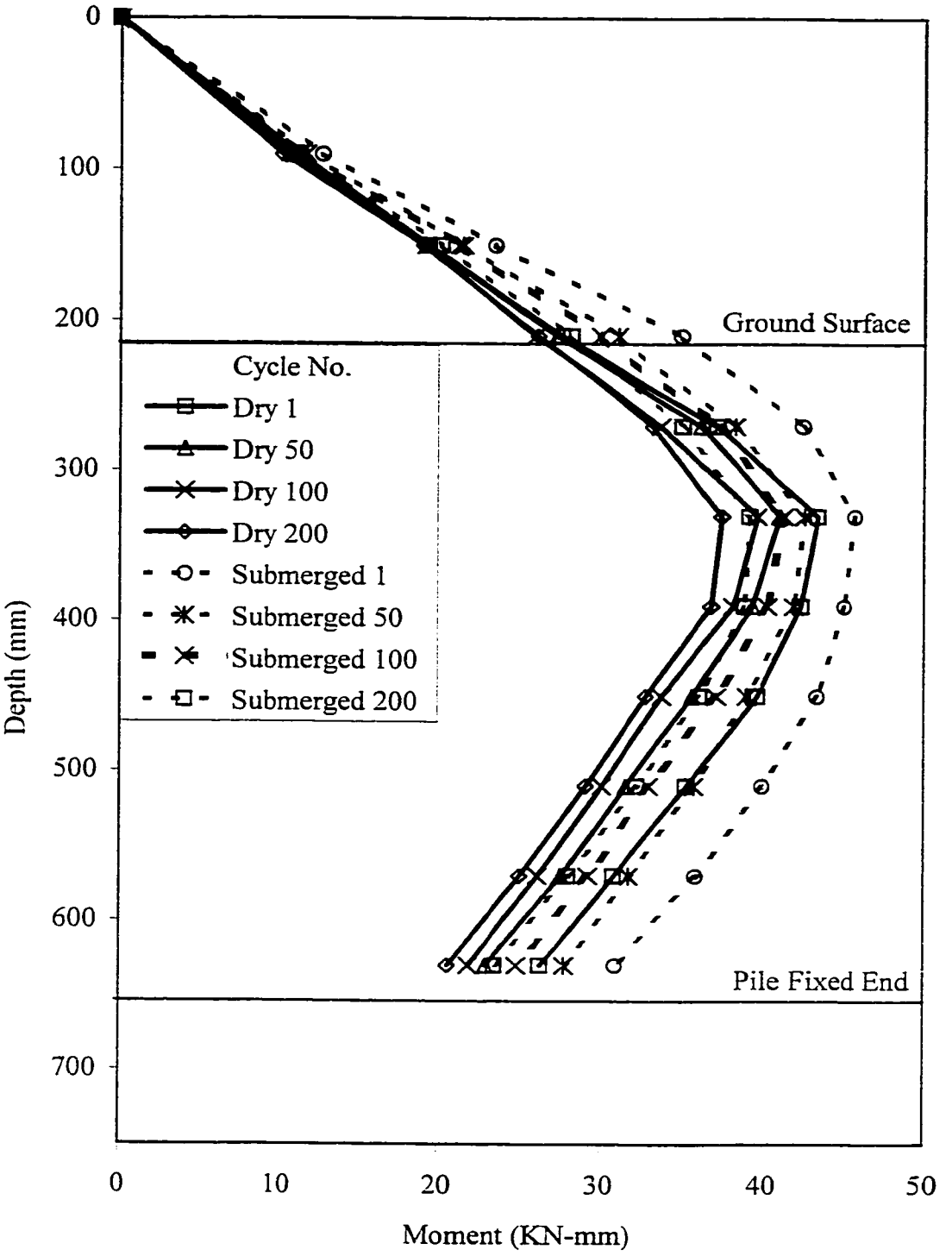

Figure 5.40: Comparison of Moment Variation with Depth for Front Row Pile in Nine Pile Group Between Dry and Submerged Sand Conditions Subjected to Cyclic Lateral Load.

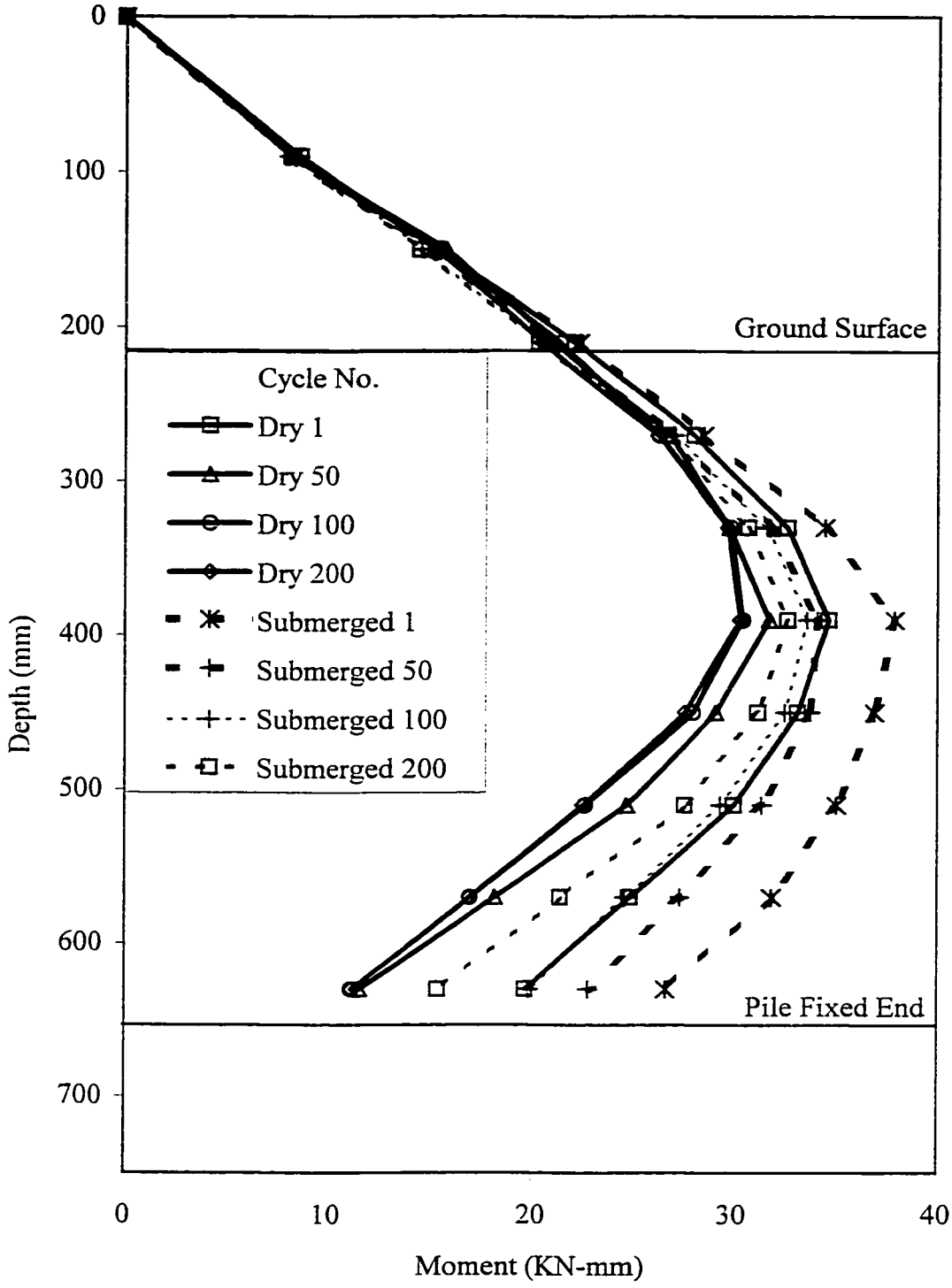

Figure 5.41: Comparison of Moment Variation with Depth for Middle Row Pile in Nine Pile Group Between Dry and Submerged Sand Conditions Subjected to Cyclic Lateral Load.

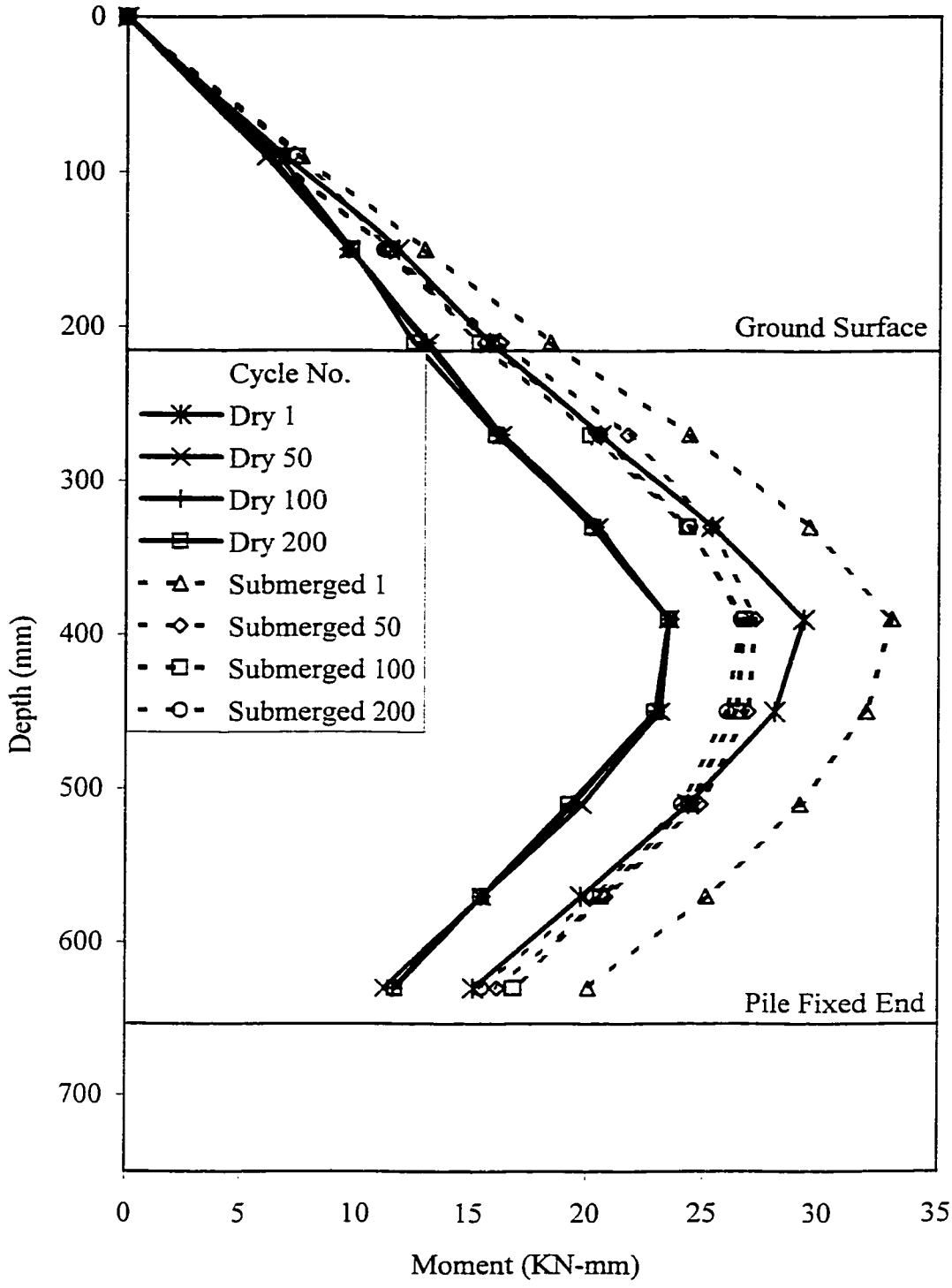

Figure 5.42: Comparison of Moment Variation with Depth for Back Row Pile in Nine Pile Group Between Dry and Submerged Sand Conditions Subjected to Cyclic Lateral Load.

Normalized Moment Diagram

Applying cyclic loading to the closely spaced piles group resulted in uneven distribution of loads to piles according to their row location. Unlike the four pile group, the number of rows in this case is higher by one row and the spacing of piles was reduced to half its value. The normalized the moment diagrams were obtained by dividing the moments by individual piles head load, similar to the procedure used earlier in chapter four for four pile group and nine pile group. Figures 5.43 and 5.44 represent the effect of normalizing the moment diagrams by pile head load for nine pile group embedded in dry and submerge sand conditions, respectively. Moreover, the resulted normalized moments for dry and submerged sand conditions are presented in table 5.1 for easier comparison. As shown in figure 5.43 the normalized moment decreases with increasing the load cycle. Similar results were obtained for the piles group embedded in submerged sand condition as represented in figure 5.44. This finding is true for piles in different row positions namely, front, middle, and back rows. Both figures reflect similar behavior, where piles in the back row attracted higher moments followed by piles in the middle and front rows, respectively.

The effect of submergence was significant in the normalized moment for the piles in the middle row. On the other hand, it was less significant for the piles in the front and back rows. These findings were presented in figures 5.45, 5.46 and 5.47. Moreover, in the middle row, the piles attract more moments in submerge sand condition if subjected to same unit

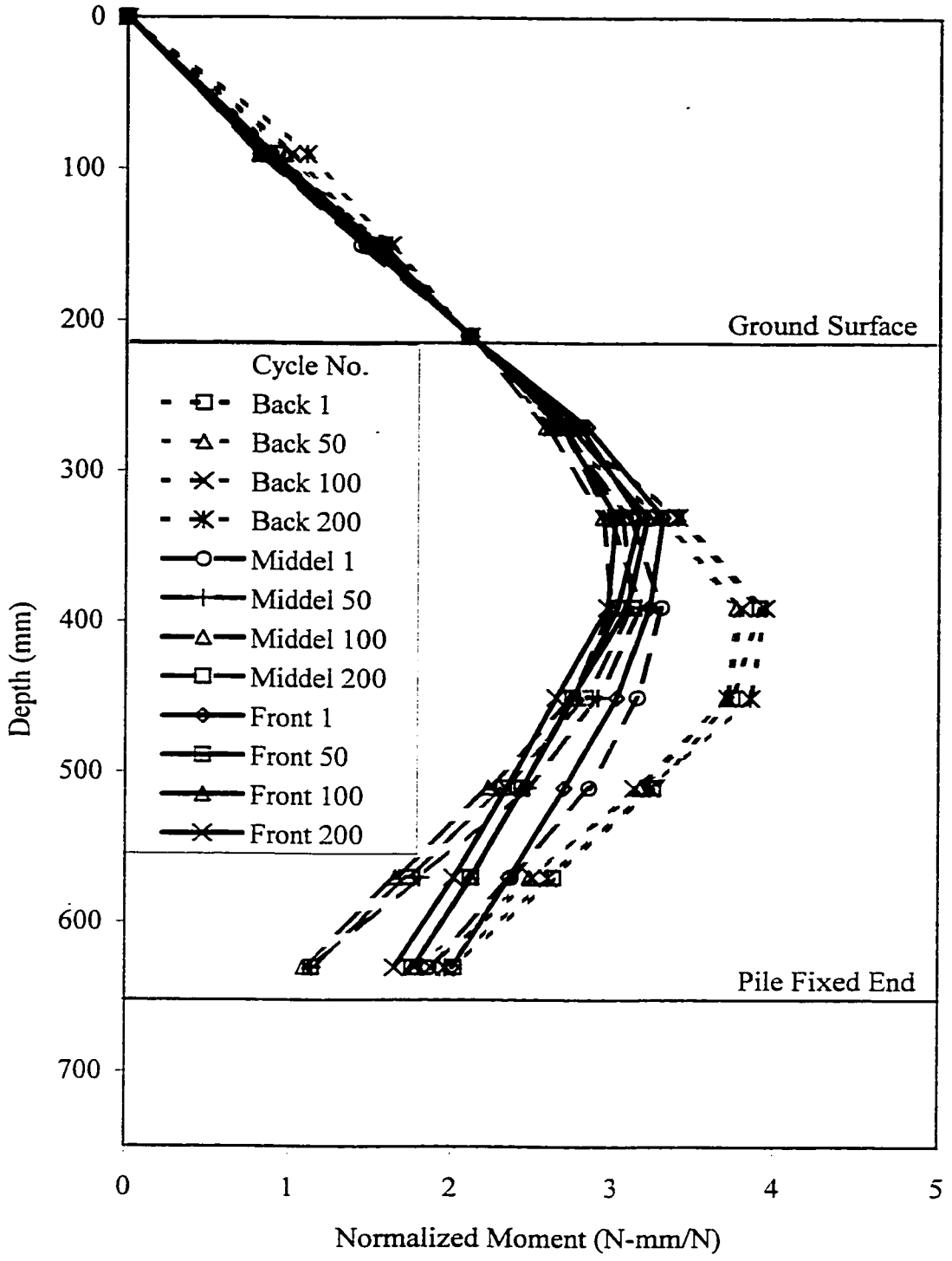

Figure 5.43: The Variation of Normalized Moment with Depth for Nine Group in Dry Sand Subjected to Cyclic Lateral Load.

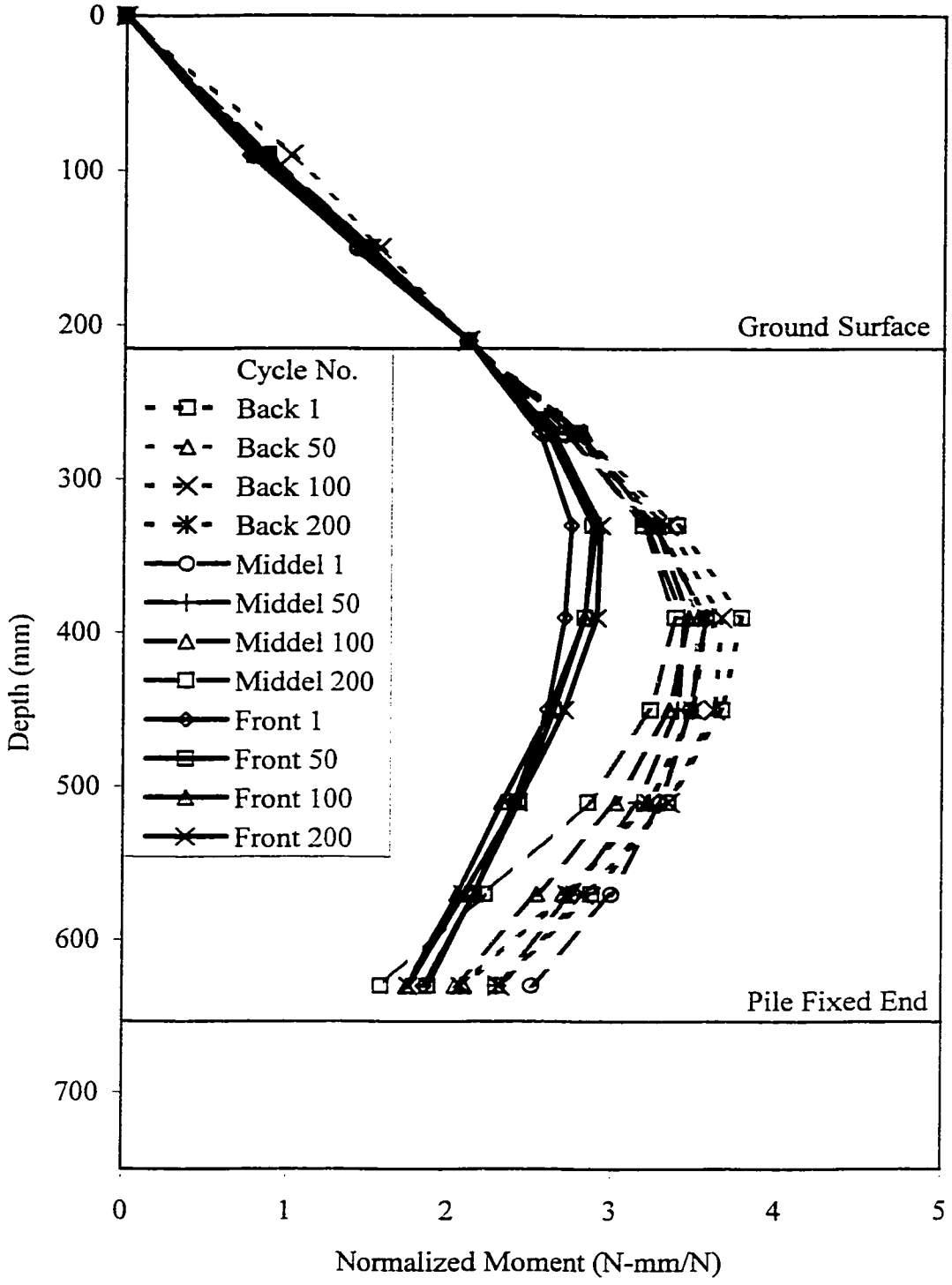

Figure 5.44: The Variation of Normalized Moment with Depth for Nine Group in Submerged Sand Subjected to Cyclic Lateral Load.

Table 5.1: Normalized Moment for Nine Pile Group Subjected Cyclic Lateral Load

Normalized Moment (N-mm/N)

Pile Position		Back Row				Middel Row				Front Row				Pile Position	
Cycle No.		1	50	100	200	1	50	100	200	1	50	100	200	Cycle No.	
Dry Sand Condition	Depth													Depth	Dry Sand Condition
	0	0.000	0.000	0.000	0.000	0.000	0.000	0.000	0.000	0.000	0.000	0.000	0.000	0	
	90	0.908	0.962	1.003	1.104	0.813	0.810	0.798	0.852	0.848	0.810	0.881	0.813	90	
	150	1.570	1.531	1.546	1.621	1.445	1.561	1.489	1.556	1.471	1.486	1.547	1.524	150	
	210	2.100	2.100	2.100	2.100	2.100	2.100	2.100	2.100	2.100	2.100	2.100	2.100	210	
	270	2.737	2.608	2.616	2.695	2.659	2.670	2.576	2.688	2.833	2.791	2.734	2.676	270	
	330	3.374	3.275	3.278	3.391	3.098	2.974	2.934	3.054	3.299	3.159	3.206	3.011	330	
	390	3.909	3.761	3.797	3.943	3.291	3.167	2.989	3.116	3.220	3.025	3.085	2.962	390	
	450	3.738	3.702	3.705	3.850	3.147	2.906	2.747	2.830	3.019	2.750	2.740	2.643	450	
	510	3.244	3.165	3.130	3.224	2.852	2.464	2.225	2.319	2.695	2.434	2.433	2.336	510	
	570	2.631	2.479	2.499	2.596	2.360	1.808	1.661	1.735	2.351	2.121	2.116	2.014	570	
	630	2.018	1.794	1.881	1.967	1.867	1.153	1.097	1.150	2.007	1.769	1.770	1.655	630	
Submerged Sand Condition															Submerged Sand Condition
	0	0.000	0.000	0.000	0.000	0.000	0.000	0.000	0.000	0.000	0.000	0.000	0.000	0	
	90	0.862	0.840	1.004	0.855	0.779	0.803	0.878	0.842	0.757	0.788	0.784	0.830	90	
	150	1.483	1.441	1.558	1.488	1.406	1.493	1.487	1.491	1.406	1.449	1.490	1.500	150	
	210	2.100	2.100	2.100	2.100	2.100	2.100	2.100	2.100	2.100	2.100	2.100	2.100	210	
	270	2.787	2.816	2.754	2.750	2.680	2.707	2.779	2.760	2.539	2.584	2.616	2.623	270	
	330	3.385	3.273	3.325	3.265	3.240	3.195	3.256	3.181	2.739	2.872	2.894	2.923	330	
	390	3.781	3.519	3.656	3.564	3.562	3.429	3.458	3.379	2.697	2.827	2.824	2.901	390	
	450	3.661	3.479	3.613	3.485	3.469	3.393	3.344	3.230	2.592	2.632	2.606	2.699	450	
	510	3.340	3.217	3.342	3.229	3.293	3.155	3.022	2.853	2.393	2.422	2.321	2.415	510	
	570	2.875	2.694	2.825	2.720	2.995	2.744	2.531	2.220	2.154	2.152	2.052	2.091	570	
	630	2.295	2.095	2.307	2.077	2.500	2.294	2.041	1.587	1.854	1.877	1.747	1.759	630	

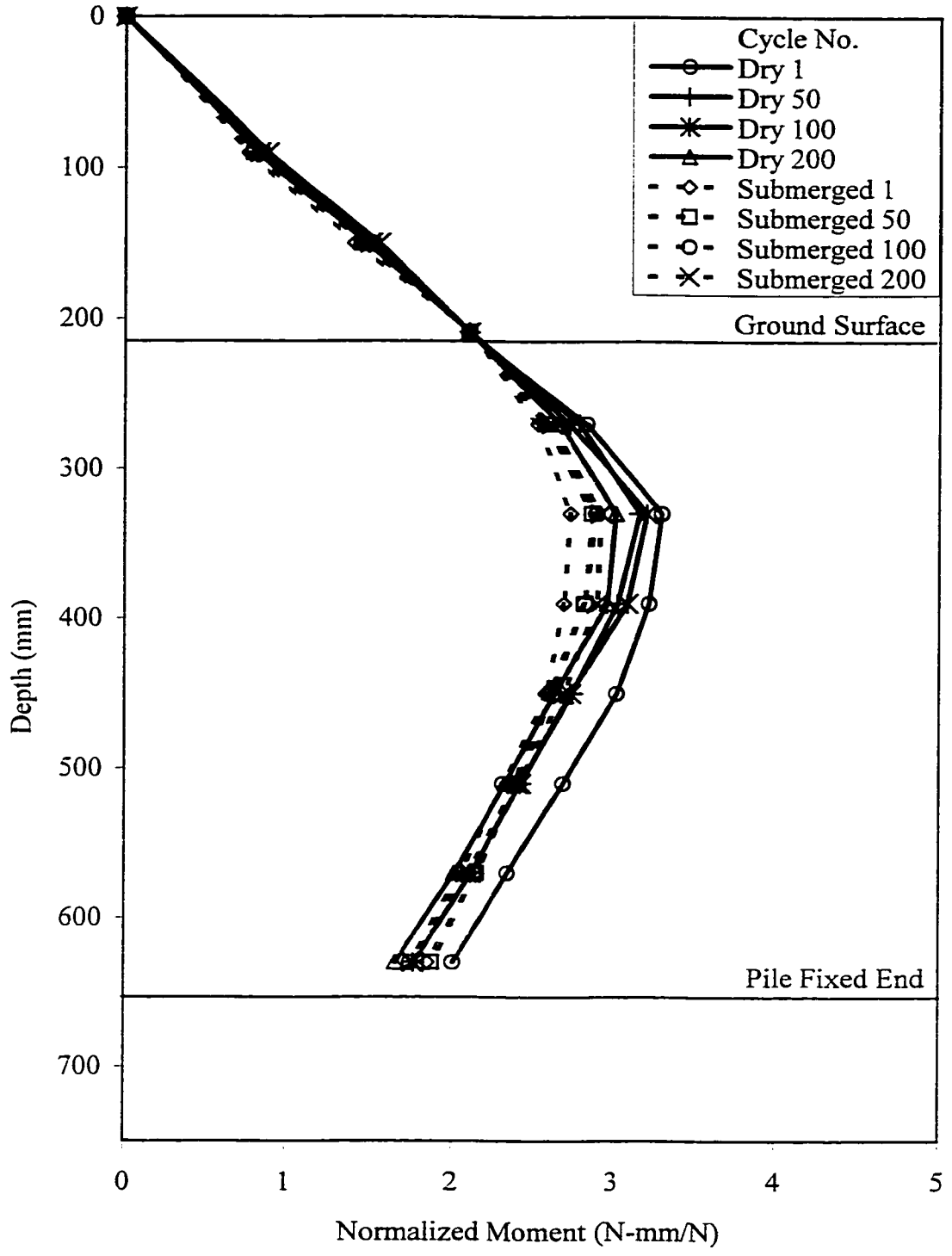

Figure 5.45: Comparison of Normalized Moment Variation with Depth for Front Row Pile in Nine Pile Group Between Dry and Submerged Sand Conditions Subjected to Cyclic Lateral Load.

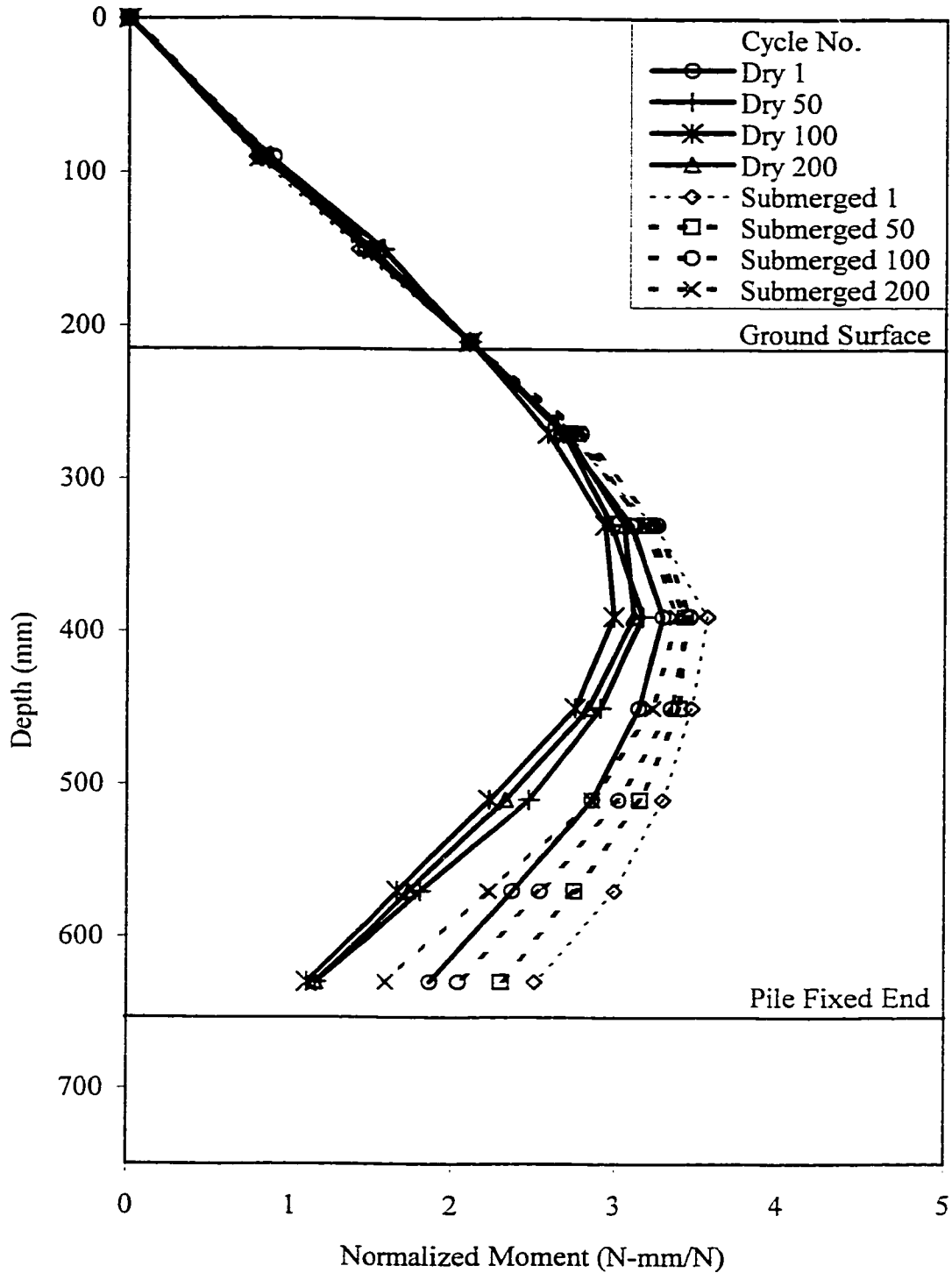

Figure 5.46: Comparison of Normalized Moment Variation with Depth for Middle Row Pile in Nine Pile Group Between Dry and Submerged Sand Conditions Subjected to Cyclic Lateral Load.

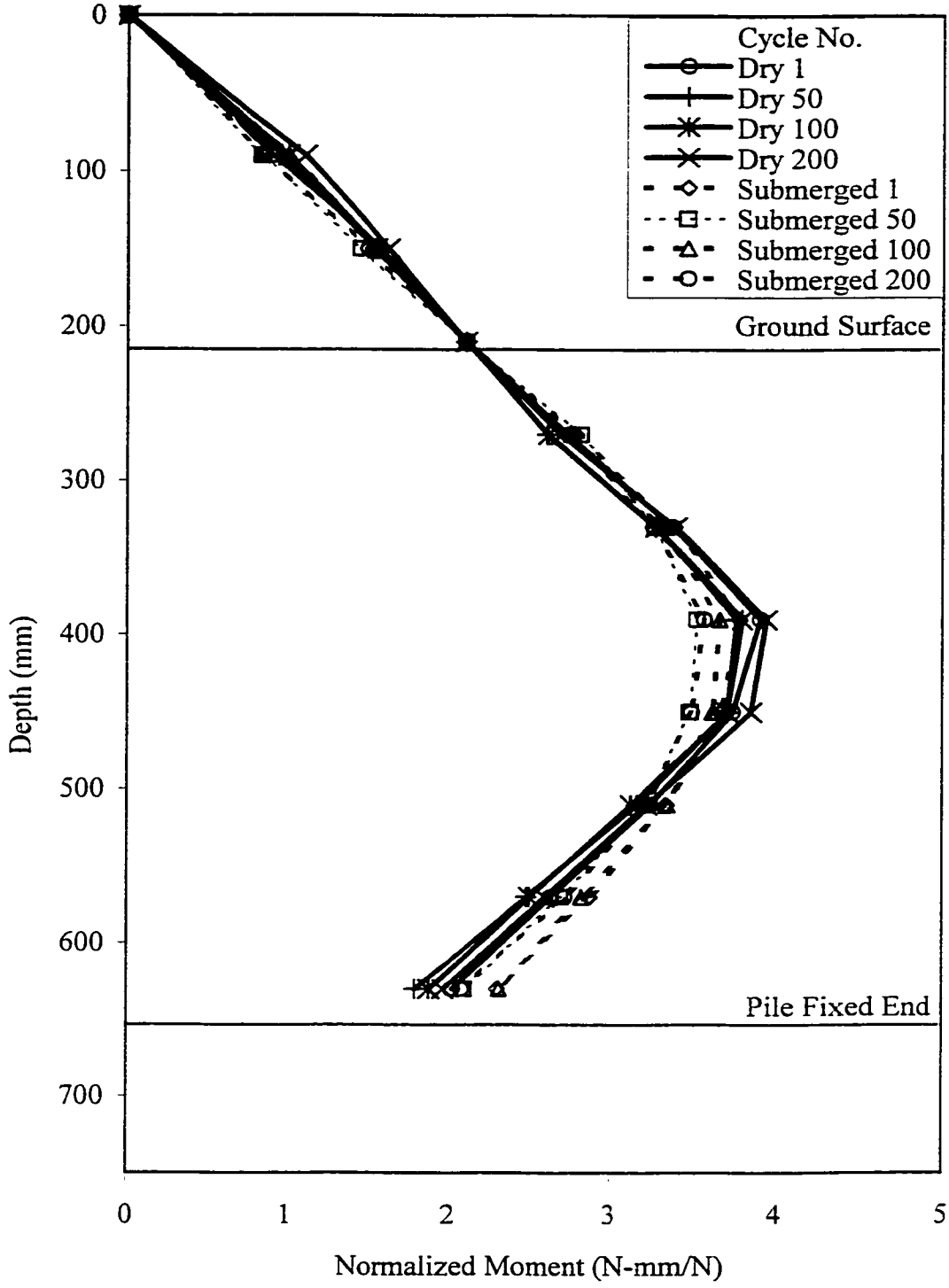

Figure 5.47: Comparison of Normalized Moment Variation with Depth for Back Row Pile in Nine Pile Group Between Dry and Submerged Sand Conditions Subjected to Cyclic Lateral Load.

load. Piles located in front and back rows attracted more moments in the dry sand. Therefore, the presence of water altered the distribution of moment.

Finally, it can be concluded for the nine pile group that piles in the front, middle and back rows behave differently if loaded to the same pile head load level. Moreover, the piles in the back and middle rows were more critical for design purposes when subject to the same pile head load.

CHAPTER SIX

CONCLUSIONS AND RECOMMENDATIONS

6.1 Conclusions

From the results presented, the following conclusions can be drawn:

- A small scale model for closely spaced group of piles can be used to explain the behavior of piles when subjected to lateral loading.
- A seventh degree polynomial equation was found the best to fit the experimental results of bending moments.
- The behavior of pile group was greatly affected by shadowing due to the shear zones in the soil around the piles in the trailing rows, which were influenced by the piles movement in the leading rows. The shadowing effect is dependent on: number of piles and spacing between the piles in the group, soil density and condition, and load level. Piles in the leading rows have attracted higher load level per pile head, leading to higher deflections and bending moments.

- The behavior of the piles at each cycle were similar to the static load condition but with different level of deflection and bending moments depending on the load level per pile head at each cycle. For the soil density used, deflections and bending moments decrease as the number of cycles increase; while the sand resistances increases due to the sand densification.
- It is more critical to study the behavior of piles under their normalized bending moments. It is always higher for piles in the trailing rows (back and Middle rows).
- The behavior of piles embedded in submerged sand was similar to the piles embedded in dry sand. However, due to the reduction in sand density, submerging yielded higher deflection and bending moments but lower sand resistance. Moreover, the percentage differences in head load sustained by the piles in different rows were higher in the dry sand condition.

6.2 Recommendations For Further Works

The following recommendations can be proposed for further studies:

- Conduct an actual scale field test with similar environmental and loading condition to establish correlation between the model and field test result.
- Produce a mathematical model formulation to present the p-y curves using the model tests results.
- Produce a mathematical model formulation to obtain p-y curves for closely spaced group of piles.

- Finite element model need to be produced in order to compare it with the test results for the model results.
- Different soil surrounding or boundary conditions can be manipulated to cover wider range of soils. For example, the effect of different type of soils and different saturation levels on piles can be experimented and studied.
- Different boundary conditions at the bottom of piles can be examined, for example, using strong spring to represent soil at such depth.

APPENDICES

APPENDIX A

SAMPLE CALCULATIONS

A.1 Calculation of Bending Moment from Stain Gage Reading

External Diameter = D_i = 40 mm

Internal Diameter = D_o = 36 mm

Strain Reading = ε = 62 x 10^{-6}

$$I = \frac{\pi}{64}(D_o^4 - D_i^4)$$

$$= \frac{\pi}{64}(40^4 - 36^4)$$

$$= 43215.749 \quad mm^4$$

$$y = \frac{D_o}{2} = \frac{40}{2} = 20$$

$$M = \frac{\varepsilon EI}{y} = \frac{62x10^{-6}\,x65450x43215.749}{20} = 8.768 \quad KN.mm$$

A.2 Calculation for Pile Head Load Normalized Moment

Moment at mud line = 8.768 KN.mm at Depth = 210mm

The Pile Head Load = Moment at Mud Line / Depth

= 8.768 x 10^3 / 210 = 41.752 N

After that all the moments at this specific pile location and load level should be divided by above Pile Head Load in order to obtain Normalized Moment.

e.g. Normalize Moment at Depth 330mm = 12.945 / 41.752 = 0.3 KN.mm/N

APPENDIX B

COMPUTER PROGRAM

```
REM THIS PROGRAM CALCULATE THE DEFLECTION AT ALL POINTS OF
THE PILE
CLS
DIM x(100), mom(100), defl(100), DEF1, DEF2, DEF3, EI, xm(100), a(100)
INPUT "Enter the input file name : "; inpt$
OPEN inpt$ FOR INPUT AS #1
INPUT #1, load, n, EI, defl1, defl2, defl3
FOR i = 1 TO n
     INPUT #1, x(i), mom(i)
NEXT i
PRINT "EI="; EI, "DEFl1="; defl1, "DEFl2="; defl2, "DEF3="; defl3
INPUT "press return to continue"; retu
CLS
PRINT " i          x(i)       mom(i)"
PRINT "=============================================="
FOR i = 1 TO n
PRINT i, x(i), mom(i)
NEXT i
INPUT "press return to continue"; retu
REM
REM TO CALCULATE THE TRAB AREA AND CENTER
REM
CLS
PRINT " i          a(i)         xm(i)"
PRINT "=============================================="
FOR i = 1 TO n - 1
   B = x(i + 1) - x(i)
   MOMNT = mom(i) + mom(i + 1)
   MOMNT1 = mom(i) + 2 * mom(i + 1)
   a(i) = B * MOMNT / (2 * EI)
   xm(i) = B * MOMNT1 / (3 * MOMNT)
 PRINT i, a(i), xm(i)
NEXT i
INPUT "press return to continue"; retu
REM
```

```
REM
REM to calculate the deflection at each point
REM
CLS
PRINT " j          x(J)        MOM(J)       DEFL(J)"
PRINT "═══════════════════════════════════════════════════════════════════════"
S1 = (defl1 - defl2 + a(1) * xm(1)) / (x(2) - x(1))
PRINT "SLOPE="; S1
     INPUT "Enter the output file name : "; out$
     OPEN out$ + ".out" FOR OUTPUT AS #3
          PRINT #3, load
PRINT #3, " j          x(J)        MOM(J)       DEFL(J)"
PRINT #3, "═══════════════════════════════════════════════════════════════════════"
S1 = (defl1 - defl2 + a(1) * xm(1)) / (x(2) - x(1))
PRINT #3, "SLOPE="; S1

FOR j = 1 TO n
     FOR i = 1 TO j - 1
          arm = x(j) - x(i) - xm(i)
          defl(j) = arm * a(i) + defl(j)
     NEXT i
     defl(j) = defl1 - S1 * (x(j) - x(1)) + defl(j)
     PRINT j, x(j), mom(j), defl(j)
     PRINT #3, j, x(j), mom(j), defl(j)
REM       'PRINT x(j), defl(j)
NEXT j
CLOSE
END
```

APPENDIX C

Dr. R.D. WOODS FAX (1996)

Department of Civil & Environmental Engineering
University of Michigan, 2340 G. G. Brown Building
2350 Hayward, Ann Arbor, MI 48109-2133
(313) 764-8495 FAX: (313) 764-4292

Today's Date June 18, 1996

Account # 103250

TO: Dr. Naser Al-Shayea, KFUPM	From: Richard D. Woods
FAX Number: 9-011-966-3-860-2879	Total pages being transmitted
State or Country: Saudi Arabia	1

REMARKS:

Dear Naser,

I have reviewed your FAX and find it very interesting. Has there been any noticeable settlement of the sand in the vicinity of the pile group? If that happens, then it would be easy to agree with your proposition that the sand is densifying during cyclic loading. It is not too clear what is meant by "medium density". Would it be possible to express it as Relative Density. If relative density is less than about 75%, cyclic compaction is likely to occur.

I am sending off this FAX to you to let you know that I am looking for references for you, but that will take the remainder of the day and it is almost 5:00 PM in Dhahran now.

Best regards

Richard D. Woods

Richard D. Woods

Department of Civil & Environmental Engineering
University of Michigan, 2340 G. G. Brown Building
2350 Hayward, Ann Arbor, MI 48109-2125
(313) 764-8495 FAX: (313) 764-4292

Today's Date June 20, 1996

Account # 103250

TO: Dr. Naser Al-Shayea, KFUPM	From: Richard D. Woods
FAX Number: 9-011-966-3-860-2879	Total pages being transmitted
State or Country: Saudi Arabia	10

REMARKS:

Dear Naser,

I have not identified any published data on cyclic lateral pile tests which show either softening or stiffening of soil with increasing number of cycles. I asked others around here and Dr. Afifi and Mr. Al Shunnar, but no ones has any recollection of such data.

I have attached to this fax, tables of contents of the most recent pile dynamics specialty conferences and the reference list from Salah Hassini's thesis.

Sounds like you have shown what we all would expect, that dry, loose sand will compact under slow cyclic testing. This kind of testing allows the sand to fill in some of the gap caused by the lateral loading and therefore, behave more stiff on later cycles. It would be interesting to repeat some tests using very loose and very dense sands. Do you have time and funding to do that?

Good luck with this research.

Best regards

Richard D. Woods

Richard D. Woods

REFERENCES

Brown D.A., C. Morrison and L.C. Reese (1988), "Lateral Load Behavior of Pile Group in Sand," Journal of Geotechnical Engineering American Society of Civil Engineering Division, Vol. 114, No. 11, November, pp. 1261-1276.

Brown, D.A. (1989), "The Influence of Cyclic Loading on the Lateral Load Response of Groups of Piles," Foundation Engineering, Current Principals and Practices, Volume I, Fred H. Kulhawy, pp. 553-564.

Cox, W.R. and J.W. McCann (1978), "Analysis of Laterally Loaded Piles," Pile Design, pp. 801-832.

Davis, E.H. and J.T. Chiristain (1971), "Bearing Capacity of Anistropic Cohesive Soil," Journal of the Soil Mechanics and Foundations Division, Proceeding of American Society of Engineers Vol. 97, No. SM5, May.

Focht, J.A., Jr. and K.J. Koch. (1973), "Rational Analysis of the Lateral Performance of Offshore Pile Groups," McCelland Engineers, American Institute of Mining, Metallurgical, and Petroleum Engineering Incorporation, The University of Taxes @ Austin, Offshore Technology Conference pp. OTC 1896.

Georgiadis, M., C. Anagnostupoulos and S. Saflkon (1992), Centrifugal Testing of Laterally Loaded Piles in Sand," Department of Civil Engineering, University of Thessaloniki, Greece. Canadian Geotechnical Journal 29, 208-216.

Matlock, H. and L.C. Reese (1961), "Foundation Analysis of Offshore Pile Supported Structures," Proceedings of the Fifth International Conference on Soil Mechanics and Foundation Engineering, Paris 17-22 July.

Matlock, H. and L.C. Reese (1988), "Tables of Non-Dimensional Solutions for Laterally Load Piles," The university of Texas @ Austin.

Poulos, H.G.(1982), "Single Pile Response to Cyclic Lateral Load," Journal of the Geotechnical Engineering Division, Proceedings of the American Society of Civil Engineers (ASCE) Vol. 108 No. GT3, March pp. 355-375.

Reese, L.C. and C.S. Desai (1974), "Chapter 9: Laterally Loaded Piles", Numerical Methods in Geotechnical Engineering pp. 297-325.

Reese, L.C., W.R. Cox and F.D. Koop (1974), "Analysis of Laterally Loaded Piles in Sand," Sixth Offshore Technology Conference, Houston, Texas, pp. 473-483.

Reese, L.C. (1977), "Laterally Loaded Piles: Program Documentation," The Journal of the Geotechnical Engineering Division, Proceeding of ASCE. Vol. 103 No. GT4, April, pp. 287-305.

Shamem M. (1988), "Study of Laterally Loaded Single Pile Model," A Thesis presented to the Faculty of the College of Graduated Studies, King Fahd University of Petroleum and Minerals, August.

Smith, T.D (1989), "Fact or Friction: A Review of Soil Response to a Laterally Moving Piles," Foundation Engineering, Current Principals and Practices, Volume I, Fred H. Kulhawy, pp. 588-598.

Swokowski E.W. (1988), Calculus with Analytical Geometry, PWS-Kent Publishing Company, pp. 717-718.

Ting J.M (1987), " Full-Scale Cyclic Dynamic Lateral Pile Responses," Journal of Geotechnical Engineering Vol. 113, No. 1, Tanvary , ASCE, pp.30-45.

Yegian, M. and S.G. Wright (1973), "Lateral Soil Resistance-Displacement Relationships for Pile Foundations in Soft Clay," American Institute of Mining, Metallurgical, and Petroleum Engineering Incorporation, The University of Taxes @ Austin, Offshore Technology Conference, pp. OTC 1893.